



UNIVERSITY OF
LEICESTER

Investigation of the function of *Campylobacter jejuni* glyceraldehyde-3-phosphate dehydrogenase in iron acquisition from lactoferrin

Thesis submitted for the degree of

Doctor of Philosophy

Department of Genetics and Genome Biology

University of Leicester

By

Mohamed-Elamen Mohamed Mahmoud Fadel

September 2017

Investigation of the function of *Campylobacter jejuni* glyceraldehyde-3-phosphate dehydrogenase in iron acquisition from lactoferrin

Mohamed-Elamen Mohamed Mahmoud Fadel

Abstract

Campylobacter jejuni is a major cause of bacterial food-borne disease, but the available knowledge of the biology and molecular basis of its pathogenesis is limited. Iron is an essential co-factor for the effective intestinal colonisation of *C. jejuni*. However, iron is not readily available due to its being tightly bound to proteins such as haemoglobin, transferrin and lactoferrin (Lf). Studies in different organisms have reported the contribution of GAPDH to iron acquisition from ferric-Tf and ferric-Lf; iron binding proteins. Therefore, this study aimed to determine the role of *C.jejuni* NCTC11168 GAPDH in iron uptake from host ferric-lactoferrin complex.

Due to essentiality of *gapA*, use of the *Campylobacter* complementation pC46 plasmids to inactivate this gene was required. Therefore, *gapA* mutated strains were successfully created in which the wild type *gapA* allele was knocked out in a *gapA* merodiploid strains while the expression of the complemented *gapA* allele is driven by promoters of different strength. In addition, site-directed mutagenesis was used to create C150S-GAPDH protein which lacks glycolytic activity. The results of gene expression studies in this research show that the mutated *gapA* strains overexpressed GAPDH. Iron growth assays in MEM α medium supplemented with low concentrations of human ferric-Lf as the sole iron source indicated that GAPDH has an important role in iron uptake from Lf. This role was supported by the inhibition of the growth of *C. jejuni* incubated with anti-GapA antibody in cultures supplemented with ferric-Lf as the sole iron source. Moreover, GAPDH was identified for the first time as an outer membrane associated protein in *C. jejuni*. Using different binding assays, it was shown that GAPDH could act as an extracellular receptor for Lf. Both purified wild type GAPDH and non-glycolytic functional C150S-cjGAPDH bound different ferric-Lf family iron binding proteins, with high affinity binding of Lf compared to the other iron glycoproteins. Therefore, the binding function of GAPDH is independent from glycolytic function.

In conclusion, this research demonstrates that GAPDH of *C. jejuni* is important agent in iron uptake from human ferric-Lf, and therefore it is probably required for successful colonisation of *C. jejuni*.

Acknowledgment

I have had fantastic time in university of Leicester, so I hope not forgetting thank those who were the source of my pleasure. First of all, all praise and glory to **Allah**, the Almighty, the Lord of the Worlds, on whom ultimately we depend for sustenance and guidance. The prayer and peace be upon His messenger. Second, I would like to express my deepest gratitude to my supervisors: **Dr. Julie Morrissey** and **Prof. Julian Ketley** for recognising and drawing out my abilities, endless support and invaluable advices and supervision at all stages of this research. I would like also to thank my thesis committee, **Professor Marco Oggioni**, **Dr Fred Tata** and also **Dr Chris Bayliss** for helpful suggestions. Special thanks for **Dr Chris Bayliss** for providing Anti-MOMP antibody. Likewise, I wish to thank **Prof Peter Moody's** Research group, especially **Dr Adnan Ayana**, **Aziz Al-Ethari** for helping me in the purification of proteins, Also **Dr Richard Cowan** who helped me using CD spectrometer of GAPDH protein. Also, I would like to thank **Dr Richard Haigh** for unlimited help during my experimental work of this research. My worm thanks should go to **Dr Caroline Cayrou** for guiding me in RT-PCR work. In addition, my thanks go to previous members of lab121, **Dr Bassam Elgamoudi**, **Dr Alex Woodacare** and **Dr Abdullahi Jama** for their advice and support. Many thanks go to **Ali**, **Khaloud**, **Norah**, and **Zaima** and all other **colleagues in lab and office 121** for their team work on the professional level.

My acknowledgment would not have sense if I did not provide my thanks to **my beloved wife, {Salmah}**. You are the best wife in the world, I could not make this work without your support. Also my children, **Abd-Elwahab**, **Mahmoud**, **Aisa Eklas** and **Husny**. Moreover, **my parents** in other life, your prayers and belief in me have made this journey possible. I must thank **my brothers** and **sisters**, **nieces** and **nephews** for all kinds of encouragement and support which are keeping me motivated throughout the completion of this thesis. My beloved brother **Zyan**: your support made me earning the success in my academic life. To **my Friends in my youth** and **childhood**, and **lovely Libyans** in Leicester. I would like to provide great thanks for good time spent together and kindly support in times of distress and prosperity.

Finally, my gratitude must go to my sponsor, the **ministry of higher education, Libya**. My teachers in all of my previous stages of education, in particular whom have great impact on my academic career progression; **Prof Ahmed Aljanga**, **Prof Ibrahim Eshnaf**, and **Dr Abubaker Mahrouf** and **Dr Nazek Al-gallas**. I could not reach this stage without you!

Table of Contents

Chapter 1. Introduction	15
1.1 Introduction.....	15
1.2 Historical background and general aspects of <i>C. jejuni</i>	15
1.2.1 Morphology and growth characteristics of <i>C. jejuni</i>	16
1.2.2 Physiological and biochemical perspectives.....	18
1.2.3 The genetics features of <i>C. jejuni</i>	21
1.2.4 Antibiotic resistance	23
1.2.5 Protein secretion pathways of <i>C. jejuni</i> :	23
1.2.6 Pathogenesis of <i>C. jejuni</i>	25
1.2.6.1 Sources of <i>C. jejuni</i> infections.....	25
1.2.6.2 Colonisation and progression of <i>C. jejuni</i> Infection.....	27
1.2.6.3 Clinical manifestations.....	29
1.3 Iron and <i>C. jejuni</i>	30
1.3.1 The importance of iron	30
1.3.2 Iron uptake systems in <i>C. jejuni</i>	31
1.3.2.1 Siderophore Uptake Systems.....	31
1.3.2.1.1 Ferric-Enterochelin	33
1.3.2.1.2 Ferrichrome.....	33
1.3.2.1.3 Rhodotorulic acid.....	35
1.3.2.2 Haem utilisation	35
1.3.2.3 Ferrous Iron Uptake.....	36
1.3.2.4 Iron uptake from Lactoferrin and Transferrin	37
1.3.2.4.1 General features of Lactoferrin and Transferrin	37
1.3.2.4.2 Iron binding and release from Lf and Tf.....	39
1.3.2.4.3 Iron binding proteins in poultry:	41
1.3.2.4.4 Utilisation of ferric-Lf and Tf by different microorganisms	41
1.3.2.4.5 Utilisation of ferric-Lf and Tf by <i>C. jejuni</i>	44

1.3.3 Role of iron in colonisation of <i>C. jejuni</i>	46
1.4 Glyceraldehyde -3- phosphate dehydrogenase (GAPDH)	46
1.4.1 The diversity of GAPDH gene among the organisms	48
1.4.2 localisation of GAPDH on the cell surface.....	49
1.4.3 Moonlighting functions of GAPDH	52
1.4.3.1 GAPDH as virulence factor.....	52
1.4.3.2 The iron uptake function of GAPDH	54
1.4.3.2.1 Role of GAPDH in iron uptake from TF and Lf in mammalian cells .	55
1.4.3.2.2 Role of GAPDH in iron uptake from TF and Lf in bacteria.....	55
1.4.4 GAPDH in <i>C. jejuni</i>	57
1.5 Aim of the research	59
Chapter 2. Material and Methods	60
2.1 Growth Media and Sterilisation procedures.....	60
2.1.1 Lysogeny broth and Agar	60
2.1.2 Mueller Hinton Broth and Agar.....	60
2.1.3 Sterilisation procedures.....	60
2.2 Growth Conditions and Bacterial Storage.....	60
2.2.1 Growth Conditions of <i>E.coli DH5α</i>	60
2.2.2 Growth Conditions of <i>C. jejuni</i>	60
2.2.3 Bacterial storage:	61
2.3 DNA methods	62
2.3.1 Extraction of plasmid DNA	62
2.3.2 Extraction of chromosomal DNA	62
2.3.3 Ethanol precipitation.....	64
2.3.4 Restriction enzyme digestion of DNA.....	65
2.3.5 DNA ligation	65
2.3.6 Polymerase chain reactions (PCR)	65
2.3.6.1 PCR reaction mix	65
2.3.6.2 Colony PCR.....	67

2.3.6.3 Inverse PCR.....	67
2.3.6.4 Primers.....	67
2.3.6.5 PCR purification.....	67
2.3.7 Estimation of DNA concentration by gel electrophoresis	67
2.3.8 Transformation of DNA.....	69
2.3.8.1 Preparation of electrocompetent <i>E. coli</i> DH5 α	69
2.3.8.2 Preparation of electrocompetent <i>C. jejuni</i>	69
2.3.8.3 Preparation of wash buffer	69
2.3.8.4 Electroporation	70
2.3.9 DNA sequencing.....	70
2.3.10 Real-time reverse transcriptase-PCR (RT-PCR)	70
2.3.10.1 Preparation of the cells	70
2.3.10.1 Extraction of RNA.....	71
2.3.10.2 Removing of DNA residuals from extracted RNA	71
2.3.10.3 Reverse transcription reaction	71
2.3.10.4 RT-PCR assay	72
2.3.10.5 Analysis of RT-PCR results	72
2.3.11 The splicing by overlap extension (SOE) PCR to tag of GAPDH at the C-terminal with mCherry fluorescent protein:.....	73
2.4 Growth assays	75
2.4.1 Growth assay of <i>C. jejuni</i> strains in Mueller Hinton Broth medium.....	75
2.4.2 Growth assay of <i>C. jejuni</i> strains in MEM α	75
2.4.3 Calculation of doubling time and growth rate	76
2.5 Protein Methods	77
2.5.1 Preparation of whole cell lysate.....	77
2.5.2 SDS Polyacrylamide gel electrophoresis (SDS-PAGE) and staining.....	77
2.5.3 Western blot.....	78
2.5.4 GAPDH enzyme activity assay.....	79
2.5.4.1 Intact <i>C. jejuni</i> cells GAPDH enzyme activity assay	79

2.5.4.2 Purified Protein GAPDH enzymatic activity assay	79
2.5.5 Fractionation of <i>C. jejuni</i>	79
2.5.6 Expression and purification of recombinant cjGAPDH	80
2.5.7 Circular Dichroism of wild and mutated GAPDH protein	81
2.5.8 Whole cell pull-down method for study role of GAPDH in binding with Lf:.....	81
2.6 Bioinformatics.....	82
Chapter 3. Characterisation of GAPDH protein in <i>C. jejuni</i> NCTC11168.....	83
3.1 Introduction.....	83
3.2 Mutagenesis of <i>gapA</i> gene	83
3.2.1 Construction of merodiploid <i>gapA C. jejuni</i> strains	86
3.2.2 Inactivation of wild-type <i>gapA</i> allele.....	89
3.2.2.1 The <i>gapA</i> is essential gene and vital for the viability of <i>C.jejuni</i>	91
3.2.3 Characterisation of constructed <i>C. jejuni</i> strains	93
3.2.3.1 The growth assay of merodiploids and mutated <i>gapA</i> strains	93
3.2.3.2 Measurement of the transcriptional levels of the <i>gapA</i> gene in constructed strains by qRT-PCR.....	96
3.2.3.3 Western blot of whole cell GAPDH among the strains.....	98
3.2.3.4 GAPDH enzyme activity measurements among the constructed strains.....	100
3.3 Identification of GAPDH as membrane associated protein in <i>C. jejuni</i>	102
3.3.1 Measurement of intact <i>C. jejuni</i> cells GAPDH enzyme activity assay after treatment with proteinase K.....	102
3.3.2 Measurement of whole <i>C. jejuni</i> cells GAPDH enzyme activity assay after treatment with anti-GapA antibody	103
3.3.3 Fractionation of <i>C. jejuni</i>	106
3.3.3.1 Detection of GAPDH activity in cell fractions.....	106
3.3.3.2 Western blot of cell fractions	108
3.4 Discussion and conclusion	110
Chapter 4. The GAPDH protein of <i>Campylobacter jejuni</i> NCTC11168 is involved in iron uptake from human ferric- lactoferrin	115
4.1 Introduction.....	115

4.2 Results.....	116
4.2.1 The response of <i>gapA</i> gene to iron stress among <i>C. jejuni</i> strains.....	116
4.2.1.1 Intact <i>C. jejuni</i> GAPDH enzyme activity assay in different iron conditions.....	116
4.2.1.2 Western blot of <i>C. jejuni</i> GapA protein in different iron conditions.....	117
4.2.2 Growth assay of the <i>C. jejuni</i> strains in MEMa	120
4.2.3 The growth of <i>C. jejuni</i> strains in optimum levels of ferric-Lf	122
4.2.4 The differences in growth kinetics were significant among the <i>C. jejuni</i> strains growing under low concentrations of human ferric-Lf levels.....	125
4.2.5 Addition of anti-GapA into iron growth assay of wild type and mutated <i>gapA</i> strains reduced significantly the growth of <i>C. jejuni</i> strains in the presence of lactoferrin as sole iron source.....	128
4.2.6 Binding assays with ferric-Lf	132
4.2.6.1 Role of cjGAPDH in binding of whole cell <i>C. jejuni</i> to lactoferrin.....	132
4.2.6.2 Far-western blot assay to study binding of purified GapA protein with different lactoferrin family proteins	134
4.2.6.2.1 Cloning, overexpression, purification of GapA protein	134
4.2.6.2.2 Far western blot assay of GapA and ferric-glycoproteins	136
4.3 Discussion and conclusion	138
Chapter 5. The binding function of GAPDH with human ferric-Lf in <i>C. jejuni</i> is independent of its glycolytic activity	142
5.1 Introduction.....	142
5.2 Site-directed mutagenesis of the <i>gapA</i> gene	144
5.3 Production and characterisation of C150S-GAPDH mutated protein.....	146
5.3.1 Overexpression and purification.....	146
5.3.2 Measurement of GAPDH enzyme activity of C150S-GAPDH mutated protein.....	148
5.3.3 Determination of the secondary structure of C150S-GAPDH by far UV circular dichroism	150
5.4 Creation of new <i>C. jejuni</i> strains lack glycolytic activity of <i>gapA</i> gene	152
5.5 Phenotyping of the hetero-merodiploid and <i>cys-ΔgapA</i> reverted strains.....	155
5.5.1 Growth curve of strains	155

5.5.2 Measurement of the transcriptional levels of gapA by RT-PCR	158
5.5.3 Western blot of whole cell GAPDH	158
5.5.4 Measurement of whole cell <i>C.jejuni</i> GAPDH enzyme activity	161
5.6 The differences in GAPDH glycolytic activity do not alter utilisation of ferric-Lf in growth of new <i>C. jejuni</i> strains	163
5.7 Binding assays with ferric- Lf.....	166
5.8 Discussion and conclusion	168
Chapter 6. General discussion	171
6.1 General discussion and future work.....	171
6.1.1 Use of <i>C. jejuni</i> complementation system coupled with allelic replacement mutagenesis method clarified essentiality of <i>gapA</i>	171
6.1.2 The cjGAPDH is a membrane associated protein in <i>C. jejuni</i> NCTC11168	172
6.1.3 The cjGAPDH is an essential element for iron uptake from ferric-Lf.....	175
6.1.4 Proposed model for iron uptake from ferric-Lf by cjGAPDH.....	177
6.2 Summary of findings and Conclusion.....	180
Appendix	181
Bibliography	187

List of tables

Table 1.1 Summary of the importance of iron to microorganisms	32
Table 2-1 Antibiotic preparation and concentrations.....	61
Table 2-2 Bacterial strains and plasmids used in this research	63
Table 2-3 conditions of PCR reactions.	66
Table 2-4 describes the PCR components.....	66
Table 2-5 primers used in this research.....	68
Table 2-6 preparation of mastermix reaction of RT-PCR experiment.....	73
Table 2-7 iron sources used in this research	76
Table 2-8 Preparation of 12% SDS-PAGE.	78
Table 3-2 Growth rate (h^{-1}) and doubling times (h) of wild type, merodiploid and mutants calculated from growth curve given in Figure 3-4.....	95
Table 3-3 Statistical differences calculated by unpaired t test between growth rate and doubling time of wild type, merodiploid and mutated strains.....	95
Table 4.1. The growth rate and doubling time of strains growing in MEM α supplemented by 0.27 μ M ferric-Lf.....	124
Table 4.2. The growth rate of strains grown in a low level of ferric-Lf.....	127
Table 4.3. The doubling time of strains grown in a low level of ferric-Lf.....	127
Table 5-1. Growth rate and doubling times of wild type, hetero-merodiploid and Cys- Δ gapA reverted strains calculated from growth curve given in Figure 5-6	157
Table (5.2) Statistical differences calculated by paired t test between growth rate and doubling time of hetero-merodiploid and mutated strains.	157
Table 5.3. The growth rate of new <i>C. jejuni</i> strains in different concentrations of human ferric- Lf.....	165
Table 5.4. The doubling time of new <i>C. jejuni</i> strains in different concentrations of human ferric-Lf.....	165

Table of figures

Figure 1-1. Electron micrograph of <i>C. jejuni</i>	17
Figure 1-2. Outline of the gluconeogenic and anaplerotic reactions of <i>C. jejuni</i> NCTC 11168. 20	20
Figure 1-3. The sources and outcomes of <i>C. jejuni</i> infection.....	26
Figure 1-4. Iron uptake systems in <i>C. jejuni</i>	34
Figure 1-5. Structure of the iron-bound (holo) form of human Lf.	38
Figure 1-6. The canonical iron binding site found in lactoferrin and transferrin.	40
Figure 1-7. Schematic representation of iron uptake pathway from Tf/Lf in <i>N. meningitidis</i> and <i>N. gonorrhoeae</i>	43
Figure 1-8. The typical structure of GAPDH in <i>S.aureus</i>	47
Figure 1-9 A & B. The distribution of GAPDH on the cell surface of (A) <i>Streptococcus pyogenes</i> and (B) <i>C. albicans</i>	51
Figure 1-10. The essential pathogenic mechanisms exploits GAPDH as virulence factor.....	53
Figure 1-11. Role of mammalian GAPDH in iron homeostasis.	56
Figure 1-12. The genomic context of <i>gapA</i> in the <i>C.jejuni</i> genome.	58
Figure 2-1. Diagram to illustrate the method used to tag <i>gapA</i> at the C- terminal end with <i>mCherry</i> fluorescent protein.	74
Figure 3-1. A, B, C. Verification of the construction of merodiploid <i>gapA C. jejuni</i> strains. ..	88
Figure 3-2. The map of pUC19 Δ <i>gapA</i> ::kanamycin- plasmid (4798 bp).	90
Figure 3-3 A, B. Verification of creation of Δ <i>gapA</i> - <i>pfdxA</i> , Δ <i>gapA</i> - <i>pmetK</i> , and Δ <i>gapA</i> - <i>pporA C. jejuni</i> strains.	92
Figure 3-4. Growth curve assay of merodiploids, <i>gapA</i> mutated and wild strain NCTC 11168. 94	94
Figure 3-5. Relative qRT-qPCR results of <i>gapA</i> gene in <i>C. jejuni</i> constructed strains.	97
Figure 3-6 A and B. Assessment of GAPDH protein expression of <i>C. jejuni</i> strains by Western blot.	99
Figure 3-7. Whole cell GAPDH enzyme activity of <i>C. jejuni</i> strains.....	101
Figure 3-8. Intact cell GAPDH-NADPH enzyme activity of <i>C. jejuni</i> strains with/without treatment of proteinase K (p k).	104
Figure 3-9. Intact cell GAPDH-NADPH enzyme activity of <i>C. jejuni</i> strains with/without treatment of anti-GapA.	105
Figure 3-10.GAPDH enzymatic activity among cell fractions of WT and Δ <i>gapA</i> - <i>pmetK</i> strains	107

Figure 3-11 A, B. Western blot results of subcellular localisation of GAPDH in cell fractions of <i>C. jejuni</i>	109
Figure 4-1. Intact cell GAPDH activity of wild type and mutated <i>gapA C. jejuni</i> strains in different iron conditions.....	118
Figure 4-2 A, B. Assessment of GAPDH protein expression of <i>C. jejuni</i> strains by Western blot in high and low iron conditions.....	119
Figure 4-3 A, B. The growth curve assay conducted in iron restricted medium MEM α	121
Figure 4-4. The growth assay of mutated <i>gapA C. jejuni</i> and wild type strains conducted in 0.27 μ M ferri- Lf supplemented MEM α	123
Figure 4-6 A, B. Growth assay of <i>C. jejuni</i> WT in the presence and absence of polyclonal anti-GapA antibody with 0.27 μ M human ferri-Lf.	129
Figure 4-7. Growth assay of wild-type NCTC 11168 in different titrations of polyclonal anti-GapA antibody with 0.27 μ M human ferri-lactoferrin in MEM α medium.	131
Figure 4-8 A, B, C, D. Western blot analysis of binding assay between anti-GapA pre-incubated <i>C. jejuni</i> with ferric-Lf.....	133
Figure 4-9. Purification of recombinant cjGAPDH protein expressed with 6xHis affinity tag. 135	
Figure 4-10 Far Western blot analysis of GapA binding with Lf iron binding proteins.	137
Figure 5-1 A, B. The Structure of cjGAPDH.....	143
Figure 5-2. Strategy applied in site-specific mutagenesis of <i>gapA</i> gene.....	145
Figure 5-3 A, B. Overexpression and purification of C150S-GAPDH protein.	147
Figure 5-4. The enzymatic activity of recombinant purified C150S-cjGAPDH mutated protein in comparison with recombinant purified cjGAPDH.....	149
Figure 5-5 A, B. The CD spectrum of cjGAPDH proteins.	151
Figure 5-6. Clarification of producing hetero-merodiploid and Cys- Δ gapA reverted <i>C. jejuni</i> strains.	154
Figure 5-7. Growth curve assay of hetero-diploids, <i>gapA</i> mutated and wild strain <i>C. jejuni</i> NCTC 11168.....	156
Figure 5-8. Relative RT-qPCR results of <i>gapA</i> gene in new <i>C. jejuni</i> strains.	159
Figure 5-9 A, B. The assessment of GAPDH expression.	160
Figure 5-11 A, B, C. The growth curve assay of mutated <i>gapA C.jejuni</i> and wild type strains conducted in low concentrations of lactoferrin.	164

Figure 5-12 A, B, C, D. Western blot analysis of binding assays between <i>C. jejuni</i> with lactoferrin.....	167
Figure 6-1. Proposed model of role of cjGAPDH in iron uptake from ferric-Lf.....	179

Abbreviations

Amp	Ampicillin
Apo-Lf	Apo-lactoferrin
Apo-Tf	Apo-Transferrin
APS	ammonium persulphate
ATP	adenosine triphosphate
bp	base pair
BSA	Bovine Serum Albumin,
C°	degrees Celsius
cDNA	complementary DNA
c.f.u	Colony forming unit
CJIE1	<i>Campylobacter jejuni-integrated elements</i>
cm	centimetres
Cm	chloramphenicol
dATP	deoxyadenosine triphosphate
dCTP	deoxycytidine triphosphate
ddH ₂ O	double distilled H ₂ O
DEPC	diethyl-pyrocabonate
dH ₂ O	distilled H ₂ O
DNA	deoxyribonucleic acid
dNTPs	deoxyribonucleotide triphosphates
DTT	Dithiothreitol
EDTA	ethylenediaminetetraacetic acid
EHEC	Enterohaemorrhagic <i>Escherichia coli</i>
EPEC	Enteropathogenic <i>Escherichia coli</i>
FBP	fructose-1,6-bisphosphate

<i>pdfxA</i>	medium expression level promoter
Fe	iron
Fe ⁺²	Ferrous iron
Fe ⁺³	Ferric iron
Ferric-Lf	Ferric-lactoferrin
Ferric-Tf	Ferric-lactoferrin
FeSO ₄	Ferrous sulphate
g	gram
G3P	glyceraldehyde-3-phosphate
GAPDH	glyceraldehyde-3-phosphate dehydrogenase
IPTG	Isopropyl β-D-1-thiogalactopyranoside
Kan	kanamycin
kb	kilobase
kDa	kilodalton
l	litre
IL-10	Interleukin-10
LbpA	Lactoferrin binding protein A
LbpB	LbpB Lactoferrin binding protein B
Lf	Lactoferrin
LOS	Lipooligosaccharides
LuA	Lysogeny agar
LuB	Lysogeny broth
M	molar
MEMα	Minimal Essential Medium Alpha
<i>pmetK</i>	Low expression level promoter
mg	milligram

MHA	Mueller-Hinton Agar
MHB	Mueller-Hinton Broth
min	minute
ml	millilitre
mM	millimolar
MOMP	major outer membrane protein
mRNA	messenger RNA
NAD(H)	nicotinamide adenine dinucleotide (reduced)
NADP(H)	nicotinamide adenine dinucleotide phosphate (reduced)
NCTC	National Collection of Type Cultures
ng	nanogram
Ni-NTA	Nickel-charged nitriloacetic acid
nm	nanometer
OD	optical density
ORF	Open reading frame
PAGE	poly-acrylamide gel electrophoresis
PBP	Periplasmic binding protein
PBS	phosphate buffered saline
PCR	polymerase chain reaction
PK	Proteinase K
PNAACL	Protein and Nucleic Acid Chemistry Laboratory
<i>pporA</i>	High expression level promoter
PV	phase variation
PVDF	Polyvinylidene fluoride
RBS	ribosomal binding site
RNA	ribonucleic acid

ROS	reactive oxygen species
rRNA	ribosomal RNA
RT-PCR	Reverse transcription PCR
SdaA	Serine dehydrogenase
SDS	sodium dodecyl sulphate
spp.	Species
TAE	Tris base, acetic acid and EDTA containing buffer
TbpA	Transferrin binding protein A
TbpB	Transferrin binding protein B
TCA	cycle tricarboxylic acid cycle (Krebs cycle)
TEMED	N,N,N',N' - tetramethylethylenediamine
Tet	tetracycline
Tf	Transferrin
U	unit
µg	microgram
µl	microlitre
µM	micromolar
UV	ultraviolet
V	volt
VAIN	Variable atmosphere incubator
VNC	Viable-non-culturable
v/v	volume/volume
w/v	weight/volume
x g	times gravity
X-Gal	5-bromo-4-chloro-3-indolyl-β-D-galactosidase

Chapter 1. Introduction

1.1 Introduction

Campylobacter jejuni subsp. *jejuni* (referred to as *C. jejuni* throughout this thesis) belongs to the epsilon class of the phylum, proteobacteria, and is a poorly characterised bacterium of medical importance. Gastroenteritis is the most common disorder observed in humans infected with *C. jejuni* (Blaser, 1997). Indeed, *C. jejuni* causes the majority of human *Campylobacter* food-borne infections and therefore the work described in this study focuses on this species.

C. jejuni needs iron to cause disease, it is one of the most important factors in the colonization of the gut by *C. jejuni* (Hermans *et al.*, 2011). Although iron is restricted in the host by binding with proteins such as transferrin (Tf) and lactoferrin (Lf), bacteria have evolved several mechanisms to combat low iron levels. The classical cytoplasmic housekeeping enzyme, glyceraldehyde 3-phosphate dehydrogenase (GAPDH) has been reported as an important factor in iron acquisition from iron binding proteins among different organisms. However, the role of GAPDH in *C. jejuni* was not identified. The present study was established in order to investigate and characterise this function.

1.2 Historical background and general aspects of *C. jejuni*

The first report of *Campylobacter* is believed to have been written in 1886 by Theodor Escherich, (Butzler, 2004). The word “*Campylobacter*” originates from the Greek campylo (“curve”), and bacter (“rod”), the species name *jejuni* was first presented by Jones *et al.* (1931) when they isolated a bacterium they called *Vibrio jejuni* (originally found in the jejunum), from calves with dysentery (Jones *et al.*, 1931).

The culture of *Campylobacter* was first successfully achieved in the early 1900's, by John MacFadyean and Stewart Stockman from the foetal tissue of aborted sheep and they referred to the isolate as “vibrios” (Butzler, 2004). However, the fastidious nature of *Campylobacter* made it difficult to have pure culture of *Campylobacter* from faeces. This problem was overcome by the utilization of a filtration technique that permitted the smaller and highly motile *campylobacter* to pass through a 0.65 µm filter, other small organisms passed through the filter were inhibited by growth on selective media (Butzler, 2004).

Development of selective culture methods have led to isolation and identification of *campylobacters* more frequently, introduction of a selective medium containing

vancomycin, polymyxin B and trimethoprim allowed routine isolation of *Campylobacter* in numerous microbiology laboratories around the world (Ketley, 1997). *C. jejuni* and *Campylobacter coli* are the most frequently reported species in human disease (Cody *et al.*, 2013). After its successful isolation from stools in the 1970s (Ketley, 1997, Butzler, 2004), *C. jejuni* has rapidly become the most commonly recognised cause for bacterial gastroenteritis in humans (Butzler, 2004). It has been reported that *C. jejuni* causes around 90% of human infections, whereas *C. coli* around 8% and other species represent about 2% of all human *Campylobacter* infections, the disease produced by *Campylobacter* is called campylobacteriosis (Cody *et al.*, 2013).

1.2.1 Morphology and growth characteristics of *C. jejuni*

C. jejuni is a member of the bacterial 16S rRNA super family VI (Ketley and Konkel, 2005). Gram-negative, non-spore forming, flagellated bacteria forming curved, S shaped or spiral rods, it is 0.2 – 0.8 µm wide and 0.5 – 5.0 µm long. *C. jejuni* is moved by a characteristic rotating movement often referred to as rapid corkscrew-like motion, using their unipolar or bipolar flagella (Butzler, 2004). Figure (1.1) shows this bacteria with bipolar flagella (Gaynor *et al.*, 2004) *C. jejuni* colonises the intestinal tract of avian species, and is thermophilic, capable of growth between 34 and 44°C but the optimal growth is at 42°C (Ketley, 1997).

C. jejuni can survive in a viable-but-non-culturable (VBNC) state following exposure to unfavourable conditions such as a poor supply of nutrients or at atmospheric oxygen concentrations. The shape of bacteria becomes coccoid, and growth cannot be detected by routine culturing methods. This process might be regulated and genetically determined process (Ikeda and Karlyshev, 2012). Subsequently, the disease could nevertheless be produced if suitable conditions are experienced (Jackson *et al.*, 2009). On the other hand, recent studies demonstrate that virulence genes in VBNC cells can be expressed and the production of metabolites carried out normally. In *C. jejuni* ATCC 33291 and *C. jejuni* 241, the expression of the Cad F in VBNC cells was detected by RT-PCR, and the *C. jejuni* VBNC population maintained an ability to adhere to intestinal cells (Zhao *et al.*, 2017).

C. jejuni grow in the guts of avian and human hosts under microaerobic conditions. (3-15% O₂, 3-10% CO₂ and ~85% N₂), therefore, it utilises alternative electron acceptors such

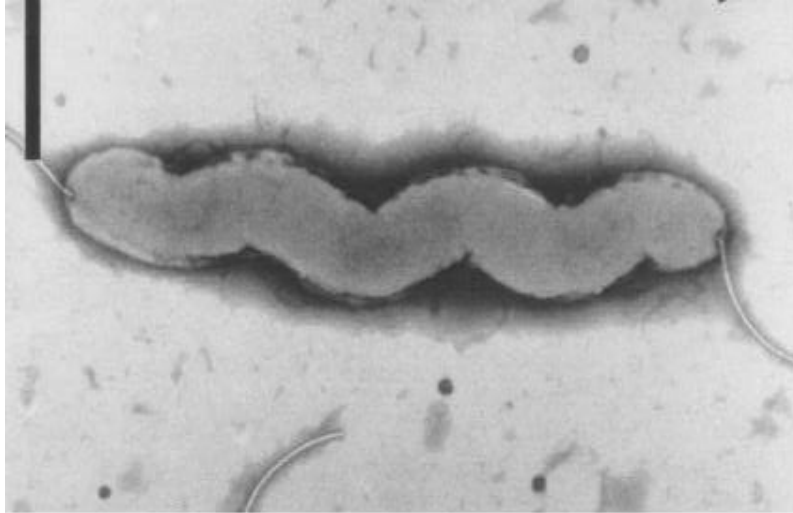


Figure 1-1. Electron micrograph of *C. jejuni*.

The bacterium in the picture is *C. jejuni* NCTC 11168; the strain used in this research. The typical spiral rod shape is recognised, the bipolar flagella; each flagellum is extended from the both poles of the cell. The flagella is not only important for movement, it is also important for intestinal colonisation by *C. jejuni*. The picture is taken from Gaynor *et al.* (2004).

as fumarate and nitrate for respiration (Guccione *et al.*, 2008). Additionally, *C. jejuni* utilises oxygen as the terminal electron acceptor (Sellars *et al.*, 2002). *C. jejuni* is capable of switching between aerobic and anaerobic metabolic systems by regulating key enzymes that participate in respiration (Mendz *et al.*, 1997).

1.2.2 Physiological and biochemical perspectives

Greater understanding of *C. jejuni* metabolism should result in deeper understanding of pathogenesis of this unique enteropathogenic bacterium and consequently research on this subject is ongoing. It has been reported that *C. jejuni* usually acquires energy from amino acids or tricarboxylic acid cycle intermediates (Crushell *et al.*, 2004). Iron uptake, which will be discussed later (section 1.3), is a very important process in survival and pathogenicity of *C. jejuni*. A better understanding of these basic physiological features of *C. jejuni* is important in order to develop new antimicrobial or vaccine targets.

The amino acids have a vital impact on the central metabolism of *C. jejuni*, amino acids are also important to colonisation of *C. jejuni* in the gut of the chicken. Certain amino acids can be used in low levels to support the growth of *C. jejuni*, these amino acids are serine, aspartate, asparagine sequentially in this order (Stahl *et al.*, 2012, Hofreuter *et al.*, 2008). In addition, *C. jejuni* can catabolise proline only under depletion conditions of other amino acids (Hofreuter, 2014). L-serine is a preferred amino acid for growth of *C. jejuni*, and *sdaA* encodes serine dehydratase (SdaA) which converts serine to pyruvate and ammonia (Stahl *et al.*, 2012). The *sdaA* mutant resulted in insufficient colonisation of chicken gut (Guccione *et al.*, 2008). However, *in vitro* experiments showed that the *sdaA* mutant was able to grow similar to wild type which might propose that the catabolism of L-serine is not vital for the growth of *C. jejuni*, but instead it is essential for colonization *in vivo* (Velayudhan *et al.*, 2004).

Catabolism of aspartate and glutamate has been suggested to be essential for the metabolism of *C. jejuni*, both amino acids are transported by a periplasmic binding protein (Peb1 uptake system). Glutamate is converted into aspartate, the produced aspartate is then deaminated to produce fumarate by reactions carried out by *aspB* (Cj0762c) and *aspA* (Cj0087) respectively (Guccione *et al.*, 2008). At the end, fumarate will be fed into TCA (Stahl *et al.*, 2012).

Unlike many other bacteria, *C. jejuni* lacks pathways, which other bacteria utilise for nutrient metabolism, for example, the glycolysis, Entner-Doudoroff, and pentose

phosphate pathways (Stahl and Stintzi, 2011). *C. jejuni* cannot ferment or oxidise carbohydrates and instead it derives its carbon from amino acids. There are two reasons behind this. First, *C. jejuni* cannot import glucose and galactose as it lacks appropriate transporters to take up these sugars. Additionally, genes encoding key enzymes within the glycolytic pathway are missing. These enzymes include glucokinase (Glc), an enzyme that facilitates phosphorylation of glucose to glucose-6-phosphate, and 6-phosphofruktokinase (6-PFK), which catalyses the phosphorylation of fructose-6-phosphate (F6P) to fructose-1,6-bisphosphate (F16BP) (Parkhill *et al.*, 2000, Hofreuter, 2014). Figure (1.2) illustrates the gluconeogenic reactions in *C. jejuni*. Nonetheless, it was proposed that *C. jejuni* may use glycerol-3-phosphate at the end of the glycolytic pathway as there is a glycerol-3-phosphate transporter system (GlpT) in strain 81-176 (Stahl *et al.*, 2012). Similarly, key enzymes were recognized in the non-oxidative part of the pentose phosphate pathway but the possibility of *C. jejuni* using this pathway for carbon and energy sources has been excluded (Stahl *et al.*, 2012). Interestingly, the early data of genomic sequencing project of *C. jejuni* indicate that the other carbohydrate metabolic pathways of *C. jejuni* were not annotated, therefore, *C. jejuni* has been considered completely asaccharolytic (Parkhill *et al.*, 2000). However, it has been recently indicated that several strains of *C. jejuni* can utilise both L-fucose and mucin as a substrate for growth, thus a novel L-fucose pathway (Cj0486/FucP) has been identified (Stahl *et al.*, 2012).

The typical biochemical reactions of *C. jejuni* include the reduction of fumerate to succinate, negative methyl red, acetoin, and indole production. *C. jejuni* reduces nitrate, and is positive for hippurate hydrolysis. Furthermore, enzymes expressed by *C. jejuni* such as superoxide dismutase (SOD), catalase, peroxidase, glutathione synthetase, and glutathione reductase may have an indispensable part in providing protection against oxygen toxicity (Crushell *et al.*, 2004). Nonetheless, the above mentioned physiological processes are so important to maintain *C. jejuni* survive in the intestinal niches of chicken and human. They collaborate to enable *C. jejuni* grow and multiply in order to manifest the clinical symptoms of Campylobacteriosis.

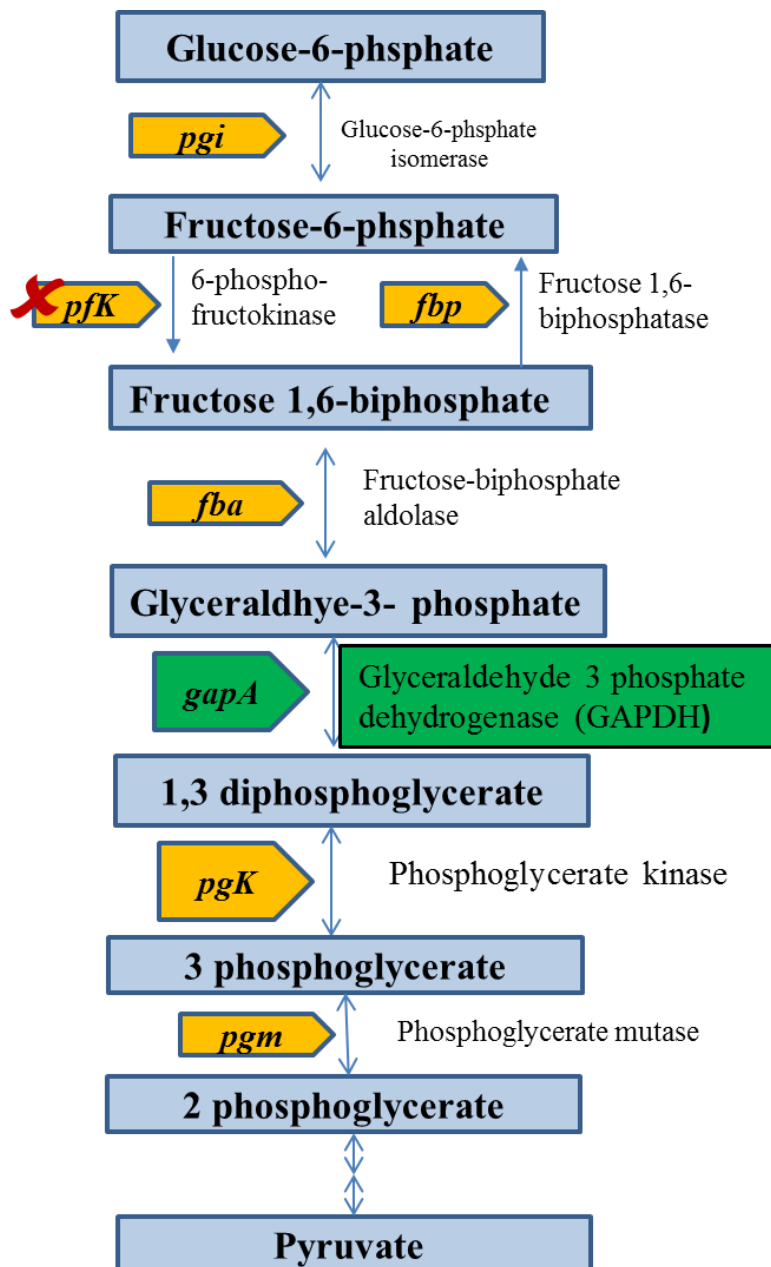


Figure 1-2. Outline of the gluconeogenic and anaplerotic reactions of *C. jejuni* NCTC 11168.

The red cross sign indicates that the *C. jejuni* genome lacks a homologue for 6-phosphofruktokinase, it means that there is no glycolysis pathway. However, all enzymes required for gluconeogenesis are present. The italic names in yellow arrows indicate the genes encoding the corresponding enzymes. Glyceraldehyde -3- phosphate dehydrogenase (GAPDH) is highlighted in green. This figure is drawn based on previously published data (Parkhill *et al.*, 2000, Velayudhan and Kelly, 2002, Kim and Dang, 2005).

1.2.3 The genetics features of *C. jejuni*

The determination of the complete genome sequence of *C. jejuni* strains and plasmids was one of the great achievements in *C. jejuni* research. Regarding the genomes of *C. jejuni* NCTC11168, 94.3% of the genome codes for proteins (Parkhill *et al.*, 2000). Generally, *Campylobacter* species have small a circular chromosome of 1,641,481 base pairs of AT rich DNA (30.6% G+C) which is expected to encode 1,654 proteins (Parkhill *et al.*, 2000, Ketley, 1997). Like the closely related bacteria, *Helicobacter pylori* (*H.pylori*), the genome of *C. jejuni* shows little organization into operons. The examples of operons and gene clusters in *C. jejuni* are ribosomal operon and gene clusters including LOS and EP biosynthesis (Parkhill *et al.*, 2000). Regarding sigma factors, *C. jejuni* is like *H. pylori* in that the genome contains only three predicted sigma factors (*rpoD*, *rpoN* and *fliA*) and the most *C. jejuni* promoters are regulated by RpoD (Wösten *et al.*, 2008).

The data of comparative genomic sequencing revealed a high degree of variability in certain regions of different strains relative to NCTC11168 strain, these include flagella, lipooligosaccharide (LOS), capsular polysaccharide (CPS), DNA restriction/modification loci and genes involved in respiratory metabolism (Parker *et al.*, 2006, Poly *et al.*, 2004, Poly *et al.*, 2005). Moreover, investigation of the genome sequence of *C. jejuni* strain RM1221 recognized four large genomic islands; *C. jejuni*-incorporated components (CJIEs1-4), which are not present in *C. jejuni* strain NCTC 11168 (Parker *et al.*, 2006). Other *C. jejuni* strains also have these islands (CJIEs1-4), but they demonstrate a high degree of variability (Parker *et al.*, 2006).

The integrated element, CJIE1, is probably encoding a Mu-like phage, it is situated in different chromosomal locations, possibly due to random insertion events, providing another mechanism to increase the genomic diversity of *C. jejuni* (Parker *et al.*, 2006). Other integrated elements (CJIE2 and CJIE4) might be phage related endonucleases, methylases or repressors whereas CJIE3 could be an integrated plasmid with 73% similarity to a *C. coli* mega plasmid (Fouts *et al.*, 2005, Parker *et al.*, 2006). Regarding *C. jejuni* strain NCTC 11168, there is only one inserted sequence within the genome and very few repeated sequences. Additionally, the NCTC11168 inserted sequence Cj0752 shares sequence similarity with *tnpB* (IS605) from *H. pylori* (Parkhill *et al.*, 2000).

Another feature of the *C. jejuni* genome is the presence of homopolymeric tracts of six or more G:C bases which can be subject to length variations among identical clones of *C. jejuni* (Parkhill *et al.*, 2000). These homopolymeric tracts are hypervariable regions due to

the potential for slipped strand miss pairing during DNA replication (Parkhill *et al.*, 2000). Therefore, homopolymeric tracts promote formation of an important process in certain *Campylobacter* spp genes, termed phase variation (PV). PV can be defined as a reversible switch between on/off of gene expression, resulting in variation in the levels of gene expression which might influence the adaption and virulence of bacteria (Bayliss, 2009). Another cause of PV is site-specific recombination, the alterations in the orientation of DNA sequences can change the positioning of promoters relative to genes (Parkhill *et al.*, 2000, Bayliss, 2009). Regarding *C. jejuni*, as poly G/C homopolymeric tracts are located within open reading frames, several genes might undergo PV (Bayliss *et al.*, 2012).

The majority of these homopolymeric tracts are intragenic having G/C contents of between approximately 8 and 13 repeats. This length polymorphism in repeat tracts of *C. jejuni* causes translational frameshift mutations, which prompt switching of expression between an on or off phase. PV enables bacteria to adopt the specific environmental niches; also, it could benefit the bacteria in host immune system evasion (Bayliss *et al.*, 2012, Parkhill *et al.*, 2000). The hypervariable sequences are mainly within the genes involved in flagellar modifications, LOS and EP biosynthesis. It suggests that these sequences are important in how the bacteria interact with their environment. Hence, these repeat tracts might be important in understanding the pathogenicity and the biology of *C. jejuni* (Parkhill *et al.*, 2000)

C. jejuni shares with other *Campylobacter* species a common pool of extrachromosomal elements. The conjugative plasmids, which carry chloramphenicol (Cm^r), kanamycin (Km^r), and/or tetracycline (Tc^r) antibiotic resistance genes, have similar distribution between *C. jejuni* and *C. coli* strains. However, there are considerable differences in size ranging from 45-50 kb with G+C content of 31-33 % (Dasti, 2007, Tenover *et al.*, 1985). Some of these plasmids are important in virulence of *C. jejuni*, particularly in the highly pathogenic strain *C. jejuni* 81-176 (Bacon *et al.*, 2000). Furthermore, the horizontal transfer of both plasmid and integrated elements of DNA occurs both *in vitro* and during colonization of the chicken (Young *et al.*, 2007). This transfer indicates that natural transformation could have an important role in genome plasticity and in the spread of new factors such as antibiotic resistance, even in the absence of selective pressure (Wassenaar and Blaser, 1999, Young *et al.*, 2007).

1.2.4 Antibiotic resistance

The medical importance of *C. jejuni* has been increased with the reporting of its resistance to different antibiotics. There is a strong relationship between the indiscriminate usage of antibiotics in animal production and emergence of resistance to antibiotics in *Campylobacter* species (Silva *et al.*, 2011). *Campylobacter* can acquire resistance determinants from both gram-positive and Gram-negative organisms, *Enterococcus* spp, which is a common commensal of the human and animal gastrointestinal tracts has apparently been able to exchange DNA with *Campylobacter* spp within this environment (Taylor and Courvalin, 1988). The *C. jejuni* is susceptible to nalidixic acid, ciprofloxacin, norfloxacin, and ofloxacin (Taylor and Courvalin, 1988), but it is intrinsically resistant to a number of antibiotics, including bacitracin, novobiocin, rifampin, streptogramin B, trimethoprim, vancomycin, and usually cephalothin.

The most recurring mechanism of antibiotic resistance in *C. jejuni* is synergy between antibiotic efflux and preventing the antibiotic reaching the cells by expression of MOMP protein (Iovine, 2013). The intrinsic resistance to novobiocin, bacitracin and vancomycin might be because absence of appropriate targets and/or low affinity binding to targets (Keo *et al.*, 2011). Regarding intrinsic resistance to trimethoprim, the different forms of dihydrofolate reductases which cannot be inhibited by trimethoprim are found in > 90% of *C. jejuni* (Gibreel and Sköld, 1998).

1.2.5 Protein secretion pathways of *C. jejuni*:

Gram-negative bacteria possess at least six different mechanisms to translocate proteins across the bacterial membranes (Konkel *et al.*, 2004). These systems were grouped based on their mechanism, composition, and evolutionary relationship. In fact, the systems are originally multiprotein complexes that allow regulated exchanges with the extracellular milieu. The secreted substrates fulfill various functions in processes such as nutrient uptake, motility, and to help during the colonization of host organisms (Green and Meccas, 2016). Different mechanisms and different sources of energy were utilised by these secretion systems to transport unfolded, partially folded, or fully folded and assembled proteins (Saier, 2006).

The most commonly-found secretion systems used to transport proteins across the cytoplasmic membrane in all domains of life are the general secretion, Sec, and twin arginine translocation, Tat, pathways (Natale *et al.*, 2008, Green and Meccas, 2016). The

Sec pathway primarily translocates proteins in their unfolded state while the Tat pathway primarily secretes folded proteins, most proteins transported by the Sec and Tat pathways remain inside of the cell, either in the periplasm or the inner membrane (Green and Meccas, 2016). However, Gram-negative bacteria can deliver the proteins from the cytosol across the outer membrane by means of other secretory systems (Yen *et al.*, 2002). Both the type I (T1SS; ABC), type III (T3SS; Fla/ Path), and type IV secretory systems (T4SS; Conj/Vir) can export proteins across both the inner and outer bacterial membranes in a single energy-coupled step (Saier, 2006). The type II secretory system (T2SS) exploits either Sec or Tat pathways to export proteins across the inner membrane, in addition to any one of several types of systems to transport proteins across the outer membrane (Yen *et al.*, 2002).

Regarding *C. jejuni*, the majority of the proteins secreted from this pathogenic bacteria have not yet been identified due probably to low levels of protein secretion under *in vitro* conditions (Christensen *et al.*, 2009). The secreted proteins of *C. jejuni* are collectively known as *Campylobacter* invasion antigens (Cia proteins) because they were found to be required for maximal invasion of intestinal epithelial cells by *C. jejuni* (Rivera-Amill *et al.*, 2001, Konkel *et al.*, 1999).

Secretory systems T3SS and T6SS were reported in different strains of *C. jejuni* to actively transport proteins across the membranes (Christensen *et al.*, 2009, Lertpiriyapong *et al.*, 2012). The T3SS is part of the flagellar apparatus of *C. jejuni* (Parkhill *et al.*, 2000). Once *C. jejuni* adheres to the host cell, it requires a functional flagellar apparatus to secrete Cia proteins (Konkel *et al.*, 1999, Rivera-Amill and Konkel, 1999). It has been demonstrated that the mutations in the basal body, hook, filament, and flagellar regulatory genes resulted in abolishing of Cia protein secretion, thereby the mutants become less invasive than wild-type strains (Fernando *et al.*, 2007, Christensen *et al.*, 2009).

The *C. jejuni* T6SS exerts crucial roles in host cell adhesion and invasion. The inactivation or down-regulation of the T6SS resulted in a reduction of adherence to and invasion of *in vitro* cell lines (Lertpiriyapong *et al.*, 2012). Furthermore, over-expression of a hemolysin co-regulated protein, which encodes a secreted T6SS component, significantly increase adhesion and invasion and probably increases the severity of the disease (Lertpiriyapong *et al.*, 2012).

1.2.6 Pathogenesis of *C. jejuni*

1.2.6.1 Sources of *C. jejuni* infections

C. jejuni is a major cause of bacterial human gastroenteritis in both developed and developing nations. The infection occurs mainly through handling or ingesting contaminated food, milk or water (Young *et al.*, 2007). *Campylobacter* species occur in the animal food chain of humans from the highest to the lowest economically developed cultures. In spite of being the most common causes of diarrhoea around the world, there are noticeable differences in the epidemiology of *Campylobacter* infections between developed and developing world. In the developed world, campylobacteriosis appears as bloody diarrhoea with mucus, and is often self-limiting. In the developing world, watery diarrhoea predominates, and infection is more frequent among children, which presumably immunising them against becoming infected as adults (Young *et al.*, 2007). Figure 1.3 shows the sources of infection and outcomes. The transmission of *C. jejuni* to patients occurs through ingestion of contaminated water, milk or food products; poultry is considered the most important source of infection (Sopwith *et al.*, 2003, Workman *et al.*, 2005). The skin of around 80% of commercially available chicken in the UK were contaminated with live thermophilic campylobacters (Corry and Atabay, 2001).

However, infection can be acquired from other sources such as environmental water sources (rivers, lakes), wild birds, domestic animals, contact with raw meat or consumption of undercooked meat or cross-contaminated food (Alter *et al.*, 2005, Workman *et al.*, 2005, Takahashi *et al.*, 2006). Regarding the infective dose of *C. jejuni*, ingesting as few as 500-800 bacteria may lead to prodromal symptoms (Ketley, 1997, Young *et al.*, 2007). The natural niche of *C. jejuni* is the intestinal tract of avian species, which can be colonised to high numbers.

The carriage rate of campylobacters in the intestines of chickens is $\sim 10^6$ to 10^7 cfu/g (Mead *et al.*, 1995). It was believed that chickens colonised with *C. jejuni* do not develop symptoms analogous to those observed in humans (Jacobs-Reitsma, 1995). Nonetheless, recent research indicates that *C. jejuni* infection may have substantial impact on animal health and welfare in intensive poultry production. Following infection of broilers by *C. jejuni* M1, significant changes in proinflammatory cytokines and chemokines were observed in the caeca of some breeds of broilers, with damage to gut mucosa, and diarrhoea (Humphrey *et al.*, 2014).

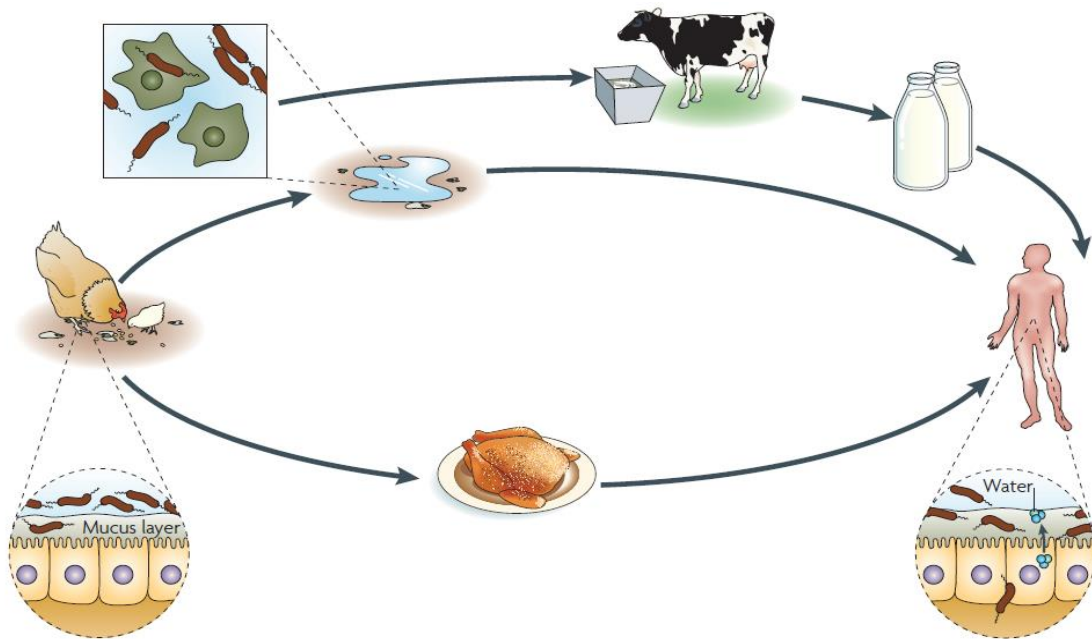


Figure 1-3. The sources and outcomes of *C. jejuni* infection.

Several environmental reservoirs can lead to human infection. *C. jejuni* colonizes the mucosal layer of chicken gastrointestinal tracts, and spreads between chicks via the faecal–oral route. It enters the water supply where it can associate with protozoans such as amoeba and form biofilms. Eventually *C. jejuni* can infect humans directly through different sources such as drinking water or consumption of contaminated milk or meat. In humans, *C. jejuni* can invade the intestinal epithelial layer, resulting in inflammation and diarrhoea. This figure is taken from (Young *et al.*, 2007).

More recently, among the strains of *C. jejuni*, there was a noticeable heterogeneity in the infection biology of *C. jejuni* in avian, mammalian and other models (Humphrey *et al.*, 2015). *C. jejuni* isolate 13126, sequence type 21 (ST21) revealed a greater ability to spread from the chicken gastrointestinal tract than other strains, the strain is also highly invasive in human epithelial cells and highly virulent in the *Galleria* infection model. Additionally, the dynamics and localisation of gastrointestinal colonisation between strains were different (Humphrey *et al.*, 2015). Indeed, such heterogeneity in infection biology of *C. jejuni* strains in the chicken and in humans might have considerable implications for control and could increase the risk to public.

New insights on *C. jejuni* localization within the gastrointestinal tract were obtained using immunofluorescent imaging of cecal and colonic cross-sections of the mouse model (Stahl and Vallance, 2015). The vast majority of *C. jejuni* cells were observed within a thin mucus layer lining the intestine and extending deep into the intestinal crypts (Stahl and Vallance, 2015). However, low numbers of this microbe were seen within the small intestine. More recently, Shang *et al.*, (2016) used infant rabbits to study colonisation of *C. jejuni* in a mammalian model. Interestingly, 24 h post-infection, this bacterium was recovered from all samples (100%) of cecum, colon, and jejunum samples, and there were fewer isolates from the duodenum and ileum (Shang *et al.*, 2016). In addition, *C. jejuni* was also recovered from the spleen, liver, kidney, and cardiac blood of experimentally infected rabbits which indicate a capability of this pathogen to produce systematic invasion (Shang *et al.*, 2016).

1.2.6.2 Colonisation and progression of *C. jejuni* Infection

C. jejuni colonise the host intestinal environment following consumption of contaminated food or water. The shape of the cell and the polar flagellum at one or both ends facilitate the entrance of bacterium to the mucus (Van Vliet and Ketley, 2001). It has been reported that *C. jejuni* can colonise chickens at very high numbers, up to 10^{10} CFU per gram of infected intestine (Young *et al.*, 2007). The mechanism by which *C. jejuni* colonizes the host is a multifactorial process, but it is not understood well. However, the knowledge about genes involved in *C. jejuni* colonization in chicks is increasing. Some cooperative functional networks such as iron metabolism/oxidative stress defence, which is important for colonization, are starting to be elucidated (Hermans *et al.*, 2011).

The polar flagella have been shown to be critical for intestinal colonization and invasion in *C. jejuni*, loss of flagella by mutation caused failure of colonisation and invasion (Yao *et al.*, 1994). The flagellum assists physical adherence (adhesion) to the epithelial cell as flagella mutants displayed reduction in adherence and invasion of epithelial cells (Van Vliet and Ketley, 2001). Due to the high motility of *C. jejuni*, chemotaxis might be an important factor in promoting *C. jejuni* migration toward favourable conditions, thus colonization of the intestinal mucosa. *C. jejuni* needs the intact gradient-sensing mechanism for successful chemotaxis, mutation in methyltransferase *cheB* and methyltransferase *cheR* involved in a methylation dependent chemotaxis pathway reduced the ability of *C. jejuni* to colonize the chick (Kanungpean *et al.*, 2011). The amino acids aspartate, cysteine, serine and glutamate, and the salts of the organic acids citrate, fumarate, α -ketoglutarate, malate, pyruvate and succinate also act as chemoattractants (Hugdahl *et al.*, 1988). However, the acquisition of essential nutrients might be not only important for survival and growth, it could be also important to the adherence of *C. jejuni* to the intestinal mucosal surfaces of the host cells.

The capability of *C. jejuni* to adhere and invade the epithelial cells of intestinal mucosa requires motility and de novo protein synthesis, in addition to host factors (Wooldridge and Ketley, 1997). As mentioned above, the flagellum is so important in colonisation, adhesion and invasion are dependent on both motility and flagellar expression (Van Vliet and Ketley, 2001). The various other adherence and invasion factors include CadF and PEB1 proteins are also important (Ziprin *et al.*, 1999). It has been suggested that CadF protein supports *C. jejuni* binding to fibronectin (Fn) on the host epithelium, the mutation in *cadF* resulted in 50% decrease in adhesion to human cells compared with the wild-type (Konkel *et al.*, 2005). The PEB1 protein is encoded by the *peb1A* locus, the adherence and invasion of *C. jejuni* to HeLa cells were significantly reduced by mutation of *peb1A*. This mutant also reduced the ability of *C. jejuni* to colonise in a mouse infection model (Pei *et al.*, 1998).

In addition, the mutated strain of *Campylobacter* invasive antigen/Cia proteins colonised chickens at approximately 1000-fold lower levels than wild-type strain (Biswas *et al.*, 2007). Other adhesins such as capsular polysaccharide (CPS) and lipooligosaccharide (LOS) are probably involved, the LOS mutant strains revealed marked decrease in translocation relative to the wild-type or complemented mutants (Javed *et al.*, 2012). Addition of chicken intestinal mucus to human epithelial cells shows that less *C. jejuni*

invasion was observed, which indicates that the chicken intestinal mucus probably has important role in the asymptomatic nature of chicken colonisation (Nachamkin *et al.*, 2000).

The invasion of epithelial cells can lead to the mucosal damage, which is associated with toxin secretion. *C. jejuni* like many Gram negative bacteria, produces Cytolethal Distending Toxin (CDT) (Bezine *et al.*, 2014), which is only verified toxin in *C. jejuni* (Dasti *et al.*, 2010). Invasion and CDT production induces a strong inflammatory response during infection which may damage epithelial organisation and causes gut ulceration (Ketley, 1997). The production of CDT triggers secretion of IL-8, a proinflammatory cytokine, induces influx of polymorphonuclear leukocytes (PMNLs) from the lamina propria in order to control bacterial spread (Pickett, 2000). Unfortunately, the strong immune response can also cause inflammatory lesions, allow bacteria accessing to the lamina propria resulting in more severe symptoms (Konkel *et al.*, 2000). However, the colonisation by *C. jejuni* in immune compromised mice was not affected by mutation of *cdtB* mutant but it impaired the invasion of bacterium into blood, spleen and liver tissues (Purdy *et al.*, 2000).

Other factors such as metabolism mechanisms may also have an impact on chicken colonisation (Lin *et al.*, 2003, Luo *et al.*, 2003). Availability of host iron is important in colonisation of *C. jejuni*, the role of iron in colonisation of *C. jejuni* will be discussed in later sections (1.3).

1.2.6.3 Clinical manifestations

C. jejuni infection commonly presents as an acute gastroenteritis, which is characterized by inflammation, abdominal pain, fever and diarrhoea. The incubation period that precedes the development of acute diarrhoea is 2–5 days and, although the disease is typically resolved in one week, symptoms can last for up to 2 weeks (Young *et al.*, 2007). Approximately 15% of patients might vomit or have stools containing occult blood (Skirrow, 2000). Regarding immune-compromised or elderly patients, *C. jejuni* infection can cause bacteraemia in < 1% of cases, in particular among the patients experienced diarrhoea (de Guevara *et al.*, 1994).

Importantly, the capability of binding with fibronectin enabled *C. jejuni* to invade other tissues leading to serious complications such as meningitis, endocarditis, hepatitis, cholecystitis, osteomyelitis, pancreatitis, splenic rupture and septic abortion (Monteville

and Konkel, 2002, Monselise *et al.*, 2004). In relation to complications of *C. jejuni* infection, other severe conditions such as arthritis, Reiter's Syndrome, Guillain-Barré syndrome (GBS) and Miller Fisher Syndrome (MFS) are associated. The risk of developing GBS following an episode of *C. jejuni* gastroenteritis is actually quite low, 1 of 3285 patients with *C. jejuni* enteritis developed GBS (McCarthy and Giesecke, 2001). However, the neurological disorders due to *C. jejuni* incidences have major effect on the morbidity and the socioeconomic status worldwide.

C. jejuni has been reported to be responsible for an average of 30- 40% of GBS cases (Nachamkin *et al.*, 2002). However, there are several factors that might be involved in developing this neuropathy disorder after *C. jejuni* infections such as LOS of *C. jejuni*, some host factors such as human leukocyte antigens (HLA) class II molecules, IgG Fc receptors (Fc R), cytokines (TNF-alpha), and matrix metalloproteinase- (MMP-) 2 and MMP-9 are risk factors for the development of GBS post-*C. jejuni* infections (Nachamkin *et al.*, 2002, Yuki and Odaka, 2005, Nyati and Nyati, 2013), LOS has been considered a crucial risk factor, the molecular mimicry between LOS of *C. jejuni* and ganglioside backbone of human; glycosphingolipids occur especially on the cellular surfaces of neuronal cells, can induce the immune system to produce anti-LOS antibodies which attack own cells gangliosides rather than *C. jejuni* and causing a paralytic neuropathologic autoimmune disease (Young *et al.*, 2007).

1.3 Iron and *C. jejuni*

1.3.1 The importance of iron

Iron is one of the important nutrient requirements for bacteria (Elli *et al.*, 2000). Iron participates in many vital biological activities such as photosynthesis, methanogenesis, hydrogen production and consumption, trichloroacetic acid (TCA) cycle, gene regulation and DNA replication (Andrews *et al.*, 2003, Faraldo-Gómez and Sansom, 2003, Schaible and Kaufmann, 2004). Table 1-1 summarises the biological importance of iron in different biological processes in the cell. Unlike other elements such as phosphate, potassium and magnesium, iron is not freely available in the host environment. Iron exists usually in two main forms; either a reduced, ferrous form (FeII) or an oxidised, ferric form (FeIII).

The ferric form is the oxidised and abundant form of iron under the oxidation conditions of the environment and, at physiological pH, most ferric iron is biologically unavailable and restricted for up-take by bacteria due to its low solubility (Ratledge and Dover, 2000). This results in an extreme reduction of freely available iron which was stated as 10^{-18} M (Andrews *et al.*, 2003). Therefore, microorganisms may be subject to conditions of severe iron limitation. To overcome this insolubility and availability problem, a number of iron binding proteins and transport processes have been developed by the bacteria to transfer the required Fe^{+3} to the cells. With regards to *C. jejuni*, iron is crucial for several biological processes. Like other bacteria, *C. jejuni* has evolved strategies to scavenge iron from the environment. To date, six different systems of iron uptake have been identified in *C. jejuni* (Miller *et al.*, 2009).

1.3.2 Iron uptake systems in *C. jejuni*

C. jejuni evolved six systems to capture iron depending on iron source, it was known that *C. jejuni* cannot synthesize siderophores but it is capable of using exogenous siderophores as an iron source (Pickett *et al.*, 1992). Figure 1-4 illustrates these systems. Three of these systems are siderophore transporters and include enterochelin, ferrochrome and rhodotorulic acid transporters, two for host iron such as haem and transferrin and one system for the ferrous iron. Apart from ferrous iron system, that diffuses readily through the general porins, all other systems are typically linked with surface ligand-gated porins which work as a specific outer membrane receptor protein. These systems have other components such as periplasmic binding protein and ABC transport system (Miller *et al.*, 2009).

1.3.2.1 Siderophore Uptake Systems

Siderophores (from the Greek: “iron carriers”) are defined as relatively low molecular weight molecules, bind and transfer iron in microorganism (Neilands, 1995). As mentioned above, siderophore production systems have not been characterised in *C. jejuni* in spite of the ability of this pathogen to utilise exogenous siderophores as sources of iron. This fact has been supported by no annotation of siderophore biosynthesis genes within the genomes of *C. jejuni* NCTC 11168, RM1221 and 81-176 (Parkhill *et al.*, 2000, Fouts *et al.*, 2005). These siderophores include enterochelin, ferrochrome, Aerobactin, and rhodotorulic acid (Miller *et al.*, 2009).

Table 1.1 Summary of the importance of iron to microorganisms

Affected Area	Effects	The Reference
Cell structure	Iron deficiency: growth inhibition, decrease in RNA and DNA synthesis, inhibition of sporulation.	(Schaible and Kaufmann, 2004)
Process of metabolism	tricarboxylic acid cycle, electron transport, oxidative phosphorylation, nitrogen fixation, aromatic biosynthesis.	(Andrews <i>et al.</i> , 2003)
Metabolic products	Examples of the products regulated by iron: porphyrins, toxins, vitamins, cytochromes, pigments, DNA and RNA synthesis	(Faraldo-Gómez and Sansom, 2003)
Enzymes (oxidoreduction, O₂ transport)	e.g: Peroxidase, superoxide dismutase, nitrogenase, hydrogenase, glutamate synthase.	(Andrews <i>et al.</i> , 2003, Riordan, 1977)

1.3.2.1.1 Ferric-Enterochelin

Enterochelin, also known as Enterobactin, is produced primarily by Gram-negative bacteria, and is perhaps the best understood siderophore. It has been considered to have the strongest siderophore to ferric ion (Fe^{+3}) binding affinity ($K = 10^{52} \text{ M}^{-1}$) (Dertz *et al.*, 2006). *C. jejuni* can utilise ferri-enterochelin to acquire iron via TonB-dependent, outer membrane receptor protein (OMRP) CfrA (Cj0755), and the binding-protein dependent inner membrane ABC-transporter system encoded by *ceuBCDE* (Parkhill *et al.*, 2000, Miller *et al.*, 2009).

The mutated strains of *C. coli* in this system revealed failure of utilising enterochelin as an iron source (Park and Richardson, 1995). In addition, the *cfrA* gene is also important in acquisition of iron from Ferrienterochelin. The *cfrA* is responsible for an outer membrane ferric enterobactin receptor, the *cfrA* mutant *C. jejuni* NCTC 11168 strain was demonstrated to be unable to grow when supplied with ferri-enterochelin as sole iron source (Palyada *et al.*, 2004).

1.3.2.1.2 Ferrichrome

Ferrichrome is a cyclic hexa-peptide that has been found to be produced by fungi of the genera *Aspergillus*, *Ustilago*, and *Penicillium* (Emery and Neilands, 1961). It is composed of three glycine and three modified ornithine residues with hydroxamate groups, Ferrichrome binds with iron atoms (Fe^{+3}) forming Ferrichrome siderophore (Krewulak and Vogel, 2008, Braun and Hantke, 2011, Emery and Neilands, 1961). *C. jejuni* strain M129 was shown to have the capability to utilise ferrichrome, and this was linked to an 80 kDa protein expressed under low iron conditions (Galindo *et al.*, 2001). This protein is encoded by an operon of three open reading frames (ORF); *cfhuABD*

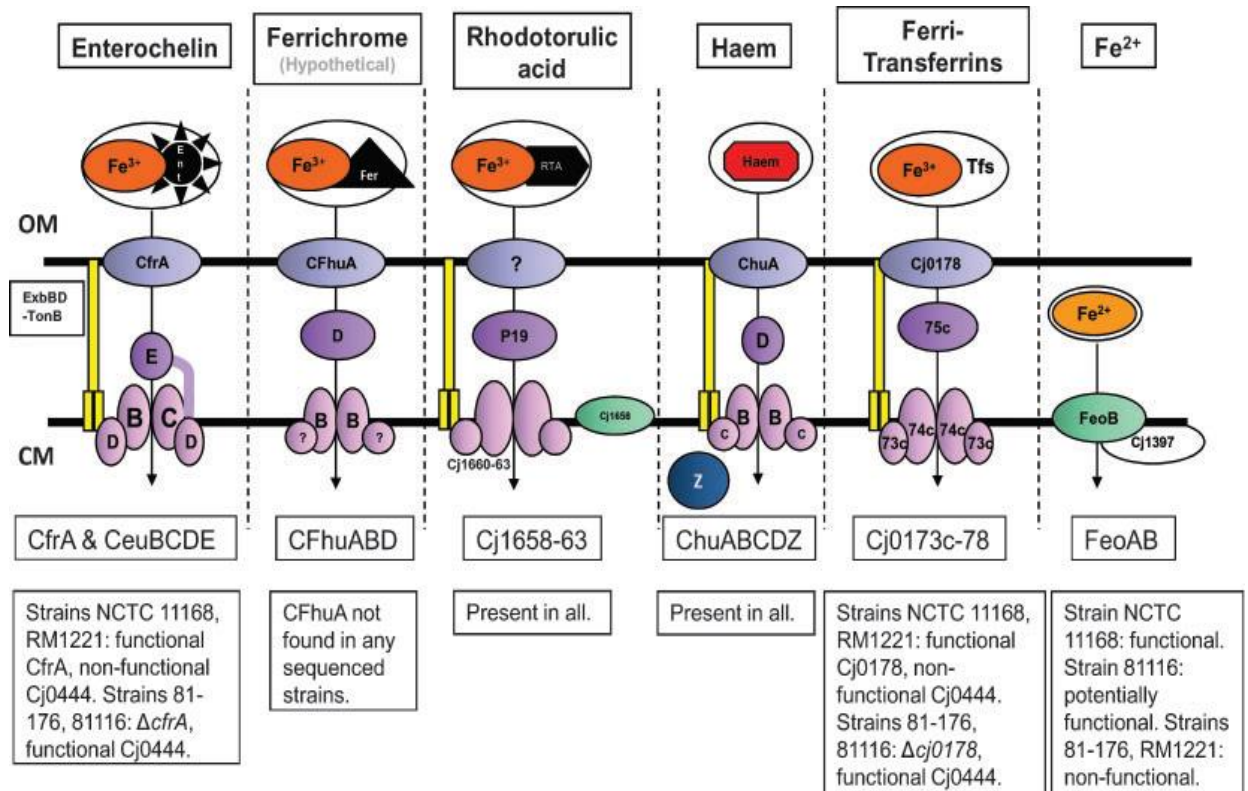


Figure 1-4. Iron uptake systems in *C. jejuni*.

OM is outer membrane and CM is cytoplasmic membrane, most of these systems are composed of an outer membrane receptor except rhodotrulic acid and ferrous iron systems. They also contain periplasmic binding protein and ABC transport system. ExbBD-TonB is energy transduction system for iron transportation across the membrane. (Miller *et al.*, 2009).

which displayed homology to a ferrichrome uptake system of *E. coli* and *Pseudomonas aeruginosa* (*P. aeruginosa*). However, this operon does not have homologue in any of the sequenced *Campylobacter* strains (Galindo *et al.*, 2001, Parkhill *et al.*, 2000, Hofreuter *et al.*, 2008). Additionally, the function of this protein was not confirmed among the strains which possess them (Galindo *et al.*, 2001).

1.3.2.1.3 Rhodotorulic acid

Rhodotorulic acid is hydroxamate siderophore which is a high-affinity chelating agent for ferric iron, produced by bacterial and fungal phytopathogens for scavenging iron from the environment (Krewulak and Vogel, 2008). Recently, it was shown that *C. jejuni* can utilize fungal hydroxamate siderophores and the Cj1658-Cj1663 locus of the *C. jejuni* NCTC 11168 was suggested to play a role in iron uptake (Xu *et al.*, 2015, Miller *et al.*, 2009). Regarding this genomic locus, *cj1658* encodes the inner membrane-associated protein that does not resemble a classical TonB-dependent OMRP, whereas *Cj1659* encodes the putative periplasmic siderophore-binding protein, and was designated P19 (Janvier *et al.*, 1998). The 19 kDa periplasmic protein (P19) was first identified by purification from *C. jejuni* 81-176 (Janvier *et al.*, 1998). However, it appears to be conserved between sequenced species of *Campylobacter* (Chaudhuri and Pallen, 2006). The *Cj1661-Cj1663* genes demonstrate homology to the components of an inner membrane ABC transporter system (Parkhill *et al.*, 2000). Moreover, the Cj1658 and P19 homologues are found in *Yersinia pestis* (*Y. pestis*) on an iron-uptake pathogenicity island (Carniel, 2001). The mutation in *cj1658* or P19 genes of *C. jejuni* NCTC 11168 causes impairment of ferri-rhodotorulic acid utilisation for growth when supplied as the sole iron source (Stintzi *et al.*, 2008).

1.3.2.2 Haem utilisation

C. jejuni has the capability to utilise haemin, haemoglobin, haemin-haemopexin and haemoglobin-haptoglobin as iron sources (Pickett *et al.*, 1992). A 70 kDa *Campylobacter* Haemin Uptake protein A (or ChuA) was identified as the outer membrane haemin/haemoglobin receptor (Van Vliet *et al.*, 1998). An undefined chemically mutagenised *C. jejuni* strain that lost the ability to utilise haem containing iron sources, was found to no longer express the ChuA protein. However, in addition to the *chuA* gene, *C. jejuni* NCTC 11168 has other three genes arranged with *chuA* together in an operon. These genes are *chuA*, *chuBC*, and *D* which encode an ABC transporter, ATP binding

protein and a periplasmic binding protein respectively (Ridley *et al.*, 2006, Parkhill *et al.*, 2000). Mutation of *chuA* gene reduced the growth of *C. jejuni* significantly compared with wild type, this indicate that *chuA* is essential for growth on haemin/haemoglobin (Ridley *et al.*, 2006).

1.3.2.3 Ferrous Iron Uptake

Ferrous iron (Fe^{+2}) is soluble at neutral pH, therefore, it can be diffused in passive transport manner through the outer membrane and into the periplasm. In the gut, iron is sustained in the ferrous state under both low pH and reduced oxygen levels. Therefore, microorganisms need ferrous iron uptake system for successful colonisation of the gut (Lau *et al.*, 2015, Ge and Sun, 2012). In contrast to its ferric counterparts, much less is known about ferrous iron transport systems. The first ferrous iron uptake system to be described was the Feo system, which in *E. coli* K12 was identified using a series of ferrous iron transport mutants (Hantke, 1987). Later on, it was found that the Feo system is an operon consisting of three genes; *feoABC* (Hantke, 2003). The *feoA* gene encodes for a 75 residue hydrophilic protein of 8.4 kDa, while *feoB* encodes for a 773 residue polytopic transmembrane protein with a molecular weight of 84 kDa. The *feoC* (*yhgG*) gene encodes for a cytoplasmic protein consisting of 78 amino acids which is only present amongst γ -proteobacteria (Hantke, 2003)

The *C. jejuni* NCTC 11168 genome contains a *feoAB*-type operon (Parkhill *et al.*, 2000). The *cj1398* gene is an homologue of the *feoB* gene of *E. coli* with 29% identity, very close to a smaller gene (*cj1397*) which demonstrates limited identity (16%) to the *feoA* gene of *E. coli* (Parkhill *et al.*, 2000, van Vliet *et al.*, 2002). The initial work on *C. jejuni* M129 and F38011 strains mutated in *feoB* demonstrated no difference in growth compared with wild type, thus it was believed that the FeoB protein is not required for Fe^{+2} uptake in *C. jejuni* (Raphael and Joens, 2003). However, another study that examined the role of FeoB in *C. jejuni* NCTC 11168, 81-176 and ATCC 43431 was carried out by Naikare *et al.* (2006). The acquisition of Fe^{+2} reduced to half in mutants compared to wild type during growth. Additionally, the colonisation of mutants of the chicken caecum was also compromised, and intracellular survival decreased (Naikare *et al.*, 2006). Therefore, it has been suggested that *feoB* is essential in transport of Fe^{+2} in *C. jejuni* (Naikare *et al.*, 2006).

1.3.2.4 Iron uptake from Lactoferrin and Transferrin

1.3.2.4.1 General features of Lactoferrin and Transferrin

Lactoferrin and transferrin collaborate to control iron in the body fluids. Both are members of an iron binding protein family, glycosylated, bilobed and monomeric proteins that have similar N-terminal and C-terminal regions. Each region consists of four domains, N1 and N2, C1 and C2 separated by deep iron binding cleft (Baker and Baker, 2004). All Lfs and Tfs from different species share the same iron binding sites, one per lobe which enables them to bind tightly, but reversibly, two ions of Fe^{+3} ($k \sim 10^{20}$ M) (Baker, 1994). The binding of metal (Fe^{+3}) is concomitant with binding to two anions of bicarbonate, this allows coordination of the Fe^{+3} in the binding cleft (Abdallah and Chahine, 2000, Baker and Baker, 2004). Lf has the capability to bind iron down to at least pH 4, in addition the affinity of Lf for iron in the pH range between 6.4 and 6.7 is greater than that of Tf (Baker and Baker, 2004). Although Lf and Tf exhibit high amino acid identity (60%), only the denatured proteins can be immunologically cross-reacted (Van Snick *et al.*, 1974). All of these glycoproteins can occur in apo-form with no loaded iron or holo form with iron saturated. The structure of holo-Lf is shown for example in figure (1-5) (Baker and Baker, 2009).

LF is synthesised by mucosal epithelial cells in different mammalian species, including humans, cows, goats, horses, dogs and rodents. By use of molecular biology techniques, Lf has been observed in rainbow trout eggs, thus Lf can be produced by fish (González-Chávez *et al.*, 2009). Lf is 80 kDa protein found in milk and various external secretions, mucosal surfaces, and granules of neutrophils thus it has been considered as a protein with multiple activities (Yen *et al.*, 2011, Adlerova *et al.*, 2008). Some of these activities are associated with iron binding, antioxidant function for instance is due to iron binding feature that prevents formation of free radicals catalysed by iron (Baker and Baker, 2004). The finding of Lf in biological fluids such as milk, saliva and seminal fluids indicate its protective role in the innate immune system (Farnaud and Evans, 2003). The other functions of Lf include antimicrobial, anti-cancer, antioxidant, and anti-biofilm formation and anti-inflammatory functions (González-Chávez *et al.*, 2009, Farnaud and Evans, 2003, Adlerova *et al.*, 2008).

Tf is produced mainly from the liver, but other organs can also synthesize Tf including brain and testis (Sertoli cells). The main role of Tf is transporting iron from the site of

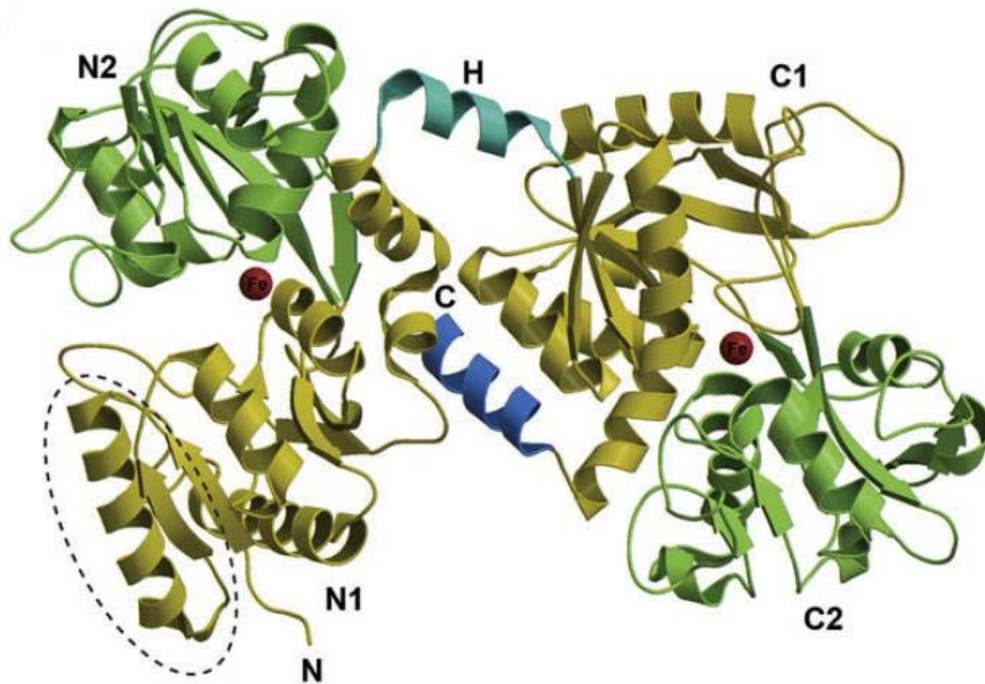


Figure 1-5. Structure of the iron-bound (holo) form of human Lf.

The C-lobe is on the right, whereas N-lobe is on the left. The N- and C-termini of the polypeptide chain are labelled N and C. The four domains are labelled N1, N2, C1, C2, with the N1 and C1 domains appearing in gold while the N2 and C2 domains are shown in green. Also, the two iron binding sites are shown with red sphere while the helix which connects the two lobes (H) and the C-terminal helix are shown in blue. The photo was taken from Baker and Baker (2009).

absorption (duodenum) or macrophages to erythropoietic bone marrow cells, and actively divided cells (Macedo and Sousa, 2008). The main function of Tf is transporting of iron; free iron can be toxic to the cells since it promotes formation of free radicals, which cause oxidative damage to the tissue. Thus, the primary role of Tf is therefore to transport iron safely around the body to supply growing cells (Gomme *et al.*, 2005).

1.3.2.4.2 Iron binding and release from Lf and Tf

Due to their high affinity to iron, the concentration of iron in extracellular compartments where Tf is the main glycoprotein is very low. This is also the case for mucosal surfaces at the site of infections due to the abundance of Lf. In both Tf and Lf, the ligands for iron binding are the same; these ligands comprise four amino acids (His253, Tyr92 and Tyr192, and Asp60). The arginine chain is responsible for binding the carbonate ion, which is crucial to stabilise iron-binding site (Baker, 1994, Baker and Baker, 2004, Adlerova *et al.*, 2008). Figure 1-6 shows iron binding sites in Tf and Lf. The binding of free or complex Fe^{+3} iron to the glycoprotein is presumably occurring in the open apo-form of the glycoprotein. According to spectroscopic studies and 3D structure, the binding of bicarbonate (CO_3^{-2}) occurs first in order to neutralise the positive charge of arginine residue (arg121) in N-lobe and associated helix. Also, it presents iron with four ligands (Tyr192, Tyr92 and the two CO_3^{-2} oxygens) clustered together on the internal surface of the N2 domain (Baker and Baker, 2004).

Regarding other ligands His253 and Asp60 on the other N1 domain, the dynamic of open apo-form through thermal fluctuations is an essential process. if it is iron free, then it simply open again, but in case of carrying iron it will be locked because of the iron atom encounters the other two ligands (Baker and Baker, 2004). The peptide that links the two lobes is important in understanding why does Lf retain iron to a much lower pH than Tf (3.0, compared with 5.5 for Tf) in spite of harbouring similar iron binding sites. While in Lf this linker peptide forms an α -helix, in all Tfs, and in ovo-Transferrin (ovo-Tf), it has a flexible, extended and irregular structure. It has been suggested that the helical linker in Lf allows a stronger interaction between the two lobes that stabilizes iron binding in the N-lobe delaying the onset of iron release due to low pH . On the other hand, there are several factors involved in releasing iron by ferric glycoprotein including; pH, temperature, receptor binding, lobe-lobe interactions, chelator and ionic concentrations (Qing-Yu *et al.*, 2000). However, it has been demonstrated that iron

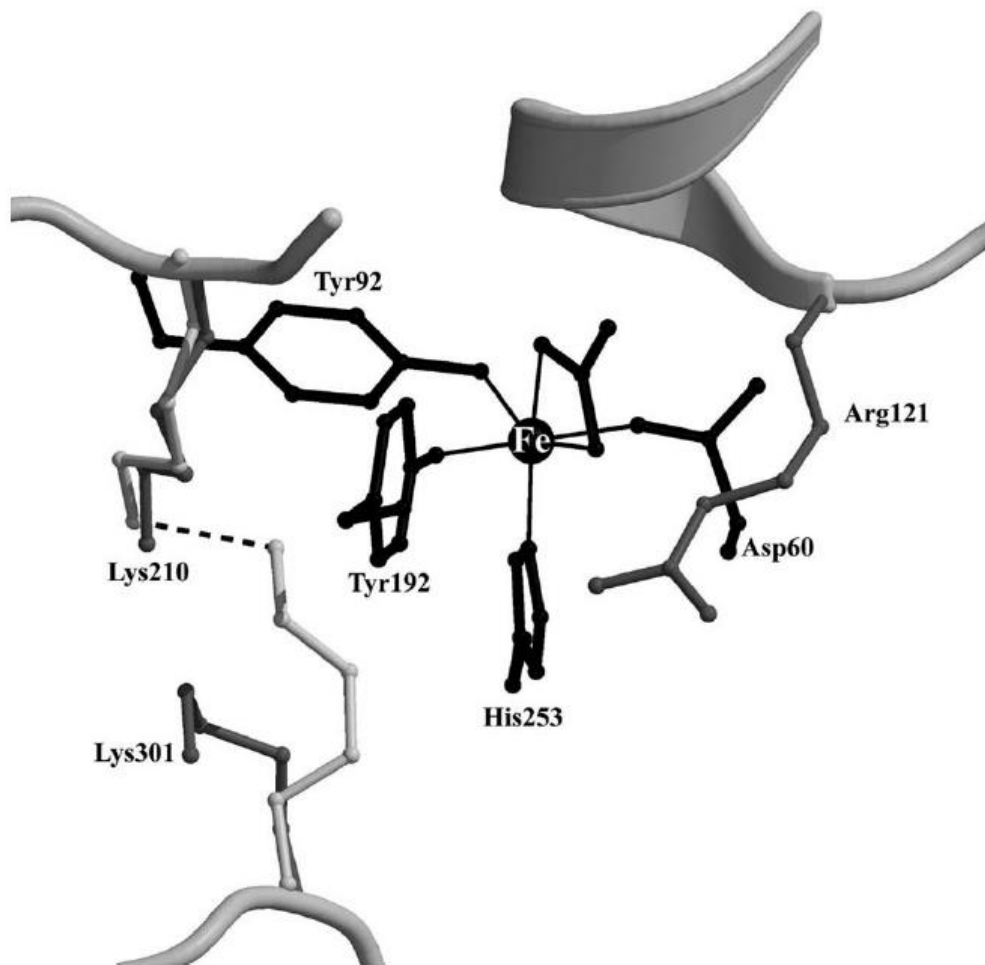


Figure 1-6. The canonical iron binding site found in lactoferrin and transferrin.

The residues of amino acids were given numbers as for the N-lobe of bovine lactoferrin. dotted line represents the two lysine residues that form a di-lysine pair, linked by hydrogen bonds, in transferrin and may modulate iron release. The figure is taken from Baker and Baker (2009).

release is delayed by chloride ion at neutral pH while the presence of chloride ions accelerates the release of iron under acidic conditions. Therefore, a combined pH–anion mechanism controls iron binding and release (Qing-Yu *et al.*, 2000).

1.3.2.4.3 Iron binding proteins in poultry:

For chickens, ovotransferrin is the only iron-binding glycoprotein found in plasma and egg white (Giansanti *et al.*, 2012). Structurally, there is strong similarity in the N-lobes of human lactoferrin, ovotransferrin and human serum transferrin (Adams *et al.*, 2003). Only a few amino acids are different and the general three dimensional structure is extremely conserved. Between chicken transferrin and ovotransferrin, the amino acid sequence is identical and the only differences were in the nature of the oligosaccharide groups linked to these proteins (Thibodeau *et al.*, 1978).

The chicken genome contains only one transferrin gene which is expressed in the liver and oviduct and is under the regulation of iron levels and steroid hormones (Dierich *et al.*, 1987). In respect to iron binding, the crystal structure of ovotransferrin shows that both iron binding sites are very similar to human transferrin and lactoferrin (Anderson *et al.*, 1989). An acidic pH could be the main factor for iron release from ovotransferrin. On the other hand, ovotransferrin, like other transferrins, can bind copper (II) ions (Fraenkel-Conrat and Feeney, 1950), in addition to several metals in the following affinity order: $\text{Fe}^{3+} > \text{Cr}^{3+}$, $\text{Cu}^{2+} > \text{Mn}^{2+}$, Co^{2+} , and $\text{Cd}^{2+} > \text{Zn}^{2+} > \text{Ni}^{2+}$ (Tan and Woodworth, 1969).

Similarly to human lactoferrin and transferrin, ovotransferrin is a multi-functional protein. It has been reported that ovotransferrin has antibacterial, antifungal and antiviral activity. Regarding antibacterial activity, some bacterial species are very sensitive to ovotransferrin such as *Pseudomonas* spp and *E. coli*, whereas others, such as some members of *Proteus* spp and *Klebsiella* spp, have been reported to be resistant (Valenti *et al.*, 1983). The exact mechanism of bacteriostatic or bactericidal effects is probably due to removal of iron from the medium, however, other non-identified complex mechanisms might be involved. In addition, other functions such as antioxidant activity, and antihypertensive subsidiary functions, were also reported in chicken ovotransferrin (CHANG *et al.*, 2006).

1.3.2.4.4 Utilisation of ferric-Lf and Tf by different microorganisms

The utilisation of Lf and Tf as iron source has been identified in different Gram positive and negative bacteria such as *Staphylococcus aureus* (*S. aureus*) (Modun and Williams,

1999), *Mycobacterium tuberculosis* (*M. tuberculosis*) (Boradia *et al.*, 2014a), *Escherichia coli* (*E. coli*) (Freestone *et al.*, 2000), *C. jejuni* (Miller *et al.*, 2008). Bacteria have developed several mechanisms to capture iron from Tf and Lf, which can be categorised into three strategies :

1- The proteolytic cleavage of the transferrin/lactoferrin molecule by surface associated and extracellular proteases. The cleavage at critical sites of iron binding or protein structure lead to the release of iron. This mechanism has been reported in several bacteria including *Pseudomonas aeruginosa* (*P. aeruginosa*) (Wolz *et al.*, 1994), *Vibrio vulnificus* (Okujo *et al.*, 1996) and *Porphyromonas gingivalis* (Lewis, 2010).

2- Reduction of the chelated iron by cell surface associated reductases. The reduction of Tf/Lf Ferric iron causes the dissociation of ferrous iron from Tf/Lf, this mechanism has been reported in Gram-negative organisms such as *E. coli*, *Ps. aeruginosa* and *Salmonella enterica* sv. Typhimurium (*S. Typhimurium*) (Vartivarian and Cowart, 1999).

3- Employing of specific outer membrane receptor complex system. This mechanism of iron uptake from Tf/Lf has been extensively described in the pathogenic *Neisseria; N meningitidis* and *N. gonorrhoeae*, it is a specific energy dependent uptake system (Schryvers and Stojiljkovic, 1999). Because this system is the subject of this research, therefore, it will be covered in this section. It is shown in figure 1-7, the process relies on specific outer membrane receptors to bind to the host's glycoproteins Tf and Lf, and transports iron across the outer membrane (Krewulak and Vogel, 2008).

Both Tf and Lf have approximately similar molecular weights (80 kDa) thus they are too large to pass through the bacterial outer membrane. Therefore, extra steps are required to remove iron from Tf or Lf at the external surface. Specific cell surface receptors that bind Tf and Lf were originally identified in *N. meningitidis*. The receptors consist of two proteins, Tf binding protein and Lf binding protein. each protein complex has two polypeptides: Tf binding protein A (TbpA) and Tf binding protein B (TbpB) for Tf; and for Lf binding protein A (LbpA) and Lf binding protein B (LbpB) for Lf (Krewulak and Vogel, 2008).

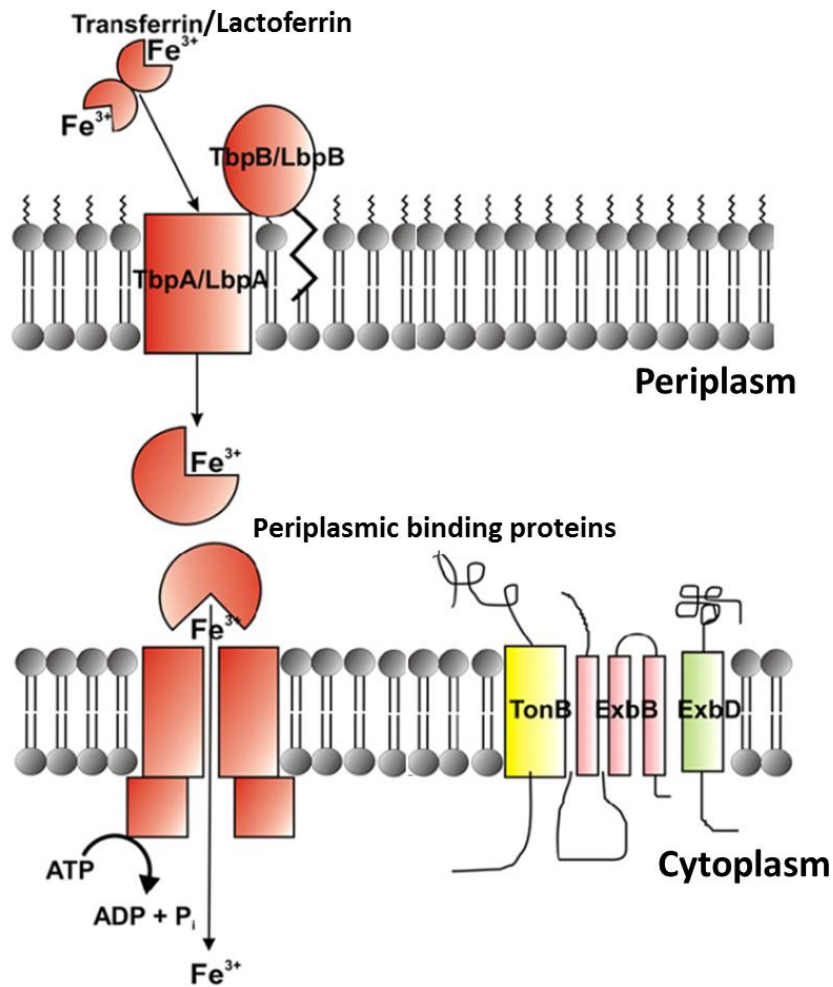


Figure 1-7. Schematic representation of iron uptake pathway from Tf/Lf in *N. meningitidis* and *N. gonorrhoeae*.

The pathway shows outer membrane receptor Tbp/Lbp, and periplasmic binding proteins. The process also requires an inner-membrane ABC transporter. The transport through the outer membrane receptor requires the action of the TonB system (TonB, ExbB, ExbD). The figure is adapted from (Krewulak and Vogel, 2008).

The LbpA mutated strain of *N. meningitidis* demonstrated a decreased ability to acquire iron and was unable to utilise lactoferrin as a sole iron source. While LbpB mutants also exhibit a reduced ability for iron uptake, they can still utilise lactoferrin as a sole source of iron (Lewis *et al.*, 1998).

The receptors Tbp and Lbp are 65 to 85 kDa, outer membrane associated with an N-terminal lipid anchor. TbpB could be the initial binding site for holo- transferrin that is assisted by subsequent binding to TbpA (Boulton *et al.*, 1999, Krewulak and Vogel, 2008). TbpA and LbpA are integral membrane proteins that are anticipated to have substantial surface loops which bind to transferrin and lactoferrin, respectively. This results in forcing the partition of the domains surrounding the iron binding sites to release iron (Schryvers and Stojiljkovic, 1999, Krewulak and Vogel, 2008).

The ExbBD-TonB complex provides energy to the receptors in order to transfer the released iron across a non-energized bacterial outer membrane (Biswas *et al.*, 1997). Binding of holo-Tf, for example, induces conformational change. The ExbBD-TonB complex transduces energy to the receptor, inducing iron release from Tf and opening of the gated pore; iron will be transported and apo-Tf is released. Once iron enters the periplasm, it is bound by the ferric ion binding protein A (FbpA). Here, it is not known whether this involves an interaction between TbpA/LbpA and FbpA (Schryvers and Stojiljkovic, 1999, Krewulak and Vogel, 2008). Iron is then moved to the cytoplasmic membrane where it is transported to the cytoplasm via the FbpB/FbpC cytoplasmic membrane transporters. FbpA is a 37-kDa periplasmic binding protein (PBP) found in the *Neisseraceae* and *Pasteurellaceae* families. Recently, the FBPs were identified in other Gram-negative bacteria such as *C. jejuni*. Interestingly, there is remarkable similarity between the structure of FbpA and the structure of one lobe of transferrin (Krewulak and Vogel, 2008).

1.3.2.4.5 Utilisation of ferric-Lf and Tf by *C. jejuni*

To date, *C. jejuni* does not have a well defined ferric-Lf or ferric-Tf iron uptake system. As previously mentioned, it was initially believed that *C.jejuni* is unable to use iron from Tf and Lf iron binding proteins (Pickett *et al.*, 1992). The genome of *C. jejuni* contains no significant homologues of *tbpA/B* or *lbpA/B* (Parkhill *et al.*, 2000). However, it has been reported that Cj0178 has some homology to the TonB-dependent outer membrane receptor protein of Tf- and Lf-binding systems (Ketley and Konkel, 2005).

Miller *et al.* (2008) demonstrated that *C. jejuni* can grow in an iron restricted medium supplemented with Tf or Lf as the sole iron source. The authors reported that the process of iron uptake is proximity-dependent, therefore *C. jejuni* needs direct contact with these ferric-glycoproteins (Miller *et al.*, 2008). The uptake of iron from Tf and Lf was attributed to genes in the cj0173c–cj0178 region of the *C. jejuni* NCTC 11168 genome (Miller *et al.*, 2008). The outer membrane receptor protein CtuA which is encoded by cj0178 was identified to be involved in iron uptake from Lf or Tf. This is in association with an ABC transporter system, namely Cj0173c – Cj0175c (Miller *et al.*, 2008). Mutation of Cj0178 (also known as CtuA) decreased the growth of *C. jejuni* significantly in the presence of Lf-bound iron and Tf-bound iron as the sole iron source (Miller *et al.*, 2008). However, as the growth of *C. jejuni* was not completely abolished, this suggests the involvement of other proteins in iron uptake from Lf and Tf.

The Cj0173c-Cj0178 system is organised into two operons, cj0176c–cj0173c and cj0177–cj0178, separated by two divergent promoters (Parkhill *et al.*, 2000). Cj0173c encodes *Campylobacter* ferric-binding protein C (CfbpC), which shows similarity to an ATPase. Cj0174c, which is CfbpB, is annotated as the permease. The structure of the periplasmic iron-binding protein Cj0175c has been identified as CfbpA. This protein consists of two domains which are connected by two β -strands, cFbpA is shown to bind iron with high affinity similar to Neisserial FbpA and displays an unusual preference for ferrous iron (oxidized subsequently to the ferric form) or ferric iron chelated by oxalate (Tom-Yew *et al.*, 2005). The gene *cj0176c* is situated upstream of *cj0175* and both genes have the same orientation of transcription. Cj0176 is an uncharacterized lipoprotein (Parkhill *et al.*, 2000, van Vliet *et al.*, 2002).

Regarding Cj0177 and Cj0178, both proteins have been proposed to function as a haem-uptake system in addition to ChuABCDZ (Chan *et al.*, 2006). However, mutants in *cj0178* are completely unaffected in haem uptake though a *chuA* mutant was significantly affected. Additionally, the *chuA* mutant was not affected for iron uptake from Lf (Miller *et al.*, 2009). Furthermore, a reduction in growth was also observed when a *cfrA* (formerly named *cj0755*) mutant strain was incubated with ferri-Lf although the difference was not similar to that obtained with the loss of *cj0178* (Miller *et al.*, 2009). However, it has been proven that the CfrA protein does not have a role in uptake of iron from Lf and Tf by *C. jejuni*. Following construction and complementation of a new *cfrA* mutated *C. jejuni* strain, no

difference was seen in iron growth assays in the presence of either Tf or Lf as sole iron source compared with wild type (Prof. Julian Ketley, unpublished data; figure 9).

1.3.3 Role of iron in colonisation of *C. jejuni*

Regulation of intracellular iron is important to secure *C. jejuni* colonisation (Hermans *et al.*, 2011). As mentioned previously (section 1.3.1), iron is essential for electron transfer pathways and acts as a cofactor for different types of enzymes. In Gram-negative bacteria, iron-regulated gene expression is controlled by the Fur (ferric uptake regulator) protein encoded by the *fur* gene. In high Fe⁺² intracellular levels, the *fur* gene responds to this increase of iron and represses the transcription of iron-regulated promoters (Stojiljkovic and Hantke, 1995). The first homologue of *fur* in *C. jejuni* was described by (Wooldridge *et al.*, 1994). *C. jejuni* has two *fur* homologs; the Fur protein regulate iron uptake and the PerR protein regulates peroxide stress defense (van Vliet *et al.*, 2002). It has been reported that the inactivation of ferric uptake regulator gene (*fur*), in addition to other important genes in iron transport such as *cfrA* and *ceuE* compromises the ability of *C. jejuni* to colonise the chicken. Furthermore, transcriptional profiling of *C. jejuni* during colonization of the chick caecum demonstrates that the transcription levels of the *chuA* gene are increased over 40-fold; *chuA* encodes the outer membrane receptor for hemin. (Woodall *et al.*, 2005).

Palyada *et al.*, (2004) demonstrated in a chick model that the mutated *cj0178* *C. jejuni* strain was significantly affected in their ability to colonize the gastrointestinal tract of chicks (Palyada, 2004). The *cj0178* was identified as important gene in iron uptake from Transferrin and Lactoferrin (Miller *et al.*, 2008). Therefore, it is clear that iron uptake systems have important role in survival and colonisation of *C. jejuni*.

1.4 Glyceraldehyde -3- phosphate dehydrogenase (GAPDH)

GAPDH is metabolic protein that is encoded by a so-called 'housekeeping gene', *gapA*. It acts as an intermediate for both glycolytic and gluconeogenic processes. The main function of this protein is in oxidative phosphorylation of glyceraldehyde-3-phosphate (G3P) to 1,3-diphosphoglycerate (1,3 dPG) in a reversible reaction during glucose metabolism, the reaction is highlighted in figure 1-2 (Kim and Dang, 2005). The crystal structure of GAPDH in most organisms has been shown to be same, GAPDH is tetrameric protein. Figure 1-8 is showing GAPDH of *S.aureus* (Mukherjee *et al.*, 2010), each monomer has two binding domains for β -nicotinamide adenine dinucleotide (phosphate)

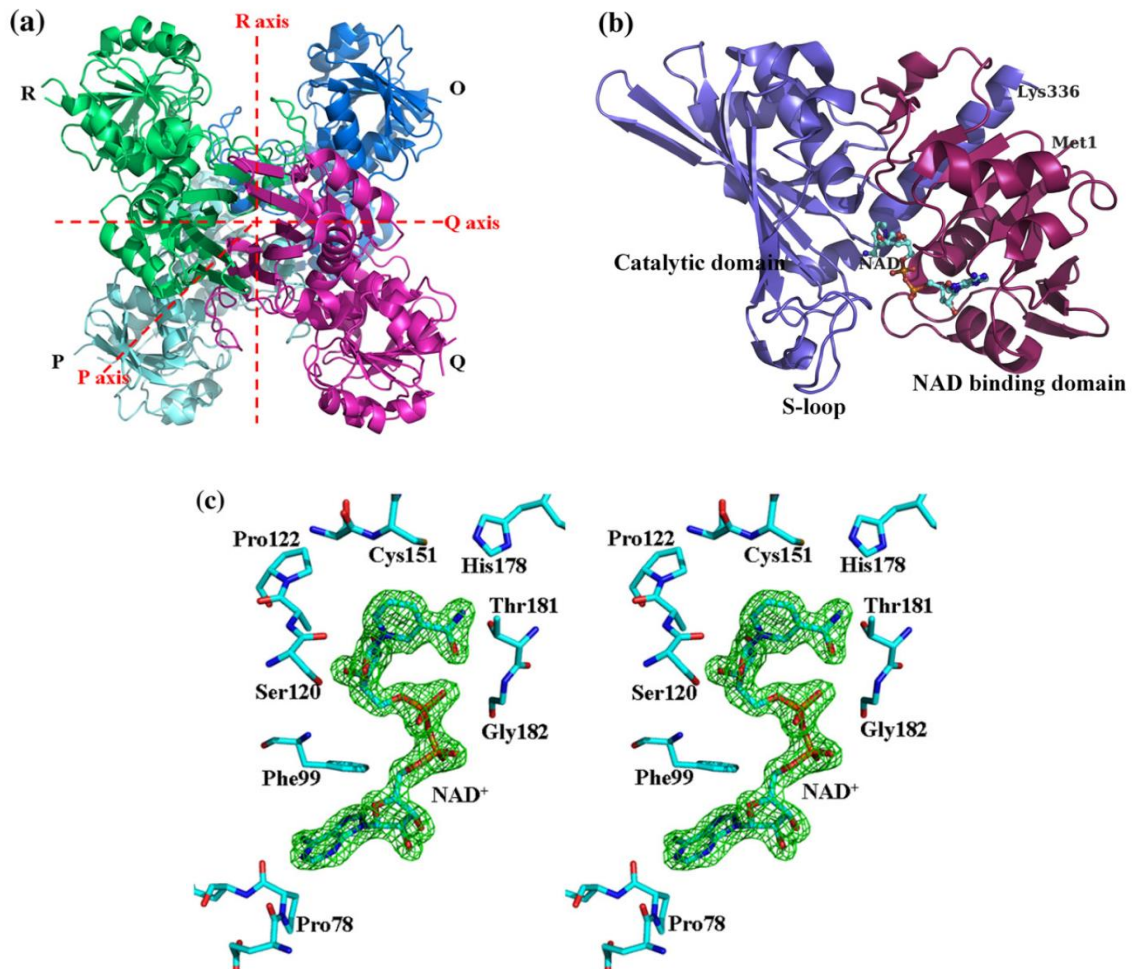


Figure 1-8. The typical structure of GAPDH in *S.aureus*.

(A) the figure shows the interaction of four identical subunits, 37 kDa, that represent the quaternary conformation of the protein. (B) Each subunit has a single catalytic site separated into two binding domains for two molecules: the domain given in purple color which binds to substrate (G3P) while pink colour domain for NAD binding unit, N terminus and C terminus at methionine and lysine respectively are also highlighted. (C) The two binding domains form a catalytic site whereby a cysteine at residue 151 and a histidine at residue 187 and NAD⁺ play the crucial role for binding the substrate G3P. This figure is from Mukherjee et al (2010).

NAD(P), a coenzyme for GAPDH metabolic reaction. GAPDH has two anion recognition sites “Ps”, for substrate binding, which is a highly conserved site in all the eukaryotic and prokaryotic GAPDH crystal structures solved so far. The other site is “Pi” for binding inorganic phosphates (Didierjean *et al.*, 2003, Mukherjee *et al.*, 2010). Two amino acids are essential for the reaction mechanism of GAPDH, Cys151 and His178 located in the active site. They are already near to each other to promote the catalytic reaction of GAPDH.

GAPDH is located in the cytoplasm of all organisms studied so far, it is essential for the utilisation of glucose, and as such is highly conserved throughout bacteria, yeast and higher eukaryotes.

1.4.1 The diversity of GAPDH gene among the organisms

There are two different classes of phosphorylating GAPDH with around 10% to 15% sequence similarity among prokaryotes and eukaryotes (Cerff, 1995). Class I GAPDH is a classic glycolytic enzyme distributed widely in both prokaryotes and eukaryotes whereas class II GAPDH is so far seemingly restricted to the archaea (Hensel *et al.*, 1989, Figge and Cerff, 2001). Class II GAPDH is a non-phosphorylating GAPDH, it cannot use NAD⁺ or NADP⁺ for oxidation of G3P and, as an alternative, it uses a ferredoxin (van der Oost *et al.*, 1998). Across bacterial genomes, the class I GAPDH gene (*gap* gene) exhibits further diversity with regard to the copy number of GAPDH homologues. In the Gram negative bacterium, *E. coli*, there are three homologues of the GAPDH gene. While *gapA* encodes the GAPDH enzyme, *gapB* encodes a E4PDH which participates in biosynthesis of pyridoxine (B₆ vitamin) (Seta *et al.*, 1997). The *gapC* gene does not exhibit any function although its open reading frame (ORF) contains 204 amino acids, most of them are conserved amino acids which are important for catalysis (Hidalgo *et al.*, 1996).

In *P. aeruginosa*, there are also three homologues of the *gap* gene. The *gapA* gene encodes for synthesis of GAPDH whereas *gapB* encodes a D-erythrose 4-phosphate dehydrogenase (E4PDH) which may also be involved in the biosynthesis of pyridoxine. The homologue *gapN* does not have an obvious function but it probably encodes a GAPDH protein (see Pseudomonas genome project: [http:// www.pseudomonas.com](http://www.pseudomonas.com)).

In contrast, the bacterium *B. subtilis* has two homologues of the GAPDH gene. However, both homologues have metabolic functions in the Calvin cycle, which occurs in photosynthetic organisms leading to production of organic compounds from carbon

dioxide and water. The *gapA* functions in the glycolytic pathway by converting G3P to 1,3dPG, whilst *gapB* catalyses the gluconeogenesis, the reverse reaction (Fillinger, 2000). In eukaryotes, although some species such as *Saccharomyces cerevisiae* have multiple GAPDH homologues and all have GAPDH activities (Delgado *et al.*, 2001), other species such as *Giardia lamblia* have two homologues of GAPDH gene and only *gap1* manifests the glycolytic activity of GAPDH (Yang *et al.*, 2002). *S. cerevisiae* has three unlinked GAPDH structural genes; TDH1, TDH2 and TDH3. None of them is individually essential for viability of this microorganism though the function of TDH2 and TDH3 is required for cell viability. Strains lacking only TDH1 do not show any growth phenotype suggesting that its product might have a function different from glycolysis. GAPDH in both wild type and strains of single and double mutants of these genes was found localised on the cell wall of *S. cerevisiae* (McAlister and Holland, 1985, Delgado *et al.*, 2001).

1.4.2 localisation of GAPDH on the cell surface

Although GAPDH was identified as a pivotal cytoplasmic element in the glycolytic pathway in 1951, over the last two decades it has become clear that GAPDH is also an anchorless surface protein (Seidler and Seidler, 2012), but signal sequences or cell wall anchoring motifs have not been yet identified. , In addition, among different organisms (Seidler and Seidler, 2012), GAPDH is essential for growth and therefore knock-out mutants might not be achievable. However, there has been rapid expansion in research to explore how GAPDH can be anchored onto the surface of organisms.

The first report describing the presence of GAPDH on the cell surface was on *Streptococcus pyogenes* (group A streptococci; GAS), the report was presented by two independent groups (Lottenberg *et al.*, 1992, Pancholi and Fischetti, 1992). They used several biochemical and serological criteria to determine the localisation and activity of GAPDH on the corresponding streptococcal cell wall extracts in this pathogenic bacterium (Pancholi and Chhatwal, 2003).

D'Costa *et al.*,(2000) provide evidence that GAPDH in *Streptococcus pyogenes* is anchored into the cell surface of bacteria by means of M-proteins. The knockout of *mga* reduced the amount of M-protein which bound fibrinogen and this was accompanied by a reduction of the amount of GAPDH released from the surface. This observation suggested that the interaction of GAPDH and M protein is essential and required the

existence of GAPDH on the surface of *S. pyogenes* (D'Costa *et al.*, 2000). Figure 1-9 A represents the surface of *S. pyogenes* and indicates GAPDH binding.

A number of later reports have indicated that GAPDH can be expressed or secreted extracellularly on the cell surface in several organisms including *Staphylococcus* species, *Lactobacillus plantarum*, *Neisseria meningitidis*, *Escherichia coli*, and *Paracoccidioides brasiliensis*, (Dumke *et al.*, 2011). In fact, although GAPDH can interact with host factors such as fibronectin, fibrinogen, albumin, laminin, collagen and plasminogen in addition to human mucin, there are several aspects of surface GAPDH localisation that need further investigation. For example, the manner of GAPDH migration onto the cell surface and the way by which GAPDH attaches on the cell surface are poorly understood (Dumke *et al.*, 2011, Seidler, 2013a).

New insight into the mechanism of the surface localisation of GAPDH has been introduced from research on *Lactobacillus plantarum* 299v, a Gram positive bacterium. It has been reported that the permeability of the plasma membrane is closely related to the efflux of GAPDH into the cell surface of this microorganism (Saad *et al.*, 2009). Double labelling of bacterial cells with anti-GAPDH antibodies and propidium iodide increased the permeability of the bacterial membrane and resulted in a 5 fold increase of GAPDH cell wall levels than unaltered cells (Saad *et al.*, 2009). In group *B streptococcus* (GBSt), Oliveira *et al.*, (2012) report that GAPDH located on the cell surface is associated with cell lysis. Electron microscopy and fluorescence-activated cell sorter (FACS) analysis demonstrated that the reduction of bacterial cell lysis levels was associated with the presence of impaired GAPDH on the surface and supernatant. Following lysis of GBS, GAPDH can associate to the surface of many living bacteria (Oliveira *et al.*, 2012).

Regarding the eukaryotes, recently in human cells GAPDH was identified to be surface-localised only on macrophages, where it seems to behave as a transferrin receptor (Rawat *et al.*, 2012). In *Candida albicans* (*C. albicans*), GAPDH was identified associated with the cell surface, representing about 35% of the total cellular GAPDH in this organism (Seidler, 2013a). Figure (1.9 B) shows the structure of *C. albicans* cell wall. Additionally, Delgado *et al.*, (2003) report that the secretion of GAPDH in *C. albicans* was promoted by GAPDH protein itself. The authors examined the ability of GAPDH polypeptide, which lacks a conventional N-terminal signal peptide, to reach the cell wall in *S.cerevisiae*. They concluded that the first half of the GAPDH amino acid sequence

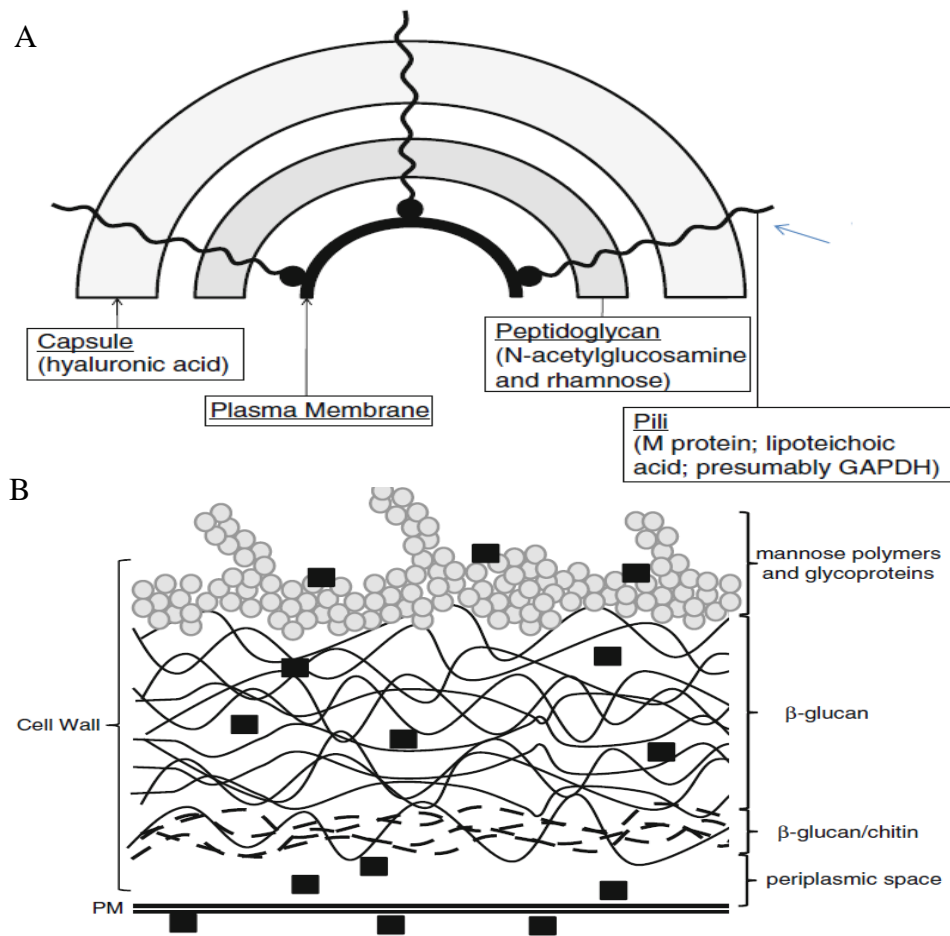


Figure 1-9 A & B. The distribution of GAPDH on the cell surface of (A) *Streptococcus pyogenes* and (B) *C. albicans*.

A- The peptidoglycan cell wall is shown as an arc surrounding the plasma membrane that is shown as the innermost arc whereas the hyaluronic acid-containing capsule is indicated as the outermost arc and covers the cell wall with a gel-like coat. GAPDH (highlighted as arrow) binds M-protein attached to the pili. The figure taken from (Seidler, 2013a).

B- GAPDH as shown as black filled boxes, wavy dashed lines are chitin and solid wavy lines are β-glucan. GAPDH can move from inside below cell membrane to the outermost of the cell wall. The localization and incorporation into the cell wall is promoted by the N-terminal half of the GAPDH from *C. albicans*. The figure taken from (Seidler, 2013a).

directs the incorporation of polypeptides into the yeast cell wall and this integration is controlled by region situated within the N-terminal half of the protein. Therefore, they suggested that the secretion of GAPDH in *Candida albicans* is specific and induced by GAPDH itself (Delgado *et al.*, 2003).

1.4.3 Moonlighting functions of GAPDH

Despite the localisation of GAPDH on the cell surface being a puzzling phenomenon, this enables GAPDH to play dual roles among different organisms. It acts as a glycolytic enzyme in the cytosol; meanwhile it can do multiple functions on the cell surfaces. Several reports indicated a potential role of GAPDH as a virulence factor in different microorganisms in addition to other functions of this protein (Egea *et al.*, 2007, Boel *et al.*, 2005). In some eukaryotes such as humans and mice, it has been reported that the accumulation of GAPDH in mitochondria is related to stimulation of proteins associated with apoptosis and it can induce pro-apoptotic mitochondrial membrane permeabilization (Tarze *et al.*, 2007). In the nucleus, GAPDH can collaborate in repair of DNA damage through catalysing Apurinic/Apyrimidinic Endonuclease (APE-1) (Sirover, 2011a). Interestingly, it has been reported that GAPDH is also associated with the progression of Alzheimer's disease and Huntington's disease; the neurodegenerative disorders (Sirover, 2011b).

Due to importance of the virulence and iron uptake functions of GAPDH, they will be explained in the following sections.

1.4.3.1 GAPDH as virulence factor

Several recent studies confirmed the importance of GAPDH as virulence factor in the pathogenesis of bacteria. Figure (1-10) illustrates the different strategies which microorganisms employ GAPDH as a virulence factor (Seidler, 2013a). In each of these strategies, GAPDH is the interacting molecule. For adherence, the surface localised GAPDH of enterohemorrhagic and enteropathogenic *E. coli* (EHEC and EPEC) binds human plasminogen and fibrinogen, this enables these pathogenic strains to interact with host intestinal epithelial cells and produce the disease (Egea *et al.*, 2007). In fact, this report was probably the first confirmation of the role of GAPDH as a virulence factor in Gram negative bacteria.

A good example of the tissue invasion mechanism for GAPDH has been identified in *S. pyogenes*. This pathogen can secrete streptokinase which has plasminogen activator-like

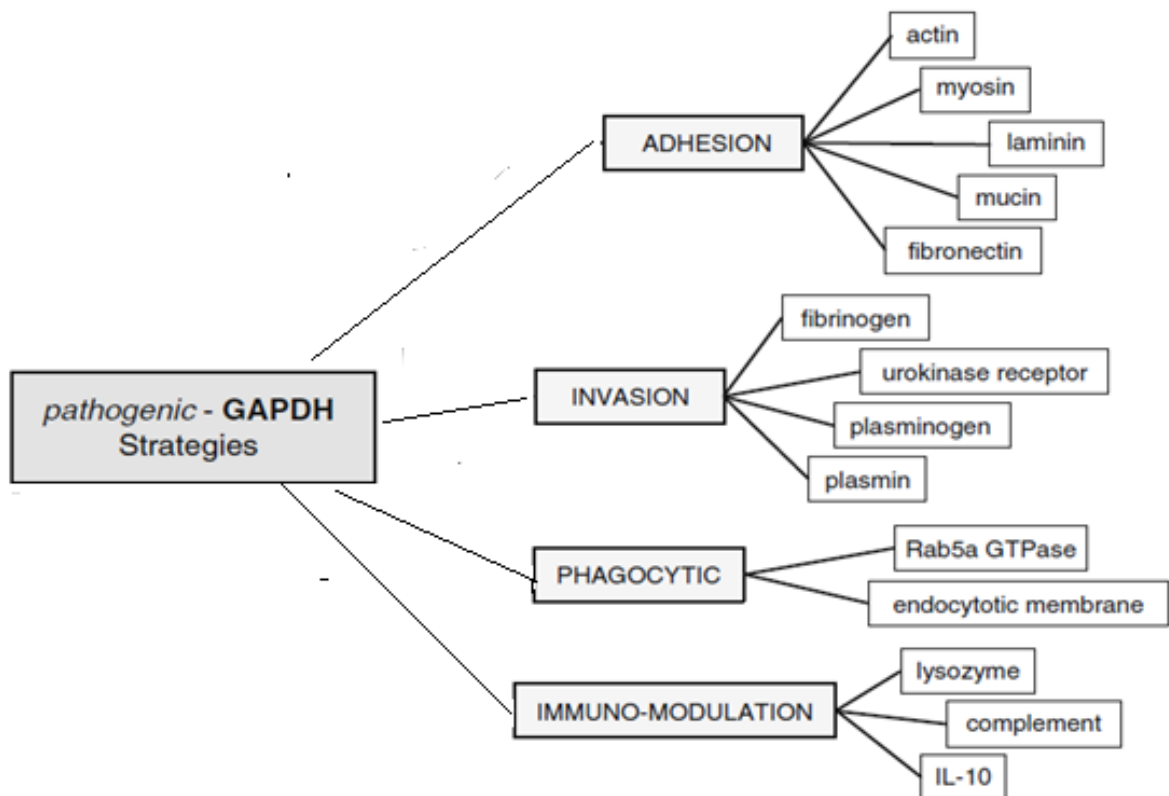


Figure 1-10. The essential pathogenic mechanisms exploits GAPDH as virulence factor.

Only the experimentally confirmed mechanisms are included in this figure. The figure taken from (Seidler, 2013a). GAPDH acts as interacting molecule in the defined mechanism, for instance, in adhesion, GAPDH binds host surface protein such as laminin, plasmin, mucin, actin and fibronectin..

activity; surface localised GAPDH in *S. pyogenes* can bind with fibrinogen leading to assembly of streptokinase-plasminogen activator which in turn promotes the generation of plasmin close to the cell surface. As a result, the co-expression of fibrinogen and plasmin binding-proteins potentially enhances the capture of the host protease activity and allows the invasion of this microorganism into the tissues of the host (D'Costa *et al.*, 2000, Seidler, 2013b).

In the intracellular pathogenic bacterium, *Brucella abortus*, GAPDH collaborates with other cellular proteins to escape from phagocytosis and lead to disease production (Fugier *et al.*, 2009). This pathogen exploits host GAPDH to bypass the endocytic pathway and replicate safely inside host cells within the endoplasmic reticulum derived replicative organelle, which is known as the Brucella-containing vacuole (BCV). GAPDH alongside the small GTPase Rab 2 protein has a crucial role in this process; both of them are present on the BCV membrane. Mutation of either GAPDH or Rab2 significantly blocks the replication of *B. abortus*. Similarly, blockage of other partner proteins of GAPDH and GTPase Rab 2, such as COPI and PKC I, decreased the replication of bacteria. Moreover, it has been suggested that the reduction of glycolysis might decrease the replication of the *B. abortus* inside the host (Fugier *et al.*, 2009).

In *Streptococcus agalactiae* (group B streptococcus), the leading cause of neonatal pneumonia, sepsis, and meningitis, surface localised GAPDH has immunomodulatory activity (Madureira *et al.*, 2007). GAPDH can induce the production of the anti-inflammatory cytokine, interleukin-10 (IL-10), which suppresses the production of antigen-presenting cells thus it assists in bacterial colonisation. Madureira and co-workers made an over-expressed GAPDH strain, and adult mice were infected by both this strain and wild type. The levels of IL-10 were elevated in the serum of mice infected by the over-expressing GAPDH strain, whereas there was a deficiency in interleukin-10 in wild type infected mice with reduced colonization. These findings suggest that GAPDH not only participates in virulence by facilitating pathogen immune evasion, but also could be acting indirectly as an immune suppressor (Madureira *et al.*, 2007).

1.4.3.2 The iron uptake function of GAPDH

The function of GAPDH in iron metabolism has been reported through an acquisition of iron from the iron-carrier proteins Tf and Lf, this function has been reported in

mammalian host tissues and in both Gram negative and positive bacteria (Boradia *et al.*, 2014b).

1.4.3.2.1 Role of GAPDH in iron uptake from Tf and Lf in mammalian cells

Mammalian GAPDH is an approximately 150 kDa protein, consisting of four identical subunits of 37 kDa (Kumar *et al.*, 2012a). Figure (1-11) shows the unique flexibility and functional variability of GAPDH in iron homeostasis in mammalian cells. There are observations of the additional dimension to the multi-functionality of GAPDH, GAPDH has important role in iron homeostasis.

Under iron depletion conditions, GAPDH can sequester iron bound Tf or Lf. The expressed GAPDH on the surface of mammalian cells functions as a dual receptor for Tf and Lf. This GAPDH can interact with Tf /Lf followed by internalization to the endosomes (Rawat *et al.*, 2012). The internalisation of GAPDH-Lf/Tf complex occurs in three different ways, Clathrin-mediated endocytosis, lipid-raft endocytosis and micropinocytosis (Kumar *et al.*, 2012b). Additionally, GAPDH can function as a soluble Tf receptor. Soluble GAPDH allows the cells to acquire Tf and associated iron in an autocrine/paracrine manner beyond their physical boundaries. This process is mediated by Urokinase plasminogen activator receptor (uPAR or CD87), a raft localized molecule (Boradia *et al.*, 2014b).

Under intracellular iron replete conditions, the isoforms of GAPDH on the cell surface are switched to recruit iron-free apo-Tf in proximity with ferroportin (Sheokand *et al.*, 2014). Ferroportin is also known as iron-regulated transporter1, which is the only known iron exporter in mammalian cells (Abboud and Haile, 2000). This occurs in order to facilitate the efflux of iron. Additionally, increase in the expression of surface GAPDH was correlated with the increase in the binding of GAPDH with apo-Tf. GAPDH-knockdown cells lost their capability of binding and showed great reduction of iron export from cells (Sheokand *et al.*, 2014).

1.4.3.2.2 Role of GAPDH in iron uptake from Tf and Lf in bacteria

It was reported that GAPDH can play a role in iron acquisition from iron glycoproteins among different bacterial species. In *S. aureus*, a transferrin-binding protein (Tpn) has been thought to be host-species specific (Modun *et al.*, 1994). However, Tpn was later reported as cell wall GAPDH and it is shown to bind human transferrin (Modun & Williams, 1999). Recently, in *S. pneumoniae*, which cannot utilise Tf and Lf as iron

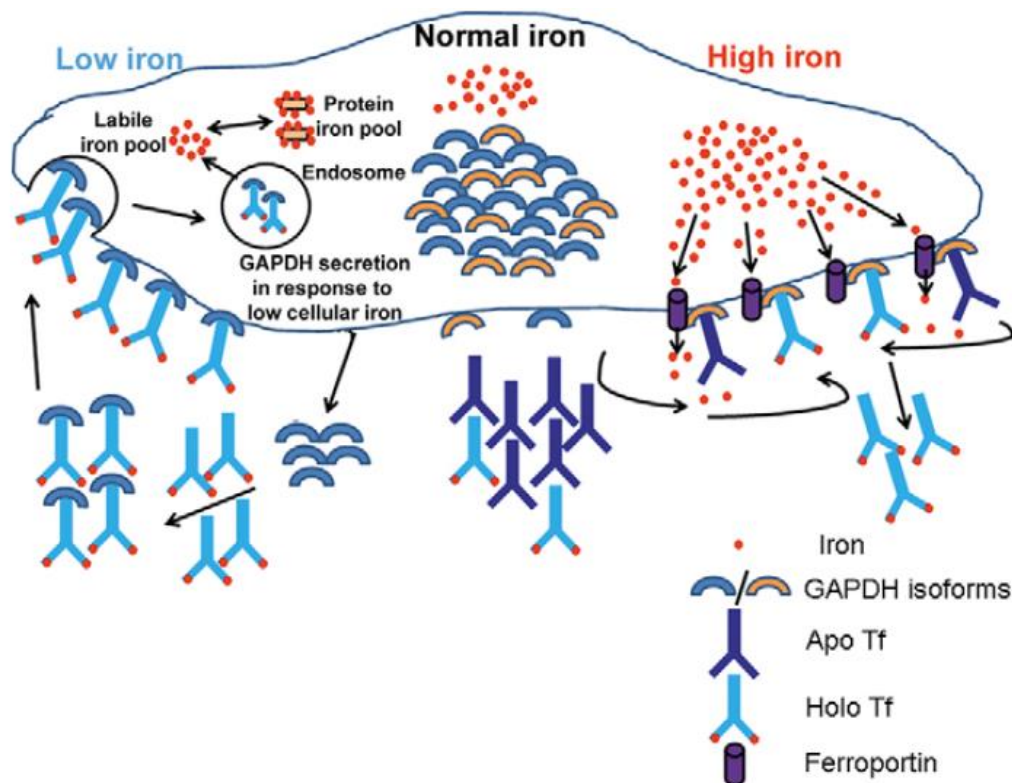


Figure 1-11. Role of mammalian GAPDH in iron homeostasis.

Under iron limitation, in order to sequester Tf iron, GAPDH functions as receptor for Tf. The similar mechanism was shown in Lf. Under high iron conditions, on the right of the mammalian cell, GAPDH switches its function to iron efflux using apo-Tf in order to export iron extracellular environment. In low iron conditions, in the left, also GAPDH isoform switched and bind with the holo-Tf to internalise iron to the cytoplasm of the cell. The figure was taken from (Sheokand *et al.*, 2014).

source but can utilise haem, it was found that GAPDH can bind haemoglobin and haem to release iron. Therefore, it has been suggested that GAPDH is essential for colonisation and penetration of this pathogen into several tissues during the infection process (Vázquez-Zamorano *et al.*, 2014).

Furthermore, GAPDH in *M. tuberculosis* (*Mtb*) and *Mycobacterium smegmatis*, along with other five proteins, facilitates the internalisation of transferrin across the mycobacterial wall and membrane when the bacterium is located within an infected macrophage (Boradia *et al.*, 2014a). More recently, it has been demonstrated for the first time that *Mtb* acquires iron by utilizing GAPDH as receptor for Lf. The findings were confirmed that GAPDH enzyme activity and Lf binding are unrelated (Malhotra *et al.*, 2017).

1.4.4 GAPDH in *C. jejuni*

Unlike many bacteria, especially closely related *H. pylori*, the GAPDH protein in *C. jejuni* (cjGAPDH) is encoded by a single and unique copy of the *gapA* gene (*cj1403c*) (Tourigny *et al.*, 2010). According to the genomic context of *C. jejuni* figure 1-13, the *gapA* gene is situated in an operon with *pgk* which encodes phosphoglycerate kinase, converting 1,3 dPG into phosphoglycerate (see figure 1.2;).

There is not much available data on the characterisation and the potential functions of GAPDH in *Campylobacter spp.* One of these studies indicated that this gene is an essential gene in *C. jejuni* by use of random insertional mutagenesis approach (Metris *et al.*, 2011). Tourigny *et al.*, (2010) cloned, expressed, purified and crystallized the GAPDH of *C. jejuni*. The results of kinetics analysis demonstrated that this enzyme can utilize both NADP⁺ and NAD⁺ in solution. Several mutants on the active site cysteine of GAPDH had been performed in order to detect any analogue, but as expected, the purified mutated GAPDH cannot convert G3P in the presence of NADP⁺ or NAD⁺ (Tourigny *et al.*, 2010).

Furthermore, the crystal structure of *C. jejuni* GAPDH (cjGAPDH) with bound NAD⁺ and NADP⁺ was solved, revealing a dual coenzyme specificity, displaying similarities with plant GAPDHs and suggesting a gluconeogenic role (Ayna, 2016). There is no published data relating to the role of cjGAPDH in iron acquisition by *C. jejuni*.

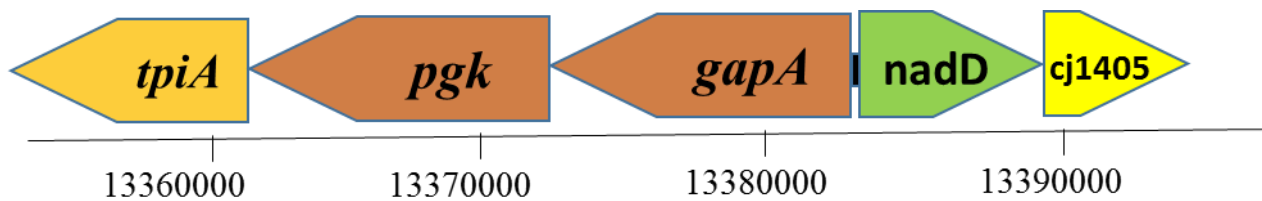


Figure 1-12. The genomic context of *gapA* in the *C.jejuni* genome.

The genome positions are indicated in base pairs (bp). Arrow direction indicates the deduced direction of transcription. The adjacent genes *tpiA*, *pgk*, *nadD* and *cj1405* encode the following proteins: triosephosphate isomerase, phosphoglycerate kinase, putative nicotinate-nucleotide adenylyltransferase and a conserved hypothetical protein respectively. .

1.5 Aim of the research

Previous findings indicate that *C. jejuni* utilises ferric-Lf and ferric-Tf for iron uptake in order to grow (Miller *et al.*, 2008). This work suggested that in addition to CtuA, which is required for intestinal colonisation, other proteins are involved in acquiring iron from Lf and Tf. The primary candidate protein appeared to be GAPDH as has been reported in other microorganisms (section 1.4.3.2.2). Therefore, the hypothesis that GAPDH is a key component in *C. jejuni* iron utilisation from Lf was addressed in the work described here with the main aim to investigate and characterise the function of cjGAPDH in uptake iron from Lf.

Indeed, obtaining new knowledge on this system of iron uptake could increase our overall understanding of the pathogenesis of *C. jejuni* and might contribute to the development of preventive methods, innovation of novel treatments and identification of new vaccine targets to prevent colonisation of this bacterium and the causation of disease.

The research objectives can be listed as follows:

- Characterisation of cjGAPDH protein expressed by newly created *C. jejuni* strains in order to demonstrate the importance of GAPDH in *C. jejuni* viability, and demonstrate cellular localisation.
- Compare the capability of utilising Lf between the newly created mutant strains of *C. jejuni* and wild type; this objective will provide evidence of GAPDH's role in iron uptake from Lf.
- Investigate binding between iron glycoproteins, such as ferric-Lf, ferric-Tf and ovo-transferrin, and cjGAPDH.
- Create and purify mutated GAPDH that lacks glycolytic activity, and also attempt to produce new strains of *C. jejuni* that do not possess GAPDH enzyme activity in order to study the potential relationship between the role of GAPDH in iron uptake from Lf and the glycolytic function of GAPDH.

Chapter 2. Material and Methods

2.1 Growth Media and Sterilisation procedures

2.1.1 Lysogeny broth and Agar

Luria Bertani broth (LuB) contains 1 % (w/v) Tryptone (Oxoid), 0.5 % (w/v) NaCl and 0.5 % (w/v) yeast extract in dH₂O. The pH was corrected to 7.5 and the medium was autoclaved. For Luria Bertani agar (LuA) 1.5 % agar was added before autoclaving.

2.1.2 Mueller Hinton Broth and Agar

This media was prepared firstly according to instructions of manufacturer; Oxoid (Basingstoke, UK). These media were supplemented by vancomycin and trimethoprim, the presence of resistance gene cassette was selected by adding of chloramphenicol (Purdy *et al.*). Table 2-1 illustrates the concentrations of the antibiotics used in this study.

2.1.3 Sterilisation procedures

Temperature resistant reagents, growth media, and PCR water were sterilised by autoclaving at 120 °C and 15 pSI for 15 minutes. Filter sterilization was used for temperature sensitive reagents. There are two different diameter sizes of membrane filters; a 0.22 µm pore diameter filter sterilisation membrane for small volumes (<50 ml) with 25 mm syringe filter membrane (PALL Life Sciences), another membrane filter is for large volumes (> 50 ml) using a vacuum driven Millipore membrane filtration system (Millipore).

2.2 Growth Conditions and Bacterial Storage

2.2.1 Growth Conditions of *E.coli DH5α*

E. coli DH5α was grown aerobically at 37 °C on LuB or LuA and supplemented where necessary with the appropriate antibiotics Amp, Cm and kan to select for mutant cells harbouring the desired plasmid.

2.2.2 Growth Conditions of *C. jejuni*

C. jejuni strains used in this study were cultured on Mueller-Hinton agar (MHA), and MH broth (MHB) (Oxoid, UK) or Minimal Essential Medium α (MEM α , GIBCO®, Invitrogen, UK) with shaking at 500 rpm (Vibrax VXR, IKA, Germany).

Table 2-1 Antibiotic preparation and concentrations.

Antibiotic	Preparation	Working Concentration	
		<i>C. jejuni</i>	<i>E. coli DH5α</i>
Chloramphenicol	10 mg/ml in 50 % ethanol in water; stored at 4°C.	10 µg/ml	20 µg/ml
Trimethoprim	5 mg/ml in 50 % ethanol in ddH ₂ O; stored at 4°C.	5 µg/ml	
Vancomycin	10 mg/ml in ddH ₂ O, stored at 4°C.	10 µg/ml	
Ampicillin	100 mg/ml in ddH ₂ O, stores at 4°C.		100 µg/ml
Kanamycin	50 mg/ml in ddH ₂ O, store at 4°C.	50 µg/ml	50 µg/ml

All strains were grown microaerobically (85 % N₂, 10 % CO₂ and 5 % O₂) at 42 °C in a variable atmosphere incubator (vain) (VA1000; Don Whitley Scientific, Shipley, UK). All media were supplemented with vancomycin and trimethoprim whereas chloramphenicol was only added to selected media in order to isolate *gapA* merodiploid strain. Kanamycin was added to isolate the mutated *C. jejuni* strains. The bacterial strains, plasmids used or constructed in this study are detailed in table 2-2.

2.2.3 Bacterial storage:

All bacterial strains were stored in glycerol stocks at -80 °C. Glycerol stocks of *E. coli* DH5α were produced by mixing of 750 µl overnight liquid cultures of LB broth with 750 µl of 50 % (v/v) glycerol, and stored in a 1.5 ml screw top microcentrifuge tube. Glycerol stocks of *C. jejuni* were prepared in the same way but by resuspending an overnight culture plate of *C. jejuni* on MHA supplemented by Vancomycin and Trimethoprim with 1-2 ml Mueller Hinton broth with 50 % glycerol. Recovery of strains from storage was performed by streaking onto appropriate solid medium containing antibiotics if required and grown overnight at proper growth conditions.

2.3 DNA methods

2.3.1 Extraction of plasmid DNA

The cloning experiments in this study were carried out using either plasmid pC46 or pUC19. The pC46 plasmid is found in 3 different types depending on the controllable promoter in its sequence; *pporA* is a highly constitutive promoter, *pfdxA* a medium and *pmetK* a lower constitutive promoter (Gaskin *et al.*, 2007a). The map of the plasmids is shown in the appendix. The plasmids were maintained in *E. coli* DH5 α and isolated after overnight incubation in 5 ml LB by using a Qiagen Mini-Prep kit (QIAGEN) according to the manufacturer's instructions.

2.3.2 Extraction of chromosomal DNA

This protocol is modified from (Chen and Kuo, 1993). Colonies of *C. jejuni* were taken from two confluent MHA plates into 10 ml tubes containing MHB, incubated microaerobically (85 % N₂, 10 % CO₂ and 5 % O₂) at 42 °C in a variable atmosphere incubator with shaking at 50 rpm. Pellet cells obtained by centrifugation at 4000 g for 15 minutes and resuspended in 0.6 ml of Buffer 1 (40 mM Tris-Acetate pH 7.8, 20 mM sodium acetate, 1 mM EDTA, 1 % SDS). The suspension was mixed gently until all the bacteria are lysed then transferred to the microcentrifuge tubes. After that, 0.2 ml of 5 M NaCl are added and mixed well by shaking. Next, the protein debris was centrifuged at 13000 g for 5 min before transferring of supernatant into new Eppendorf tubes. Then, 0.6 ml chloroform/iso-amyl alcohol (24 : 1) was added and mixed by inverting the tubes approximately 100 times before centrifugation of the samples at 13000 g for 1 min. The top layer of liquids was transferred to sterilised microcentrifuge tubes, chloroform/iso-amyl alcohol (24:1) and centrifugation steps were repeated twice. Finally, 1 ml 100 % ethanol was added and mixed by inverting the tubes (and the pellet of DNA was obtained by centrifugation at 13000 g for 5 min. The supernatant was discarded and 0.8 ml of 70% ethanol was added and mixed well. DNA was precipitated again by centrifugation at 13000 rpm for 2 min. The 70 % ethanol was discarded and desiccator was used to aspirate the residues of ethanol. The pellet of DNA was resuspended in 50-100 μ l of sterile deionised water.

Table 2-2 Bacterial strains and plasmids used in this research

Bacterial strains and plasmids	characteristics	Reference
A- Bacterial strains		
1- <i>E. coli</i> DH5 α	Cloning host strain	Lab strain
2- <i>E. coli</i> Rosetta DE3	GAPDH protein expression and purification	Lab strain
3- <i>C. jejuni</i> Wild type (wt)	<i>C. jejuni</i> NCTC11168 Motile variant, wild-type genome strain	Lab strain
4- 2 <i>gapA</i> - <i>pfdxA</i>	merodiploid <i>gapA</i> gene with <i>pfdxA</i> promoter	This study
5- 2 <i>gapA</i> - <i>pmetK</i>	merodiploid <i>gapA</i> gene with <i>pmetK</i> promoter	This study
6- 2 <i>gapA</i> - <i>pporA</i>	NCTC11168 diploid <i>gapA</i> gene with <i>pporA</i> promoter	This study
7- Δ <i>gapA</i> - <i>pfdxA</i>	Inactivated wild <i>gapA</i> allele while complemented allele with <i>pfdxA</i> promoter	This study
8- Δ <i>gapA</i> - <i>metK</i>	Inactivated wild <i>gapA</i> allele while complemented allele with <i>pmetK</i> promoter	This study
9- Δ <i>gapA</i> - <i>porA</i>	Inactivated wild <i>gapA</i> allele while complemented allele with <i>pporA</i> promoter	This study
10-Ser-2 <i>gapA</i> - <i>pfdxA</i>	Hetero-diploid <i>gapA</i> has wild <i>gapA</i> allele and cys150ser- <i>gapA</i> allele with <i>pfdxA</i> promoter	This study
11-Ser-2 <i>gapA</i> - <i>pmetK</i>	Hetero-diploid <i>gapA</i> has wild <i>gapA</i> allele and cys150ser- <i>gapA</i> allele with <i>pmetK</i> promoter	This study
12-Ser- <i>fdxA</i>	Inactivated wild <i>gapA</i> allele while Cys150Ser- <i>gapA</i> mutated complemented allele with <i>pfdxA</i> promoter	This study
13-Ser- <i>metK</i>	Inactivated wild <i>gapA</i> allele while complemented allele with <i>pmetK</i> promoter	This study
B-plasmids	characteristics	Reference

1- pC46fdxA	Suicide plasmid, CaT ^R , fdxA is medium gene expression constitutive promoter	(Gaskin <i>et al.</i> , 2007a)
2- pC46fdxA-gapA	pC46fdxA plasmid cloned with gapA gene	This study
3- pC46metK	Suicide plasmid, CaT ^R , metK is low gene expression constitutive promoter	(Gaskin <i>et al.</i> , 2007a)
4- pC46metK-gapA	pC46metK plasmid cloned with gapA gene	This study
5- pC46porA	Suicide plasmid, CaT ^R , fdxA is high gene expression constitutive promoter	(Gaskin <i>et al.</i> , 2007a)
6- pC46porA-gapA	pC46porA plasmid cloned with gapA gene	This study
7- ΔgapA-kan-pUC19	Mutated gapA by invPCR with insertion of kanamycin cassette in pUC19 plasmid	This study
8- pC46fdxA-cys150sergapA	pC46fdxA plasmid cloned with cys150sergapA	This study
9- pC46metK-cys150sergapA	pC46metK plasmid cloned with cys150sergapA	This study
10- pET151/D-gapA	topoisomerase vector for expression of GAPDH protein	(Ayna, 2016)
11- pET151/D-cys150sergapA	topoisomerase vector for expression of mutated GAPDH protein	This study

2.3.3 Ethanol precipitation

This procedure was performed before any digestion reaction or transformation in order to reduce amount of ethanol and salts in DNA sample. To each 1 volume of DNA sample the following were added, 2.5 volumes of 100 % ethanol to remove H₂O from DNA and 0.1 volume of 3 M sodium acetate (at pH 5.2) to condense DNA. The mixture was left at 4° C (on ice) for 10 minutes then centrifuged at 14,000 g for 8 minutes. The supernatant was discarded and the pellet washed carefully with 1 ml cold 70 % ethanol. The pellet was then centrifuged for 2 minutes at 14,000 g. After that, ethanol was discarded, the open tube was placed in the vacuum pump to allow complete evaporation of any ethanol residues. The pellet was then re-suspended in 25-30 µl dH₂O.

2.3.4 Restriction enzyme digestion of DNA

All restriction endonuclease enzymes and buffers were purchased from New England Biolabs and used according to the directions of the manufacturer. The restriction digestion reactions were routinely carried out in a 50 µl final volume. 1 µg of DNA was digested with appropriate enzymes and compatible buffers. Reactions were incubated at 37 °C for 1-3 hours or overnight. For cloning purpose, the vector was de-phosphorylated to prevent re-ligation of the vector alone. This was achieved by adding 1 µl of Antarctic phosphatase alongside 5 µl Antarctic phosphatase buffer to the sample following digestion and incubating for 1 hour at 37 °C, and then incubated at 65 °C for 15 min to deactivate the phosphatase. After that, the reaction was purified by using the QIA quick PCR purification kit (Qiagen) according to the manufacturer's instructions.

2.3.5 DNA ligation

Appropriate amounts of vector and insert DNA were combined in 1:3 ratio and the reactions were assembled in final volume of 20 µl. The concentrations of restriction digested vector and insert DNA fragments were estimated by gel electrophoresis as explained below. Typically, 50 ng of vector and 150 ng of insert DNA were used in the total volume of 20 µl reaction mixture. The other reaction components were 400 U/ml of T4 DNA Ligase (New England Biolabs), this enzyme catalyzes the formation of phosphodiester bonds between the 5' phosphate and 3' hydroxyl groups in DNA. The reactions also contain 1 × T4 DNA Ligase reaction buffer. 10mM of ATP were added to the ligation reaction to avoid any changes of ATP in Ligase reaction buffer. The reaction then adjusted to final volume of 20 µl by dH₂O. Finally, reactions were incubated overnight at 16 °C. Before any further applications, the ligation reactions were purified by using the QIA quick PCR purification kit (Qiagen).

2.3.6 Polymerase chain reactions (PCR)

2.3.6.1 PCR reaction mix

All PCR reactions were assembled in 20 µl final volume using sterile 200 µl PCR tubes and cycled using (Mastercycler® pro, Eppendorf, Germany). A master mix containing all of the PCR components except template DNA was prepared in a pre-chilled, sterile micro centrifuge tube and thoroughly mixed by vortex. Following a brief centrifugation, 18 µl aliquot of master mix was dispensed into PCR tubes and 2 µl appropriate template DNA were added and finally the tubes were spun prior to placement in the thermal cycler. One

tube contains 2 μ l of dH₂O rather than DNA template in addition 18 μ l of master mix aliquot was used as the negative control sample. A gradient PCR was employed to establish the best conditions and concentrations of components to amplify the gene, and then the best result of this PCR was considered as the standard condition for the next PCR targeting this gene. The best reaction volumes and conditions of DNA polymerase; Phusion which is high fidelity DNA and Kappa Taq DNA polymerase used in this research are detailed in tables 2-3 and 2-4, these are in regard of *gapA* amplification of *C. jejuni* chromosomal DNA.

Table 2-3 conditions of PCR reactions.

Step	Temperature	Duration	Cycles
Initial denaturation	94 °C	3 minutes	1
Denaturation	94 °C	15 seconds	30
Annealing	55.7 °C	30 seconds	
Extension	72 °C	Phusion: 30 seconds/ 1000 bp	
		Kappa: 60 seconds/ 1000 bp	
Final extension	72 °C	10 minutes	1

Table 2-4 describes the PCR components.

Component	Phusion	Kappa
Forward primer (2 pmol/ μ l)	1.6 μ l	2 μ l
Reverse primer (2 pmol/ μ l)	1.6 μ l	2 μ l
PCR buffer	4 μ l	2 μ l
dNTPs (contains 10 mM each deoxynucleotide)	0.32 μ l	0.4 μ l
DNA polymerase	0.2 μ l	0.25 μ l
Sterilised dH ₂ O	10.28 μ l	11.35 μ l
DNA template	2 μ l	2 μ l
Total volume	20 μ l	20 μ l

2.3.6.2 Colony PCR

A transformed colony was removed from selective media by a sterile pipette tip and part of it was sub-cultured onto new selective media divided into small numbered squares (one square for each tested colony) and grown overnight, then the other part of same colony was added to 200 μ l dH₂O and mixed thoroughly. The cell solution was then heated in a thermo cycler for 5 minutes at 96 °C before being centrifuged at 14,000g for 2 minutes. A 2 μ l aliquot of the resulting supernatant was used as the template in a PCR reaction, this PCR was performed by Kappa DNA polymerase. Table 2-4 lists the components of PCR reaction. The same PCR conditions in table 2-3 were applied.

2.3.6.3 Inverse PCR

The oligonucleotide primer pairs with 5' restriction enzyme sites were designed to anneal just within the coding region of initial construct and amplify outwards. Amplification will be resulted in the production of a linear inverse PCR product containing the regions flanking the gene of interest and the vector, but the majority of the interested gene will be deleted. The inverse PCR product and selectable marker will be restricted with the appropriate enzyme and ligated to produce the final construct. The same above mentioned PCR conditions and components in tables 2-3 and 2-4.

2.3.6.4 Primers

All oligonucleotide primers used are listed in table 2-5.

2.3.6.5 PCR purification

E.N.Z.A Cycle Pure kit (Omega Biotek) was used to purify PCR products with following the manufacturer's instructions.

2.3.7 Estimation of DNA concentration by gel electrophoresis

The concentration of DNA in samples was estimated by agarose gel electrophoresis. 2-3 μ l of molecular weight marker (Hyperladder 1) of known concentration with different sizes ranged from (200-10000 bp) was loaded onto a 1% agarose gel containing ethidium bromide. 1 μ l of DNA solution (unknown concentration) was mixed with 4 \times sample loading buffer and loaded into an adjacent well. The gel was subjected to electrophoresis then DNA was visualised under UV light. DNA concentration was estimated visually by comparing the band intensity of the sample to the known concentration of the molecular weight markers.

Table 2-5 primers used in this research

Name	Sequence	Use
<i>gapA</i> -Forward	5'-CATGCCATGGCTGTAAAAGTTGCTATAAAATGGTTTTG-3'	Amplification of <i>gapA</i>
<i>gapA</i> -Reverse	5'-CATGCCATGGTTAAGCCTTATTTGCAATATATACTG-3'	Amplification of <i>gapA</i>
<i>Cj0046</i> - Forward	5'-CTCTCTCCGCTAGAAATTAATCC-3'	Clarification by colony PCR
CATinvR	5'-GCGGTCCTGAACTCTTCATGTC-3'	Clarification by colony PCR
Flanking <i>cj0046</i> -F	5'-AATTCCCATTTTTCAATTAGGCTAG-3'	Clarification by colony PCR
Flanking <i>cj0046</i> -R	5'-AGTTTATGGATACAAAAATTCCTGG-3'	Clarification by colony PCR
Flank- <i>gapA</i> -For	5'-TCTAGAATTCCTTCTTCTAAAAGTGAATTCCTATA-3'	Cloning of <i>gapA</i> into pUC19
Flank- <i>gapA</i> -Rev	5'-CTATGTCGACGCGATTGGCAATAACAAATCTACTA-3'	Cloning of <i>gapA</i> into pUC19
Inv <i>gapA</i> -For	5'-ATAAGGATCCGGGCTATTCAAGTCGTCTAG-3'	Mutagenesis of <i>gapA</i>
Inv <i>gapA</i> -Rev	5'-AAGAGGATCCTTGCAACACATCTGCCTATG-3'	Mutagenesis of <i>gapA</i>
Kan-For	5'-ATAAGGATCCATTAATACTGTAGAAAAGAGGAAGG-3'	Amplification of kanamycin
Kan-Rev	5'-TGACGGATCCACTAAAACAATTCATCCAGTAAA-3'	Amplification of kanamycin
Flank- <i>pgK</i> -For	5'-TGCTCTTGTGTGATTGCATTTTAAATTTG-3'	Clarification of mutants
Flank- <i>nadD</i> -Rev	5'-CTCGCTCATGTCAATGGTTTTGATATTT-3'	Clarification of mutants
Cys150Ser- <i>gapA</i> -For	5'-AATGCAAGTCCACAACAAATTGTTTAGGTC-3'	Site directed mutagenesis of <i>gapA</i> gene
Cys150Ser- <i>gapA</i> -Rev	5'-ATTTGTTGTGGA ^{ACTTGCATTAGAAATAATGC} -3'	Site directed mutagenesis of <i>gapA</i> gene
<i>gapA</i> -qPCR-For	5'-AAATGGTTTTGGACGCATAG-3'	Real-time PCR of <i>gapA</i> gene
<i>gapA</i> -qPCR-Rev	5'-ACTATCAACACTGCCTTTAAAT-3'	Real-time PCR of <i>gapA</i> gene
<i>rpoA</i> -qPCR-For	5'-CGAGCTTGCTTTGATGAGTG-3'	Real-time PCR reference gene
<i>rpoA</i> -qPCR-Rev	5'-AGTTCCCACAGGAAAACCTA-3'	Real-time PCR reference gene
<i>gapA</i> -F-PciI	5'-ACATGTATGGCTGTAAAAGTTGCTATAAAATG-3'	mCherry tagging
<i>gapA</i> -mChe-R	5'-CAGTATATATTGCAAATAAGGCTATGGTGAGCA-3'	mCherry tagging

mCherry- <i>gapA</i> -F	5'-CAAATAAGGCTATGGTGAGCAAGGGCGAGGA-3'	mCherry tagging
mCherry-R-PciI	5'- <u>ACATGTTT</u> ACTTGTACAGCTCGTCCAT-3'	mCherry tagging

2.3.8 Transformation of DNA

2.3.8.1 Preparation of electrocompetent *E. coli* DH5 α

5 ml of LB broth was inoculated with *E. coli* DH5 α and incubated with shaking overnight at 37 °C. The grown culture was diluted 1/100 in new LB broth and incubated again with shaking at 37°C until reaching an optical density (OD) between 0.4-0.6 at 600 nm. The cells were placed on ice and centrifuged at 4 °C for 15 minutes, at the maximum speed to pellet the cells. The cells were washed 3 times by re-suspending them and centrifuged at 4°C in decreased volumes of ice cold dH₂O (50 ml, 25 and 10), the last washing step with 10% glycerol (v/v). After this final 4 °C centrifugation, the pelleted cells were resuspended in 1 ml of ice cold 10 % glycerol. The cells were then either transformed immediately or were divided into 200 μ l aliquots on dry ice and stored at -80° C. The cells were thawed on ice before use.

2.3.8.2 Preparation of electrocompetent *C. jejuni*

C. jejuni was grown up in two confluent plates and incubated overnight microaerobically in the vial. 2 mls of MHB were added to plates and the cells were scrapped off with sterile spreader and transferred into a new tube. The cells were then centrifuged 3 min at the maximum speed 13,400 g. The supernatant was removed and the cells re-suspended in 1 ml of ice cold wash buffer (272 mM sucrose and 15 % v/v glycerol); the preparation is below. The wash step was repeated twice. Finally, the cells were re-suspended in 700-1000 μ l of wash buffer. The competent cells were either transformed immediately or divided into 200 μ l aliquots on dry ice and stored at -80 ° C.

2.3.8.3 Preparation of wash buffer

For 10 ml stock, the following components were added: 0.931 g sucrose, 1.5 ml glycerol and 8.5 ml sterile dH₂O. The mixture then was sterilised by membrane filter into a clean universal tube.

2.3.8.4 Electroporation

The electroporation in both *E. coli DH5a* and *C. jejuni* was carried out using electrocuvettes with a 2 mm gap (Cell Projects Ltd, GeneFlow, UK) and a BioRad Gene Pulser (BioRad, UK) settled at 1.5 kV, 200 Ω and 25 μ F and the time constant should be between 18-23. Electrocuvettes were pre-chilled in 4 °C on ice before use. The cells were pulsed once and recovered by immediately flushing out the cuvette with 1 ml LB broth and incubated in water bath at 37 °C for 1 hour. Then they were cultivated on selective media and incubated overnight at 37 °C. The electroporation of *C. jejuni* was slightly different, the settings of BioRad Gene Pulser were: 2.5 kV, 200 Ω and 25 μ F and the time constant should be around 8. The recovery was performed by flushing out the cuvette with 200 μ l MH broth (with trimethoprim and vancomycin) and incubated overnight at 37 °C under microaerobic conditions. Then the transformant cells were selected by growing in MH agar (with trimethoprim and vancomycin) in addition to chloroamphenicol.

2.3.9 DNA sequencing

DNA sequencing was performed by PNAACL (Protein and Nucleic Acid Chemistry Laboratory), University of Leicester. The reaction mixture was carried out in 10 μ l using a BigDye ®Terminator v3.1 Cycle Sequencing Kit (ABI Applied Biosystems®). Two different primers were used in separate reaction. The reactions were cycled in a PCR machine using the following settings, an initial 5 minutes 96°C denaturing step was followed by 29 cycles of a 10 second denaturing step at 96 °C, a 10 second annealing step at 50 °C, and a 4 minute extension step at 60 °C. The reaction then cleaned up by adding 2.2 % SDS (2 μ l SDS and 8 μ l of dH₂O), reaction), placed in a thermal cycler at 98 °C for 5 minutes then 25 °C for 10 minutes. The reaction then purified by using Performa column kit in accordance with the manufacturer's instructions in order to remove any unincorporated dye from the sequencing reaction.

2.3.10 Real-time reverse transcriptase-PCR (RT-PCR)

2.3.10.1 Preparation of the cells

C. jejuni strains were grown overnight in MHB under microaerobic conditions. Then, the cells were equalised on OD₆₀₀=0.025 and incubated again in the same conditions to reach the mid-log of the growth curve OD₆₀₀=0.1. 1 ml of cold RNA stabiliser (95% ethanol + 5% phenol) was added to each 5ml of culture and incubated at 4 °C for 30 minutes. The

cells were spun down and transferred to new Eppendorf tubes, spun briefly to discard the remaining amount of RNA stabiliser and cells then were either kept at -80 °C for longer storage or proceeded into RNA extraction experiment.

2.3.10.1 Extraction of RNA

Norgen total RNA kit was used to extract RNA from *C. jejuni* cells. Briefly, the cells were taken from -80 °C, resuspended in 100 µl (TE pH= 8 + 3mg lysozyme) and incubated for 10-20 minutes at 37 °C until lysed. 300 µl of lysis buffer (RL buffer 300 µl /prep + 10 µl /ml β mercaptoethanol) were added, vortexed, and tubes were spun 14000 g for one minute. 200µl of 100% ethanol were added to each sample and vortexed for 10 seconds, directly transferred to column and spin down at 14,000 g for one minute. After that, washing step by using 400 µl of washing buffer was performed three times and finally the column placed to clean micro tubes and 50 µl of Elution buffer were added to column and centrifuged for two minutes at 1700 rpm and then again two minutes at full speed. The concentration and purity of RNA were assessed by use of Nanodrop 2000C system (Thermo Scientific, UK) at absorbance of 260 nm, 1 µl of extracted RNA putted onto the centre of the measuring area of Nanodrop. The blank sample was 1µl of elution buffer. The purity of RNA was estimated by the ratio of absorbance at different wavelengths: the 260/280 ratio and 260/230 ratio.

2.3.10.2 Removing of DNA residuals from extracted RNA

Turbo DNase treatment kit was used to clear any potential DNA in the samples. The 0.1 volume of 10 x Turbo DNase buffer (Ambion) and 1 µl of Turbo DNase (Ambion) were added to the samples, mixed gently and incubated at 37 °C for 30 - 60 minutes. After that, 0.1 volume of DNase inactivation reagent (Ambion) was added and tubes were mixed gently, then incubated at room temperature for two minutes and centrifuged at max speed for 1.5 minute. The supernatant was transferred to a new microfuge tube and concentration of RNA was measured again by Nanodrop, samples were kept at -80 °C.

2.3.10.3 Reverse transcription reaction

RNA to cDNA Applied Biosystems kit was used to synthesis of cDNA. According to the instructions, 20 µl final volume reaction was set up containing 10 µl of 2x buffer, 1 µl of Reverse transcriptase, 0.5 µg of RNA and volume completed by adding of Diethyl pyrocarbonate (DEPC) water. The reactions were incubated at 37 °C cycle for 60 minutes and then at 95 °C for 5 min and then stored at -20 °C.

2.3.10.4 RT-PCR assay

Fast SYBR green (Qiagen) Applied Biosystems kit was used in RT-PCR analysis of *gapA* gene among *C. jejuni* strains. To normalise the results, *rpoA* gene was used as reference gene (Ritz *et al.*, 2009). The primers were designed by Clone Manager (version 9) (Scientific and Educational Software, 2012) to amplify around 160 bp of the sample and reference genes. The important features of primers such primer self-dimer, hetro-dimer and hairpin were analysed by online tool: <https://www.idtdna.com/calc/alyzer>

Table 2-6 summarises the RT-PCR mastermix components, the reactions were carried out in triplicates using AB Applied Biosystems, 7500 Fast real time PCR system (Life Technologies) apparatus. The negative controls included no RNA template added, master mix was prepared with considering calculate the number of sample tested plus the negative/positive controls multiply by 3 and finally added 1 for the pipetting error. The PCR conditions were holding stage at 95 °C for 20 seconds, cycling stage (annealing/extension) at 95°C for 3 seconds and 60°C for 30 seconds in overall 40 cycles. Melt curves were produced for each amplification product. Amplification plots and melt curves were analysed by Applied Biosystems. In the negative control no RNA template was present. Samples were normalized using *rpoA* gene as a housekeeping gene (Ritz *et al.*, 2009). All the samples, including controls, were analyzed in triplicate and each experiment was repeated three times in three different days.

2.3.10.5 Analysis of RT-PCR results

The Ct based method was used in analysis of the results, the Relative *n*-fold changes in the transcription of the examined genes between the new *C. jejuni* strains (treated) and wild strain (non-treated) were calculated using the relative quantification (Fugier *et al.*) as following: $\Delta Ct_1 = Ct_{\text{untreated control (gapA)}} - Ct_{\text{endogenous control gene untreated (rpoA)}}$

$\Delta Ct_2 = Ct_{\text{treated sample (gapA)}} - Ct_{\text{endogenous control treated (rpoA)}}$; where ΔCt_1 is wild type and ΔCt_2 is the new created strain. $\Delta \Delta Ct = \Delta Ct_2 - \Delta Ct_1$; Fold value = $2^{-\Delta \Delta Ct}$;

RQ = $1 \div \text{fold value}$

The Ct is the threshold cycle value for the amplified genes, the statistical analyses then performed using Excel 2013 (MicrosoftCorp.) to calculate statistically significant differences when P = 0.05 by applied Student's t-test.

Table 2-6 preparation of mastermix reaction of RT-PCR experiment

Reagent	Concentration	Volume for one reaction (1x)		Final concentration	
		<i>rpoA</i>	<i>gapA</i>	<i>rpoA</i>	<i>gapA</i>
Fast SYBR green	2 x	10		1 x	
Forward primer	10 μ M	0.4	0.8	200 nM	400 nM
Reverse primer	10 μ M	0.4	0.8	200 nM	400 nM
cDNA	500 ng	2 μ l			
dH ₂ O		Up to 20			

2.3.11 The splicing by overlap extension (SOE) PCR to tag of GAPDH at the C-terminal with mCherry fluorescent protein:

The SOE PCR was used to fuse two DNA fragments; *gapA* gene and mCherry fluorophore. The latter was amplified by PCR (gift from Dr Ezio Rosato, department of genetics and genome biology, university of Leicester), the fusion reaction was carried out without using restriction enzymes or T4 DNA ligase. The method is illustrated in figure 2-1. Phusion DNA polymerase was used for the amplification and fusion reactions. The inner primers (3 and 4) for the initial PCR products contain 10-15 bp of complementary sequence that allows the fusion of the two fragments in the second PCR. The outer primers (1 and 2) contain *PciI* restriction sites which has compatible end with *Esp31*, and were used to amplify the final product. The sequences of primers are indicated in table 2-5. PCR conditions were similar to phusion PCR and similar to mentioned in table 2-4. The final product (*gapA-mCherry*) was cutted and ligated into *cj0046* plasmids the ligated plasmids were transformed by electroporation into *E. coli* (DH5 α) (section 2.3.8.4). Transformants were plated on selective LB agar plates containing 20 μ g/ml chloramphenicol and incubated for 24 hours at 37 $^{\circ}$ C.

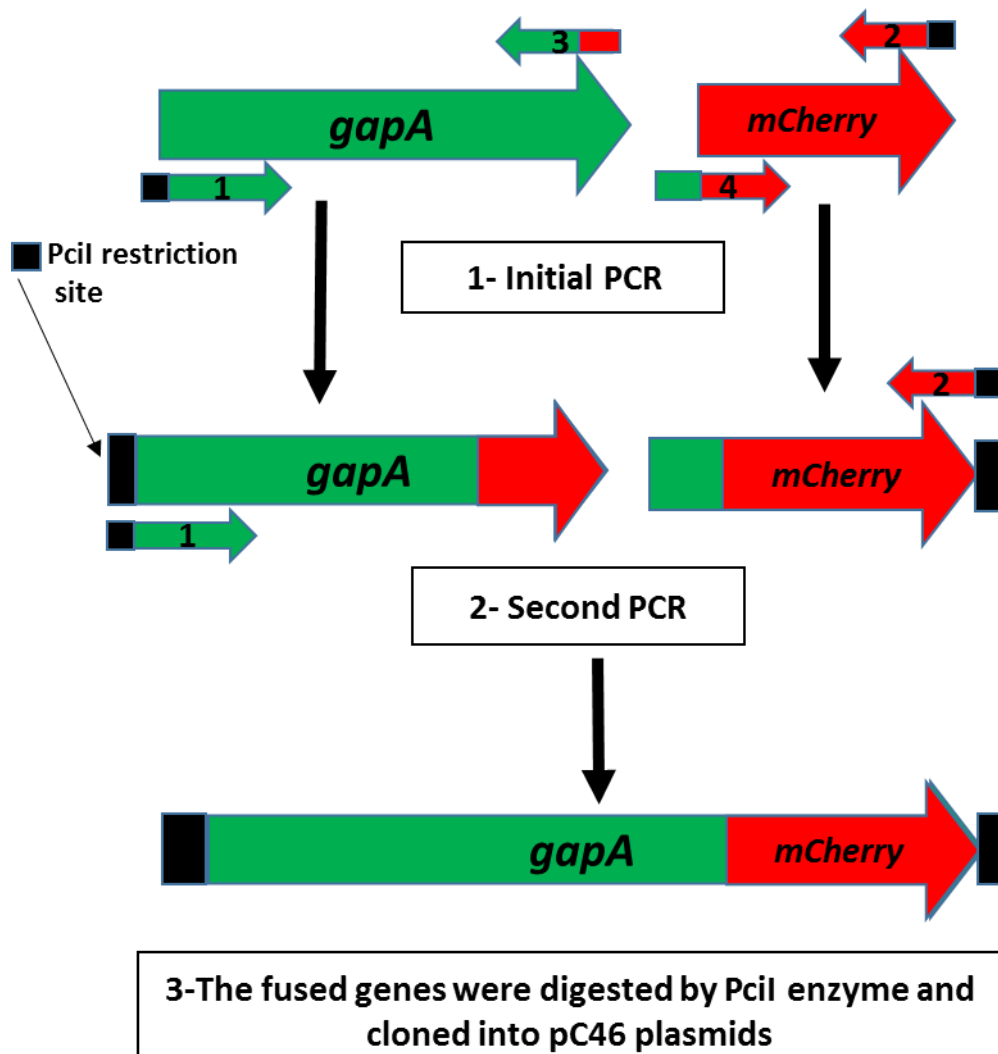


Figure 2-1. Diagram to illustrate the method used to tag *gapA* at the C- terminal end with *mCherry* fluorescent protein.

The small arrows with numbers indicate the primers used in this approach, 1 and 2 (outer primers), 3 and 4 (the inner primer; overlapping sequences contained primers). In the initial PCR, two separate PCR fragments are produced which contain overlapping sequences. In the second PCR, the outer primers (1 and 2) were used to amplify *gapA* overlapped to *mCherry* in the C-terminal region in order to produce the *gapA*-*mCherry* fused gene.

2.4 Growth assays

2.4.1 Growth assay of *C. jejuni* strains in Mueller Hinton Broth medium

The colonies of *C. jejuni* were recovered from -80 °C and streaked to confluency on MHA plates and incubated in the Vain, then inoculated into 5 mL MHB supplemented by trimethoprim and vancomycin and incubated with shaking (50 g) overnight in the Vain. The optical density (600 nm) of each culture was measured after overnight incubation, the cultures were then diluted in fresh MHB+VT to give a final OD₆₀₀ of 0.025 (about 2.5×10^7 c.f.u/ml as calculated by (Reeser, 2007 #352). Next, multiple 200 µl aliquots of diluted cultures were added into individual wells of a 96 well microplate. For this experiment, 8 replicates were used for each strain and four MHB blanks per strain. After that, the plate was sealed with a gas permeable pre-pierced seal and then incubated in the FLUOstar Omega at 37 °C Atmospheric Control Unit set to independently control the O₂ and the CO₂. Absorbance at 600 nm was measured (20 flashes/cycle) for 48 cycles of 30 minutes with continual shaking (double orbital) at 500 g between measurements. The growth kinetics parameters, doubling time and growth rate were calculated (see section 2.4.3), and used to compare between the strains.

2.4.2 Growth assay of *C. jejuni* strains in MEMα

C. jejuni strains were grown on two confluent MHA plates under standard growth conditions of this bacterium. The strains were harvested with phosphate-buffered saline (PBS; 2 ml/plate) and centrifuged at 4000 g for 5 min. the cells then suspended in MEMα and the centrifugation repeated twice. After that, the cells were suspended in 5 ml of MEMα and the absorbance of all strains adjusted to an initial optical density at 600 nm (OD₆₀₀) of 0.1. The strains then incubated microaerobically for 12 to 16 h with agitation to achieve iron depletion. Next, the cells were harvested, the supernatants were discarded and the pellets were resuspended again in fresh MEMα 10 ml cultures to an initial OD₆₀₀ of 0.05, This value of absorbance contains (5×10^7 c.f.u/ml) (Reeser *et al.*, 2007). The cultures of each strain then transferred into microcentrifuge tubes supplemented with the appropriate iron sources. Table 2-7 illustrate the iron sources used in this experiment, negative control samples do not contain iron source whilst the positive control was supplemented with 40 µM ferrous sulphate 40µM FeSO₄. 200 µl of each culture were dispensed into 96 well microplate 3 replicates were used for each strain and iron source, and nine MEMα blanks. The plate was sealed with a gas permeable pre-pierced seal and

incubated in the FLUOstar Omega at 37 °C Atmospheric Control Unit set to independently control the O₂ and the CO₂. Absorbance at 600 nm was measured (20 flashes/cycle) for forty-eight cycles of 30 minutes with continual shaking (double orbital) at 500 rpm between measurements. OD readings were taken at intervals. The differences in doubling time and growth rate were analysed by an unpaired Student's *t* test.

Table 2-7 iron sources used in this research

Iron source	Preparation of stock solution	Final concentration	storage
FeSO ₄	10 mM in sterilised dH ₂ O + 5 µl concentrated sulphuric acid	40 µM	Only use fresh
Human ferric-Lf	10 mg/ml in 1x P.B.S (pH 7.5)	0.27 µM	2-8 °C
human ferric-Tf	10 mg/ml in 10 mM Tris-HCl (pH 7.5)	0.27 µM	-20 °C
ferric-ovo-Tf	10 mg/ml in 10 mM Tris-HCl (pH 7.5)	0.27 µM	-20 °C

2.4.3 Calculation of doubling time and growth rate

Computer program Excel 2013 (Microsoft Corp.) was used to calculate the growth rate and doubling time. After drawing the growth curve by plotting the values of OD and time obtained from experiment of either section 2.4.1 or 2.4.2, the Y axis of the curve was changed into the log scale. After that, only the OD values in the graph which represent the exponential phase of the growth were chosen to build new curve. After that, the trend line was added to the curve and exponential function was chosen for this trend line. The growth rate (μ_{\max} h⁻¹) is represented by the value of “x” in the formula appeared on the curve. Growth rate was represented per hour (h⁻¹). To calculate the doubling time (d.t), the following formula was used:

$$[d.t = \text{Ln}2 (\text{natural log of } 2) / \text{growth rate}];$$

d.t is given in hours (h).

2.5 Protein Methods

2.5.1 Preparation of whole cell lysate

C. jejuni cells grown on MHA were re-suspended in PBS and the cell concentrations were equalised to an optical density ($OD_{600} = 0.1$). The cell pellets were obtained by centrifugation at 4000 g for 5 minutes. Lysis of whole cells was achieved by resuspending pellets in 200 μ l of 2 x SDS loading buffer (10% SDS, 1M Tris pH 6.8, 1 % Bromophenol blue, 2.5 ml glycerol, 200 mM DTT and up to 10 ml dH₂O), transferred into 500 μ l tube followed by heat treatment (98 °C, 5 minutes) and spin for 2 min. If SDS-PAGE was not conducted immediately, the cell lysate was kept on -20 °C.

For purified proteins, certain concentration of protein mixed with 2x SDS loading buffer, followed by heat treatment (98 °C, 5 minutes) and spin for 2 min.

2.5.2 SDS Polyacrylamide gel electrophoresis (SDS-PAGE) and staining

The preparation of 12 % SDS-PAGE is shown in Table 2-8 . The separating gel consisted of a mixture of buffer A (0.75 M Tris, 0.2 % SDS, pH=8.2 HCl), 30nit. About 1 ml of isopropyl alcohol was added to the gel to remove the air bubbles and to enhance the straightness of the gel. Once the bottom separating gel had solidified, a stacking gel which consists of buffer B (0.25 M Tris, 0.2 % SDS, pH= 6.8 Hcl), 30 % (v/v) acrylamide, 1 % APS and TEMED, was loaded on top of the separating gel and the comb was instantly inserted into the gel.

Soon after the gel had solidified, the gel casting unit was transferred into the electrophoresis tank which was filled with 1x SDS-PAGE running buffer (25 mM Tris-HCl, 192 mM Glycine, 1 % (w/v) SDS), and the comb was removed. The pre-stained protein marker was loaded, followed by loading of the samples. The tank was connected to power supplier and run constantly at voltage 100 for 120 min. Regarding the staining, following the SDS-PAGE the gel was immersed in Coomassie blue dye solution (10% glacial acetic acid, 45 % methanol and 0.25 % w/v Brilliant Blue R (Sigma-Aldrich)) for 60 min with shaking (40 rpm). After that, destaining solution (7.5 % glacial acetic acid, 20 % methanol) was used to display the protein positions on the SDS-PAGE gel.

Table 2-8 Preparation of 12% SDS-PAGE.

component	Separating gel (2 gels)	Stacking gel (2 gels)
Buffer A	7.5 ml	-
Buffer B	-	3.75 ml
Acrylamide	6 ml	1.5 ml
10 % APS	375 μ l	75 μ l
TEMED	7.5 μ l	3.75 μ l
dH ₂ O	1.05 ml	2.175 ml

2.5.3 Western blot

The expression of GAPDH protein from *C. jejuni* strains, the binding with Lf iron binding protein and other investigations were investigated by immunoblotting technique; Western blotting, by using of different primary antibodies depending on the assay such as polyclonal rabbit anti-GapA, polyclonal rabbit anti-Lf, and rabbit monoclonal anti-GroEL. The samples were loaded on 12 % polyacrylamide gel (SDS-PAGE gel) and electrophoresed constantly at a current of 100 volts. After that, proteins separated from SDS-PAGE were transferred into polyvinylidene fluoride (PVDF) membrane (pre-activated with 100% methanol). Transfer was performed in a tank containing cold transfer buffer (192 mM glycine, 25 mM Tris pH ~8.3, and 20% methanol) at a constant current of 100 A for 1 hour. The membrane subsequently blocked with blocking buffer (0.05% Tween-20, 5 % non-fat dry milk in 10 x PBS) at 4°C. The blocking buffer was contained BSA rather than milk in case of Lf investigations. The primary antibody was added in appropriate amount to the membrane in blocking buffer then incubated for 1 hour with shaking followed by washing in T.P.B.S buffer (10 x PBS, 0.05 % tween; in 1000 ml H₂O). Next, appropriate amount of secondary antibody (anti-rabbit HRP) in blocking buffer was added to the membrane and incubated for 1 hour at room temperature. The washing in T.P.B.S followed to remove unbound secondary antibody. An EZ-ECL Chemiluminescence detection kit was used to detect the signals for HRP and the bands were quantified with ImageJ software.

2.5.4 GAPDH enzyme activity assay

2.5.4.1 Intact *C. jejuni* cells GAPDH enzyme activity assay

C. jejuni strains were recovered from frozen glycerol stock onto two confluent plates and used to inoculate 5 ml of MHB medium. The cultures were incubated overnight, and OD₆₀₀= 0.1 was used to equalise the cultures for cell growth which contains approximately (4.8 x 10⁸ cfu/ml). Each strain was represented by two samples, one sample for the test and another for control. The samples for the test were resuspended in 1 ml of GAPDH assay buffer containing 50 mM Na₂HPO₄, 5 mM EDTA, 40 mM Triethanolamine, 2 mM Glyceraldehyde-3-phosphate (G3P), and 2 mM of cofactor NAD⁺ or NADP⁺ while control samples were also suspended in the same buffer but free of G3P. Samples were incubated in a 37 °C water bath for 30 minutes, and then the cells were pelleted by centrifugation at 12,000 xg for 10 minutes. The pellet was investigated under the 40 x objective microscope in order to estimate the lysis level and the supernatant was transferred into new cuvette. The production of NAD(P)H was detected by measuring the absorption of the supernatant at 340 nm in a UV/visible Spectrophotometer (6705 uv/vis spec JENWAY). The results of GAPDH assay were corrected by subtracting the absorbance readings of control from the test samples.

2.5.4.2 Purified Protein GAPDH enzymatic activity assay

This assay was taken from (Purves *et al.*, 2010). Purified protein was prepared at 20 ng/μl, 10 μl of this solution (200 ng) were mixed in a 96 well plate with 190 μl GAPDH assay buffer (50 mM Na₂HPO₄, 5 mM EDTA, 40 mM Triethanolamine, 4 mM G3P, and 2 mM of cofactor NAD⁺ or NADP⁺). The assay was carried out in triplicate for each sample, and the plate was incubated at 37 °C in a FLUOstar Omega plate reader (BMG Labtech). The absorption was measured at 340 nm after 30 minutes, and an average reading from the 3 wells was recorded for each sample.

2.5.5 Fractionation of *C. jejuni*

C. jejuni cells were fractionated into cytosol, total membrane and outer membrane fractions, the fractionation steps were performed at 4 °C or on ice (this method is similar to van Vliet *et al* 1998). Cells were harvested by centrifugation at 4000 rpm for 15 min re-suspended in 1.0 ml envelope buffer (EB; 10 mM Tris-HCl, pH 7.5), and transferred to Eppendorf tubes (250 μl/tube). Cells were frozen at -80°C for at least 30 minutes, defrosted, and lysed by sonication (10 minutes total, with 15 sec on/off). The non-lysed

cells were removed by centrifugation, the supernatants were transferred to 2 ml clear Beckman tubes (Miconai *et al.*) and crude total membranes pelleted by ultracentrifugation at 50,000 g for 10 min at 4 °C in the Beckman TL-100 ultracentrifuge. Supernatants (soluble fraction containing cytosolic and periplasmic contents) were divided and transferred into two new Eppendorf tubes, one for GAPDH enzymatic assay and other for precipitation by 10 % tricarboxylic acid (TCA) for SDS-PAGE and Western blot, stored at -20 °C. The pellets (total membranes) were washed once with 1.0 ml of EB, re-ultracentrifuged and then the pellets were re-suspended in 100 µl EB and 100 µl 2 x SDS-PAGE loading buffer, stored at -20 °C. For extraction of outer membrane fraction, the pellets (total membranes) were re-suspended in 1.0 ml of EB containing 0.6% (w/v) sodium sarkosyl (*aka* N-lauryl-sarcosine; EBS) and incubated at 4°C for 30 min. Sarkosyl insoluble fractions were pelleted by ultracentrifugation (as above), the supernatant discarded and the pellets re-extracted in 1.0 ml of EBS for a further 30 min at 4 °C. Finally, a second ultracentrifugation step (as above) the supernatants are discarded and the pellets (outer membrane) are re-suspended either in 100 µl 0.5M Triethanolamine (pH= 7.5) for GAPDH enzymatic assay, or in 100 µl EB and 100 µl 2 x SDS-PAGE loading buffer for SDS-PAGE and Western blot and stored at -20 °C.

2.5.6 Expression and purification of recombinant cjGAPDH

Wild and mutated cjGAPDH were expressed for purification using IPTG induction of recombinant plasmids in *E.coli* Rosetta followed by His-tagged chromatography. The constructed vectors were transformed into *E. coli* (Rosetta DE3). The transformed colonies were added to 50 ml LuB as an overnight starter culture supplemented with 50 µg/ml ampicillin and 34 µg/ml chloramphenicol and incubated with shaking overnight. After that, the culture was diluted one hundred times into 1000 ml LuB medium containing same previously added antibiotics and incubated at 37 °C. Once the OD₆₀₀ of the cells reached to 0.6 - 0.7, the temperature was dropped to 18 °C and IPTG was added to a final concentration of 200 µM for induction. After 2-3 hours, the temperature was raised again into 37 °C and the cells were grown overnight in incubator with agitation.

On the next day, the cells were harvested re-suspended in lysis buffer (20 mM Na₂HPO₄, 500 mM NaCl, 20 mM imidazole pH 7.4 and 1 Roche complete EDTA free protease tablet; protease inhibitors. The suspension was sonicated at 10 kHz (10 seconds on, 20 s off) for five cycles and the cell debris was removed by centrifugation at 18000 g for 30 min. The binding step was performed by loading the supernatant onto 2 ml slurry Ni-

NTA in 50 ml falcon and left on roller at 4 ° C for 30 min. Next, the solutions were spun at 4000 rpm for 2 min and both supernatant and resin were collected. The resin was washed in wash buffer (20 mM Na₂HPO₄, 500 mM NaCl, 40 mM imidazole pH 7.4) to remove protein bound non-specifically to the resin. After that, the proteins were eluted with a buffer containing high imidazole concentration (20 mM Na₂HPO₄, 500 mM NaCl, 500 mM imidazole, pH 7.4) elution buffer. The concentration of the protein was measured using Bio-Rad assay after elution.

Part of eluted His-tagged protein was stored at -80 °C, the other part was further treated to remove 6xHis-tag from the proteins. The eluted protein was treated with 1:100 TEV protease (protease: protein ratio) and dialysed against imidazole (20 mM Na₂HPO₄, 50 mM NaCl, 1 mM DTT pH 7.4) at room temperature. The dialysed sample was loaded onto 1 ml slurry Ni-NTA to remove 6xHis tag from the protein, concentrated to 10 mg/ml, and finally was flash freezing in liquid nitrogen and stored at -80 °C following..

For the requirements of circular dichroism (Biswas *et al.*) assay, part of the purified proteins was buffer exchanged into (20 mM phosphate buffer pH= 7.4., 200 mM sodium fluoride) and concentrated to 5 mg/ml.

2.5.7 Circular Dichroism of wild and mutated GAPDH protein

Around 0.3 mg/ml of both GAPDH forms were used in CD spectrum assessment. The experiments were carried out in buffer containing 20 mM phosphate buffer pH= 7.4., 200 mM sodium fluoride and performed at room temperature using wavelengths with a range between 185-260 nm with a 0.1 cm path length. Additionally, each spectrum recorded were the average of 13 accumulations at scan speed of 20 nm-1 min, with bandwidth 1 nm at 0.5 nm stepwise and a 3 seconds time constant. A CD spectrum is obtained as a function of wavelength and is reported in molar ellipticity. The CD experiment was conducted with Prof Peter Moody and Dr Richard Cowan in Department of Molecular and Cell Biology, University of Leicester.

2.5.8 Whole cell pull-down method for study role of GAPDH in binding with Lf:

In order to characterise the role of GapA protein in iron uptake from lactoferrin, a binding assay was developed to study how *C. jejuni* strains pre-exposed to polyclonal anti-GapA antibody interacted with lactoferrin. *C. jejuni* strains were grown in MEM α medium to deplete intracellular iron stores. On the next day, a certain number of cells (OD₆₀₀=0.1; about 1 x 10⁸ cfu/ml) of each strain were incubated with anti-GapA for four hours. These

cells were washed with 1 ml of sterilised MEM α medium and incubated with 0.27 μ M lactoferrin for 1-2 hours. After this, the cells were washed gently with the same medium and lysed with 1X SDS-PAGE loading buffer. The same procedure was applied to control samples which had not been exposed to anti-GapA, only lactoferrin was added to these samples. Additionally, the same procedure was followed with cells pre-incubated with anti-MOMP as negative control. The samples and controls were subjected to SDS-PAGE and then Western blotting. Rabbit Anti-lactoferrin antibody was used to probe the membrane. The differences in intensity of lactoferrin bands between test samples and control groups on Western blot film was detected using the Image J programme (1.49v, National institute of Health, USA).

2.6 Bioinformatics

The analysis of sequences was performed by the Blast programmes on the NCBI website (<http://www.ncbi.nlm.nih.gov/blast/Blast.cgi>), and also by Clone Manager Professional Suite (Sci Ed Central, version 9.0, copyright 1994-2005, Scientific and Educational Software). Clone manager was used also to design all primers in this research. The sequence trace files were viewed using finch TV version 1.4.0 (Geospiza Research team). *C. jejuni* genome sequence data was firstly obtained from the web site: <http://xbase.bham.ac.uk/campydb/>.

After closing of this website, NCBI database was used.

SignalP 4.1 Server was used to examine if cjGAPDH has signal peptide for surface localisation or not, from this website

: <http://www.cbs.dtu.dk/services/SignalP/>.

Protein alignment was performed by using of clustal omega online programme from the website: <http://www.ebi.ac.uk/Tools/msa/clustalo/>.

Chapter 3. Characterisation of GAPDH protein in *C. jejuni* NCTC11168

3.1 Introduction

GAPDH is a metabolic enzyme that acts as an intermediate during glucose metabolism. It is located in the cytoplasm of the cell and it catalyses reversible oxidative phosphorylation of glyceraldehyde-3-phosphate (G3P) to 1,3-diphosphoglycerate (1,3 dPG) (Kim and Dang, 2005). Over the last two decades, researchers reported GAPDH can also be located as an anchorless cell surface protein in different prokaryotic and eukaryotic organisms, making GAPDH a potentially multifunctional protein (Sirover, 2011a). Interestingly, several studies demonstrated the capability of different bacterial pathogens using GAPDH to uptake iron from the host, particularly from the iron carrier proteins transferrin and lactoferrin (Lf) (Modun and Williams, 1999, Modun *et al.*, 2000, Boradia *et al.*, 2014a, Grenier and Tanabe, 2011).

Little is known about GAPDH in *C. jejuni* (cjGAPDH or GapA), therefore the “moonlighting” functions of cjGAPDH are yet to be elucidated. *C. jejuni* has one homologue of the GAPDH gene (*gapA*) which is located in an operon with *pgk*. Random transposon mutagenesis experiments indicated *gapA* is an essential gene (Metris *et al.*, 2011). One of the aims of work described in this chapter was clarifying whether *gapA* is essential in *C. jejuni*, and whether mutation of this gene can be complemented. In the case of *gapA* essentiality, the effect of changing the expression levels on the potential function of GAPDH in iron uptake will be examined. The creation of newly *C. jejuni* strains which have an inactivated wild type *gapA* gene complemented with another functional *gapA* allele elsewhere in the genome will be explained in the next section. Therefore, another aim of the work described here is the characterisation of these newly created strains of *C. jejuni* in terms of growth patterns, the expression of the *gapA* gene (transcription and translation), GAPDH enzymatic activity, and GAPDH sub-cellular localisation. The characterisation of these strains is important to investigate the potential function of GAPDH in iron acquisition from Lf iron binding proteins which will be described in the following chapters.

3.2 Mutagenesis of *gapA* gene

As described in section (1.4.4), the *gapA* gene in *C. jejuni* encodes only one copy of GAPDH. Therefore, it does not have another homologue to provide essential metabolic function of cjGAPDH. Therefore, due to this essentiality and in order to investigate its

function, chromosomal *gapA* was cloned and integrated into a non-functional region within the *C. jejuni* genome and placed under the control of different promoters in terms of gene expression levels. This strategy allows expression of GAPDH at different levels, which could be important in investigating the potential role of GAPDH in capturing iron from Lf.

To this end, we have used the pC46 plasmid complementation system, which involves recombination of complementing genes into *cj0046*, which is a pseudogene. The pseudogene *Cj0046* is conserved among the *C. jejuni* strains (NCTC11168, 81116, 81–176 and RM1221). Three types of pC46 plasmid have been used in this research; these plasmids have different heterologous promoters that can be used to drive expression of the complementing gene at different levels. The high (*porA*), medium (*fdxA*) and lower (*metK*) level promoter (Gaskin *et al.*, 2007b). The main features of these promoters are presented in table 3-1. All of these promoters originated from *C. jejuni*.

In this work, the *gapA* gene of *C. jejuni* NCTC11168 was cloned into the pC46 plasmids downstream of the three individual promoters driving gene expression at relatively different levels. These recombinant plasmids were used in transforming *C. jejuni* NCTC11168 in order to create the merodiploid *gapA* strains of *C. jejuni* which have different levels of *gapA* expression, followed by inactivation of *gapA* at the native location.

Table 3-1. Features of promoters in pC46 plasmids

Promoter	Length (bp)	Type of promoter	The gene	Function	Reference
<i>pfdxA</i>	72	iron responsive	Ferredoxin (<i>fdxA</i>)	FdxA is electron carrier in different metabolic reactions	(van Vliet <i>et al.</i> , 2001)
<i>pmetK</i>	86	constitutive	S- adenosyl methionine synthase (<i>metK</i>)	The major biological methyl donor	(Zano <i>et al.</i> , 2014)
<i>pporA</i>	253		Major outer membrane protein (<i>porA</i>)	Formation of functional porins	(Goulhen <i>et al.</i> , 2004)

3.2.1 Construction of merodiploid *gapA* *C. jejuni* strains

As *C. jejuni gapA* is considered an essential gene in *C. jejuni*, production of *C. jejuni gapA* merodiploid strains was a necessary first step before mutation of the wild-type *gapA*. The *gapA* gene was cloned into the three different pC46 plasmids, then recombinant *gapA*-pC46 plasmids were purified from *E. coli* DH5 α and transformed into *C. jejuni* NCTC11168. The *C. jejuni* transformation was based on the allelic genetic exchange between the chromosomal pseudo gene *cj0046* and its allele carried on the suicide pC46 plasmid. The aim was to produce three different merodiploid (2ngapA) strains of *C. jejuni*, with different expression levels of the complemented *gapA* gene.

Initially, *gapA* primers tailed with the restriction sites for *Nco*I were designed (see table 2.5) and used to amplify *gapA* from chromosome of *C. jejuni* NCTC11168 using Phusion PCR (see table 2.4), the vector's ribosome binding site was used. Both the insert (*gapA* gene) and vectors (pC46 plasmids) were cut and ligated, and transformed by electroporation into *E. coli* DH5 α . Transformant cells were screened by colony PCR, using *gapA*-Forward and *cj0046*-forward primers which ensure amplification of only the cloned *gapA*. Additionally, using these primers clarified the orientation of *gapA* in the pC46 plasmids. After that, the transformed cells were grown in LuB and the plasmids were extracted. The *gapA* cassettes on these plasmids were sequenced to ensure that they did not contain any mutation in *gapA* and promoters. The Blast program was used to analyse the sequencing data. The results showed that there were no errors on *gapA* gene, ribosome binding site (RBS) and the promoter regions in all plasmids. Therefore, these recombinant plasmids were suitable to transform into *C. jejuni* NCTC11168. The plasmid maps of these plasmids are shown in the index.

After obtaining these clones successfully, the next step was transformation of these recombinant plasmids into competent *C. jejuni* NCTC11168 by electroporation (see section 2.3.8.4). Colony PCR was carried out to investigate and confirm the generation of these strains. For this purpose, were used primers that target the chromosomal sequences flanking the *cj0046* gene, these sequences were not involved in the allelic exchange. The position of these primers are shown in figure 3-1 A & B.

Figure 3-1 C shows the results of PCR, the size of the PCR product from the wild type is around 2197 bp which is smaller than the other PCR products. The size in the other strains is larger because of insertion of the pC46 cloned cassette; figure 3-2 A & B.

C. jejuni NCTC11168 was used as a negative control, because it was not transformed by any of *gapA*-pC46 recombinant plasmids.

Overall, PCR results confirmed the achievement of obtaining three different merodiploid *gapA C. jejuni* strains. In addition to *gapA* in wild type locus, each strain has an additional copy of *gapA*, under the control of a different promoter, inserted into *cj0046* pseudogene:

C. jejuni gapA, cj0046::pfdxA-gapA (2gapA-pfdxA)

C. jejuni gapA, cj0046::pmetK-gapA (2gapA-pmetK)

C. jejuni gapA, cj0046::pporA::gapA (2gapA-pporA)

DNA sequencing for both *gapA* copies and promoters in these strains showed no errors suggesting that they can be used for the further work. The notation of each strain given in brackets will be used subsequently.

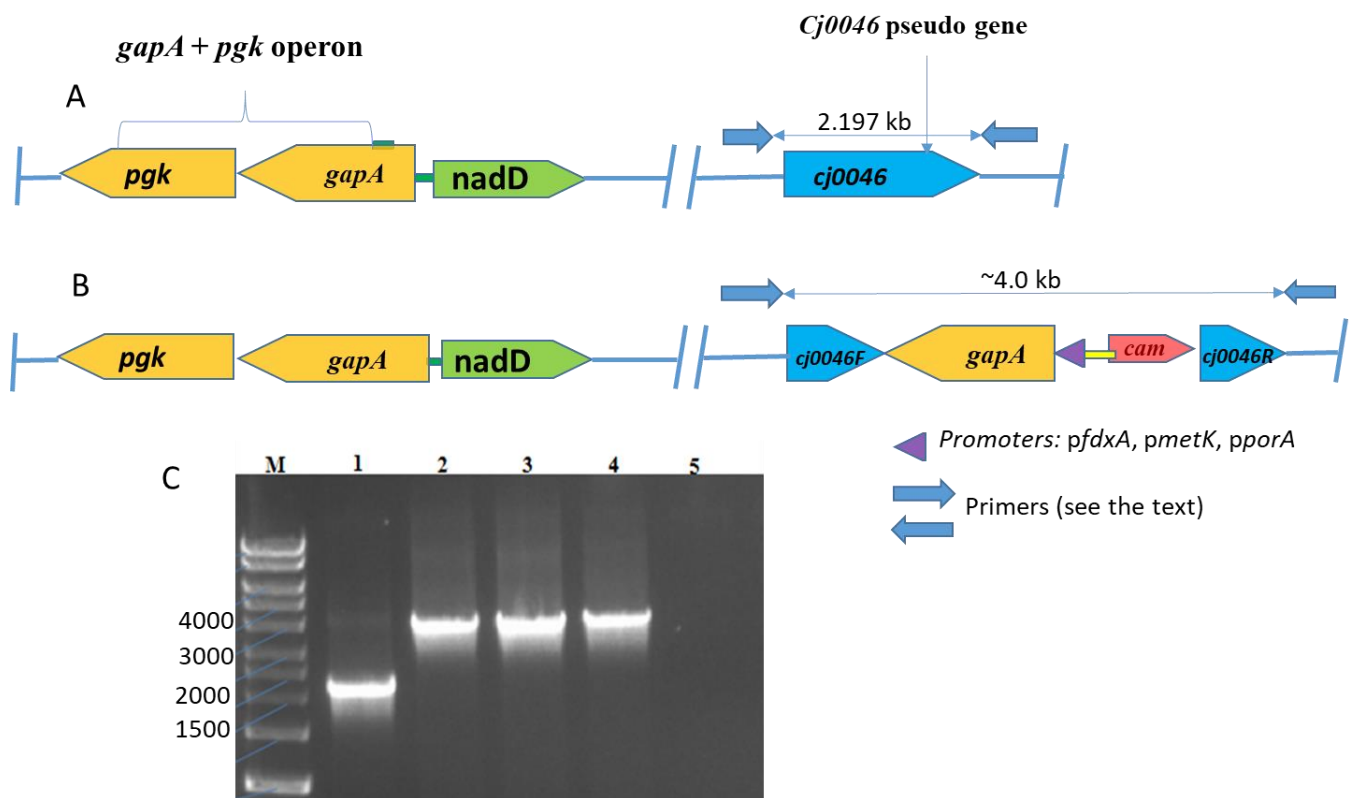


Figure 3-1. A, B, C. Verification of the construction of merodiploid *gapA* *C. jejuni* strains.

(A) and (B) show genomic context in WT and merodiploid strains respectively. The blue arrows indicate the primers that flank the cassette insertion site (flanking *cj0046-F*, and flanking *cj0046-F*), the sequences of primers were given in table 2.6. The *gapA* wild-type allele is in an operon with the *pgk* gene.

(C) Agarose gel electrophoresis of PCR products from the flanking region of *cj0046* to confirm creation of merodiploid *gapA*. M is hyperladder1 marker, lane 1 is *C. jejuni* WT. Lanes 2-4 are *2gapA-pfdxA* (3956 bp), *2gapA-pmetK* (3981 bp) and *2gapA-pporA* (4184 bp) respectively. The lane 5 is negative control (PCR mastermix + dH₂O).

3.2.2 Inactivation of wild-type *gapA* allele

An important objective in this research was to create *C.jejuni* strains in which the wild type *gapA* is inactivated while maintaining an active complemented *gapA* copy expressed at different levels. The cloning strategy applied to create new *C. jejuni* strains with an inactivated wild type chromosomal *gapA* gene will be described.

First, primers with incorporated restriction enzymes site (*SalI* and *EcoRI*); (see table 2.5), were designed to amplify the *gapA* gene and also part of the sequences flanking genes *pgk* and *nadD* which were about 700 bp and 400 bp respectively. Next, the PCR product (*gapA* with flanking sequences = insert) and pUC19 plasmid (vector) were digested with *SalI* and *EcoRI* and they were ligated together. The recombinant plasmid (*gapA*-pUC19) was electroporated into *E. coli* DH5 α and the transformant cells screened by blue/white screening system in which the white colonies were chosen for colony PCR to verify cloning of *gapA* into pUC19.

After that, deletion / insertion mutagenesis was performed to disrupt the *gapA* gene cloned in pUC19 by inverse PCR using *InvgapA*-F and *InvgapA*-R primers tagged with restriction site of *Bam*H1 (see table 2.5). Next, a terminator-less, promoter-less kanamycin resistance gene was introduced into the mutated gene and resultant ligations transformed into *E. coli* DH5 α . The LB agar plate supplemented with ampicillin (100 μ g/ml) and kanamycin (50 μ g/ml) was used to grow overnight the transformant cells at 37 °C in order to select the *E. coli* colonies that have pUC19 Δ *gapA*::kanamycin- plasmid. The grown colonies were screened by PCR to ensure the presence of a kanamycin cassette within the mutated *gapA* gene cloned in the pUC19 plasmid, and this was further confirmed by DNA sequencing reactions. Each of the flanking *gapA* genes, *pgk* and *nadD*, were sequenced and no errors detected. Finally, pUC19 Δ *gapA*::kanamycin plasmid figure 3-2, was transformed into competent *C. jejuni* wildtype and merodiploid *gapA* strains by electroporation. Transformants were plated onto MHA supplemented with vancomycin and trimethoprim in addition to kanamycin for the selection of the recombinant cells. Also the cultures were supplemented by glycerol, and horse blood to enhance recovery of the mutants (Purves *et al.*, 2010). The plates were incubated microaerobically (85 % N₂, 10 % CO₂ and 5 % O₂) at 42 °C in a variable atmosphere incubator for 3-5 days.

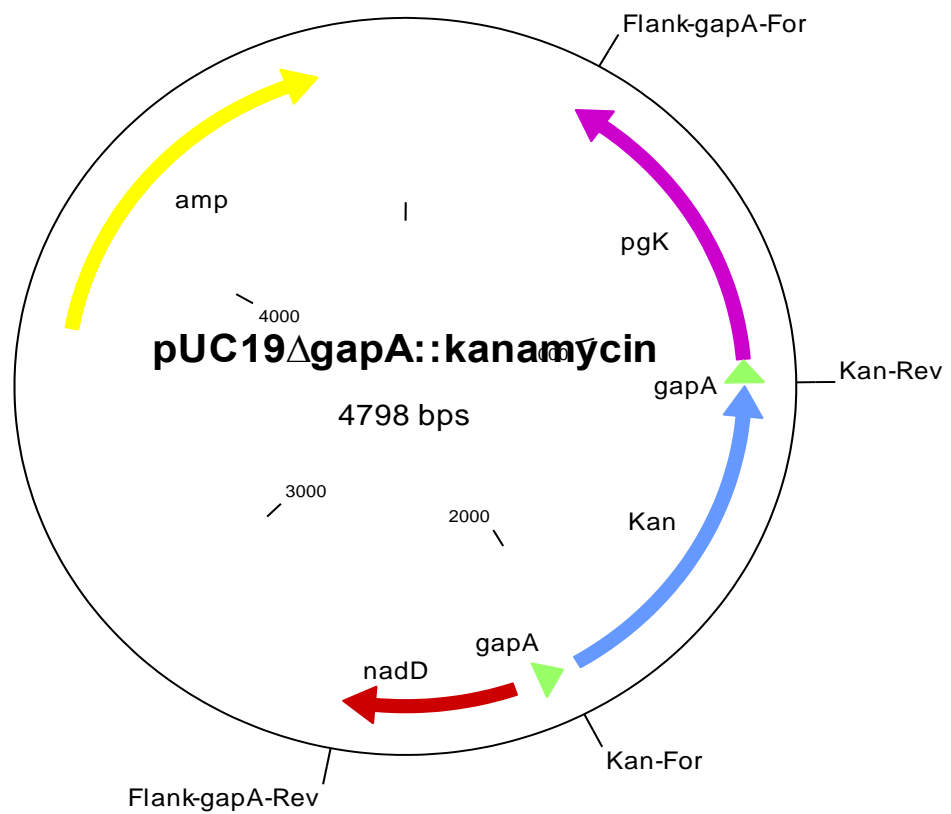


Figure 3-2. The map of pUC19 Δ gapA::kanamycin- plasmid (4798 bp).

The *gapA* gene was inactivated by deletion by inverse PCR and insertion of kanamycin cassette. The location of cloning PCR primers; Flank-*gapA*-For and Flank-*gapA*-Rev are indicated in addition to kanamycin primers kan-F and kan-R. The details of primers were given in table 2-5.

3.2.2.1 The *gapA* is essential gene and vital for the viability of *C.jejuni*

After three days of incubation, no colonies of the transformed wild type strain containing a single copy of the *gapA* gene were detected on selective medium with supplements (glycerol/ horse blood) nor without them. The experiment was repeated three times, the merodiploid strains were used as control. The concentration of kanamycin was decreased twofold in some MHA plates to enhance isolation of mutated cells. This result clarifies the essentiality of *gapA* gene in *C. jejuni* confirming that *gapA* gene is vital to the viability of this pathogen.

Regarding the transformation of merodiploid *gapA* strains, there were around 10-25 of *C. jejuni* colonies on kanamycin containing plates were obtained after 3 days of incubation. Ten colonies of each strain were randomly chosen for screening by PCR to confirm presence of terminator-less, promoter-less kanamycin cassette in the correct location of the *C. jejuni* genome. Different sets of primers were used for PCR amplification as shown in Figure 3-3 A, B. The primer set A; kanamycin forward and *pgk* forward were used to ensure presence of kanamycin cassette adjacent to the *pgk* gene. The primer set B are chromosomal flank primer of *pgk* gene and kanamycin forward for extra confirmation of kanamycin cassette position in native locus of *gapA*, and the red arrows indicate primer set C which are chromosomal flanking primers of *pgk* and *nadD* genes. The size of the PCR product in primer set C should be similar between wild type strain and mutated *gapA* strains (3000 bp) due to the fact that the deleted sequences of *gapA* during the mutagenesis were about 800 bp which is close to the size of inserted kanamycin cassette. At the end, three strains of *C. jejuni* were constructed:

- 1- *C. jejuni* $\Delta gapA::kanR$ *cj0046::pfdxA-gapA* ($\Delta gapA$ -*pfdxA*),
- 2- *C. jejuni* $\Delta gapA::kanR$ *cj0046::pmetK-gapA* ($\Delta gapA$ -*pmetK*)
- 3- *C. jejuni* $\Delta gapA::kanR$ *cj0046::pporA-gapA* ($\Delta gapA$ -*pporA*).

DNA sequencing for the complemented *gapA* gene, DNA sequencing of promoters and *pgk* gene in these new strains showed no errors. The notation of each strain given in brackets will be used in all upcoming work of this project.

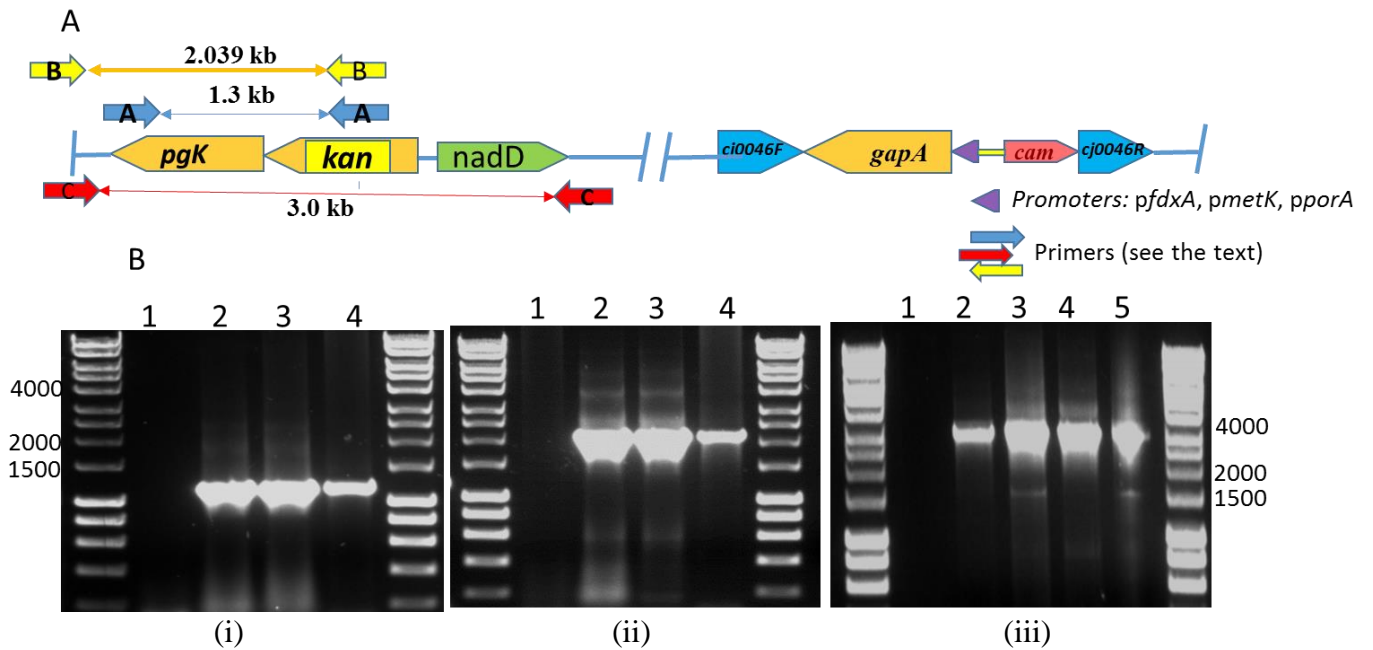


Figure 3-3 A, B. Verification of creation of $\Delta gapA$ -*pfdxA*, $\Delta gapA$ -*pmetK*, and $\Delta gapA$ -*pporA* *C. jejuni* strains.

(A) *C. jejuni* genomic context of inactivated *gapA* strains. Kanamycin cassette was inserted in *gapA*. The blue arrows indicate primer set A; kanamycin forward (*kan*-F) and Flank-*gapA*-For, yellow arrows are primer set B; chromosomal flank primer of *pgk* gene (Flank-*pgK*-For) and *kan*-F, and the red arrows indicate primer set C which are Flank-*pgK*-For and Flank-*nadD*-Rev.

(B) Agarose gel electrophoresis to confirm the creation of mutated *gapA* strains.

(i) Primer set A on the left hand photo, PCR product is 1300 bp, 1= WT as negative (-ve) control 2, 3, 4 are $\Delta gapA$ -*pfdxA*, $\Delta gapA$ -*pmetK* and $\Delta gapA$ -*pporA* strains respectively.

(ii) is primer set B in the middle, PCR product is 2039 bp 1= WT as (-ve) 2, 3, 4 are $\Delta gapA$ -*pfdxA*, $\Delta gapA$ -*pmetK* and $\Delta gapA$ -*pporA* strains respectively.

(iii) is primer set C on the right hand photo, PCR product is 3000 bp; 1= H₂O added to PCR reaction as -ve control, 2= WT while 3, 4, 5 are $\Delta gapA$ -*pfdxA*, $\Delta gapA$ -*pmetK* and $\Delta gapA$ -*pporA* strains respectively.

3.2.3 Characterisation of constructed *C. jejuni* strains

3.2.3.1 The growth assay of merodiploids and mutated *gapA* strains

Growth assays for merodiploid and inactivated *gapA* strains were performed in order to detect any alteration in the phenotype compared to the wild type strain. The MHB medium was chosen as culture medium as it supports the growth of *C. jejuni* (Davis and DiRita, 2008). The growth assay was accomplished as mentioned previously (see section 2.4.1). The growth kinetics parameters; doubling time and growth rate of merodiploid and inactivated *gapA* strains were calculated as mentioned in (section 2.4.3) and compared with wild type strain. The resulting OD₆₀₀ values were log transformed and plotted versus time to determine the slope at the exponential growth phase and to calculate the specific growth rate (μ_{\max} h⁻¹) and doubling time (Widdel, 2007).

The results are shown in Figure 3-4 and tables 3-2 and 3-3. Generally, the growth kinetics reveals similar trends between the merodiploid and wild type strains as there was no differences in growth rate and doubling time in MHB; table 3-2. The mutated native *gapA* strains $\Delta gapA-pmetK$ and $\Delta gapA-pfdxA$ strains also revealed no significant differences with the wild type strain. However, the doubling time and growth rate of $\Delta gapA-pporA$ were significantly higher than the wild type strain. Additionally, there was a rapid decline in growth and entry into the stationary and death phases was observed in the merodiploid *gapA* strains; *2gapA-pporA*, *2gapA-pfdxA* and also mutated strains $\Delta gapA-pfdxA$ and $\Delta gapA-pporA$.

Between the merodiploids and mutated strains, no difference in growth kinetics parameters were observed except *2gapA-pporA* and $\Delta gapA-pporA$ strains. The latter demonstrated a faster growth rate ($0.32 \text{ h}^{-1} + 0.02 \text{ SD}$) as compared to the growth rates of both the wild-type ($0.58 \text{ h}^{-1} + 0.05 \text{ SD}$) and *2gapA-pporA* ($0.6 \text{ h}^{-1} + 0.04 \text{ SD}$) strains. The reason for this difference is not clear as the complemented *gapA* allele in both of the mutants is driven by the same constitutive promoter.

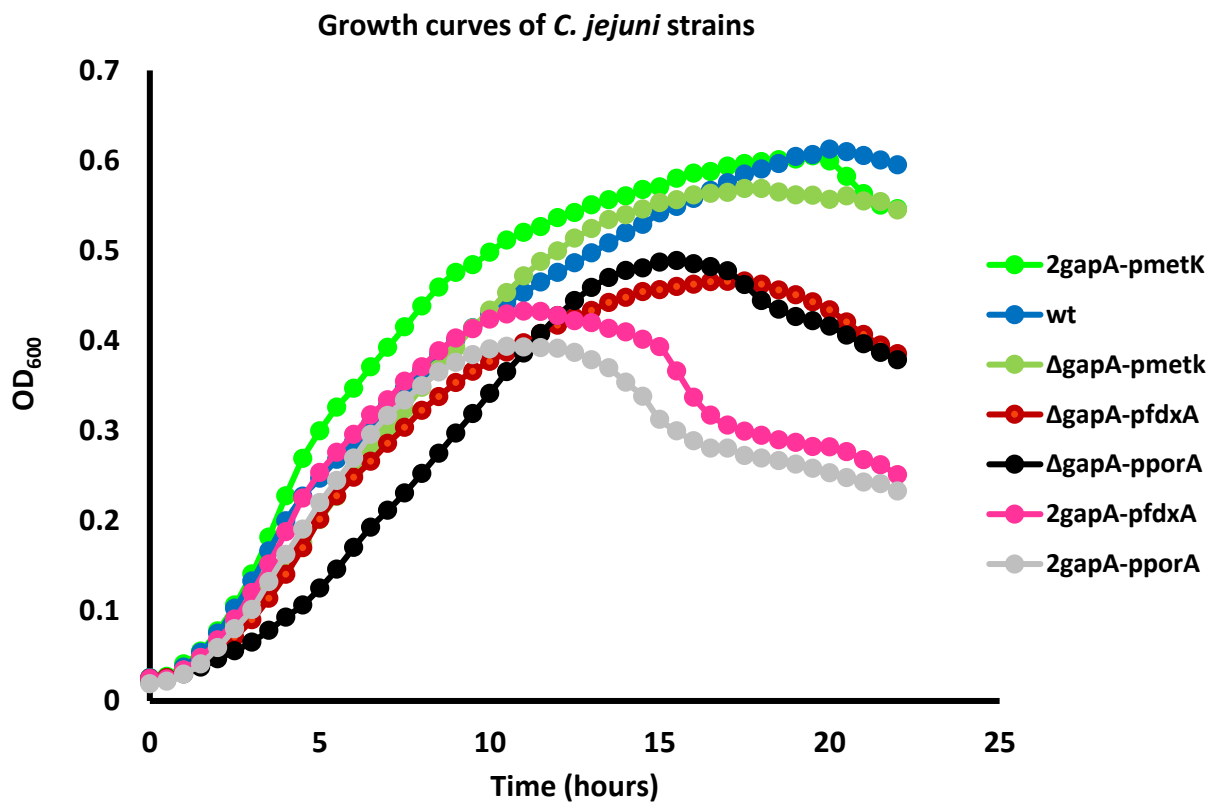


Figure 3-4. Growth curve assay of merodiploids, *gapA* mutated and wild strain NCTC 11168.

The strains were grown in MHB under microaerobic conditions at 42° C. The optical density (OD) of the initial cell suspension was adjusted to OD₆₀₀= 0.05, the growth was measured as the optical density of the culture at 600 nm. The readings of OD were taken every 30 minutes for 24 hours by FLUOSTAR omega plate reader. This figure represents the combination of three biological repeats.

Table 3-2 Growth rate (h^{-1}) and doubling times (h) of wild type, merodiploid and mutants calculated from growth curve given in Figure 3-4

Strains Growth parameters	WT	Diploids			Complements		
		<i>2gapA-pfdxA</i>	<i>2gapA - pmetK</i>	<i>2gapA - pporA</i>	<i>ΔgapA-pfdxA</i>	<i>ΔgapA-pmetK</i>	<i>ΔgapA-pporA</i>
1- Growth rate (h^{-1}) (P value vs WT)	0.58 ± 0.05	0.54 ± 0.06 (0.52)	0.56 ± 0.03 (0.62)	0.60 ± 0.04 (0.72)	0.47 ± 0.01 (0.09)	0.45 ± 0.01 (0.08)	0.32 ± 0.01 (0.02)*
2- Doubling time (h) (P value vs WT)	1.16 ± 0.08	1.21 ± 0.15 (0.58)	1.18 ± 0.1 (0.74)	1.29 ± 0.25 (0.43)	1.43 ± 0.01 (0.07)	1.37 ± 0.14 (0.08)	2.15 ± 0.1 (0.02)*

* p<0.05

Table 3-3 Statistical differences calculated by unpaired t test between growth rate and doubling time of wild type, merodiploid and mutated strains.

	Growth Rate			Doubling time		
Diploids vs Complements	<i>2gapA-pfdxA</i> Vs <i>ΔgapA-pfdxA</i>	<i>2gapA - pmetK</i> Vs <i>ΔgapA-pmetK</i>	<i>2gapA - pporA</i> Vs <i>ΔgapA-pporA</i>	<i>2gapA-pfdxA</i> Vs <i>ΔgapA-pfdxA</i>	<i>2gapA - pmetK</i> Vs <i>ΔgapA-pmetK</i>	<i>2gapA - pporA</i> Vs <i>ΔgapA-pporA</i>
P value	0.23	0.06	0.02*	0.14	0.16	0.01*

* p<0.05

3.2.3.2 Measurement of the transcriptional levels of the *gapA* gene in constructed strains by qRT-PCR.

Transcription levels of *gapA* were measured by real time PCR (qRT-PCR) in order to determine the expression levels of the different promoters. *C. jejuni* strains were grown to mid-log phase then total RNA was extracted, Dnase treated, and reverse transcribed into cDNA (see section 2.3.10.4). The mRNA transcripts levels of *gapA* gene and *rpoA* (reference gene) were quantified by qPCR using ddCt method (Scheffe *et al.*, 2006, Ritz *et al.*, 2009). The qPCR assay was carried out in three replicates at three different times for each sample and results were combined and averaged, the results are given in figure 3-5.

The results show that the transcription levels of GAPDH are relevant to the controlled promoter, high in *porA*, medium in *fdxA* and lower in *metK* *C. jejuni* strains. The mRNA transcripts levels in merodiploid strains were higher than that of mutated *gapA* strains but were significantly different, *2gapA-porA* strain has the highest level of mRNA transcriptional levels among all the strains with approximately a 97-fold increase versus wild-type. Interestingly, the results show the mRNA transcription level of *gapA* in *C. jejuni* wild stain was considerably lower than all other strains. Therefore, all of these constructed *C. jejuni* strains can be considered *gapA* over-expressed strains. In relation with growth assay, the strains shown high transcriptional level of *gapA*, *2gapA-fdxA*, *2gapA-porA* and Δ *gapA-pporA* have entered stationary and death phases of growth earlier than WT strain.

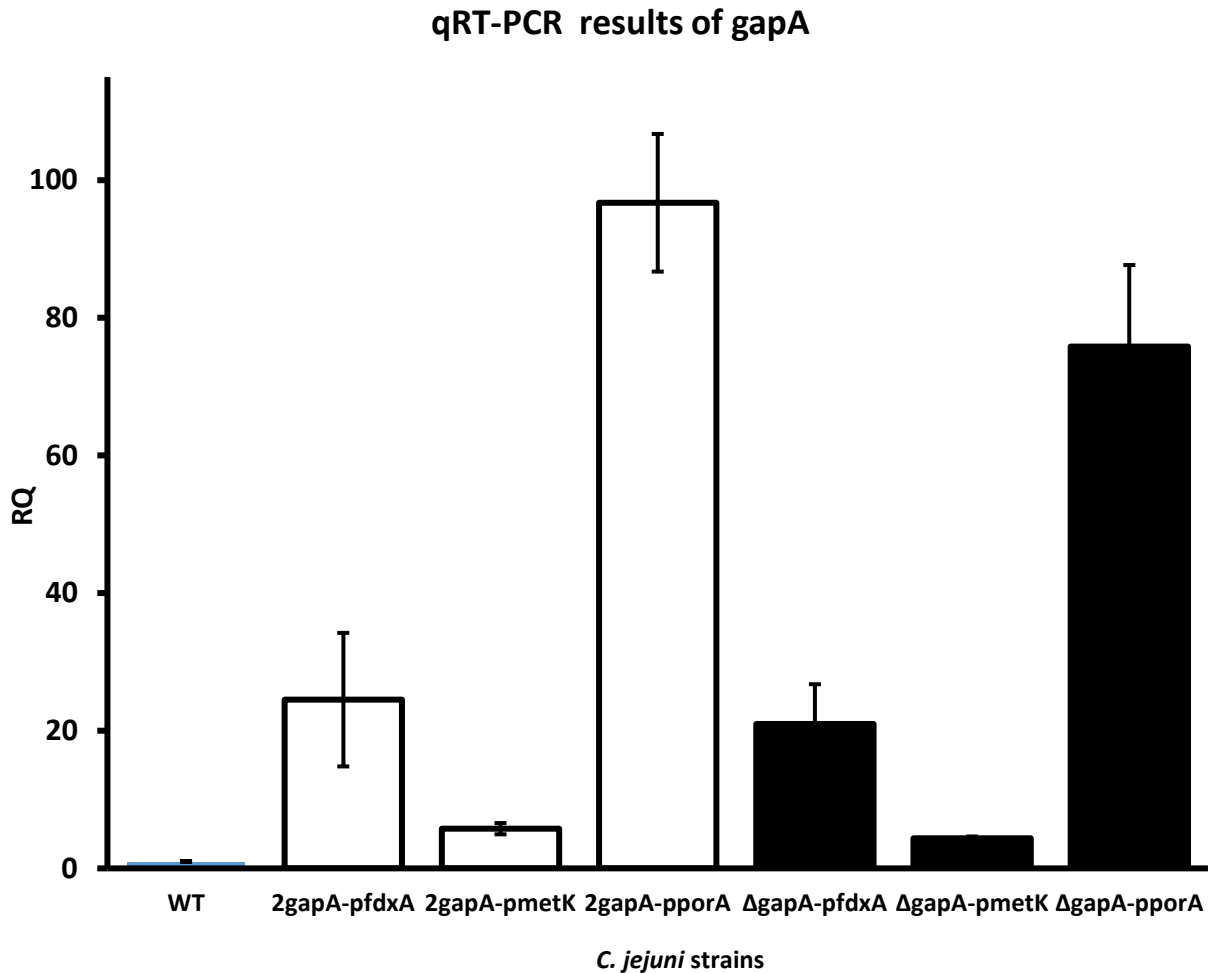


Figure 3-5. Relative qRT-qPCR results of *gapA* gene in *C. jejuni* constructed strains.

The mRNA transcripts levels of *gapA* were measured by qPCR and compared with *rpoA*. The blue column represent the wild type strain, whereas the white and black columns represent the merodiploid and mutated *gapA* strains, respectively. The results represent the combination of three biological repeats (each with three replicates). The error bars are indicated by standard deviation. Level. The transcription levels were relative to wild type strain.

3.2.3.3 Western blot of whole cell GAPDH among the strains

Western blot analysis was used to identify the expression of *C. jejuni* GAPDH protein among the strains. *C. jejuni* strains were grown on MHA supplemented with selective antibiotics, the growth was scraped off with MHB and equalised for all strains at OD₆₀₀=0.1. After that, the cells were grown to mid-log phase of growth, the whole cell lysis was prepared and western blot analysis was accomplished as mentioned in (section 2.5.3).

Rabbit polyclonal anti-GapA primary antibody was used to probe the membrane. This antibody was produced by Eurogentec (<http://www.eurogentec.com/eu-home.html>) following overexpression and purification of GapA protein, the antibody was tested successfully for detection of expressed GAPDH from *C. jejuni* (Prof. Julian Ketley, unpublished data). The results illustrated in figure 3-6 A, B show that there is a prominent \approx 43 kDa, which represents GAPDH polypeptide in all *C. jejuni* strains. However, an additional \approx 30 kDa band can be seen in most overexpressed GapA strains. No bands were seen on the membrane probed only with secondary antibody (data not shown), this indicated that the all detected bands were specific to primary antibody.

Fiji Image J programme was used to estimate the levels of GAPDH proteins based on the measurement of band intensity of each strain. As the concentration of proteins of tested strains was equalised before conducting Western blot, GAPDH protein expressed by wild type strain was used to normalise the results of GAPDH expression levels. The bar chart Figure 3-6 B shows the result of Image J analysis. The results indicated that the level of normalised GAPDH protein was high in *2gapA-porA* strain; 8 fold higher than wild type. These results are in correlation with RT-PCR, the levels of GAPDH were relevant to the strength of the promoter and the number of expressed *gapA* genes.

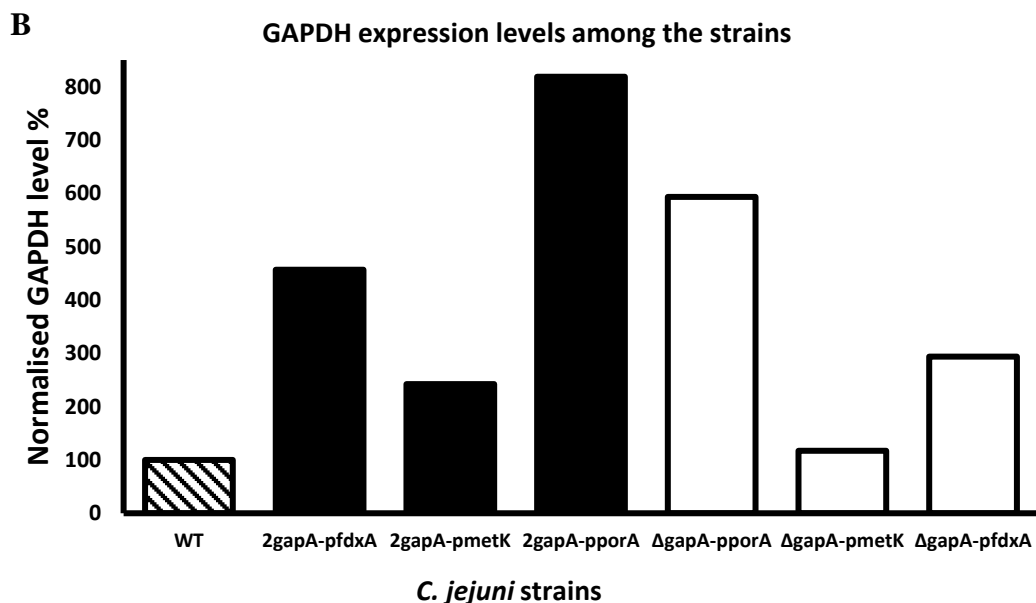
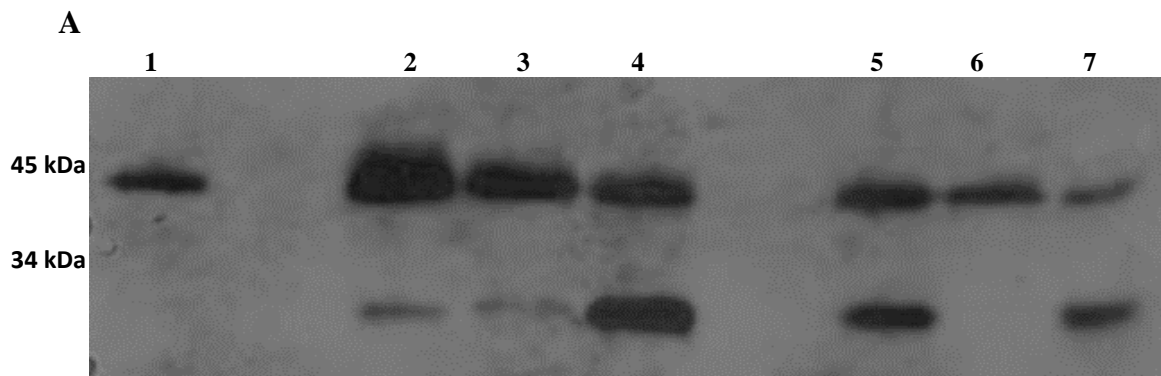


Figure 3-6 A and B. Assessment of GAPDH protein expression of *C. jejuni* strains by Western blot.

(A) Western blot of *C. jejuni* proteins, 1= WT, 2= 2gapA-pfdxA, 3= 2gapA -pmetK, 4=2gapA-pporA, 5=ΔgapA-pporA, 6= ΔgapA-pmetK and 7= ΔgapA-pfdxA. The cells were normalised to an OD₆₀₀ of 0.025 and grown until they reached the mid-log phase of growth. 10 μl of cell lysate were loaded onto an SDS-PAGE gel. The proteins were transferred to PVDF membranes and probed with 1:5000 dilution of primary antibody (polyclonal rabbit anti-GapA), washed and secondary antibody (Goat anti-rabbit HRP tagged) added with 1:5000 dilution.

(B) The expression level of proteins detected by anti-GapA measured from the Western blot, using Fiji Image J normalised to expression of GapA in WT strain. The data was obtained by use of Fiji Image J1.49 (Rasband, W.S., ImageJ, U. S. National Institutes of Health, Bethesda, Maryland, USA). The intensity of both bands were combined.

3.2.3.4 GAPDH enzyme activity measurements among the constructed strains

The GAPDH assay of intact cells was carried out in order to determine the enzyme function of GAPDH in mutant and diploid strains compared to the wild type. It is hypothesised that GAPDH activity will reflect the strength of the promoter controlling the complemented copy of *gapA*. Moreover, as this assay is not based on lysis of the cells, the detection of GAPDH activity of the intact *C. jejuni* cells might indicate the cell surface localisation of GAPDH. In this experiment, the *C. jejuni* strains were grown overnight and then assayed for GAPDH activity in the presence of 2 mM G3P and either 2 mM NAD or NADP cofactor as mentioned in section (2.5.4.1). Both NAD and NADP coenzymes were tested to clarify that new created strains of *C. jejuni* are dual coenzyme specificity. GAPDH activity was measured by taking the absorbance reading of the supernatant at 340 nm.

The results illustrated in figure 3-7 show that the levels of GAPDH enzymatic activity were significantly higher in merodiploid and *gapA* mutated strains than the WT strain because *gapA* gene is overexpressed in these strains. Additionally, the results are in correlation with previously observed in RT-PCR and Western blot and might be related to growth patterns observed in figure 3-4. Interestingly, these results could suggest extracellular activity of GAPDH in *C. jejuni*.

On the other hand, the results also indicate that GAPDH in *C. jejuni* demonstrates dual coenzyme specificity towards NADH and NADPH. However, the levels of NADPH formed were significantly higher than NADH so GAPDH protein in *C. jejuni* is preferentially utilizing NADP more than NAD.

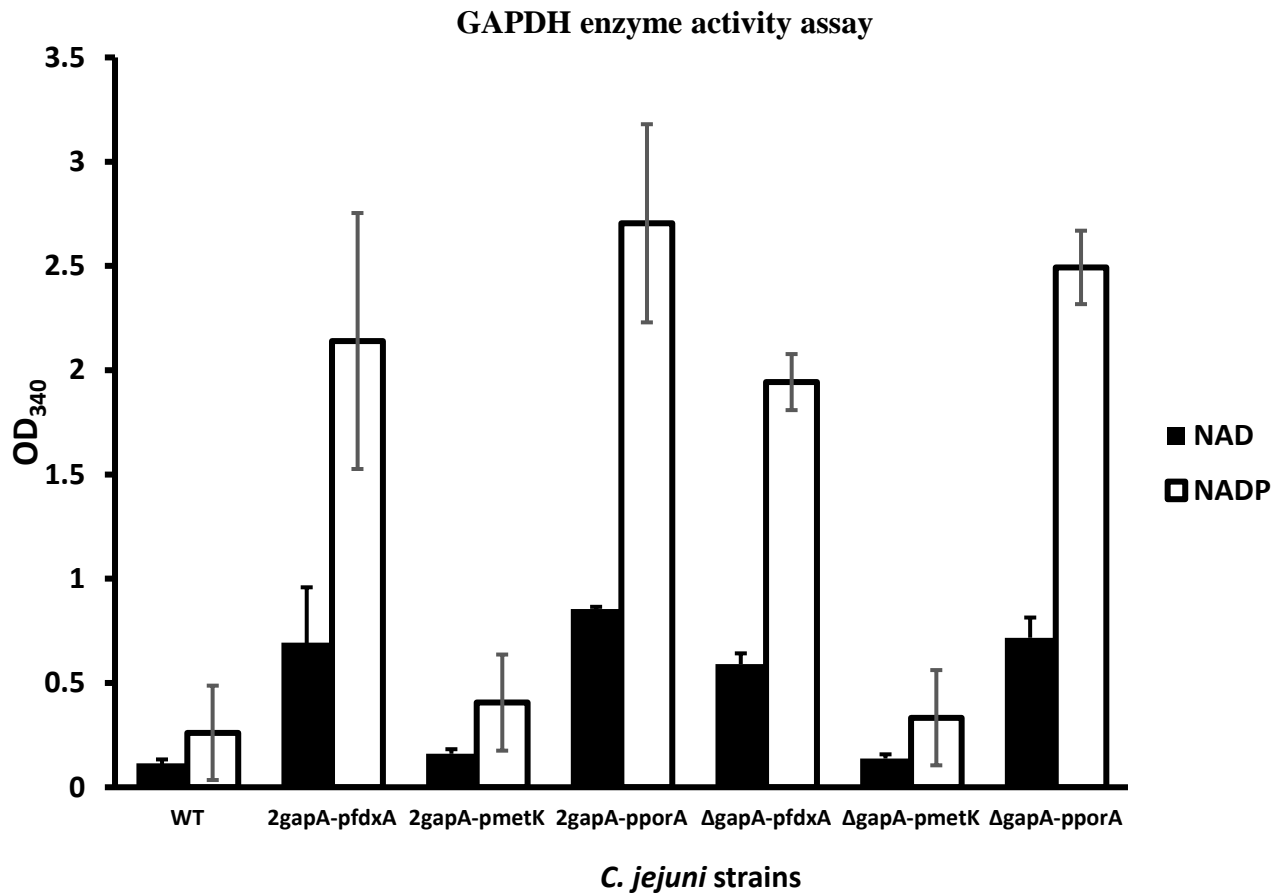


Figure 3-7. Whole cell GAPDH enzyme activity of *C. jejuni* strains.

The graph shows the NADH dependent GAPDH activity (black columns) and NADPH dependent GAPDH activity (white columns) determined from whole cell GAPDH assays of WT, 2gapA-pfdxA, 2gapA-pmetK, 2gapA-pporA, ΔgapA-pfdxA, and ΔgapA-pmetK, ΔgapA-pporA *C. jejuni* strains. The amounts of cells used were normalised to an OD₆₀₀ of 0.1. The data presented is an average of at least 3 independent biological repeats and corrected by control samples as mentioned in chapter 2 (Materials and Methods). The error bars indicate the standard deviations of the data.

3.3 Identification of GAPDH as membrane associated protein in *C. jejuni*

The subcellular localisation of GAPDH in *C. jejuni* has not previously been determined, but knowledge of the GAPDH localisation in *C. jejuni* is essential to understand its function. In a number of different organisms, although GAPDH does not have an N-terminal signal sequence (peptide signal) or a C-terminal hydrophobic tail which are necessary for export to the cell surface, the research reported GAPDH as an anchorless surface protein (Seidler and Seidler, 2012). This resulted in GAPDH being considered as a multi-function protein apart from its fundamental role in metabolism and energy production. In *C. jejuni*, it is important to determine the localisation of GAPDH, cell surface localisation will open new insights in research on this enteropathogenic bacterium and link this location with potential, non-identified multiple functions of cjGAPDH.

In this section, the subcellular localisation of GAPDH in *C. jejuni* NCTC11168, wild type *gapA* mutated strains will be examined in order to identify GAPDH localisation. The results of whole cell enzymatic activity of GAPDH in section (3.2.3.3) provided evidence of the possible localisation of GAPDH on the cell surface of *C. jejuni*. Therefore, further experiments carried out to attempt to clarify if cjGAPDH is surface associated.

3.3.1 Measurement of intact *C. jejuni* cells GAPDH enzyme activity assay after treatment with proteinase K

The levels of whole cell GAPDH enzyme activity was estimated after treating the cells with protein digestion enzyme proteinase K. This enzyme can digest the proteins located on the surface of the cells, this should result in a decrease in GAPDH levels if it is located on the cell surface of *C. jejuni*. Overnight growth of wild type, the lowest GAPDH over-expressed mutated strain ($\Delta gapA-pmetK$) and the highest ($\Delta gapA-pporA$) in MHB medium was equalised to OD₆₀₀= 0.1 in 1.5 ml microcentrifuge tubes. The tubes then were centrifuged, the pellets were re-suspended in 50 μ l of 20 mg/ml of proteinase K and incubated at 37 °C in a water bath for 1 hour. The cells were then centrifuged for 10 minutes at 13,000 xg and washed once with sterilised MHB medium and centrifuged again for 1 minute. The GAPDH assay buffer was added and whole cell GAPDH measured as previously mentioned (section 2.5.4.1).

The results shown in figure 3-8 indicate that the levels of GAPDH-NADP were always significantly higher in the cells not treated with proteinase K than cells treated with proteinase K (p value<0.05). Overall, these results indicate that the cjGAPDH protein is

present on the surface of the *C. jejuni* cells. Although proteinase K reduces the amount of GAPDH on the cell surface, there is still a considerable amount of GAPDH detected by this enzymatic assay as seen in figure 3-8. Under the microscope, there was not a great difference in the bacterial populations (number and shape) between the control and test samples either after proteinase K or after GAPDH assay buffer treatment. However, it is unknown whether this enzyme activity represents undigested cell surface GAPDH or leaked intracellular GAPDH.

3.3.2 Measurement of whole *C. jejuni* cells GAPDH enzyme activity assay after treatment with anti-GapA antibody

To confirm the findings obtained from the proteinase K-treated whole cell GAPDH assay, anti-GapA antibody was used to investigate the localisation of GAPDH on the cell surface of *C. jejuni*. The anti-GapA antibody should only bind the GAPDH protein if the protein is located on the surface of the cells resulting in the inactivation of GAPDH. Accordingly, the levels of GAPDH enzyme activity should be decreased due to this interaction.

Apart from incubation of *C. jejuni* strains with anti-GapA at titration of 1:200 in the tubes equalised with $OD_{600} = 0.1$ of the cells, all other steps of the assay were similar to the previous proteinase k treatment. The results in figure (3-9) show that the levels of GAPDH activity measured by the assay decreased significantly after incubation with anti-GapA, the p values of two paired *t* test are : WT =0.03, $\Delta gapA$ -*pmetK*=0.02, $\Delta gapA$ -*pporA* =0.01.

Similarly to the previous results of proteinase k treatment, there are detectable levels of GAPDH activity in strains treated with anti-GapA. However, the microscopic investigation did not indicate to great alterations in the count and the shape of bacterial populations during the assay. Nevertheless, the findings are consistent with the previously obtained, which indicate the association of GAPDH protein on the surface of *C. jejuni*.

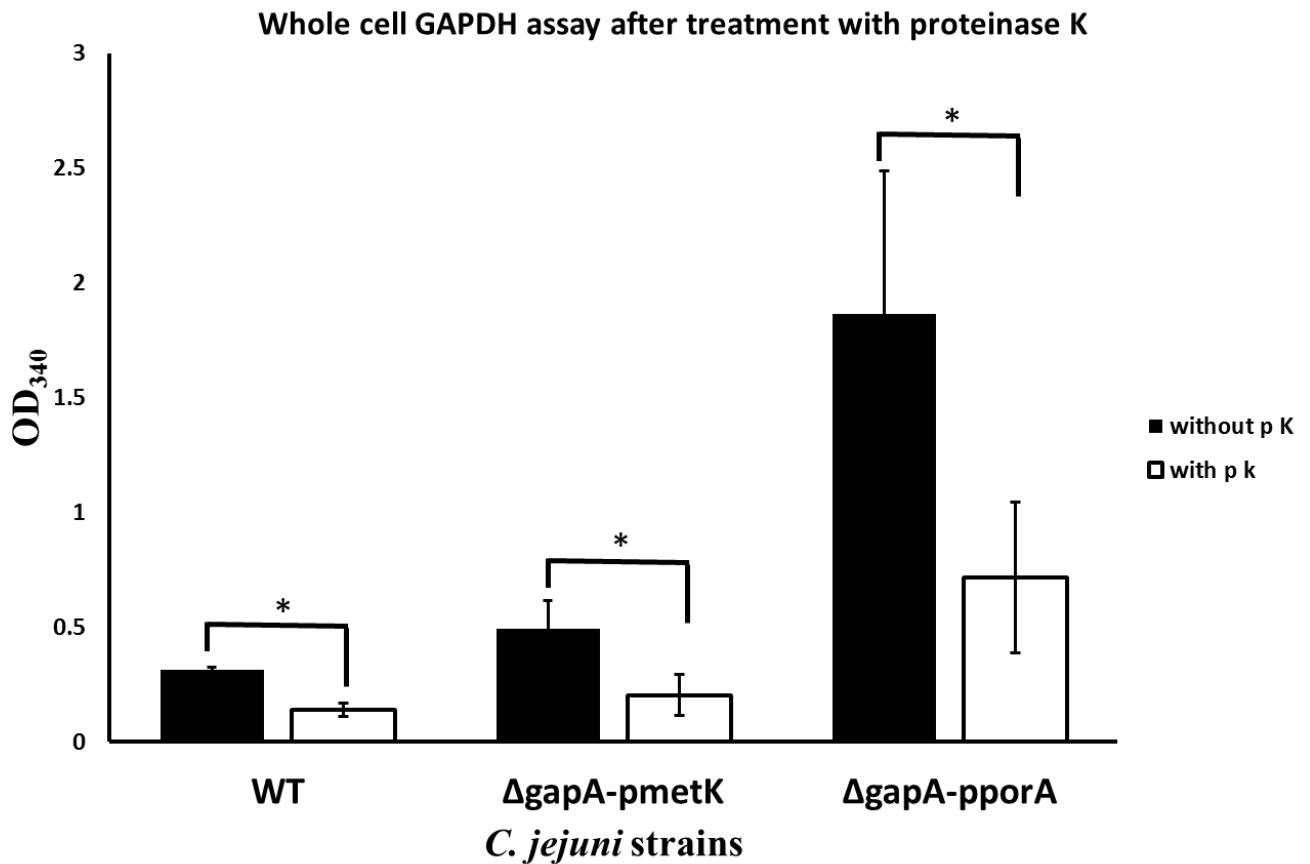


Figure 3-8. Intact cell GAPDH-NADPH enzyme activity of *C. jejuni* strains with/without treatment of proteinase K (p k).

After overnight growth in MHB, the cells were equalised on OD₆₀₀ = 0.1, spun at 13,400 rpm for 2 minutes followed by incubating with 20 mg/ml p k at 37° C for 1 hour. Cells were spun and washed by sterilised MHB and spun again before adding of GAPDH assay buffer. The P value of the differences in GAPDH enzyme activity between each individual strain treated with/without proteinase K was as following: WT = 0.03, $\Delta gapA$ -pmetK = 0.05, $\Delta gapA$ -pporA = 0.03; (* = p < 0.05). The data presented is an average of at least 3 independent biological repeats, the error bars indicate the standard deviations of the data.

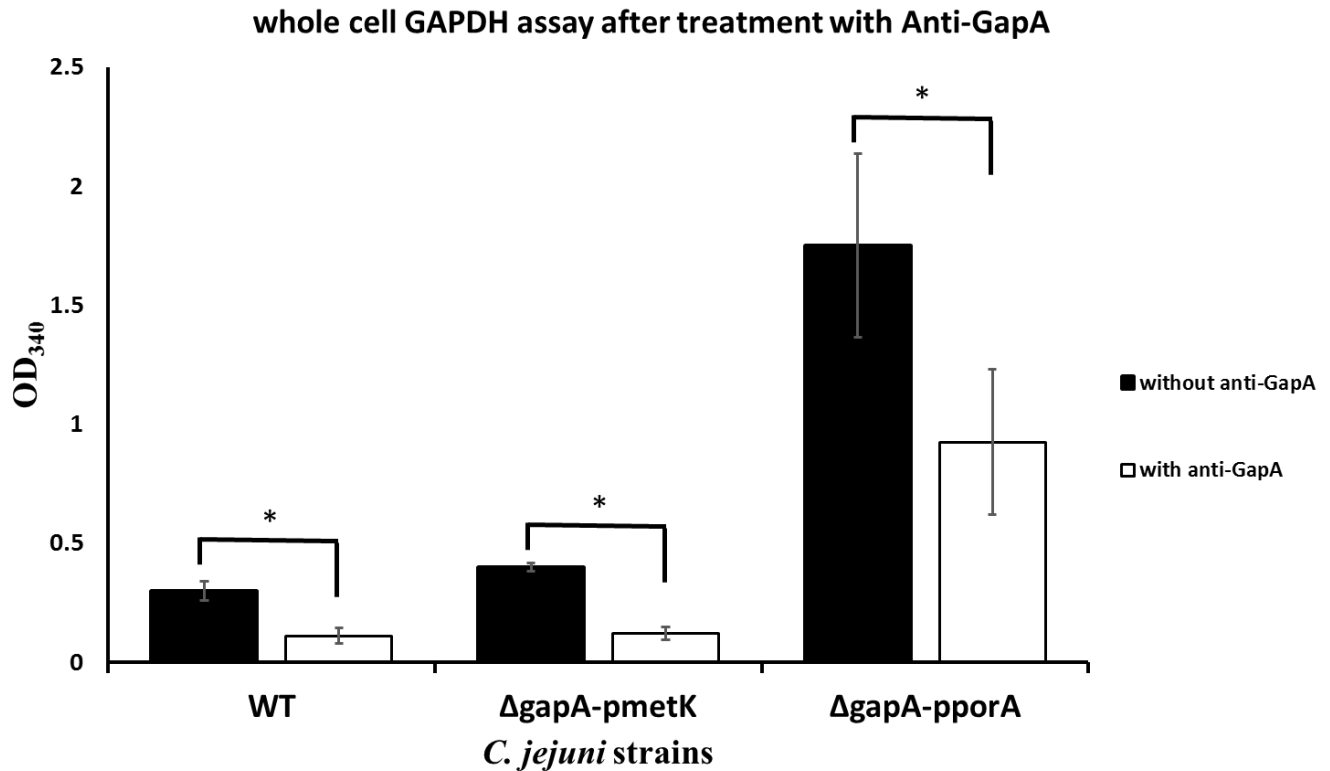


Figure 3-9. Intact cell GAPDH-NADPH enzyme activity of *C. jejuni* strains with/without treatment of anti-GapA.

The same procedure in previous section was followed to prepare the cells. The anti-GapA was added to the equalised cells by 1:200 titration. P value of the differences in GAPDH enzyme activity between each individual strain treated with/without anti-GapA was as following: WT =0.03, Δ gapA-pmetK=0.02, Δ gapA-pporA =0.01, (* = p<0.05).. The data presented is an average of at least 3 independent biological repeats, the error bars indicate the standard deviations of the data.

3.3.3 Fractionation of *C. jejuni*

In order to investigate the sub-cellular localisation of GAPDH within *C. jejuni* NCTC11168, cell fractionation experiments were carried out on *C. jejuni* wild type and *gapA* mutated strains. The method used was similar to that developed previously (Van Vliet *et al.*, 1998) based on differential solubility in Sarkosyl; see section (2.5.5). Three fractions of *C. jejuni* were extracted, cytosol, total membranes (inner and outer membranes) and outer membrane fractions. Each fraction was divided into two aliquots, one for determination of GAPDH enzymatic activity and the other for western blot analysis.

Accomplishment of this work needs immunoblot protein marker in order to control subcellular contamination of outer membrane fraction by cytoplasmic proteins. Liu *et al.*, (2014) had used *E. coli* anti-GroEL antibody (sigma), which can cross-react with *C. jejuni* GroEL protein (~62 kDa) (Liu *et al.*, 2014). Therefore, this antibody was used in this experiment for this purpose. GroEL is a cytoplasmic protein important for proper folding of 10% of newly synthesized proteins (Liu *et al.*, 2014, Houry *et al.*, 1999).

3.3.3.1 Detection of GAPDH activity in cell fractions

GAPDH enzymatic activity was evaluated in cell fractions by the method described previously (Villamón *et al.*, 2003, Boradia *et al.*, 2014a) with minor modifications. Briefly, 10-50 μ l (200 ng/ μ l) of proteins of cell fraction were added to 200 μ l of GAPDH assay buffer in a 96 well plate. The other steps are similar to those mentioned in section 2.5.4.2, the control samples were the same cell fractions incubated with GAPDH buffer without G3P. The cytosol and outer membrane fraction from WT and $\Delta gapA$ -*pmetK* strains were investigated and results are shown in figure 3-10. The $\Delta gapA$ -*pmetK* strain was chosen because its expression levels of *gapA* is close wild type, therefore, the probable effects of high overexpression on GAPDH localisation might be minimised.

The results demonstrate the presence of GAPDH enzymatic activity in both fractions, the enzymatic activity of GAPDH was observed in both cytosol and outer membrane fractions. No significant difference were observed between fractions. However, these results provide another indication of membrane association of GAPDH protein in *C. jejuni* which is in agreement with results given in previous sections (3.2.1 and 3.2.2).

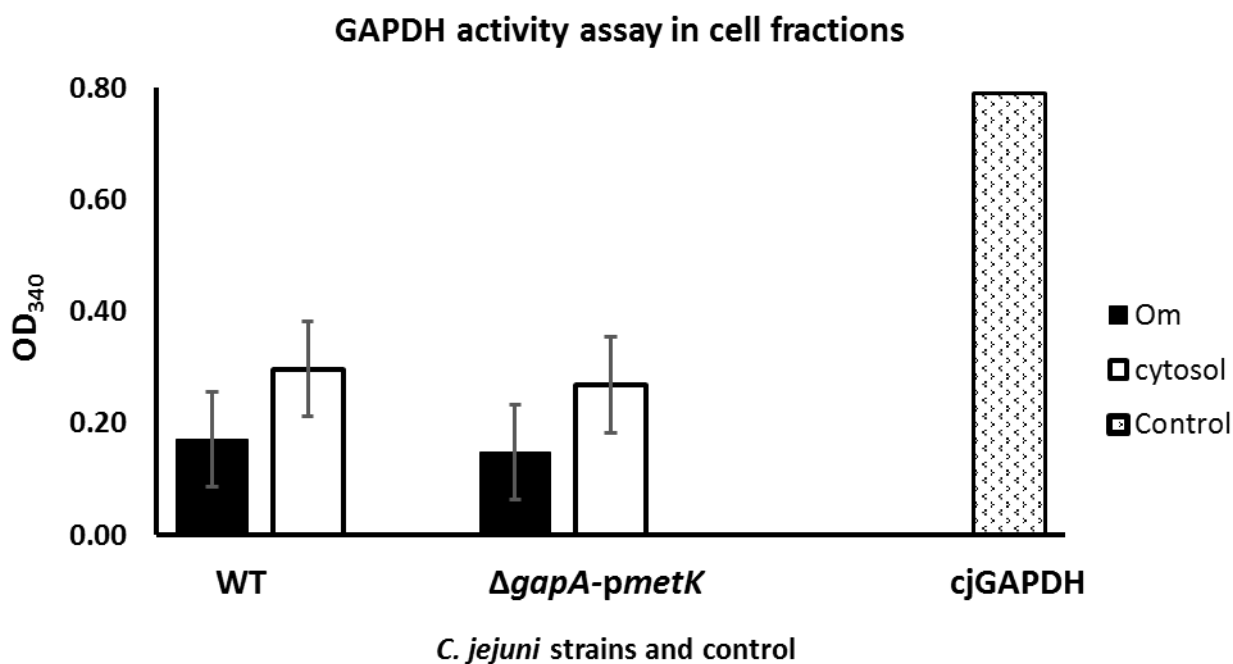


Figure 3-10. GAPDH enzymatic activity among cell fractions of WT and $\Delta gapA-pmetK$ strains.

The assay based on measurement the absorbance of formed NADP at 340 nm, the samples are cytosol and outer membrane fractions. The controls were similar to samples but G3P not added to their reactions, the value of samples OD₃₄₀ were corrected by subtracting the OD₃₄₀ of controls. GAPDH activity was detected in each cell fraction, purified cjGAPDH protein was used as positive control (10 μ l of 20 ng/ μ l purified protein; 200 ng). The assay was repeated three times with triplicate of each fraction in each run. The results represent the average and error bars are standard deviation of the data.

3.3.3.2 Western blot of cell fractions

The previous results of subcellular localisation of GAPDH proteins in *C. jejuni* requires confirmation by other methods such as immunoprecipitation, immunoblotting, and immunocytochemistry techniques. Here, Western blot as immunoblotting technique was chosen to prove the localisation of expressed GAPDH protein in purified outer membrane fractions.

After the extraction of *C. jejuni* fractions, they were subjected to SDS-PAGE followed by transfer of the proteins onto PVDF membrane as explained in section 2.5.3. Rabbit polyclonal Anti-GapA antibody (1:5000) was used to probe the membrane as primary antibody, after washing, the anti-rabbit HRP secondary antibody was applied to the membrane (1:5000) to detect GAPDH protein (~43 kDa). Concurrently, in order to detect the cross-subcellular contamination of the outer membrane fraction, another membrane was used as a control and probed with anti-GroEL primary antibody (1:80,000). After washing, the membrane was incubated with anti-rabbit HRP secondary antibody to detect GroEL protein bands. The EZ-ECL Chemiluminescence detection kit was used to develop the bands as previously mentioned in section 2.5.3. The fractions from *C. jejuni* wild strain and $\Delta gapA-pmetK$ and $\Delta gapA-pporA$ strains were examined and results are shown in figure 3 -11 A, B.

The results revealed the presence of GAPDH bands in all *C. jejuni* fractions (figure 3-11 A) with high abundance in the cytosol compared with other fractions. Additionally, all fractions show the smaller band with different intensities, which might be degradation products of GAPDH protein. In comparison as seen in figure 3-11 B GroEL protein bands were only detected in the cytosol fractions so the outer membrane fraction is free of major contamination from other subcellular contaminants. Together these results show that the *C. jejuni* GAPDH protein is found on the cell surface and is a membrane-associated protein.

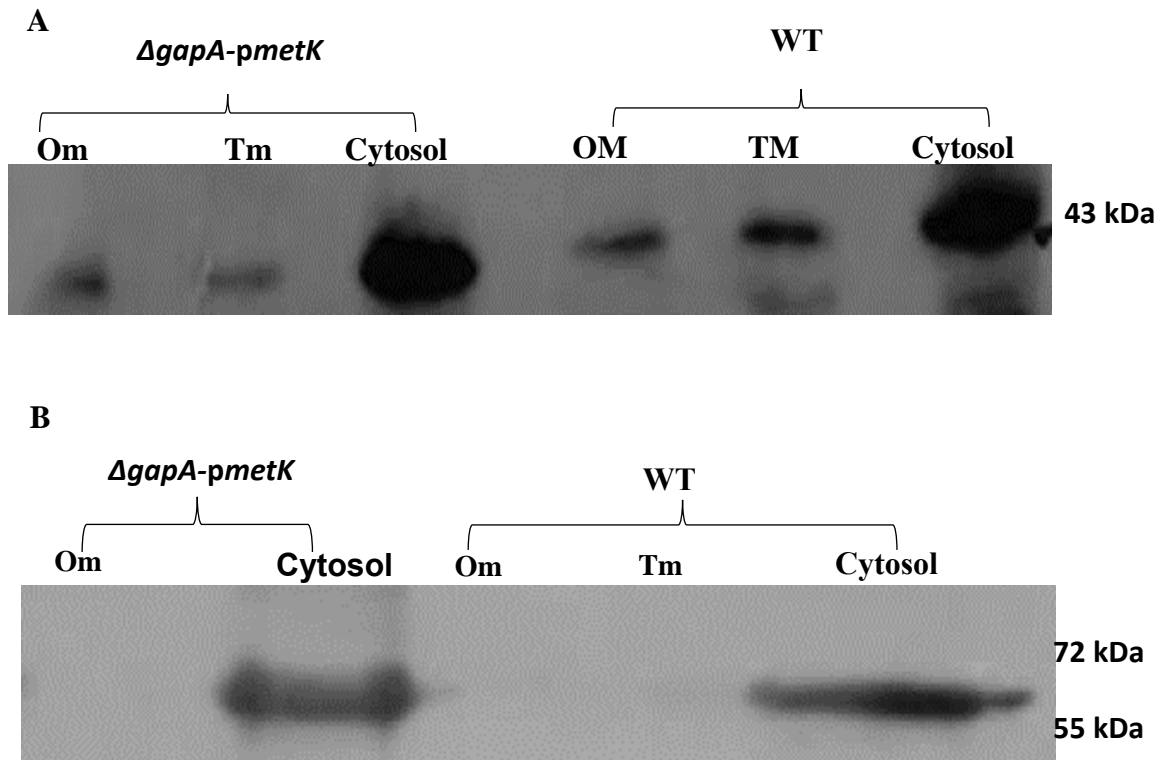


Figure 3-11 A, B. Western blot results of subcellular localisation of GAPDH in cell fractions of *C. jejuni*.

(A) The proteins of different fractions as labelled in the figure transferred into PVDF membrane which was then probed with primary anti-GapA antibody (1:5000), and secondary antibody (1:5000) after washing. All fractions showed a prominent 43 kDa band indicating the existence of GAPDH protein. Tm= total membrane, Om= outer membrane.

(B) The control, the same proteins of tested fractions in (A) were examined for subcellular contamination. Anti-GroEL (1:80,000) antibody was used to probe this membrane, an approximate 62 kDa distinct band was detected only in the cytosol fractions. *ΔgapA-porA* strain was also tested here to evaluate its purity. The corresponding sizes of pre-stained protein marker are given on the right of the photos A and B.

3.4 Discussion and conclusion

Surface localisation of GAPDH in a number of different pathogens has enabled this metabolic protein to play several functions that are not related to the metabolism. Here, it has been shown that GAPDH is a membrane-associated protein in *C. jejuni*, which was not known before in this enteropathogenic bacterium. The previous work of Miller (2008) suggested that a surface-associated protein of *C. jejuni* was involved in uptake of iron from ferric-Tf and ferric-Lf. Furthermore, evidence of *gapA* essentiality was also provided indicating that GAPDH is crucial for the viability of *C. jejuni*.

The GAPDH protein in *C. jejuni* is transcribed from a unique copy of the *gapA* gene (cj1403c) (Tourigny *et al.*, 2010). A previous study showed that the *gapA* gene is essential through the use of random insertional mutagenesis, different transposons were inserted randomly along the genome which lead to disruption of the targeting regions or genes where the transposon is inserted (Metris *et al.*, 2011). However, this strategy has some limitations such as random insertion of transposon which might cause inaccurate annotation of *gapA* (Liberati *et al.*, 2006, Deng *et al.*, 2013). Therefore, allelic replacement mutagenesis method was chosen in this research to clarify the essentiality of *gapA* in *C. jejuni*. The results obtained by this method were consistent with the results of a random insertional mutagenesis strategy and provide further evidence that *gapA* is an essential gene.

Evidence supporting the essentiality of *gapA* was established by creating mutated *gapA* strains from *gapA* merodiploid cells. This achievement was not feasible by knocking out *gapA* in the wild type strain. *C. jejuni* NCTC11168 was unable to grow after inactivation of *gapA*, the cultures were supplemented by glycerol and 5% defibrinated horse blood as further enhancement of cultures in order to recover any mutated cells. No clones of the mutated wild type strain were obtained. Moreover, mutation following complementation shows that this effect was neither due to polarity effects of *pgk*, nor technical problems were the reasons behind a lack of recovery of mutants. Indeed, use of the pC46 complementation system provides advantages for achieving the three mutated strains of *C. jejuni* as they have a range of *gapA* expression from low or relatively equal to the native *gapA*, to high levels of expression. Obtaining various expression levels of GAPDH helps in exploring its function in iron uptake from Lf iron binding protein in the next chapter and overcomes the inability to create a *gapA* deletion mutant.

Regarding the process of *gapA* mutagenesis, the pseudogene *cj0046* was chosen in the complementation system for integration of genes onto *C. jejuni* chromosome in order to reduce the deleterious effect of insertions on the cells (Jervis *et al.*, 2015). The purpose of using a terminator-less kanamycin cassette was to disrupt only the *gapA* open reading frame while allowing the remainder of this operon to be expressed. The kanamycin cassette is also promoter-less, this was in order to reduce the potential secondary polar effect on the genes downstream of the operon. The expression of kanamycin was driven by the promoter of the operon thus it was necessary during the construction and screening of the mutants to determine the orientation of the kanamycin cassette (Figure 3-3 B, ii).

The complementation of *gapA* within the region of *cj0046* does not affect the growth rate of the new created *C. jejuni* strains except $\Delta gapA-porA$ strain. The reason behind the significant alteration in growth pattern of $\Delta gapA-porA$ strain was not clear. Despite the relatively similar trends of exponential phase, figure 3-4, it can be noticed that the entry of strains into the stationary and death phases of bacterial growth was related with the expression levels of GAPDH. Referring to the figure 3-4, the optical density of the bacterial growth was gradually decreased, from the highest expressed GAPDH strain to the lowest. Therefore, it might be the excessive expression of *gapA* by the strong constitutive promoters caused toxic effects on the cell in rich nutrient conditions. Performing a growth assay based on calculating CFU of each strain in certain time point could be beneficial to relate these observations to the overexpression of GAPDH.

There was effort to create new *C. jejuni* strains that have GAPDH tagged with mCherry fluorophore in order to study the localisation of GAPDH and its role in iron uptake. The *gapA* was successfully tagged with mCherry using overlap extension (SOE) PCR (section 2.3.11). The cloning of mCherry-*gapA* on pC46 plasmids was performed and all *E. coli* Dh5 α grown colonies have recombinant pC46-*gapA* plasmids, but mCherry-*gapA* gene was ligated inversely, opposite to the promoter. Therefore, cjGAPDH-mCherry protein will not be expressed as the encoded gene was not situated downstream of *pfdxA*, *pmetK* and *pporA* promoters. The reason of not obtaining bacterial colonies with proper orientation of mCherry-*gapA* was not clear, expression of GAPDH-mCherry protein might be toxic to *E. coli* Dh5 α .

Another main finding was surface localisation of GAPDH. This study demonstrated for the first time that *C. jejuni* GAPDH is a membrane-associated protein exported and

localised on the cell surface of *C. jejuni*. Although GAPDH enzymatic assays were designed and performed carefully to avoid cell lysis, there were still detectable levels of GAPDH which might be intracellular forms of this protein. However, Western blot was used to prove the observations obtained from enzymatic assays. Existence of GAPDH in the outer membrane fraction, but not the GroEL protein make it less likely that the localisation of GAPDH in *C. jejuni* was due to cell lysis and subcellular contamination. This agrees with other studies showing that localisation of GAPDH on the cell surface has been shown with other organisms (Egea *et al.*, 2007, D'Costa *et al.*, 2000, Modun and Williams, 1999, Gao *et al.*, 2014b, Dumke *et al.*, 2011). However, surface localisation of *cj*GAPDH raises questions about the other potential functions of this protein, and also support its probable roles in iron uptake and pathogenicity of *C. jejuni*.

As mentioned in previous sections, GAPDH lacks a signal peptide (N-terminal signal sequence), or transmembrane regions (C-terminal hydrophobic tail) which are essential to export proteins onto the cell surface, so the mechanism of association with the outer membrane needs further investigation. Indeed, more studies on the secretion of other cytosolic moonlighting proteins into surrounding environment are required. A proteomic study on the Gram positive bacteria, *Listeria monocytogenes* demonstrated that some cytosolic proteins such as enolase and EF-Tu that also lack signal peptides are exported into the cell surface throughout the SecA2-dependent secretion system (Lenz *et al.*, 2003). Interestingly, many Gram negative and positive bacteria including *C. jejuni* have evolved outer-membrane vesicle mediated export system to deliver the proteins and virulence factors such as proteases, phospholipases and haemolysin into cell surface and ultimately into the host cells (Rompikuntal, 2012). It is unclear if *cj*GAPDH is transported by similar ways or not, Egea *et al* (2007) reported that GAPDH in both pathogenic *E. coli* EHEC and EPEC strains is an extracellular protein but its secretion was not mediated by vesicles and depended on the external medium conditions like concentration of glucose (Egea *et al.*, 2007). In our work, the blast alignment analysis showed *cj*GAPDH has 47% homology with GAPDH of pathogenic *E. coli* strains. In spite of fact that among bacterial species, GAPDH is conserved metabolic protein, this similarity in amino acids residues might also reflect the resemblance in some biological features such as excretion and membrane association.

Clarifying the expression strength of heterologous promoters was essential in the primary work of this research. The expression levels of *gapA* among newly created *C. jejuni*

strains were relevant to the expression strength of the promoters. The relative RT-PCR results revealed that the mRNA transcriptional levels of *gapA* in wild type strain was relatively lower than other created strains which may suggest that these new strains are over-expressed *gapA* strains. The western blot studies of GAPDH among overexpressed strains revealed two bands instead of one band compared with wild strain. The first prominent band is approximately 43 kDa representing the GapA protein of *C. jejuni* and the additional band is around 30 kDa. Several reasons might explain this finding of having an extra polypeptide (30 kDa). A likely possibility is that the extra polypeptide represents a degraded GAPDH molecule. It might be the post-translational modification (PTM) mechanism of *C. jejuni* randomly misfolded or unfolded extra synthesised molecules of GAPDH protein. This might result in accumulation into insoluble aggregates or fast degradation of GAPDH protein.

Regarding the whole cell GAPDH enzyme activity assay, the results showed dual activity of NADP and NAD coenzymes. The levels of NADP⁺ are two fold higher than NAD⁺, therefore, these findings mirror those of previous studies that have found GAPDH in *C. jejuni* phosphorylates NADP- GAPD⁺ and also indicate the ability of *C. jejuni* to utilise both of the coenzymes according to the energy status of the pathogen (Tourigny *et al.*, 2010). As *C. jejuni* lacks a complete set of ORFs for the enzymes of glycolytic pathway (Parkhill *et al.*, 2000), it can be proposed that gluconeogenesis is more important rather than glycolysis. The preferable utilisation of NADP⁺ and characteristics of anabolic pathways could reflect this proposal (Ayna, 2016). In *Bacillus subtilis* and *H. pylori*, non-photosynthetic organisms, NADP⁺ dependent GAPDH homologues were functioning in gluconeogenic function (Fillinger, 2000). However, the genomes of these microorganisms contain two *gap* genes for anabolic and catabolic reactions. Accordingly, it could be argued that GAPDH in *C. jejuni* evolved to harbour dual activity of NADP⁺ and NAD⁺ coenzymes in anabolic and catabolic contexts (Ayna, 2016).

Regarding the analysis of *gapA* expression, the results showed a correlation in amount of transcribed mRNA detected by RT-PCT and translated GAPDH polypeptide estimated by Western blot. The expression of *gapA* was higher in the new created strains than wild type in both transcription and translation levels, this was probably due to having 2 expressed copies of *gapA* and importantly the expression strength of promoters driving the expression of complemented *gapA* allele is apparently stronger than native promoter of wild type *gapA* gene. Therefore, GAPDH enzyme activity phenotypes of the new

created strains and wild type strain were also different and related to *gapA* expression levels.

In conclusion, new *C. jejuni* strains have been successfully created. These strains have an inactivated wild type *gapA* allele, with a functional copy of *gapA* under different strength promoters. This is the first report of an association of GAPDH protein with the cell surface of *C. jejuni*, and provides extra evidence on *gapA* essentiality.

Chapter 4. The GAPDH protein of *Campylobacter jejuni* NCTC11168 is involved in iron uptake from human ferric- lactoferrin

4.1 Introduction

Campylobacter jejuni has been shown to utilise the iron from host iron binding proteins Lf and Tf (Miller *et al.*, 2008). These proteins are very closely related glycoproteins with an extremely high affinity for iron. Transferrin is important in transport and recycling iron through the blood circulation of the host while lactoferrin is found in secretions such as tears, saliva, gastrointestinal fluids, but it differs from transferrin by having the capability to maintain affinity to iron in low pH conditions (pH <5.5). The affinity of Lf to bind iron is 260-fold greater than that of transferrin (Legrand *et al.*, 2008, Weinberg, 1984, Aisen and Leibman, 1972). During infection, bacteria express specialized cell-surface molecules to sequester and capture iron from Tf and Lf iron binding proteins. The cell-surface associated GAPDH has been reported as a receptor for host transferrin in extra cellular organisms such as *Staphylococcus aureus* (Taylor and Heinrichs, 2002, Modun and Williams, 1999) and also intracellular pathogens such as *Mycobacterium tuberculosis* (Boradia *et al.*, 2014a).

In the context of *C. jejuni*, the process of iron uptake from ferric-Lf is poorly understood, but appears to be receptor-dependent and require proximity (Miller *et al.*, 2008). The CtuA outer membrane receptor protein was shown to be involved in this pathway. The mutation of *Cj0178* (the encoding gene of CtuA) decreased the growth of *C. jejuni* significantly in the presence of ferric-Lf and ferric-Tf iron as sole iron sources (Miller *et al.*, 2008). However, the growth of *C. jejuni* was not completely abolished, this suggests the involvement of other proteins in iron uptake from Lf and Tf. Apparently, Lf and Tf are too large molecules to pass through the bacterial outer membrane and extra steps such as iron removal are required (Krewulak and Vogel, 2008). Thus, the process of iron uptake from these iron glycoproteins requires a surface protein to provide iron for growth of *C. jejuni*. In the previous chapter, it was shown for the first time that the GAPDH protein is a surface associated protein in *C. jejuni* NCTC11168. Therefore, with consideration of previous reports of the role of GAPDH in iron uptake from lactoferrin family proteins, it could be hypothesized that cjGAPDH has a role in iron uptake from ferric-Lf.

C. jejuni gapA mutated strains, characterised in the previous chapter will be used to determine the role of GAPDH in iron uptake from host iron binding proteins. Lf was chosen for study in most experiments during this research due to the fact that it is a preferred source of host derived-iron in *C. jejuni* (Rock, 2003). Lactoferrin is the most abundant iron binding protein in the intestinal mucosal niche where *C. jejuni* colonises and causes gastro-intestinal disease (Rock, 2003).

4.2 Results

4.2.1 The response of *gapA* gene to iron stress among *C. jejuni* strains

It was important to study the effect of iron stress on the translation and enzymatic function of the *gapA* gene product in *C. jejuni* to understand the behaviour of *C. jejuni* in different iron conditions. Previous research revealed that there was no effect of iron on the transcription of *gapA* in *C. jejuni* when 40 μ M FeSO₄ was used to promote iron replete conditions. (Butcher and Stintzi, 2013, Holmes *et al.*, 2005). However, in other pathogenic bacteria, for example, *S. aureus* GAPDH is iron regulated in a strain dependent manner (Purves *et al.*, 2010). In *M. tuberculosis*, GAPDH expression and localisation on the surface are affected by iron depletion of this pathogen (Boradia *et al.*, 2014a). Here, the intact cell GAPDH enzyme assay and Western blot of whole cell lysis of wild type strain and mutated *gapA* strains ($\Delta gapA$ -*pmetK* and $\Delta gapA$ -*pporA*) were performed under both low and replete conditions of iron.

4.2.1.1 Intact *C. jejuni* GAPDH enzyme activity assay in different iron conditions

The purpose of this quantitative assay was to observe the differences in NADP-GAPDH enzyme activity in high and low iron conditions. Therefore, wild type *C. jejuni*, merodiploid and mutated *gapA* strains were microaerobically grown overnight in restricted iron medium (MEM α) to achieve iron depletion. On the next day, OD₆₀₀ of all strains were measured and equalised to OD₆₀₀= 0.1. The equalised cells were then divided into two groups representing different iron conditions. Iron restricted was MEM α only without any supplementation of iron, and iron replete, MEM α was supplemented by 40 μ M ferrous sulphate (Fe₂SO₄), the standard level for high iron growth (Pickett *et al.*, 1992, Ridley *et al.*, 2006). Mutated strains which have only one allele of functional *gapA* controlled by different strength promoters were investigated. Cultures were incubated microaerobically until stationary phase (12-16 hours). GAPDH enzyme activity was measured as previously mentioned (section 2.5.4.1). To assess cell lysis, each strain was

investigated under the microscope. This work was carried out with three biological repeats, the results shown in Figure 4-1 illustrate that no significant differences in the level of intact cell GAPDH-NADP enzyme activity were observed between the two iron conditions. Therefore, GAPDH enzymatic activity is not affected by iron conditions.

4.2.1.2 Western blot of *C. jejuni* GapA protein in different iron conditions

In order to detect any differences in the expression of *C. jejuni* GAPDH in iron replete and restricted conditions, Western blot analysis was performed for *C. jejuni* wild type, and the *gapA* overexpressed *2gapA-pmetK*, and the mutant Δ *gapA-pmetK* strains. The strains were grown over night in MEM α , then transferred to new fresh MEM α supplemented or not supplemented with 40 μ M FeSO₄, incubated until logarithmic phase (4-9 hours). After that, the strains were centrifuged, equalised into OD₆₀₀= 0.1. The cells were lysed by SDS-PAGE lysis buffer, the cells were subjected to SDS-PAGE and transferred to PVDF membranes as explained previously (chapter 2; materials and methods). The GAPDH of *C. jejuni* polypeptide (43kDa) was detected by polyclonal anti-GapA antibody as shown in figure 4-2.

Image J software was used to estimate the quantity of GAPDH in each band on the blotted membrane. The intensity of GAPDH (43kDa) in each strain as measured by Image J was not shown significantly different between high and low iron conditions. Therefore, it can be concluded that gene expression level of *gapA* in *C. jejuni* strains was not altered by different iron conditions.

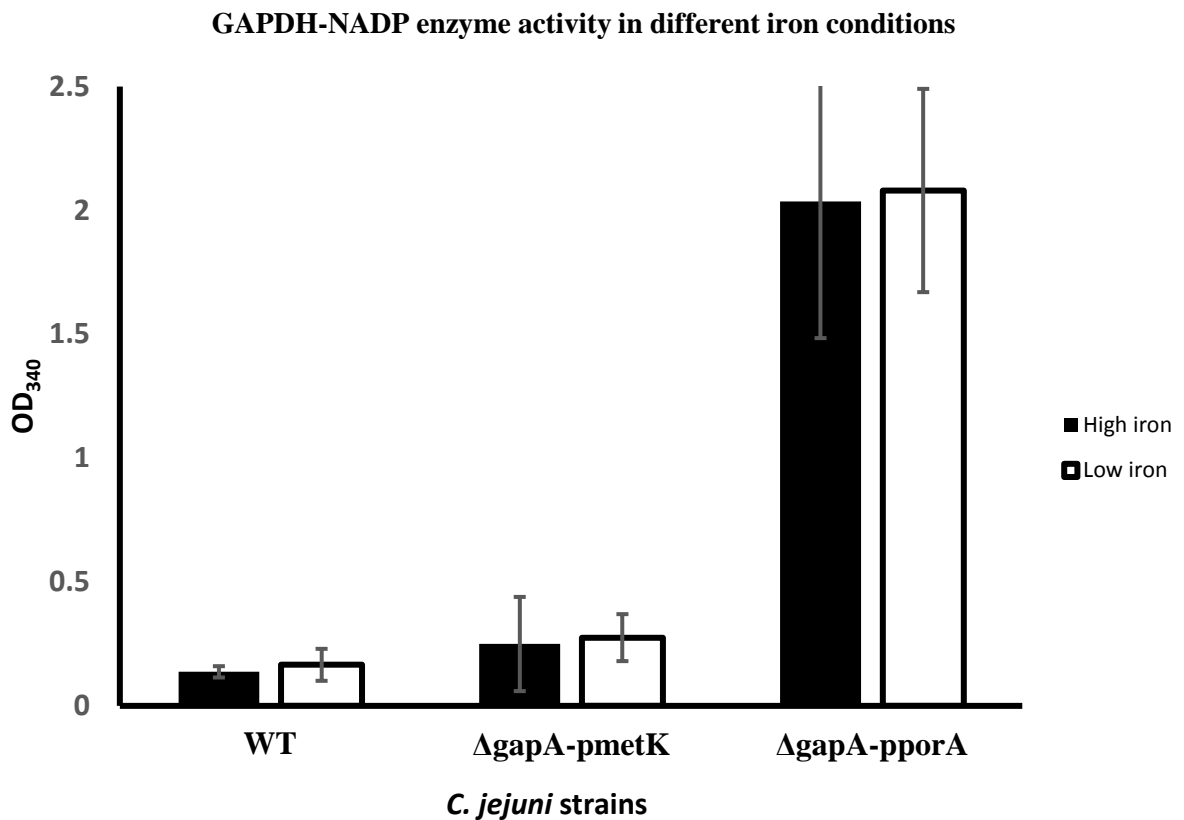


Figure 4-1. Intact cell GAPDH activity of wild type and mutated *gapA* *C. jejuni* strains in different iron conditions.

The graph shows the NADPH dependent GAPDH activity in different iron conditions; high iron (black columns) and low iron (white columns) determined from whole cell GAPDH assays of WT, $\Delta gapA$ -pmetK, $\Delta gapA$ -pporA *C. jejuni* strains. The data presented is an average of at least three independent biological repeats and corrected by control samples as mentioned in materials and methods. P values of t test between strains were: WT= 0.47, $\Delta gapA$ -pmetK= 0.159, $\Delta gapA$ -pporA= 0.16. The error bars indicate the standard deviations of the data.

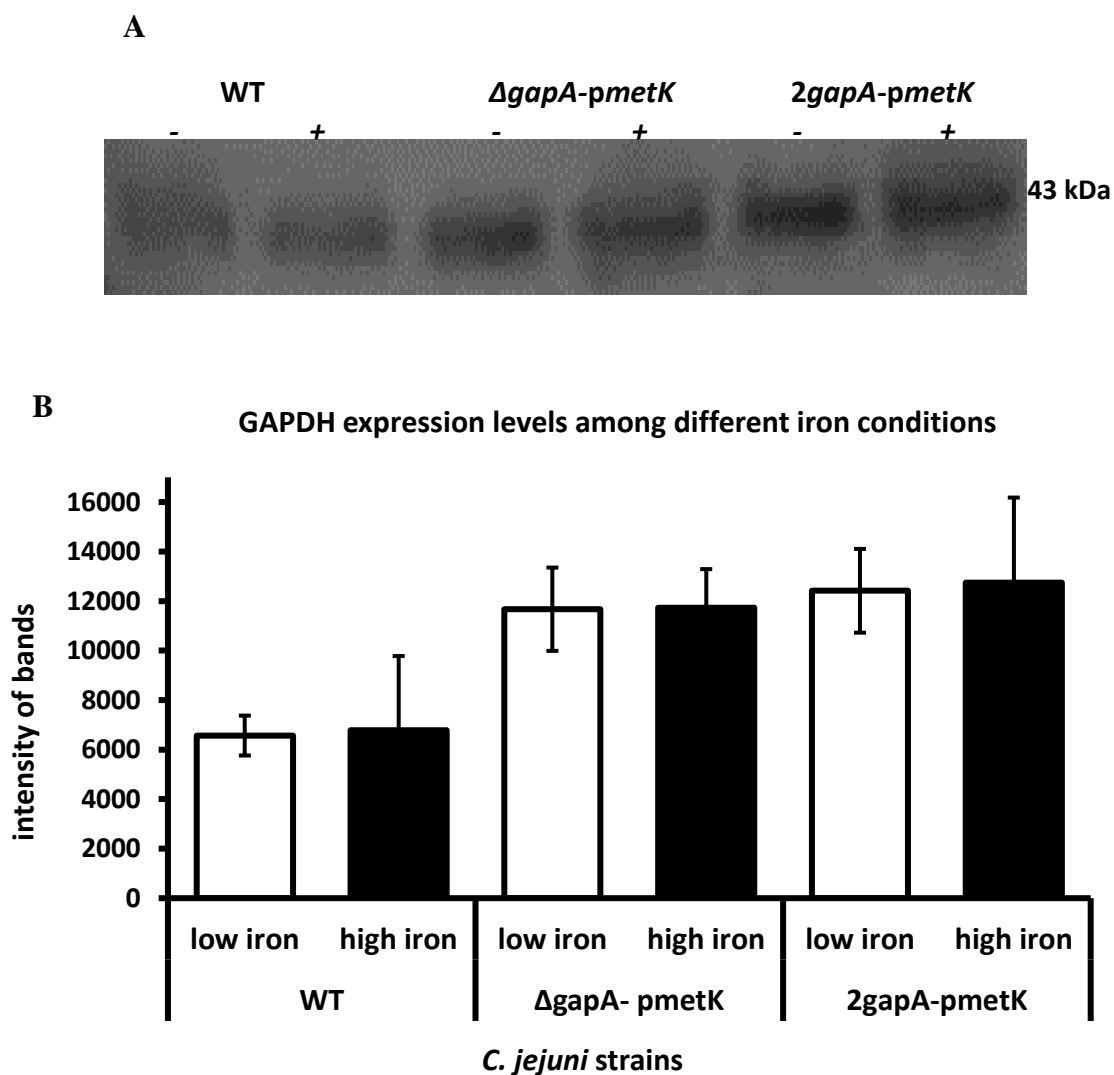


Figure 4-2 A, B. Assessment of GAPDH protein expression of *C. jejuni* strains by Western blot in high and low iron conditions.

(A) Western blot of whole cell *C. jejuni* strains WT, $\Delta gapA-pmetK$ and $2gapA-pmetK$ in different iron conditions (+) High and (-) low. The titration of 1:5000 anti-GapA was used to probe the membrane, 1:5000 anti-rabbit as HRP secondary antibody. 10 μ l of cell lysis were loaded. (43 kDa) prominent band among all strains were shown. (B) The intensity of each band detected by anti-GapA in Western blot was estimated by image J software. The error bars represented by the standard error and p values of t test between two iron conditions were WT= 0.9, $\Delta gapA-pmetK$ = 0.6 and $2gapA-pmetK$ = 0.8.

4.2.2 Growth assay of the *C. jejuni* strains in MEM α

In order to establish the growth patterns of mutated strains in defined iron-restricted medium, MEM α , the 24 hour growth curve assay of *C. jejuni* strains were performed as mentioned previously (chapter 2, section 2.4.2). The 24 hour growth assays in MEM with and without 40 μ M iron sulphate were used. The experiment was repeated three times on different days, with three technical replicates for each iron source in a 96 well microplate. The statistical analysis of the growth of the strains was performed by the student *t* paired test where the results are significant when *P value* = <0.05. The colony forming unit (CFU) of wild strain was assessed for each run of the experiment to confirm that the obtained OD is equivalent to the number of viable cells in the culture.

The results are shown in figure 4-3 A, B. All strains grew poorly in non-supplemented MEM α cultures figure 4-3 A. None of the strains reached OD₆₀₀= 0.1 of the growth and the differences in their growth pattern were not significant. However, supplementation of growth by 40 μ M FeSO₄ improved the growth of strains to exceed OD₆₀₀= 0.2, but there was no differences between the growth patterns of strains.

It is clear that none of these strains grew well in MEM α unless supplementation with FeSO₄. Therefore, supplementation with ferrous sulphate has been used as a positive control in the subsequent iron assays. The growth of the strains in non-supplemented MEM α will also be used, but as a negative control to clarify iron restricted conditions.

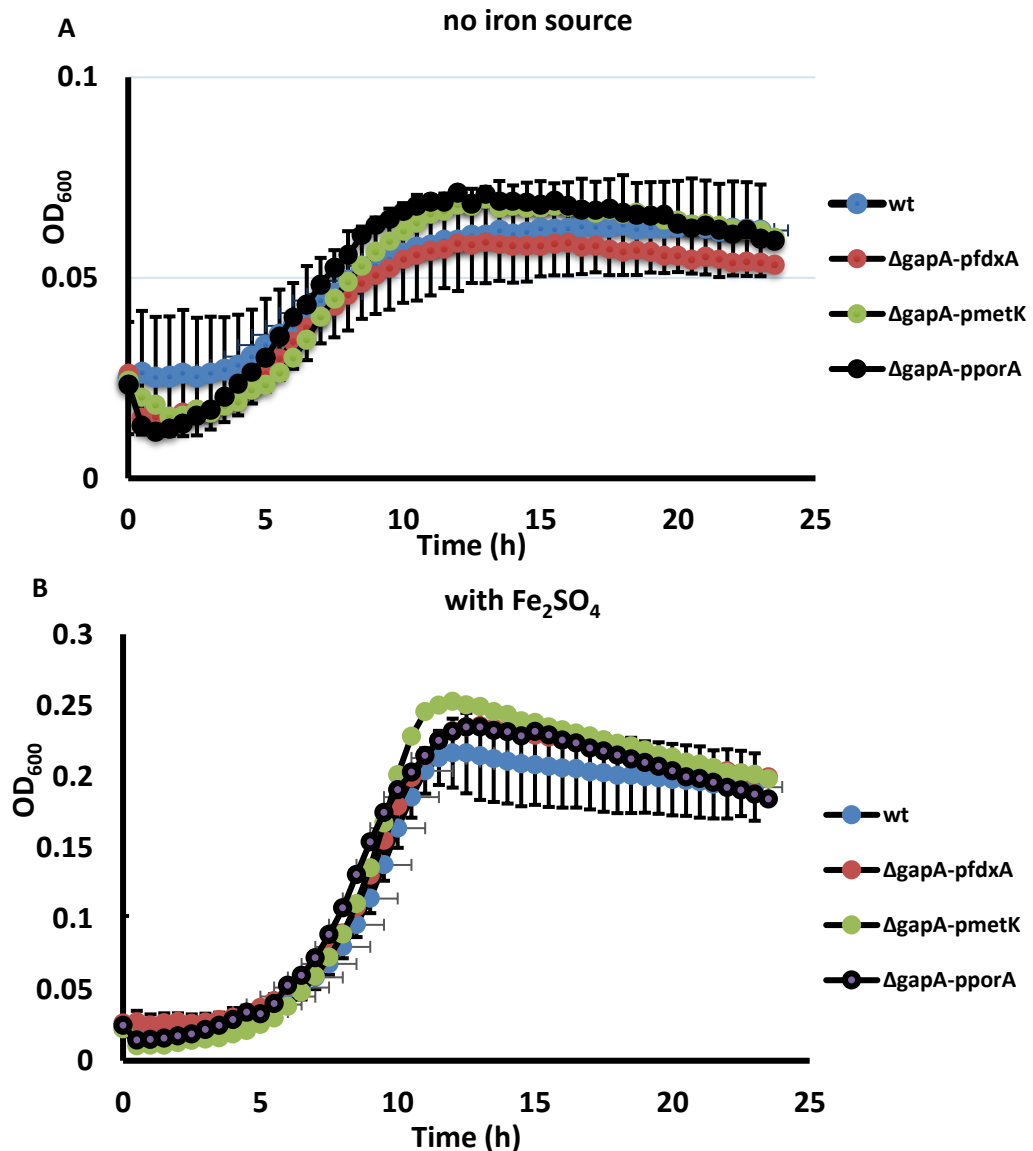


Figure 4-3 A, B. The growth curve assay conducted in iron restricted medium MEM α .

All assays were conducted using MEM α with cultures incubated microaerobically with agitation. *C. jejuni* strains WT (—●—), $\Delta gapA-pfdxA$ (—●—), $\Delta gapA-pmetK$ (—●—) and $\Delta gapA-pporA$ (—●—) were grown over night in MEM α to deplete iron stores. The assay performed in FLUOSTAR omega plate reader. Each data point in both curves represents the mean of the three replicates carried out in three different days. The error bars represent the standard deviation of the wild type strain. (A) non-supplemented MEM α and (B) 40 μ M ferrous sulphate supplemented MEM α .

4.2.3 The growth of *C. jejuni* strains in optimum levels of ferric-Lf

To compare the capability of utilising ferric-Lf in iron uptake between WT and mutated strains $\Delta gapA$ -*pfdxA*, $\Delta gapA$ -*pmetK* and $\Delta gapA$ -*pporA*. *C. jejuni* strains were grown in iron restricted medium (MEM α medium) supplemented with the optimum concentration (0.27 μ M) of human ferri-Lf as sole iron source (Miller *et al.*, 2008). The growth rate and doubling time were calculated to define the differences between the strains.

The results shown in figure 4-4 revealed no differences in the growth between the mutated *gapA C jejuni* strains and wild type in iron uptake from human ferric-Lf. Likewise, the mutated strain in other iron binding proteins such as transferrin and ovotransferrin, were grown in similar patterns of growth obtained by adding ferrous sulphate without displaying any difference (data is shown in appendix). Therefore, these results suggest that the high levels of GapA protein do not affect growth of *C. jejuni* with Lf as the sole iron source.

The growth rate was in range between (11 ± 1 to 14 ± 1) minutes. Interestingly, the highest *gapA* expression level strain ($\Delta gapA$ -*pporA*) showed rapid entering into s phase of growth curve which was not seen in MEM α supplemented with either FeSO₄ or other Lf iron binding proteins. However, this observation was reported for this strain in MHB, rich nutrient medium section 3.2.3.1.

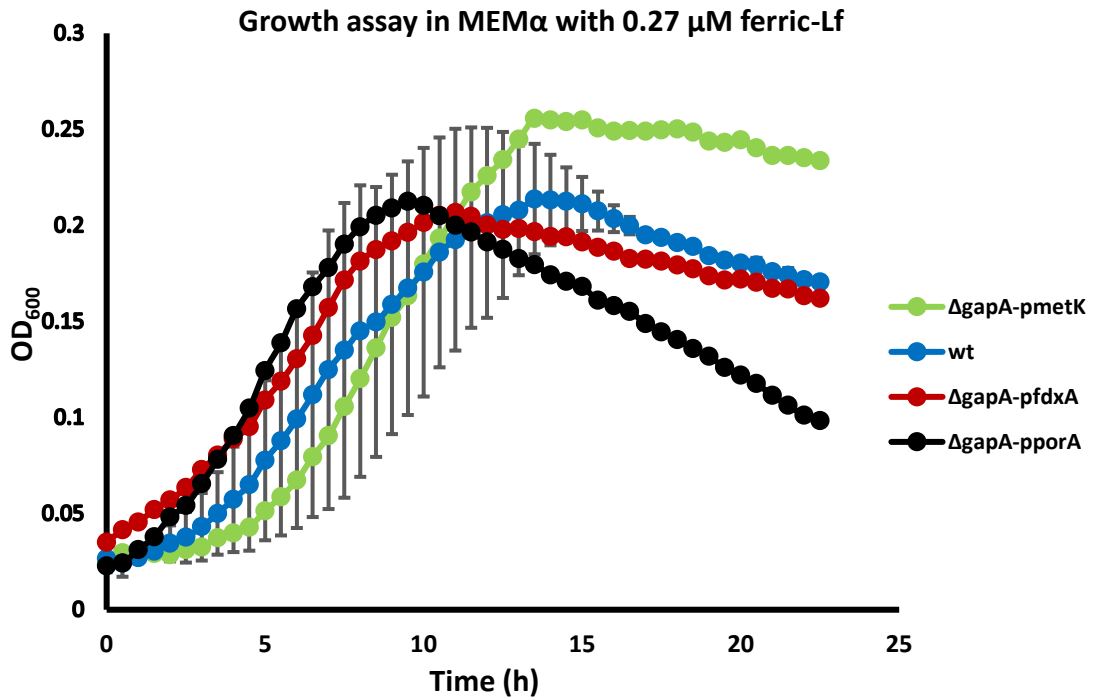


Figure 4-4. The growth assay of mutated *gapA* *C. jejuni* and wild type strains conducted in 0.27 μ M ferri- Lf supplemented MEM α .

All assays were carried out using MEM α with cultures incubated microaerobically with agitation. *C. jejuni* strains WT (—●—), *ΔgapA-pfdxA* (—●—), *ΔgapA-pmetK* (—●—) and *ΔgapA-pporA* (—●—) were grown over night in MEM α to deplete iron stores. The cells were equalised at OD₆₀₀= 0.025 in MEM α supplemented by 0.27 μ M ferric-Lf.. The 200 μ l of each culture of strains were distributed in 96 well plate, and placed in FLUOSTAR omega plate reader to perform 24 hours growth assay. Each data point in the curve is the mean of the three biological repeats, the error bars represent the standard deviations of wild strain.

Table 4.1. The growth rate and doubling time of strains growing in MEM α supplemented by 0.27 μ M ferric-Lf.

Table shows the growth rate and doubling time of each strain after growing in MEM α supplemented by 0.27 μ M ferric-Lf. The growth rate and doubling time were compared between wild type and mutated strains by student paired *t* test. No significant differences were observed, $P > 0.05$.

Strains Growth parameter	WT	<i>ΔgapA-pfdxA</i>	<i>ΔgapA-pmetK</i>	<i>ΔgapA-pporA</i>
Growth rate (h⁻¹)	0.22 ± 0.03	0.18 ± 0.01	0.23 ± 0.03	0.23 ± 0.03
(P value vs WT)		(0.23)	(0.83)	(0.90)
Doubling time (h)	3.17	3.81	3.06	3.03
(P value vs WT)		(0.16)	(0.80)	(0.86)

4.2.4 The differences in growth kinetics were significant among the *C. jejuni* strains growing under low concentrations of human ferric-Lf levels

Growing of *C. jejuni* strains in MEM α medium supplemented with optimum concentrations of ferric-Lf (0.27 μ M) showed no differences in growth patterns. As creating strains lacking functional *gapA* was not possible in this research, supplementing the cultures with a range of low concentrations of ferric-Lf might reveal the effect of GAPDH in iron uptake from this pathway. It has been demonstrated in the previous chapter that mutated *gapA* strains ($\Delta gapA$ -*pfdxA*, $\Delta gapA$ -*pmetK*, and $\Delta gapA$ -*pporA* are overexpressing GAPDH cells, therefore, it has been assumed that the redundancy of GAPDH in these strains might be important to determine the differences in iron uptake between these strains and wild type. Therefore, the levels of lactoferrin were reduced gradually by tenfold less than the highest optimum concentrations (1.11 μ M) and the growth assay of *C. jejuni* strains were accordingly performed. The concentrations of (0.111 μ M, 0.0111 μ M, and 0.006 μ M) human ferric-Lf were used to supplement MEM α medium, the 0.006 μ M is approximately half of 0.0111 μ M ferric-Lf concentration. The doubling time and growth rate were determined.

The results are shown in figure 4-5 A, B, C. There are significant differences in the growth between mutated strains and wild type. The growth rate and doubling time in different concentrations of ferric-Lf are shown in tables 4.2 and 4.3 respectively. The data show that there is a decrease in growth of all strains, proportional with the decrease in ferric-Lf concentrations. However, the growth of mutated strains in 0.1 μ M gave similar patterns to the positive control cultures which supplemented with 40 μ M, figure 4-3 B. The growth kinetics of WT strain were extremely reduced with the lowest concentration of ferric-Lf (0.006 μ M) which was similar to the negative control; no iron added as shown in figure 4-3A.

The results of this experiment suggest that *gapA* gene does play a role in the acquisition of iron from Lf by *C. jejuni*. In the next experiment, this potential function of *gapA* gene will be further investigated but in the presence of antibody against GapA protein.

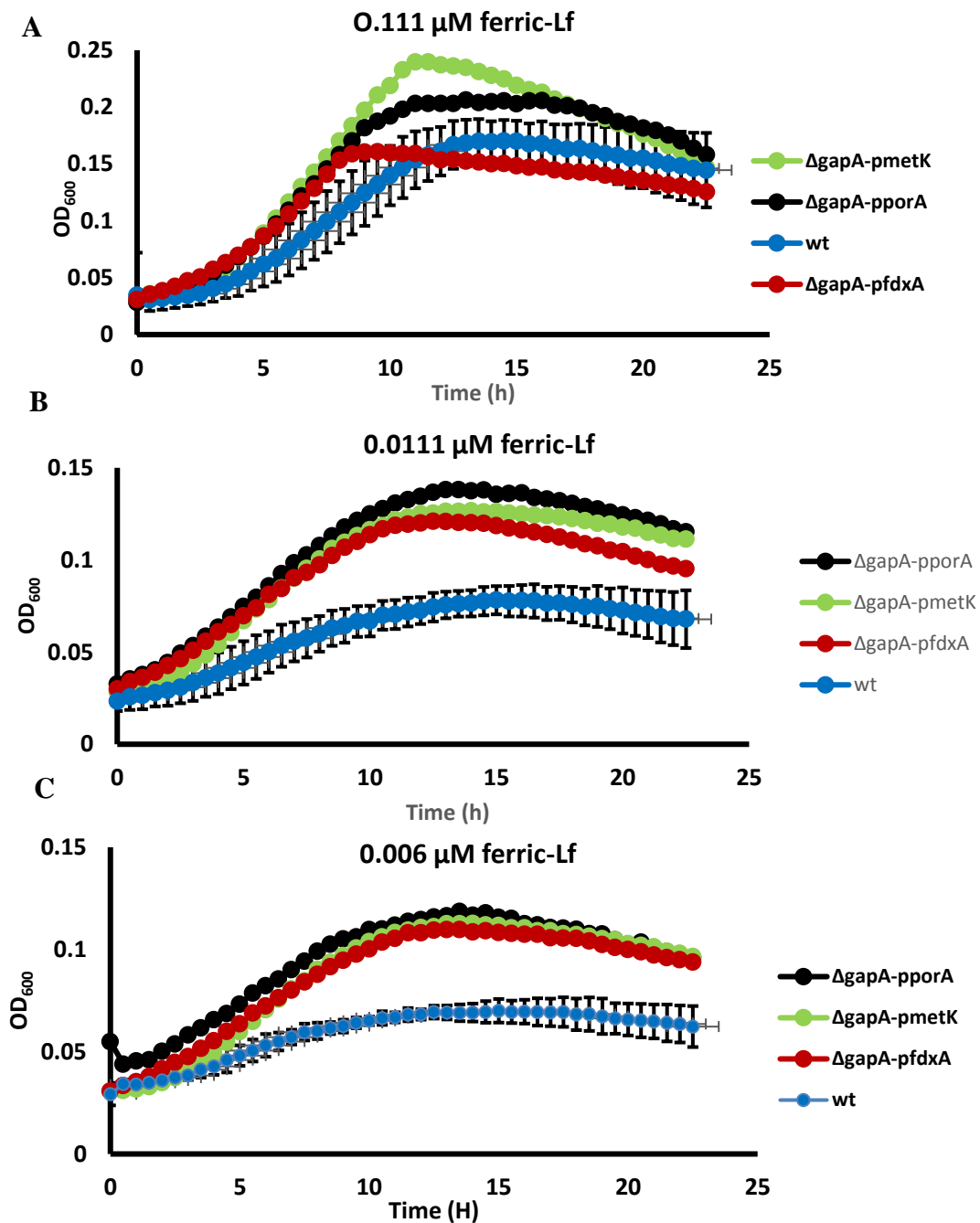


Figure 4-5 A, B, C. The growth curve assay of mutated *gapA* *C.jejuni* and wild type strains conducted in low concentrations of lactoferrin.

This graph shows the growth of *C. jejuni* strains WT (—●—), *ΔgapA-pfdxA* (—●—), *ΔgapA-pmetK* (—●—) and *ΔgapA-pporA* (—●—) in MEM α supplemented with different concentrations of ferric-Lf. (A) = 0.111 μM , (B) = 0.0111 μM in and (C) = 0.006 μM . Each data point is the mean of three replicates. The data presented is an average of at least three experiments carried out on different days. The error bars represent the standard deviation of WT.

Table 4.2. The growth rate of strains grown in a low level of ferric-Lf.

Table shows the growth rate of each strain calculated from data given in figure 4-5 A, B, C in MEM α supplemented by low concentrations (0.1, 0.01 and 0.006 μ M) of ferric-Lf. The growth rate was compared between wild type and mutated strains by student paired *t* test and differences observed are significant $P < 0.05$.

Growth rate (h^{-1})	WT	$\Delta gapA-pfdxA$	$\Delta gapA-pmetK$	$\Delta gapA-pporA$
0.1 μM (P value vs WT)	0.16 \pm 0.004	0.23 \pm 0.01 (0.004)	0.27 \pm 0.01 (0.002)	0.23 \pm 0.01 (0.01)
0.01 μM (P value vs WT)	0.09 \pm 0.02	0.16 \pm 0.02 (0.019)	0.22 \pm 0.06 (0.03)	0.17 \pm 0.01 (0.01)
0.006 μM (P value vs WT)	0.08 \pm 0.01	0.13 \pm 0.02 (0.04)	0.12 \pm 0.02 (0.03)	0.13 \pm 0.02 (0.03)

Table 4.3. The doubling time of strains grown in a low level of ferric-Lf.

Table shows the doubling time of each strain calculated from data given in figure 4-5 A, B, C in MEM α supplemented by low concentrations (0.1, 0.01 and 0.006 μ M) of ferric-Lf. The doubling time was compared between wild type and overexpressed strains by student paired *t* test and differences observed are significant $P < 0.05$.

Doubling time (h)	WT	$\Delta gapA-pfdxA$	$\Delta gapA-pmetK$	$\Delta gapA-pporA$
0.1 μM (P value vs WT)	4.28 \pm 0.13	3.05 \pm 0.13 (0.0003)	2.55 \pm 0.07 (0.0002)	2.99 \pm 0.14 (0.003)
0.01 μM (P value vs WT)	7.72 \pm 0.1	4.39 \pm 0.2 (0.04)	3.38 \pm 0.08 (0.03)	4.04 \pm 0.1 (0.03)
0.006 μM (P value vs WT)	7.93 \pm 0.3	5.39 \pm 0.14 (0.04)	5.63 \pm 0.22 (0.03)	5.36 \pm 0.13 (0.03)

4.2.5 Addition of anti-GapA into iron growth assay of wild type and mutated *gapA* strains reduced significantly the growth of *C. jejuni* strains in the presence of lactoferrin as sole iron source

To further investigate the role of GAPDH in iron uptake from ferric-Lf, polyclonal anti-GapA antibody derived from serum of rabbit was added into the cultures to inactivate the surface GAPDH protein on *C. jejuni* strains and observe its impact on the growth kinetics of these strains in MEM α medium supplemented with ferric-Lf as sole iron source. Experimentally, *C. jejuni* WT was grown in MEM α with ferric chloride (FeCl₃) or 0.27 μ M ferric-Lf in the presence and absence of anti-GapA to determine if the inhibition of extracellular GAPDH affects iron uptake from ferric-Lf. No iron MEM was used as a negative control. Polyclonal anti-major outer membrane protein (anti-MOMP) antibody was included in this assay (gifted from Dr Christopher Bayliss, Department of Genetics at University of Leicester) to clarify the specific role of GAPDH in this iron uptake process.

Results are show in figure 4-6 A, B, it is clear that FeCL₃ and ferric-Lf support growth of *C. jejuni* in MEM α . Interestingly, anti-GapA inhibits growth in ferric-Lf but not FeCl₃. Therefore, cjGAPDH is required for iron uptake from ferric-Lf. To confirm, *C. jejuni* WT is grown in ferric-Lf and FeCl₃ in presence of a different antibody; anti-MOMP. Results show no difference in growth in presence of anti-MOMP compared to anti-GapA, figure 4-6 B. This work was repeated on other strains and show same effect (results in appendix).

These findings support the results of previous section and provide evidence that *gapA* in *C. jejuni* NCTC11168 can be important element of iron uptake from ferric-Lf.

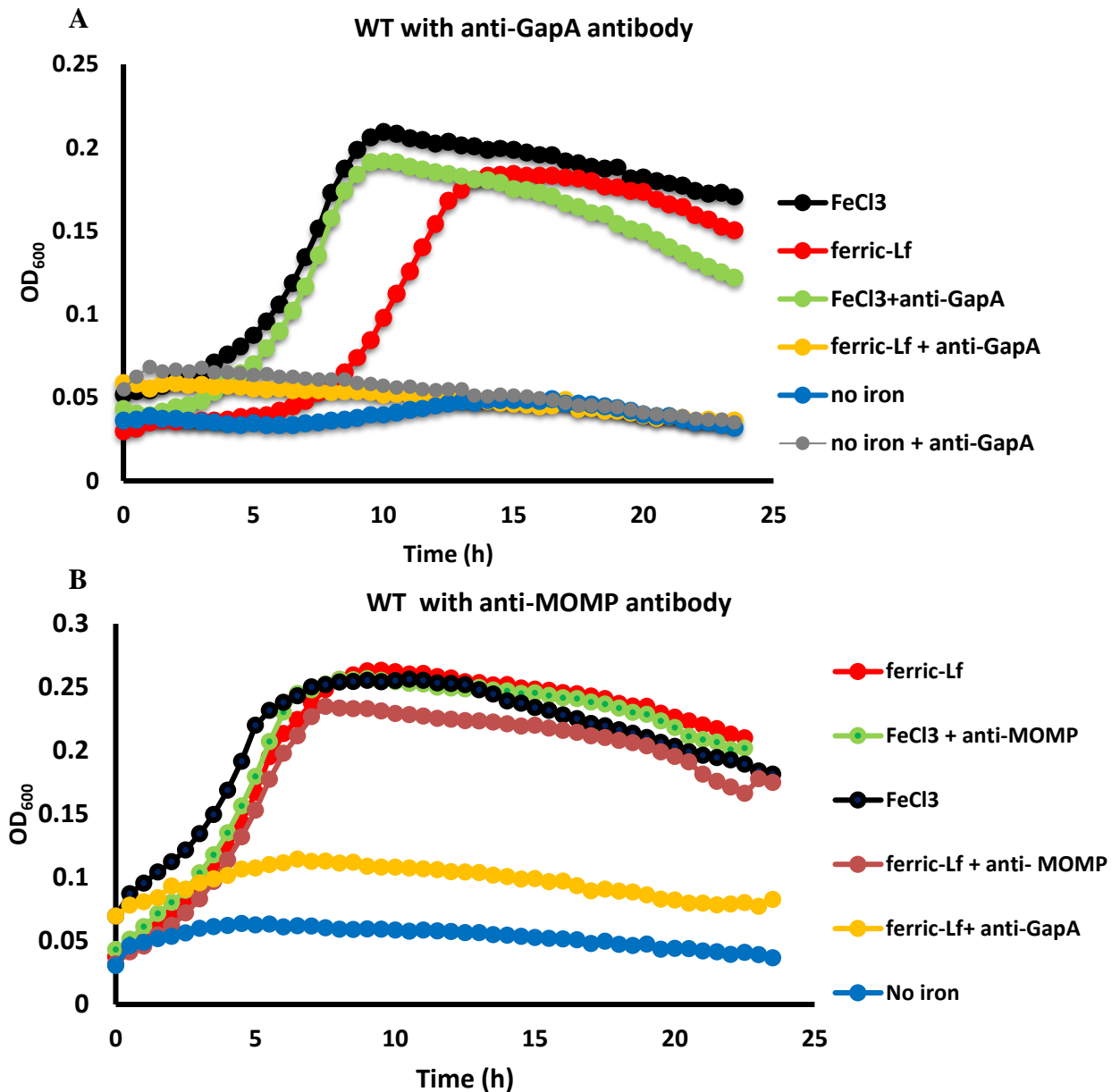


Figure 4-6 A, B. Growth assay of *C. jejuni* WT in the presence and absence of polyclonal anti-GapA antibody with 0.27 μ M human ferri-Lf.

The graphs show the 24 growth assays of WT strain in MEM α , the cultures incubated microaerobically in FLUOSTAR Omega plate atmosphere reader with agitation. (A) The growth assay with inclusion of anti-GapA antibody, whereas (B) growth assay with anti-MOMP antibody. Each data point is the mean of the three replicates, all conditions were tested in triplicate in three different days. Cultures included no antibody or the addition of antibody to 1:200 final concentration, 0.27 μ M human ferri-lactoferrin, 40 μ M FeCl₃ (iron-replete conditions, positive) and non-supplemented MEM α (iron-limited conditions, negative).

Furthermore, to confirm that obtained phenotypes in lactoferrin supplemented cultures corresponded to the concentration of anti-GapA, different titrations of anti-GapA were added into *C. jejuni* NCTC11168 in the presence of 0.27 μ M of human ferri-Lf. The results shown in Figure 4-7 indicated that the reduction of culture growth were proportional to the amount of antibody. Therefore, the inhibition of iron uptake system from Lf by anti-GapA was in a concentration dependent manner.

The response of WT to different titrations of anti-GapA

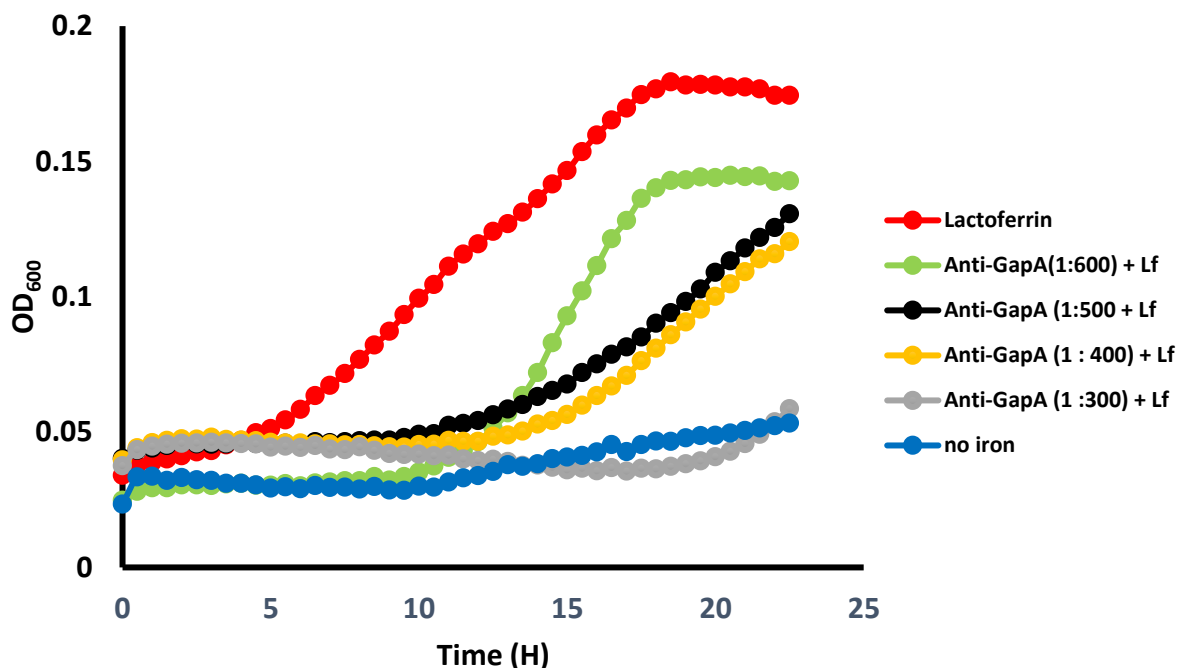


Figure 4-7. Growth assay of wild-type NCTC 11168 in different titrations of polyclonal anti-GapA antibody with 0.27 μ M human ferri-lactoferrin in MEM α medium.

This graph shows the growth of *C. jejuni* WT in MEM α supplemented with different titrations of anti-GapA antibody; 1:300, 1:400, 1:500 and 1:600 with 0.27 μ M human ferric-Lf. The ferric-Lf without added antibody was a positive control, no iron added was a negative control. The cultures were incubated microaerobically in FLUOSTAR Omega plate atmosphere reader with agitation. Each data point is the mean of three replicates. The data presented is an average of three experiments carried out on different days.

4.2.6 Binding assays with ferric-Lf

Previous studies showed that iron uptake from Lf was receptor specific and required proximity (Miller *et al.*, 2008). Here, the data shown in the last sections indicate the involvement of GAPDH in iron uptake from ferric-Lf. Therefore, the next work focus on characterisation of this function, to determine if the extracellular cjGAPDH binds human ferric-Lf or not.

4.2.6.1 Role of cjGAPDH in binding of whole cell *C. jejuni* to lactoferrin

C. jejuni strains pre-exposed to polyclonal anti-GapA antibody were incubated with ferric-Lf in order to explore the role of cjGAPDH in the binding process. Theoretically, anti-GapA antibody can bind with membrane-associated cjGAPDH reducing its capability to act as receptor for ferric-Lf. This should result in decreased binding of ferric-Lf with *C. jejuni*. Anti-MOMP antibody was used as negative control.

C. jejuni WT, $\Delta gapA$ -*pporA*, and $\Delta gapA$ -*pmetK* strains were grown in MEM α medium to deplete iron stores. On the next day, cells (OD₆₀₀= 0.1; about 1 x 10⁸ cfu/ml) of each strain were incubated with anti-GapA, anti-MOMP or no antibody for one hour, then exposed to 0.27 μ M human ferric-Lf for 1 hour, the cells were lysed and subjected to SDS-PAGE and then Western blot probed by rabbit anti-Lf antibody. This was done to determine and confirm that human ferric-Lf specifically binds to extracellular GAPDH. The expected size of human ferric-Lf band is 92 kDa. The differences of intensity of Lf bands between test samples and control groups on Western blot film was detected by Image J programme (1.49v, National institute of Health, USA).

Figure 4-8 A, B illustrates the results of binding assay of WT strain, other strains are given in the appendix. There is a noticeable decrease in the intensity of bands of test samples (+Ab) compared to controls (-Ab). The presence of anti-GapA reduced the amount of lactoferrin bound to *C. jejuni* strains by approximately more than 50%. The treatment of the cells with anti-MOMP did not affect binding of ferric-Lf; figure 4-8 B and D.

These results show that GAPDH plays a role in *C. jejuni* binding of ferric-Lf, and probably this binding is important to iron release from Lf iron binding protein.

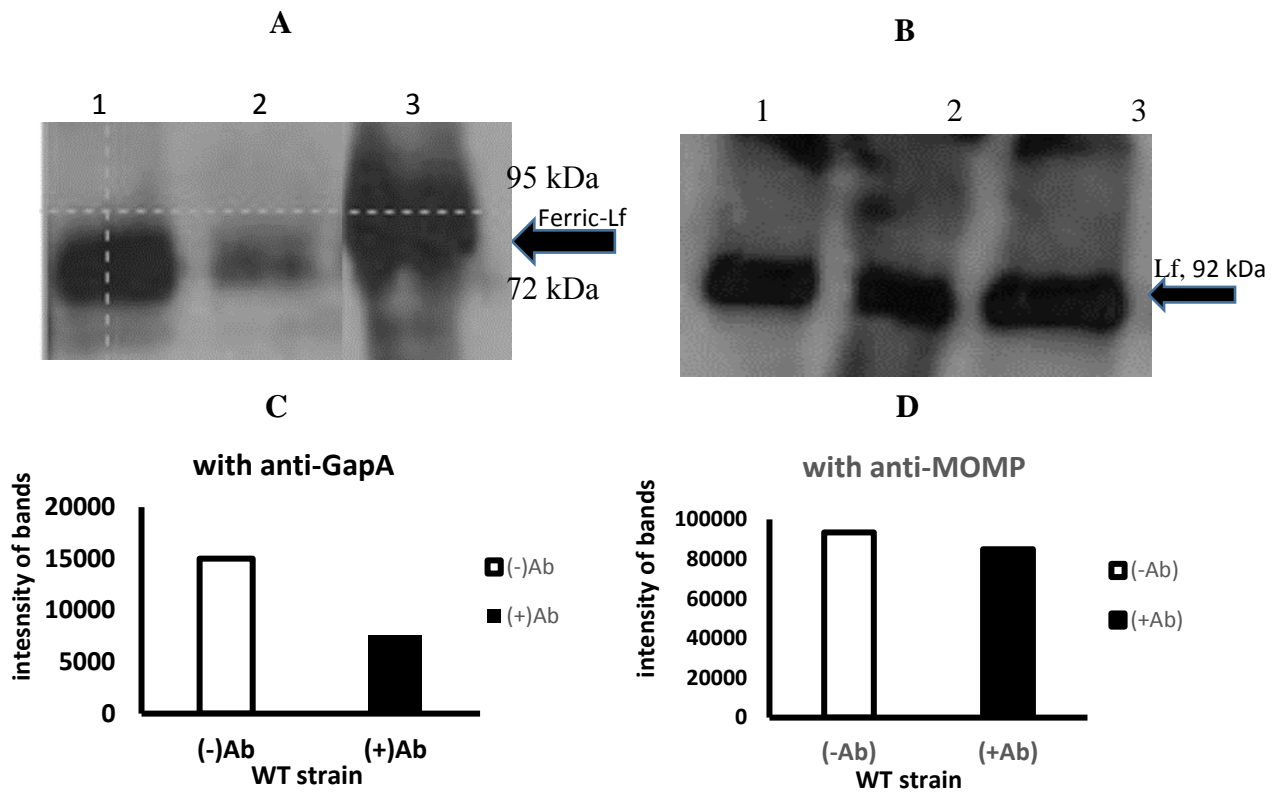


Figure 4-8 A, B, C, D. Western blot analysis of binding assay between anti-GapA pre-incubated *C. jejuni* with ferric-Lf.

Figure (A) Western blot analysis of solubilised *C. jejuni* proteins (approximately 25 μ g of protein separated by SDS-PAGE) prepared from iron-restricted WT strain treated with (+) / without (-) (1:200) anti-GapA antibody (Ab), washed and incubated with 0.27 μ M ferric-Lf. Lane 1 = WT (-Ab), 2= WT (+Ab), and 3= human ferric-Lf (~5 μ g; positive control indicated by arrow at approximately 92 kDa). (B) Similar to A, WT strain was pre-incubated with anti-MOMP 1:200 and the samples were in similar order in blot A. All Blots probed with rabbit anti-lactoferrin antibody, Protein ladder band sizes are indicated in kDa to the right of each blot. (C) Assessment of Western blot bands of the blot (A). Image J was used to estimate the intensity of the bands, differences between presence / absence of anti-GapA of WT strain =49.5%. (D) Assessment of Western blot bands of the blot, the difference was about 9.1% between two conditions of WT strain.

4.2.6.2 Far-western blot assay to study binding of purified GapA protein with different lactoferrin family proteins

The far-Western method is a modification of the standard Western blot analysis, also called ligand blotting or West-Western. In this method, proteins immobilized on suitable membranes such as PVDF can be detected by their ability to bind to soluble recombinant proteins of interest (Takayama and Reed, 1997). It is a rapid and highly reproducible assay for investigating the protein—protein interactions between protein binding partners (Walsh *et al.*, 2012). Here, the purpose of this assay was to identify if cjGAPDH protein can bind human ferric- Lf iron binding proteins, ferric-Lf, ferric-Tf and ferric-ovo-Tf.

4.2.6.2.1 Cloning, overexpression, purification of GapA protein

To purify GapA protein, the *gapA* gene was cloned into pET151/D topoisomerase vector (recombinant plasmid was gifted from (Dr Adnan Ayna and Professor Peter Moody, Department of Molecular and Cell Biology, University of Leicester). The *gapA* was tagged with an N-terminus Tobacco Etch Virus (TEV) protease cleavable 6xHis tag. The map of recombinant *gapA*- pET151/D topoisomerase plasmid is shown in the appendix.

The recombinant GapA protein of *C. jejuni* was purified according to the protocol described by (Elliott, 2009, Ayna, 2016), see (section 2.5.6). The plasmid was transformed into the overexpression bacterial host *E. coli* Rosetta DE3, the protein was purified and eluted using slurry Ni-NTA (Nickel-Nitrilotriacetic acid). The recombinant GapA protein was further purified via dialysis membrane to remove unwanted molecules such as salts from the protein, and a cleavage step with TEV protease to remove the 6xHis-tag. The purity of the protein was estimated via SDS-PAGE, the gel of the purification process of recombinant GapA is shown in figure 4-9.

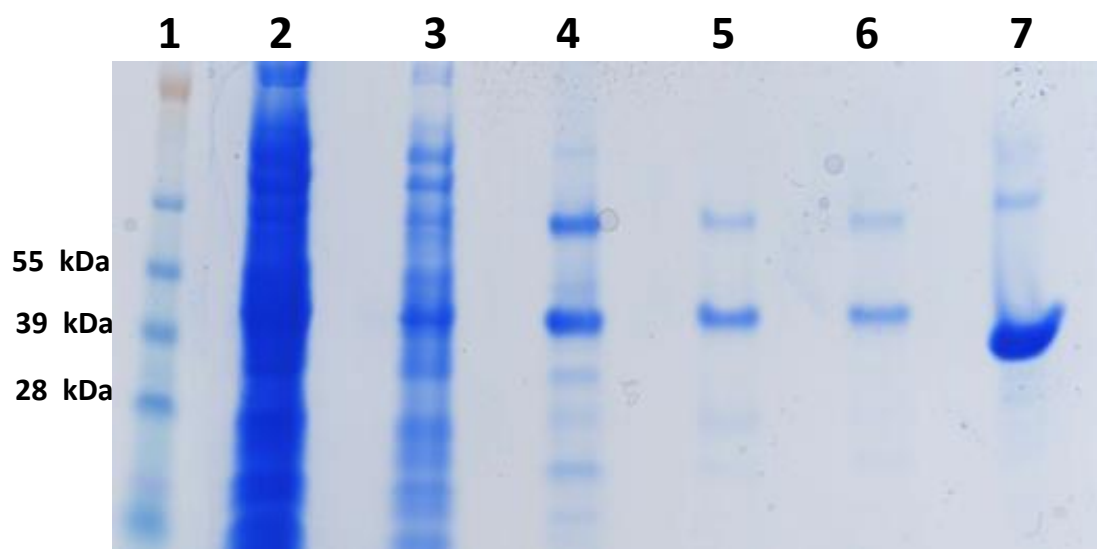


Figure 4-9. Purification of recombinant cjGAPDH protein expressed with 6xHis affinity tag.

SDS-PAGE (12% gel) was run for samples which were taken at each stage of the purification, 10 µl of sample mixed with 10µl 2 x SDS sample buffer. The wells are : 1= SeeBlue2 (Life Technologies) protein marker was loaded for size comparison. 2= soluble cell extract, 3= unwashed Ni-NTA resin-GapA, 4= washed Ni-NTA-GapA, 5 and 6= protein elution 10 and 5 µl respectively, and well 7= 5 µl human GAPDH protein, which was around 37 kDa and purity >90% (sigma-Aldrich). SeeBlue2 and human GAPDH have been gifted by Dr Adnan Ayna and Professor Peter Moody, Department of Molecular and Cell Biology, University of Leicester).

4.2.6.2.2 Far western blot assay of GapA and ferric-glycoproteins

After the purification of recombinant GapA, the binding of this protein with the lactoferrin family of proteins was investigated. 5 µg of GapA (positive control) and 3 µg of lactoferrin, transferrin, ovo-transferrin proteins in addition to bovine serum albumin (BSA, negative control) were subjected to SDS-PAGE and transferred to PVDF membranes as explained previously (chapter 2; materials and methods). Immediately after blocking step, membranes were washed with binding buffer (50 µg/ml pure GapA in 1x PBS-T) and incubated for 2-3 hours. The membrane was washed by blocking buffer (10% (w/v) BSA in 1x PBS-T) as 3 x 5 min, 2 x 15 min, 3 x 5 min., then probed by primary antibody anti-GapA (1:5000), washed and incubated with a secondary antibody anti-rabbit HRP conjugated (1:5000). For quality control purpose, another identical blot was run in parallel and incubated with GapA- free binding buffer as a control to detect any cross reactions that might be produced by these antibodies. Image J was used to quantify interaction between GapA and iron-binding proteins.

The results of probing these membranes with anti-GapA antibody shows that GapA protein binds to itself, as expected, and also binds to Lf, Tf and ovo-Tf figure 4-10 B. There is no GapA protein binding to BSA. In the absence of supplemented GapA protein, the anti-GapA antibody only binds to GapA showing that GapA protein specifically binds to Lf, Tf and ovoTf. Furthermore, the binding appears to be with different degrees of infinity with lactoferrin showing the highest intensity of binding. Image J analysis figure (4-10 D) showed ferric-Lf binds GapA protein approximately three times higher than ferric-Tf and ferric-ovo-Tf. Interestingly, all of these bound proteins including GapA were denatured prior to being subjected to 12% SDS-PAGE, this means that they maintained the capability of binding even though they are misfolded.

Overall, the results of these binding assays not only provide further evidence of GAPDH function in iron uptake from ferric- Lf, but they also indicate that GAPDH can bind iron binding proteins. Moreover, this finding and outer membrane association of cjGAPDH suggest that cjGAPDH might act as receptor and interact directly with ferric-Lf to release iron.

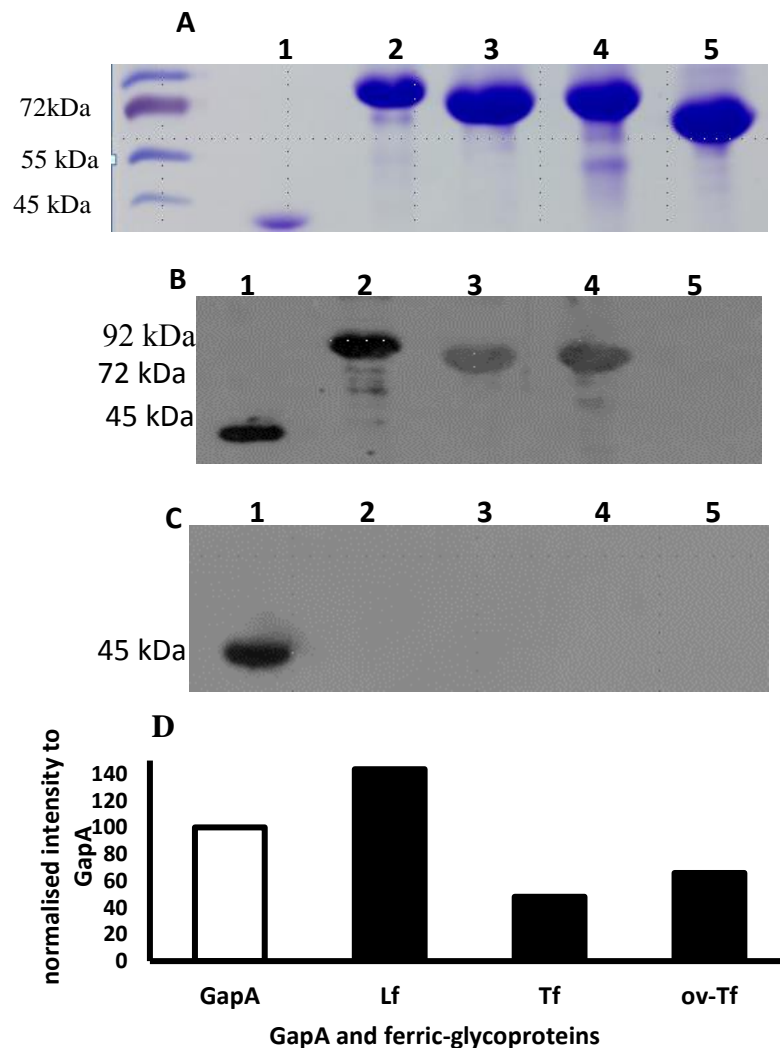


Figure 4-10 Far Western blot analysis of GapA binding with Lf iron binding proteins.

Panel A shows 12% SDS-PAGE of 5 μ g GapA and Lf iron binding proteins and BSA was normalised at \sim 3 μ g each. The following order of loaded samples was the same throughout this assay: 1= purified GapA, 2= human ferric-Lf, 3= human ferric-Tf, 4= , ferric-ovo-Tf and 5= BSA. (B) is far Western blot, immobilised proteins on PVDF membrane incubated with 50 μ g/ml binding buffer, washed and probed with anti-GapA antibody. (C) Identical to B, but GapA- free binding buffer was incubated with the proteins on PVDF membrane. (D) Bar chart estimation of binding by image J. The band intensity was normalised by GapA in lane 1. Iron binding proteins are approximately 90 kDa, the protein ruler is appearing on the left of the gels.

4.3 Discussion and conclusion

GAPDH is a highly conserved protein in bacteria (Fillinger, 2000). Numerous studies reported the contribution of GAPDH in iron acquisition from lactoferrin iron binding proteins in different organisms (Modun and Williams, 1999, Raje *et al.*, 2007, Sheokand *et al.*, 2013, Boradia *et al.*, 2014a). The findings of this chapter demonstrated for the first time the involvement of GAPDH in iron acquisition from ferric-Lf in *C. jejuni*. Additionally, the results also show that extracellular cjGAPDH binds ferric-Lf specifically.

The growth of WT and mutated strains in MEM α supplemented with low levels of ferric-Lf showed significant differences in the growth kinetics. The mutated strains grew better than wild type and this was the first indication of GAPDH function in iron uptake from ferric-Lf. This finding has not been reported previously in *C. jejuni* or related bacteria *H. pylori*, but it has been indicated in other pathogenic bacteria such as *M. tuberculosis* (Malhotra, 2017). However, there was considerable reduction in growth of all strains due to the inadequate level of ferric-Lf in the cultures. The mutated strains showed better growth due to overexpression of GAPDH as shown in section (3.2.3.4), the high amount of cjGAPDH in mutated strains could provide more opportunity to interact with ferric-Lf and release iron. Rawat *et al.*, (2012) reported that under low iron conditions, macrophage cells prefer to use GAPDH to acquire Lf. The reason for this preference was the increased expression of GAPDH in iron depletion of macrophages. Our findings show that different iron conditions do not affect the expression of GAPDH. No difference in growth between WT and mutant strains under optimum concentrations of Ferric-Lf was observed, this is probably because the amount of ferric-Lf was adequate for the demand of the cells. Unfortunately, it was not possible to have another complementation system to create new *C. jejuni* strains, which can express GAPDH in levels lower than wild type *gapA*. Therefore, it is unknown if very low levels of GAPDH can affect the release of iron from lactoferrin or not.

The inclusion of anti-GapA into ferric-Lf supplemented cultures showed inhibition of growth, while pre-exposing of *C. jejuni* to anti-GapA antibody caused marked decrease in binding to ferric-Lf. These results indicate the direct involvement of cjGAPDH in the binding and acquisition of iron for growth of *C. jejuni* from ferric-Lf. Results of anti-MOMP supplemented cultures proved that the observed effects are specific to GAPDH

and they are not random attachment of anti-GapA components to the cell surface of *C. jejuni*. Interestingly, these findings also demonstrate the surface localisation of cjGAPDH on *C. jejuni* and support the results obtained in the previous chapter. In previous work (Miller *et al.*, 2008), inactivation of *ctuA* did not completely impair the growth of *C. jejuni* in the presence of ferric-Lf as the sole iron source which proposes the contribution of other genes in this iron uptake system. Our findings suggest that *gapA* of *C. jejuni* could be an essential element in this pathway of iron uptake. Furthermore, far Western blot showed the capability of GapA protein to bind a range of Lf family proteins, this also provides extra evidence of the role of GapA in iron uptake. The high affinity of GAPDH to bind Lf might explain why *C. jejuni* prefers utilising lactoferrin rather than other iron glycoproteins. It has been reported that *C. jejuni* obtains iron more readily from ferric-Lf than ferric-Tf (Rock, 2003). High affinity to bind Lf was also reported in closely related bacteria, *H. pylori*, Lf is very important for *in vivo* growth of *H. pylori*, but the role of GAPDH in this binding has not been investigated. However, the binding of bacteria to iron glycoprotein due to GAPDH was assessed in *M. tuberculosis*, the affinity of *Mtb* GAPDH to bind Lf is 5 fold greater than affinity to bind Tf (Malhotra *et al.*, 2017).

Taken together, these findings demonstrate direct interaction between GAPDH and ferric-Lf to release iron into the cells. *C. jejuni* likely has a specific binding site for Lf rather than non-specific adherence to the cell surface and it is probably cjGAPDH.

Organisms that cannot produce siderophores usually have specific Tf or Lf receptors to sequester iron from these proteins (Senkovich *et al.*, 2010). For example, *Neisseria* species, and *Haemophilus influenzae*; are pathogenic bacteria which have specific receptors for Tf and Lf (Krewulak and Vogel, 2008, Herrington and Sparling, 1985). As mentioned previously (section 1.3.3.1), *C. jejuni* lacks siderophore synthesis genes but can use external siderophores. The capability of cjGAPDH to bind specifically both Lf and Tf supposes that *C. jejuni* has dual receptor to bind Lf and Tf which is most likely GAPDH. Dual receptor function of GAPDH to bind both Lf and Tf was determined in human GAPDH and *Mtb* GAPDH (Kumar *et al.*, 2012a, Malhotra *et al.*, 2017). In *H. pylori*, the role of GAPDH was not yet investigated, however, this bacterium might have dual receptor for Lf and Tf and other receptors act only for Lf (Senkovich *et al.*, 2010). The role of energy transduction system ExbBD-TonB1-3 was not shown in iron uptake from Lfs in *C. jejuni* (Prof. Julian Ketley, unpublished data; figure 6a-f). The growth

kinetics of single and double *tonB* mutant strains showed no differences in the presence of ferri-Lfs as the sole iron source due to probable redundancy in the *tonB* system. However, further investigation of energy dependency might be required.

The mechanism of how GAPDH protein contributes to the release of iron bound Lf family proteins is better understood in *M. tuberculosis*. GAPDH, with another five interacting proteins, facilitates the sequestering of transferrin on the cell surface of *M. tuberculosis*. A Tf-GAPDH complex internalises transferrin across the mycobacterial wall and membrane within infected macrophage and perhaps ferric reductases in the cytoplasm of *M. tuberculosis* participate in the removal of iron from transferrin (Boradia *et al.*, 2014a). Regarding Lf, a recent study demonstrated that GAPDH can act as an external receptor to sequester iron from Lf (Malhotra *et al.*, 2017). In vitro experiments proved that GAPDH is the receptor involved in binding with Lf, the overexpression of GAPDH in *M.tb* H37Ra cells led to significant increase in binding and uptake of Lf and also internalized of Lf into the bacterium. The mechanism of internalisation of this process is still unclear (Malhotra *et al.*, 2017).

In the extracellular pathogen *S. aureus*, the exact mechanism for iron sequestration from Tf/Lf proteins has yet to be elucidated. One mechanism suggests that GAPDH provides localised acidification which promotes release of iron from Tf, Another mechanism states that GAPDH can sequentially remove iron from N-lobe and then C-lobe of transferrin (Taylor and Heinrichs, 2002, Modun and Williams, 1999). In other pathogens such as *Trypanosoma brucei*, the causative agent of human sleeping sickness, GAPDH was recognised as a receptor to bind bovine lactoferrin (Tanaka *et al.*, 2004). In mammalian cells, the role of GAPDH in this context is better characterised. Indeed, GAPDH function here is not only in the iron uptake. It is involved in iron homeostasis and the balance of intracellular iron levels (Boradia, 2014 #266). Once the cells needs iron, GAPDH interacts with either lactoferrin or transferrin and internalise them into the endosomes (Rawat *et al.*, 2012). Upon conditions of intracellular iron excess, GAPDH switches its function to be iron efflux. GAPDH can be converted into another isoform which is high affinity receptor of apo-transferrin (Sheokand *et al.*, 2014). However, the exact mechanism of how iron flow out the cells remains unclear.

A number of organisms have been documented to utilise Lf to acquire iron, but the role of GAPDH in iron uptake was not identified. These include some pathogenic bacteria

such as some of *Haemophilus* and *Neisseria* species (Gray-Owen and Schyvers, 1996), *H. pylori* (Senkovich *et al.*, 2010), *Vibrio cholera* (Ascencio *et al.*, 1992), in addition to some parasites such as *Schistosoma mansoni*, *Leishmania infantum*, *Trypanosoma cruzi*, (Soares *et al.*, 1992, Tanaka *et al.*, 2004).

To conclude, the findings of this chapter have indicated for first time that cjGAPDH is involved in iron uptake from ferric-Lf. In addition, the results demonstrate that cjGAPDH can potentially serve as a specific receptor of lactoferrin. In the subsequent chapter, the relation between glycolytic activity of GAPDH, particularly the function of Cys150 in the active site of GAPDH and iron acquisition from lactoferrin will be investigated.

Chapter 5. The binding function of GAPDH with human ferric-Lf in *C. jejuni* is independent of its glycolytic activity

5.1 Introduction

GAPDH protein is one of the most intriguing proteins because it exhibits a variety of functions unrelated to its classical role in energy production. However, the molecular mechanisms that underpin GAPDH's role as a multifunctional protein are poorly understood (White and Garcin, 2016). The structure and function of GAPDHs among different organisms are well-characterised, overall crystal structures are solved and they seem similar to each other. The asymmetric unit in crystal structure has two domains; one NAD(P)⁺ binding domain and one catalytic domain (Mukherjee *et al.*, 2010). In *C. jejuni*, the crystal structure of cjGAPDH and active site controlling the glycolytic function has been successfully solved (Elliott, 2009). The active site of cjGAPDH is similar to that of other GAPDHs, the structure of the monomeric form and the active site of cjGAPDH is shown in Figure 5-1 A, B.

The catalytic cysteine150 (C150) residue interacts with Histidine177 (H177), which facilitates the increase of C150 acidity by proton extraction (Tourigny *et al.*, 2011, Elliott, 2009). Therefore, the mutation of these important amino acid residues could significantly affect the function of GAPDH. It has been reported that the cysteine residue in the active site of GAPDH has a very important role in the regulation of oxidative stress, GAPDH is a major target of oxidative stress (Hwang *et al.*, 2009). Oxidative stress may convert the normal conformation of GAPDH to an abnormal one via modification of the cysteines, resulting in protein aggregation (Nakajima *et al.*, 2007). In addition, the cysteine residue in the active site of GAPDH is critical in a signal transduction pathway regulating heme metabolism (Sirover, 2014). The cys mutated GAPDH and chemically modified histidine in the active site prevented heme from binding with GAPDH (Hannibal *et al.*, 2012).

The mechanism of the GAPDH reaction is well-elucidated, C150 and H177 have important roles in this reaction. The substrate of GAPDH (D-G3P) binds the active site with its C₃ phosphate positioned in the conserved "Ps" site. It is stabilized by a neighbouring NAD⁺, the cavity of binding is mostly formed by basic amino acid residues (Mukherjee *et al.*, 2010). The thiol group of C150 attacks the carbonyl carbon (C₁) of

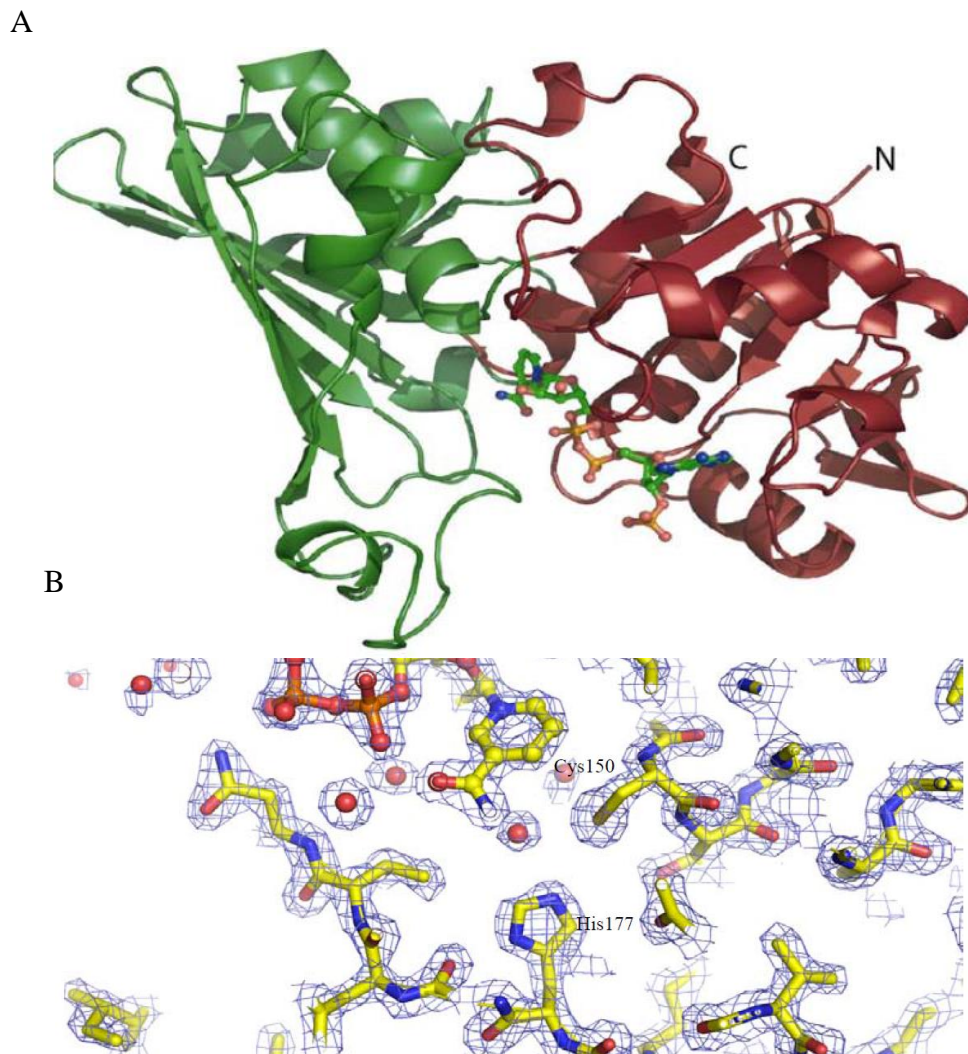


Figure 5-1 A, B. The Structure of cjGAPDH.

In panel A the structure of the monomeric form of cGAPDH bound to NADP, each of NADP⁺ binding domain and the catalytic domain are represented in red and green respectively. The binding domain is corresponding to residues 1-147 and 312-328, while catalytic domain is composed of residues 148-311. The NADP⁺ molecule is shown as a ball and stick structure. In panel B, the essential amino acid residues in the active site of cjGAPDH, Cys150 and His177 are labelled. The figures were taken from Elliott (2008).

D-G3P creating a hemithioacetal intermediate. The H177 assists the transfer of hydride from C₁ of bound G3P to the C₄ atom of the nicotinamide ring NAD⁺, this transfer oxidizes the substrate with the formation of a thioacylenzyme intermediate while NAD⁺ is reduced to NADH (Mukherjee *et al.*, 2010).

In the previous chapter, the results indicated that cjGAPDH is involved in iron uptake from human ferric-Lf. The results of the binding assays with Lf suggest that GAPDH could act as a specific receptor to bind ferric-Lf. However, the role of the glycolytic reaction of GAPDH in this function still needs clarification. In this context of GAPDH, there is not much available knowledge about ferric-Lf in the literature. A recent study reported no relationship between binding of GAPDH with Lf and enzymatic activity of GAPDH in *M. tuberculosis* (Malhotra *et al.*, 2017). In the work of this chapter, it is hypothesised that the glycolytic activity of GAPDH can mediate iron release from ferric-Lf. Therefore, the main aim was to investigate the role of enzymatic activity in iron uptake from ferric-Lf by cjGAPDH. One approach to address this is to substitute the cysteine C150 in the active site of GAPDH with serine (C150S) by site directed mutagenesis. The mutated *gapA* was cloned, over-expressed and purified. The enzyme activity of purified mutated GAPDH will be measured and compared with wild protein. The major objective was to create *C. jejuni* strains lacking the enzymatic activity of GAPDH, and then examine its capability to utilize ferric-Lf in iron uptake and growth of *C. jejuni*.

5.2 Site-directed mutagenesis of the *gapA* gene

Site-directed mutagenesis was used to substitute the active site amino acid, cysteine, in GAPDH protein of *C. jejuni* with serine. Figure 5-2 illustrates the strategy of the mutagenesis described in this chapter. Briefly, inverse PCR primers were designed (table 2.5), in which the 5' end of forward and reverse primers tailed with about 10-15 bp overlapping sequences, the primers also contain the desired mutation in the DNA sequence of *gapA* encodes the amino acids which control the glycolytic function. The recombinant *gapA*- pET151/D plasmid (see section 4.2.6.2.1) was used as a template in the PCR reaction. The entire plasmid was amplified and PCR products were digested with *DpnI* in order to eliminate the parental plasmids, which harbour C150. After that, digested PCR products were alcohol precipitated and electroporated into *E. coli* DH5 α . The LB agar plate supplemented with 100 μ g/ μ l Amp was used to recover the transformant cells. All PCR conditions and all other subsequent work such as DNA electrophoresis and DNA sequencing were performed as described in chapter 2. Colonies were screened by PCR

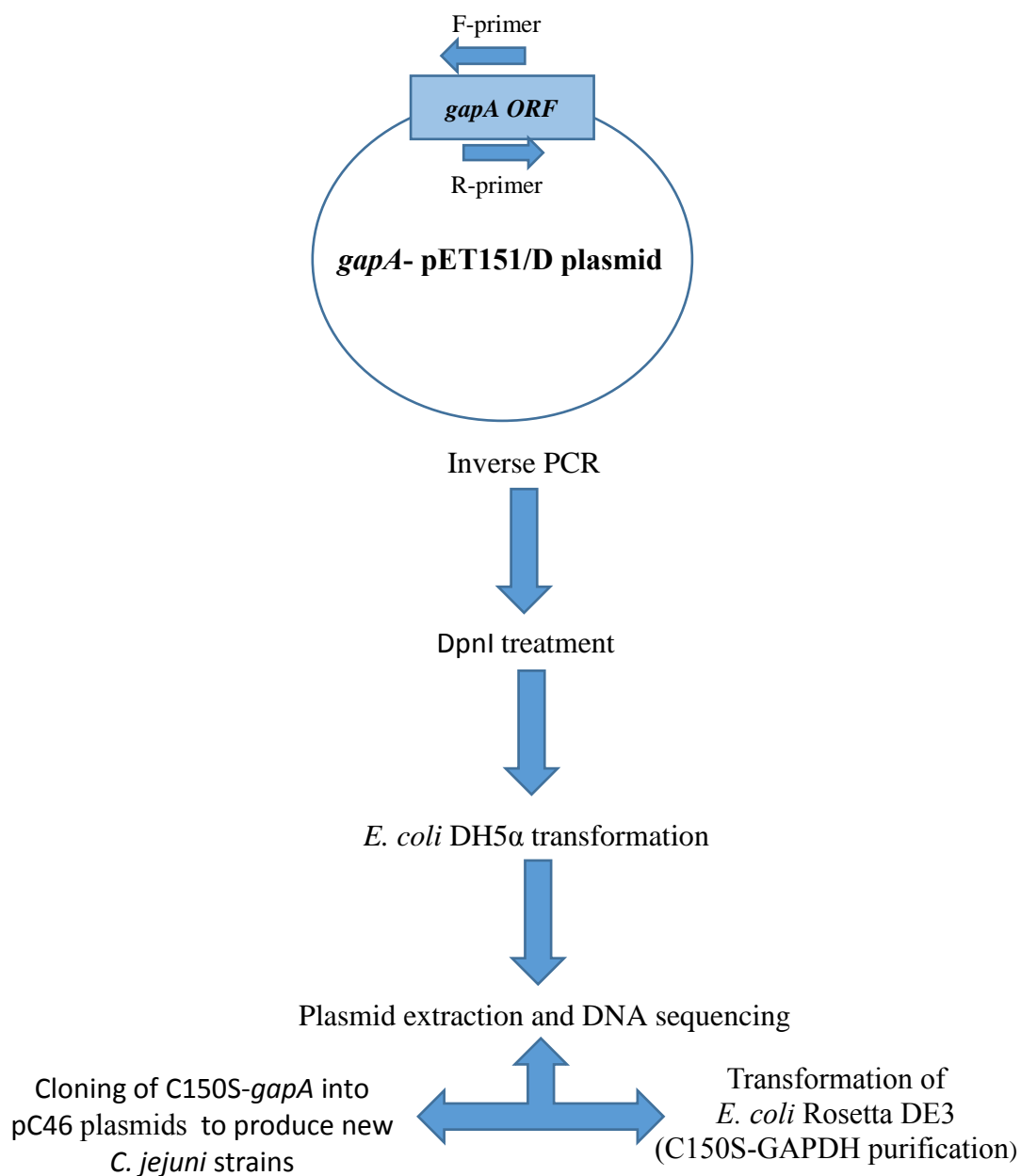


Figure 5-2. Strategy applied in site-specific mutagenesis of *gapA* gene.

The figure illustrates the procedure for construction of C150S-*gapA*. The details of F-primer and R-primer is given in table (2.6). DNA sequencing was performed by use of *gapA*-For and *gapA*-Rev primers to ensure substitution of C150S in ORF of *gapA*.

and those that might harbour C150S-*gapA*-pET151/D plasmid were chosen for plasmid extraction. DNA sequencing of mutated *gapA* was used to confirm the mutation and to select the plasmids to be transformed to *E. coli* Rosetta DE3 for expression and purification of C150S-GAPDH mutated protein. Additionally, C150S-*gapA* mutated gene cloned in pET151/D plasmid was exploited to construct new C150S-*gapA*-pC46 recombinant plasmids in order to create new strains of *C. jejuni* that are deprived of GAPDH glycolytic activity.

5.3 Production and characterisation of C150S-GAPDH mutated protein

It was important to express and purify C150S-GAPDH mutated protein in order to determine the role of C150 in iron acquisition from ferric-Lf. The hypothesis is that iron acquisition depends on the basic function of GAPDH. Additionally, the purification of C150S-GAPDH was important to investigate the changes in characteristics of this new modified protein such as solubility, enzyme activity, secondary structure and folding.

5.3.1 Overexpression and purification

The previous conditions applied for purification of wild type cjGAPDH were followed as described previously (Elliott, 2009, Ayna, 2016), section 2.5.6. Briefly, C150S-*gapA*-pET151/D plasmid was transformed into the overexpression host *E. coli* Rosetta DE3, and the same steps in section (4.2.6.2.1) were followed.

The results of protein over-expression in *E. coli* Rosetta DE3 are shown in figure 5-3 A,B. It is clear that the solubility of recombinant C150S-GAPDH mutated protein was similar to recombinant cjGAPDH wild-type protein, the mutated protein was expressed extensively in the soluble fraction of the cells (figure 5-3A). The presence of mutated cjGAPDH in the soluble fraction was confirmed by Western blot assay, a dense band was detected by anti-GapA antibodies in the soluble fraction of *E. coli* Rosetta DE3 at 43 kDa which is most likely recombinant C150S-cjGAPDH protein. A similar sized, but less dense band was also seen in the insoluble fraction. In addition, the induction of C150S-GAPDH expression by IPTG was similar to wild-type cjGAPDH. Inducing of the cells by IPTG yielded more protein, although the absence of IPTG also resulted in a considerable level of expression, this feature was also observed with wild-type cjGAPDH. Therefore, all the subsequent steps in protein purification were performed with soluble fraction of the *E. coli* Rosetta DE3 with induction by 150 μ M IPTG.

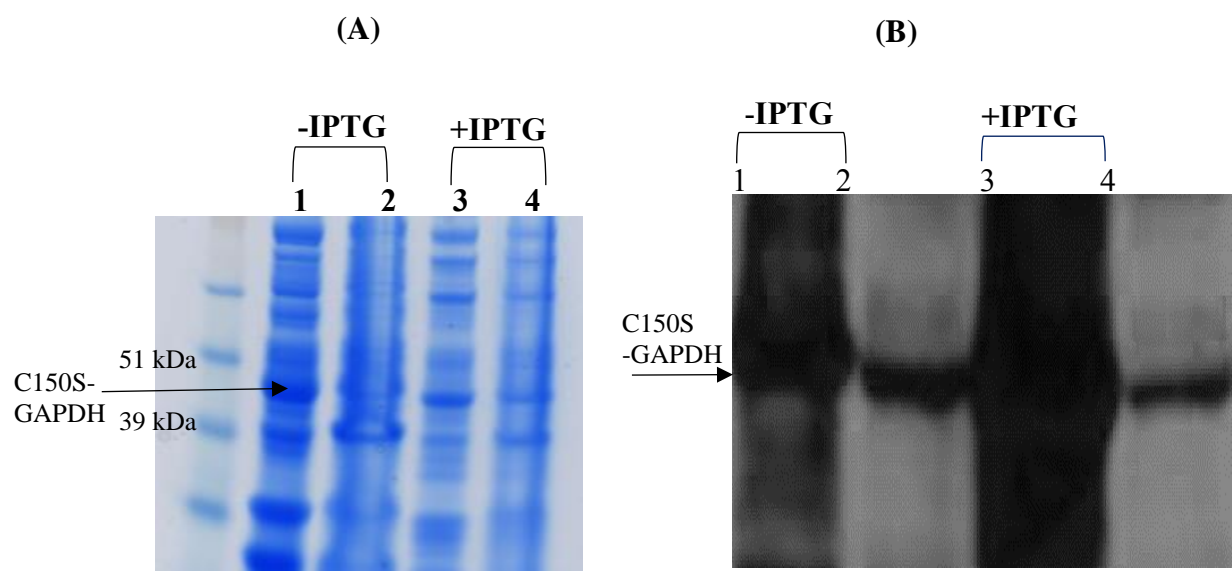


Figure 5-3 A, B. Overexpression and purification of C150S-GAPDH protein.

Panel A shows the Coomassie stained 12% SDS-PAGE gel of overexpressed C150S-GAPDH *E. coli* Rosetta DE3 fractions. The lanes 1, 3= soluble fractions, and 2, 4 = insoluble fractions. The cells were grown at 37°C and induced by 150 μ M IPTG, with overnight incubation. The cells were lysed by sonication and centrifuged, the supernatant was taken as soluble fraction while the pellet was insoluble. SeeBlue2 protein marker and C150S-GAPDH sizes are indicated on the left of the gel. Panel B is the Western blot of fractions shown in Panel A in the same order; the blot was probed with 1:5000 rabbit anti-GapA, the expressed C150S-GAPDH is indicated by the arrow on the left of the blot.

5.3.2 Measurement of GAPDH enzyme activity of C150S-GAPDH mutated protein

Numerous publications have indicated cysteine as the crucial amino acid in the active site of GAPDH among different organisms (Mukherjee *et al.*, 2010, Didierjean *et al.*, 2003, Tourigny *et al.*, 2011). Therefore, it was essential to investigate the enzymatic function of C150S-GAPDH mutated protein in converting G3p to 1, 3-diphosphoglycerate in the presence of coenzyme NADP. The same method described previously was followed (Purves, 2011). The purified cjGAPDH was used as a positive control.

The assay was conducted in triplicate for sample and control, and the plate was incubated at 37°C for 30 minutes. After that, the absorption was measured at 340 nm by a FLUOstar Omega plate reader (BMG Labtech). For each sample and control, an average reading from the three wells was recorded to represent the enzyme activity of the protein. The results are shown in figure 5-4, there is a large decrease in the enzymatic activity of C150S-GAPDH mutated protein in comparison with recombinant cjGAPDH protein. The mutated protein is enzymatically inactivated due to the substitution of cysteine with serine in the active site of the protein.

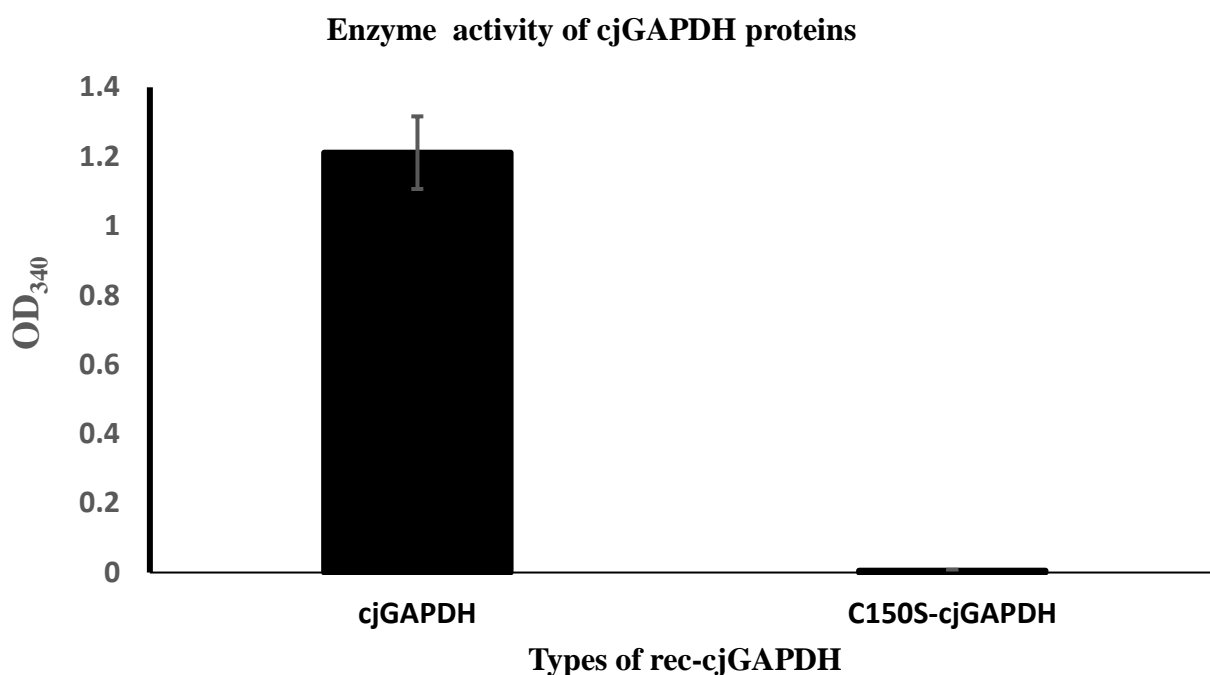


Figure 5-4. The enzymatic activity of recombinant purified C150S-cjGAPDH mutated protein in comparison with recombinant purified cjGAPDH.

The graph shows the NADPH-GAPDH activity of different forms of cjGAPDH, recombinant wild type protein cjGAPDH (black column) and recombinant mutated C150S-GAPDH (unfilled column). 10 μ l of 20 ng/ μ l purified protein (200 ng) were added to enzymatic reaction. The assay was performed as described in the text, the data presented is an average of at least 3 independent biological repeats. The error bars indicate the standard deviations of the data.

5.3.3 Determination of the secondary structure of C150S-GAPDH by far UV circular dichroism (CD)

Circular dichroism (CD) is a rapid technique used to estimate the secondary structure, folding and binding properties of the protein. Here, this method was used to investigate whether the C150S-GAPDH protein was folded or not, and to measure the secondary structure at different wavelengths. The procedure was described in section 2.5.7. To calculate the signals of CD spectrum, the difference between the absorbance generated from counter-clockwise (L) and clockwise (R) rotating circularly polarized light is calculated and accordingly the secondary structure of protein can be predicted at wavelengths between 160-250 nm (Kelley and Sternberg, 2009). In relation to GAPDH protein, it has been reported by CD spectroscopy method as an α -helical protein (Boradia *et al.*, 2016, Palamalai and Miyagi, 2010).

The reference CD spectrum of secondary structure of polypeptide chains is shown in figure 5-5 A. The helix, sheet and random coil are represented by yellow, blue and red respectively. This figure was taken from <http://www.proteinchemist.com/cd/cdspec.html>. As indicated in the figure, α -helical proteins have one positive band at approximately 193 nm and negative bands at around 208 and 222 nm. Proteins rich in antiparallel β -pleated sheets (β -helices) will show a one-dip curve at 218 nm and one positive peak at 195 nm while random coil proteins will have very low ellipticity above 210 nm and negative band around 195 nm (Greenfield, 2006, Kelley *et al.*, 2015).

The results of comparative CD spectra between cjGAPDH and C150S-GAPDH proteins are shown in figure 5-5 B. The spectra of both proteins show the features of α -helix pattern, there is one positive band at approximately 193nm in both proteins, two negative bands at about 209 and 223 nm. However, the negative bands are not so distinct.

Overall, the results of CD spectra of GAPDH secondary structure acquired here suggest that the proteins are folded and the secondary structure of mutated C150S-GAPDH protein was not altered and still similar to the wild type protein. Both wild type GAPDH and C150S-GAPDH proteins are comparable α -helical secondary structure proteins.

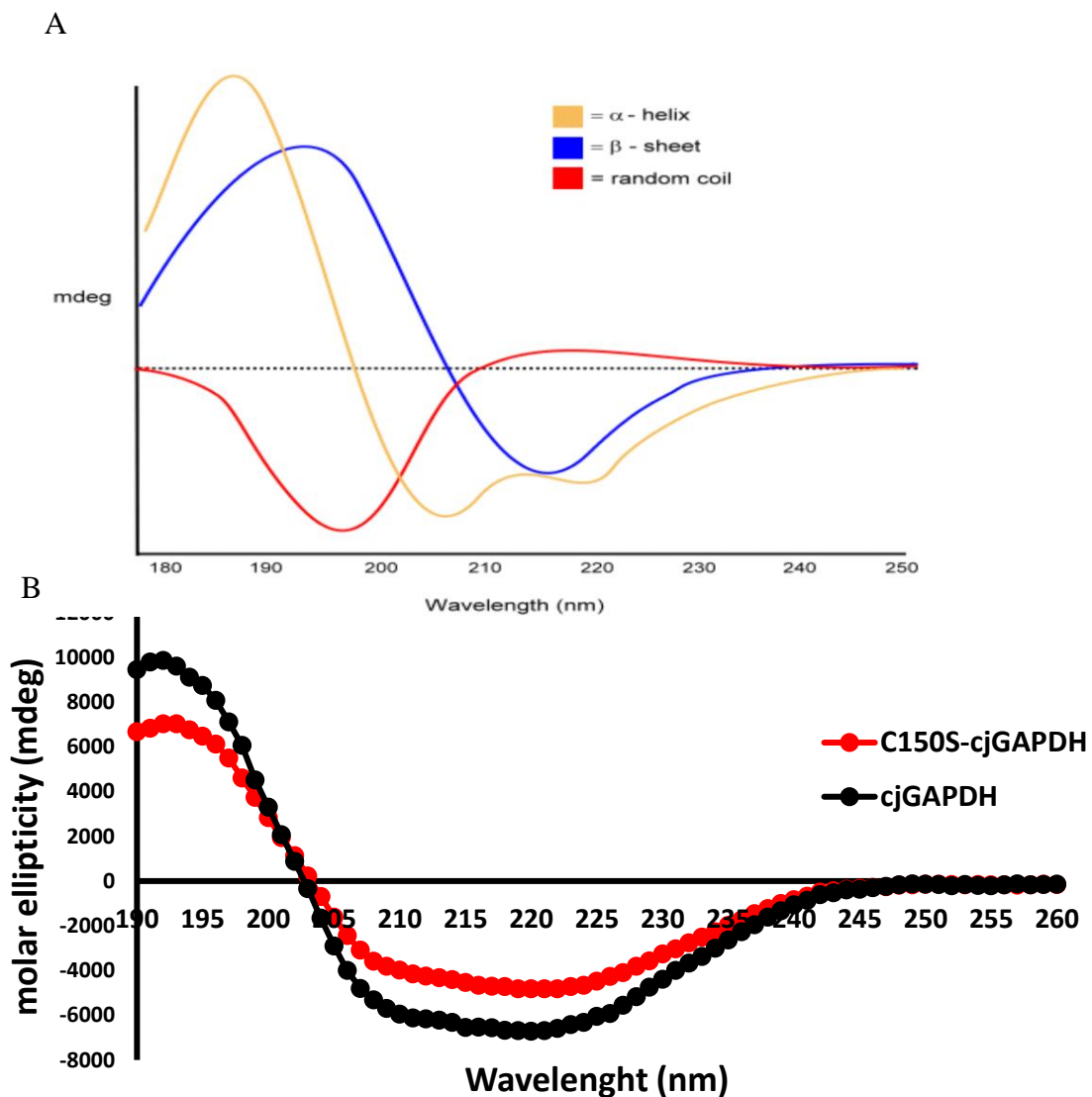


Figure 5-5 A, B. The CD spectrum of cjGAPDH proteins.

Figure (A) shows the reference CD spectrum of the secondary structures of a polypeptide chain helix (yellow), sheet (blue), random coil (red). Figure (B) shows CD spectra of cjGAPDH and C150S-GAPDH proteins. The final concentration of about 20 μM cjGAPDH proteins was used, the experiment was performed in buffer containing 20 mM phosphate buffer pH= 7.4, 200 mM sodium fluoride. The wavelengths used were ranged between 185 to 260 nm with a bandwidth of 1 nm using a quartz cuvette with 0.1 cm light path. The CD spectrum was reported in molar ellipticity (mdeg).

5.4 Creation of new *C. jejuni* strains lack glycolytic activity of *gapA* gene

As mentioned previously, the cysteine residue has an important function in the active site of *gapA*. Therefore, it was important to know if the substitution of cysteine with serine in *cjGAPDH* active site can affect the capability of *C. jejuni* to utilise human ferric-Lf as a sole iron source. The open reading frame (ORF) of C150S-*gapA* in C150S-*gapA*-pET151/D plasmid was amplified and cloned into pC46 plasmids; the *C. jejuni* plasmid delivery system. The same procedure of *gapA* complementation in *C. jejuni* described in section 3.2.1 was followed. Two plasmids were constructed, C150S-*gapA*-p*CfdxA* and C150S-*gapA*-p*CmetK* which are medium and low gene expression plasmids respectively. Unfortunately, no clones of *E. coli* DH5 α were obtained for C150S-*gapA*-p*CporA* plasmid. *C. jejuni* NCTC11168 was transformed by these two newly created plasmids by electroporation. The selection marker in the transformation was resistance to chloramphenicol, the resistant colonies were further investigated by colony PCR to ensure the existence of the C150S-*gapA* within pseudo gene *cj0046* DNA sequences. Additionally, DNA sequencing of the complemented *gapA* gene was also performed to prove the presence of the C150S mutation. Figure 5-6 shows the agarose gel electrophoresis for PCR used to prove construction of the hetero-merodiploid *gapA* *C. jejuni* strains.

Overall, PCR results confirmed the successful transformation of two new *C. jejuni* strains:

- 1- *C. jejuni* 2*gapAcj0046::pmetK*-C150S-*gapA* (Ser-2*gapA*-*pmetK*).
- 2- *C. jejuni* 2*gapAcj0046::pfdxA*-C150S-*gapA* (Ser-2*gapA*-*pfdxA*).

DNA sequencing for both *gapA* alleles and promoters in these strains showed no errors suggesting that they can be used for the further work. The notation of each strain given in brackets will be used in all further work in this project.

Finally, *gapA* wild type allele was inactivated by transformation with pUC19 Δ *gapA::kanamycin* plasmid; see figure 3-2. The procedure followed in mutagenesis and clarification of mutants is identical to that described in section 3.2.2. The transformant cells were selected based on resistance to kanamycin and further investigated by colony PCR and DNA sequencing.

Around 10 colonies of *C. jejuni* on MHA plates supplemented by kanamycin were obtained after 3 days of incubation. All colonies were screened by PCR to confirm the presence of terminator-less, promoter-less kanamycin cassette in the correct location of

the *C. jejuni* genome (figure 5-6). In addition, DNA sequencing analysis of the ORF of C150S-*gapA* complemented gene was performed by use of different primers; *gapA*-For, *gapA*-Rev and *Cj0046*-Forward primers (see table 2.5 for primer sequences). Additionally, DNA sequencing analysis of *pfdxA* and *pmetK* promoters, which drive the expression of C150S-*gapA* was also carried out in these newly produced strains. Interestingly, the results of DNA sequencing revealed no colonies maintained the C150S-*gapA* mutation. The genetic codon of serine 5'-TCC-3' was reverted to cysteine 5'-TGT-3'. No errors were observed in DNA sequences of the promoters and RBS. The experiment was repeated three times.

As transformation controls, the merodiploid *2gapA-pfdxA* and *2gapA-pmetK* were used as positive controls for the mutagenesis to ensure that the transformation procedure was working properly. In addition, hetero-merodiploid strains; Ser-*2gapA-pmetK* and Ser-*2gapA-pfdxA* were also electroporated with sterilised water free of DNA, incubated on MHA containing Cm. The grown colonies were sequenced and results showed no reversion in genotype of complemented *gapA*. Therefore, these results mean that the transformation procedure was not involved in the reversion of the strains genotype.

The results indicate the importance of C150 in metabolic functions of cjGAPDH and consequently *C. jejuni*. Two reverted strains, mutated in *gapA* were produced:

1- *C. jejuni* $\Delta gapA::kanR$ *cj0046::pfdxA-gapA* (Cys- $\Delta gapA$ -*pfdxA*),

2- *C. jejuni* $\Delta gapA::kanR$ *cj0046::pmetK-gapA* (Cys- $\Delta gapA$ -*pmetK*).

The notation of each strain given in brackets will be used in all incoming work of this chapter.

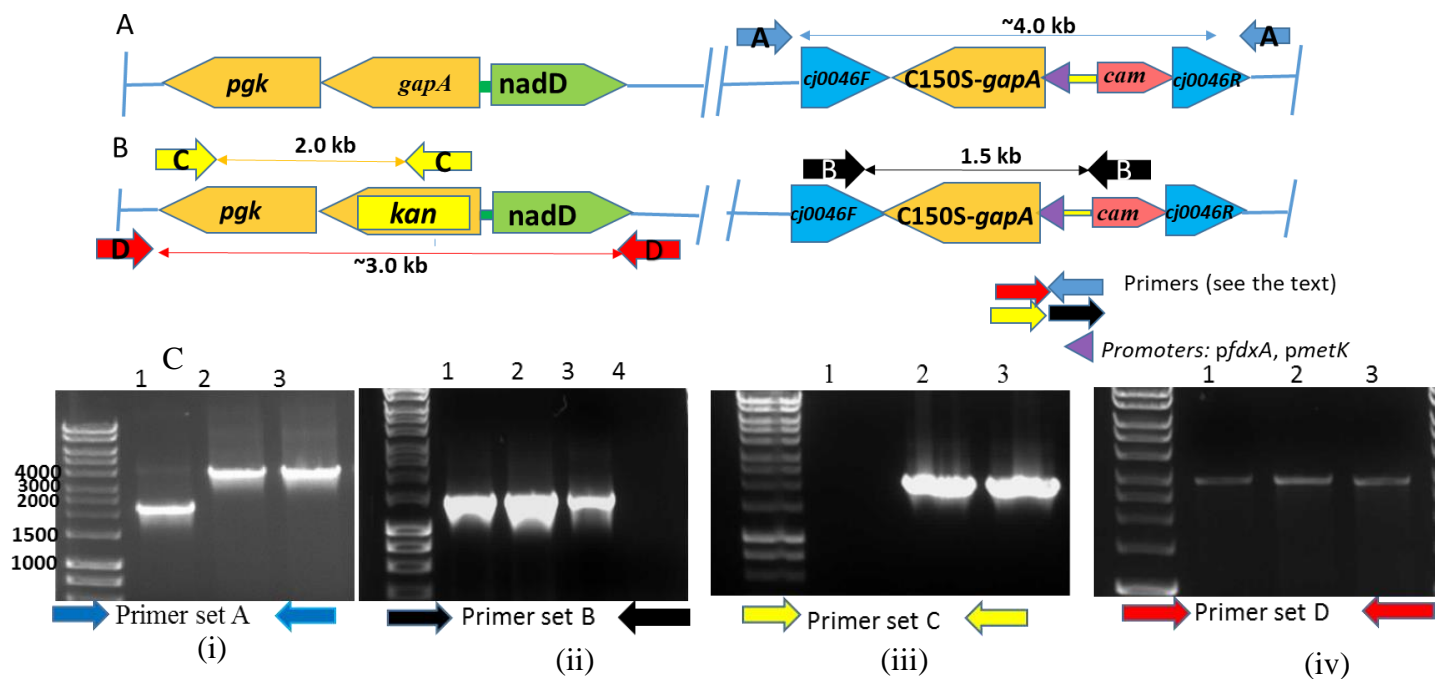


Figure 5-6. Clarification of producing hetero-merodiploid and Cys- Δ gapA reverted *C. jejuni* strains.

(A, and B) *C. jejuni* genomic context of hetero-merodiploid and inactivated *gapA* strains respectively. The blue arrows indicate primer set A; chromosomal flank primer of *cj0046* pseudo gene to clarify creation of hetero-merodiploid strains, black arrows are primer set B; *cj0046*-For and CATinv-R, yellow arrows are primer set C; chromosomal flank primer of *pgk* gene (Flank-*pgk*-For) and kanamycin-F, and the red arrows indicate primer set D which are Flank-*pgk*-For and Flank-*nadD*-Rev.

(C) Agarose gel electrophoresis to confirm the creation of these new strains. The gel (i) shows PCR products by primer set A; 1= WT product size=2197, 2= Ser-2*gapA*-*pfdxA*, product size=3965bp, and 3= Ser-2*gapA*-*pmetK*, product size=3981bp. The gel (ii) is PCR products by primer set B, 1= Cys- Δ *gapA*-*pfdxA*, product size=1468 bp, 2= Cys- Δ *gapA*-*pmetK*, product size =1447 bp, 3= Δ *gapA*-*fdxA* ;+ve control, and 4 = WT as -ve control. The gel (iii) is PCR product by primer set C; the product size is 2039bp, 1= WT as -ve control, 2= Cys- Δ *gapA*-*pfdxA* and 3= Cys- Δ *gapA*-*pmetK*. Finally, (iv) is PCR products by primer set D, product size=3000 bp, same order of gel (iii) but WT was +ve control. The marker is hyperladder I, the standard sizes indicated on the right side of the gel (i).

5.5 Phenotyping of the hetero-merodiploid and *cys-ΔgapA* reverted strains

Starting from this section, the assays applied in chapter 3 and 4 for phenotyping new created *C. jejuni* strains were used here for the same purpose. Thus, some information might not be given to avoid the repetition.

5.5.1 Growth curve of strains

Growth curves of the new merodiploid and reverted *Cys-ΔgapA* strains were carried out in order to detect the alterations of the growth patterns compared with wild type strain. The doubling time and growth rate were calculated for each strain as have been shown previously in chapter two, and compared with wild type.

The results shown in figure 5-7 illustrate no statistical differences between wild type and complemented C150S-*gapA* strains. In addition, no differences were observed between hetero-merodiploid and *Cys-ΔgapA* reverted strains. The statistical analysis of growth kinetics parameters between the strains are given in tables 5-1 and 5-2. All strains have close doubling times ranging from 1.77 to 1.97, which is approximately two hours to multiply its population to double in size or value at a constant growth rate. The observation here was the minor delay of entering into log phase of growth by all strains including the WT. It is likely that this is due to technical issues of the initial supply of optimum levels of CO₂ and O₂ in the plate reader during the running of this experiment, thus this affected all strains.

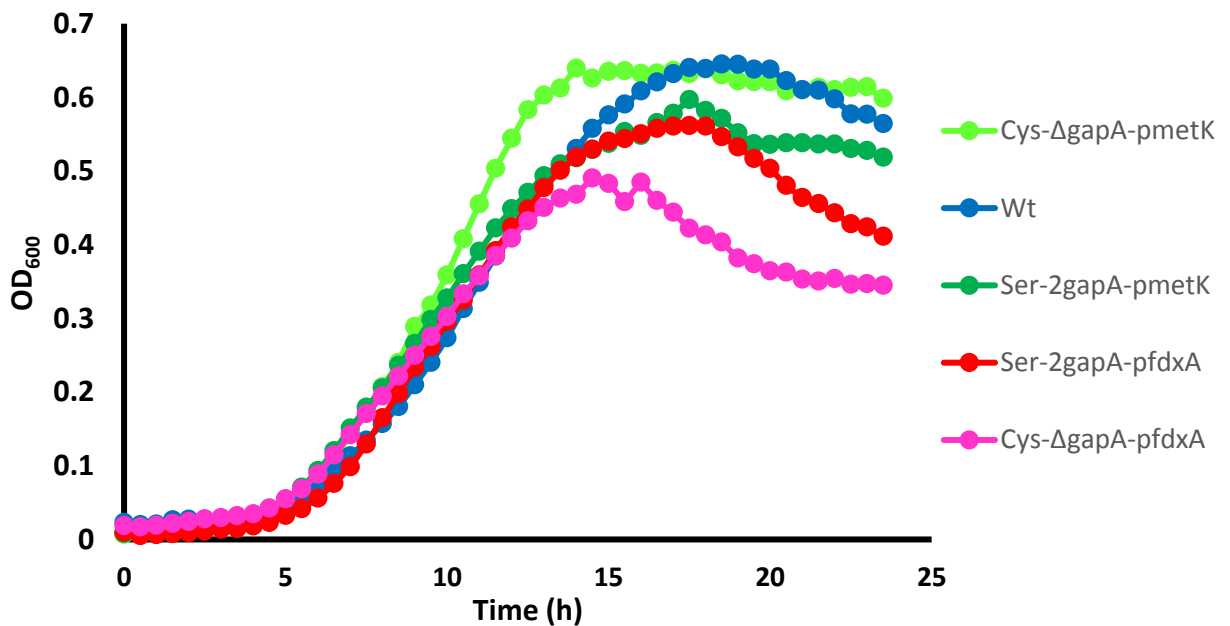


Figure 5-7. Growth curve assay of hetero-diploids, *gapA* mutated and wild strain *C. jejuni* NCTC 11168.

C. jejuni strains were grown in MHB under microaerobic conditions at 42° C. The optical density (OD) of the initial cell suspension was adjusted to initial OD₆₀₀= 0.025, the growth was measured as the optical density of the culture at 600. The readings of absorbance were taken every 30 minutes for 24 hour by FLUOSTAR omega plate reader. Each data point represents the average of the 5 replicates, each experiment was repeated 3 times in three different times.

Table 5-1. Growth rate and doubling times of wild type, hetero-merodiploid and Cys- Δ gapA reverted strains calculated from growth curve given in Figure 5-6

Strains Growth parameters	WT	Hetero-merodiploid		Cys- Δ gapA reverted	
		Ser-2gapA-pfdxA	Ser-2gapA-pmetK	Cys- Δ gapA pfdxA	Cys- Δ gapA pmetK
1- Growth rate (h ⁻¹) (P value vs WT)	0.36 ± 0.03	0.39 ± 0.05 (0.34)	0.39 ± 0.004 (0.07)	0.36 ± 0.05 (0.95)	0.38 ± 0.01 (0.15)
2- Doubling time (h) (P value vs WT)	1.95 ± 0.13	1.80 ± 0.21 (0.35)	1.77 ± 0.02 (0.16)	1.97 ± 0.31 (0.95)	1.80 ± 0.07 (0.16)

Table (5.2) Statistical differences calculated by paired t test between growth rate and doubling time of hetero-merodiploid and mutated strains.

	Growth rate		Doubling time	
Hetero-merodiploid Vs cys- Δ gapA reverted	Ser-2gapA-pfdxA vs Cys- Δ gapA pfdxA	Ser-2gapA-pmetK vs Cys- Δ gapA pmetK	Ser-2gapA-pfdxA vs Cys- Δ gapA pfdxA	Ser-2gapA-pmetK vs Cys- Δ gapA pmetK
P value	0.51	0.52	0.49	0.51

5.5.2 Measurement of the transcriptional levels of gapA by RT-PCR

Real-Time PCR was carried out in order to evaluate the mRNA levels of both *gapA* heterologous copies in the newly created *C. jejuni* strains. The hypothesis is that mRNA transcript levels of C150S-*gapA* is relevant to the strength of the promoter. The results show that the transcription levels of GAPDH was relatively higher in hetero-merodiploid and Cys- Δ *gapA* reverted strains than WT. The results were in agreement with those obtained from *C. jejuni* merodiploid and mutated *gapA* strains characterised previously (section 3.2.3.2). Overall, the transcriptional levels of GAPDH were compatible and related to the strength of the promoters.

The results are shown in figure 5-8, the Ser-2*gapA*-*pfdxA* strain exhibits the highest transcriptional levels among all the strains, the wild strain demonstrated mRNA transcription levels were relatively lower than other *C. jejuni* strains.

5.5.3 Western blot of whole cell GAPDH

Western blot analysis was used to assess GAPDH protein levels in hetero-merodiploid and Cys- Δ *gapA* reverted strains, it has been assumed that the levels of cjGAPDH in these strains correspond to the strength of promoters. The western blot analysis was carried out as mentioned previously (section 2.5.3).

The results are shown in figure 5-9, all strains show the prominent 43 kDa which represents GAPDH polypeptide in all *C. jejuni* strains. Like the overexpressed *C. jejuni* strains described in section 3.2.3.4, there is an extra \approx 30 kDa band in the C150S-*gapA* complemented strains. Therefore, the levels of GAPDH in each strain was relevant to the strength of the corresponding promoter. The image J programme was used to estimate the levels of cjGAPDH proteins. Figure 5-9 shows the result of the Image J analysis. The level of GAPDH protein was the highest in Ser-2*gapA*-*pfdxA*, it was approximately 8 fold greater than WT. These results correlate with transcription levels determined by RT-PCR (section 5.4.2.2), therefore, the levels of GAPDH were related to the strength of the promoter and the number of transcribed *gapA* genes.

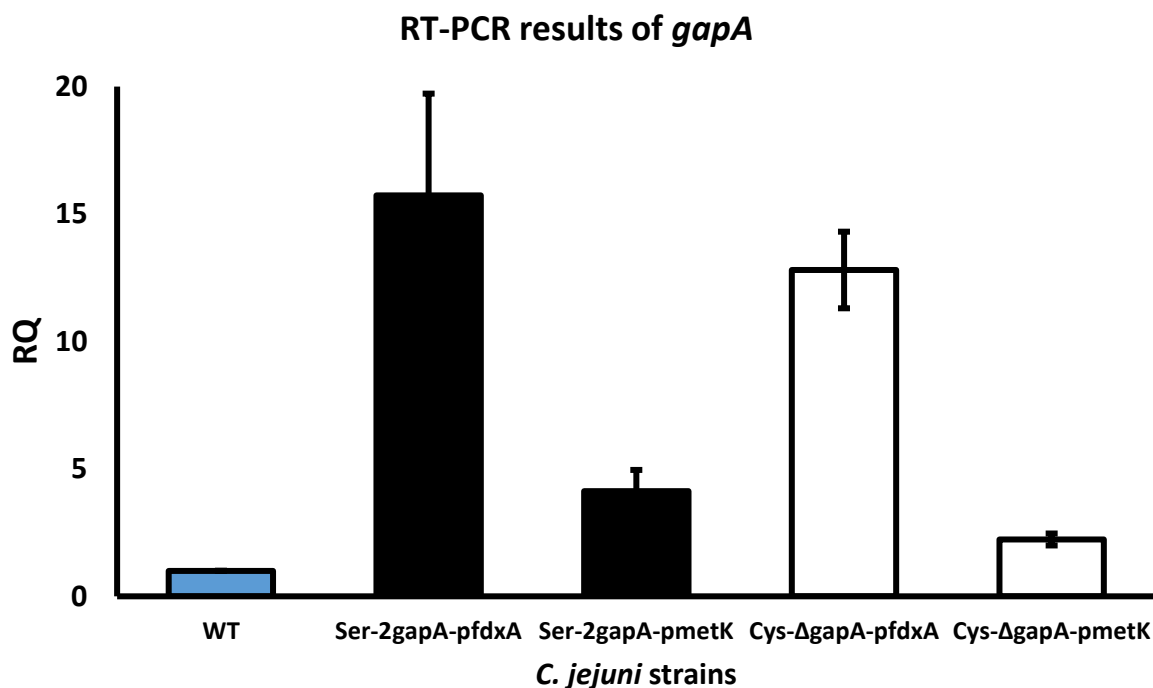


Figure 5-8. Relative RT-qPCR results of *gapA* gene in new *C. jejuni* strains.

The mRNA transcripts levels of *gapA* were measured by qPCR and compared with WT, the *rpoA* was used as endogenous gene. The blue column represents WT, whereas the black and white columns are representing the hetero-merodiploid and *Cys-ΔgapA* reverted strains respectively. The conditions are identical to same experiment described in 3.2.3.2. The data presented is an average of three independent biological repeats. The error bars indicate the standard deviations of the data.

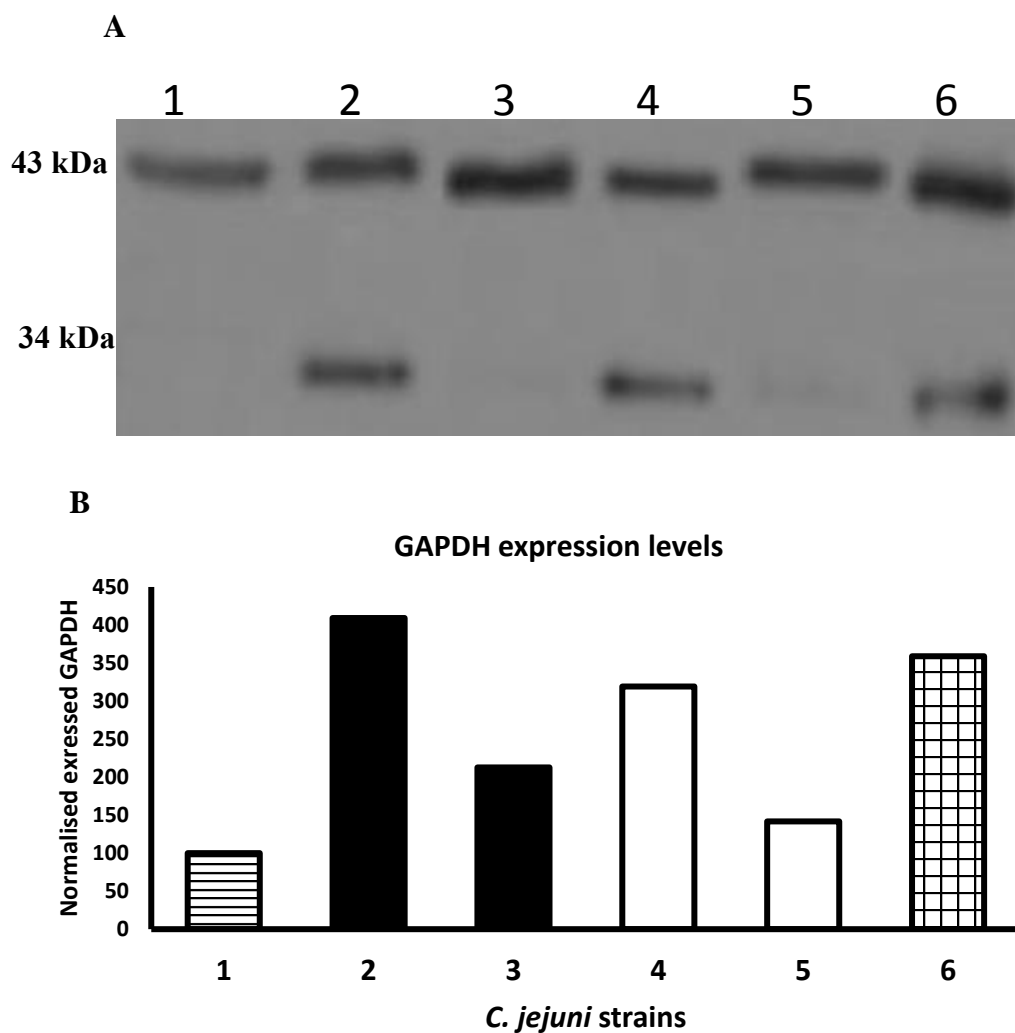


Figure 5-9 A, B. The assessment of GAPDH expression.

(A) Western blot of *C. jejuni* proteins. The proteins transferred to PVDF membranes and probed with 1:5000 dilution of primary antibody (polyclonal rabbit anti-GapA), washed and secondary antibody (Goat anti-rabbit HRP tagged) added with 1:5000 dilution. 1= WT, 2= Ser-2*gapA*-*pfdxA*, 3= Ser-2*gapA*-*pmetK*, 4= Cys- Δ *gapA*-*pfdxA*, 5= Cys- Δ *gapA*-*pmetK*, and 6= Δ *gapA*-*pfdxA* positive control *C. jejuni* strain.

(B) The expression level of GAPDH measured from the Western blot using Image J normalised to expression of *cjGAPDH* in WT strain. The data was obtained by use of Image J1.49 (Rasband, W.S., ImageJ, U. S. National Institutes of Health, Bethesda, Maryland, USA). The WT was represented by column with horizontal black lines. The black columns are hetero-diploid strains whereas white are Cys- Δ *gapA* reverted strains.

5.5.4 Measurement of whole cell *C.jejuni* GAPDH enzyme activity

Accomplishment of this assay was very important to clarify the recovery of the wild phenotype of the C150S-GAPDH among *Cys-ΔgapA* reverted strains. The whole cell GAPDH enzyme activity was measured in hetero-merodiploid and *Cys-ΔgapA* reverted strains and compared with wild type *C. jejuni* strain. The assay was performed as mentioned previously (section 2.5.4.1).

The results in figure 5-10 showed significant differences between hetero-merodiploid *Ser-2gapA-pfdxA* and reverted *Cys-ΔgapA pfdxA* strains. The hetero-merodiploid *Ser-2gapA-pfdxA* which have 2 heterologous copies of *gapA* gene showed GAPDH enzyme activity close to the WT strain which more likely means that the complemented C150S-*gapA* allele does not express its canonical function. On the other hand, reverted *Cys-ΔgapA- pfdxA* strain displayed high GAPDH enzyme activity phenotype due to restoring the wild type genotype. The differences between strains harbouring *metK* promoters and wild type were not significant, this is because the expression levels of GAPDH between them is not huge and reversion of *ser-metK* into the wild genotype.

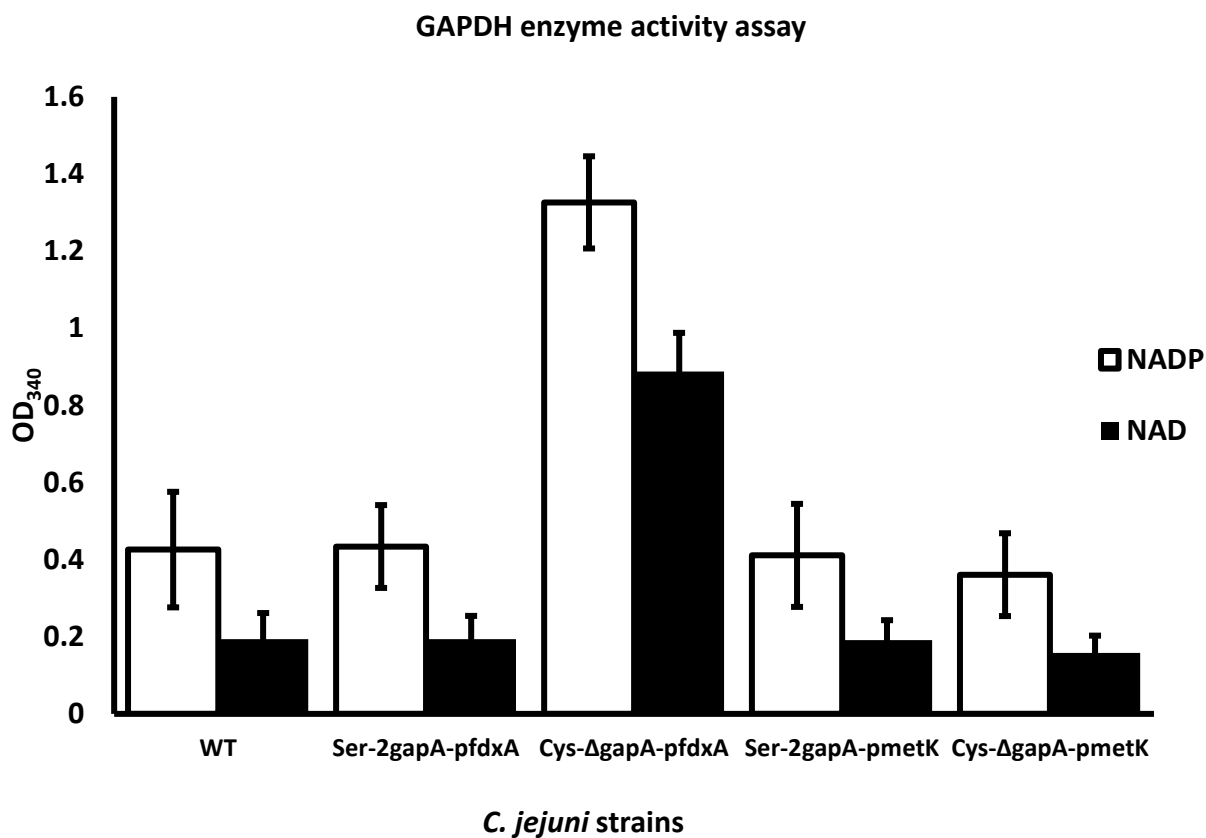


Figure 5-10. Whole cell GAPDH enzyme activity of new *C. jejuni* strains.

The graph shows the NADH dependent GAPDH activity (black columns) and NADPH dependent GAPDH activity (white columns) determined from whole cell GAPDH assays of WT, Ser-2gapA-pfdxA, Cys-ΔgapA-pfdxA, 2gapA-pmetK and Cys-ΔgapA-pmetK *C. jejuni* strains. The optical density OD₃₄₀ of formed NADH and NADPH from GAPDH reaction was measured, the data presented is an average of at least 3 independent biological repeats. The error bars indicate the standard deviations of the data.

5.6 The differences in GAPDH glycolytic activity do not alter utilisation of ferric-Lf in growth of new *C. jejuni* strains

The 24 hour growth assay in iron restricted medium (MEM α) was carried out on the new *C. jejuni* strains. The purpose of this assay was to examine the effect of glycolytic activity of GAPDH in iron uptake from ferric-Lf. Ideally, it was planned to create strains inactivated in native *gapA* gene with a complemented, non-glycolytic functional *gapA* allele. In other words, they completely lack GAPDH enzymatic activity. Unfortunately, the complemented allele in the mutated *gapA* strains reverted to wild genotype with recovery of high enzymatic activity levels of GAPDH. Therefore, the provision of the planned strains to perform this experiment was not feasible.

However, to partially overcome this obstacle, the assay was performed using of strains selected based on different gene expression levels determined in the previous sections. The hetero-merodiploid strain, Ser-2*gapA*-*pfdxA* has shown low GAPDH activity level close to WT although it is expressing high amount of GAPDH. Therefore, it was chosen to compare with Cys- Δ *gapA*-*pfdxA* reverted strain, which has similar high levels of GAPDH expression, but high GAPDH enzymatic activity. In addition, the WT and other hetero-merodiploid and Cys- Δ *gapA*-*pmetK* *C. jejuni* strains were included in this assay. Experimentally, the strains were grown in MEM α medium supplemented with different concentrations (0.27 μ M, 0.1 μ M, 0.01 μ M) of human ferric-Lf. The same procedure mentioned in section 4.2.4 was followed.

The results of growth assays are shown in figure 5-11. With optimum levels of ferric-Lf (0.27 μ M), no differences were observed in the growth patterns between all the examined strains, figure 5-10 A. Therefore, this finding suggests that the optimum levels of ferric-Lf support the growth of the *C. jejuni* strains as observed in section 4.2.4. Under decreasing levels of human ferric-Lf tenfold lower than optimum level, no differences between hetero-merodiploid Ser-2*gapA*-*pfdxA* and Cys- Δ *gapA*-*pfdxA* reverted strains were observed. The doubling time and growth rate were also calculated and the results showed no significant differences between Ser-2*gapA*-*pfdxA* and Cys- Δ *gapA*-*pfdxA* strains, tables 5-3. However, the iron growth assay showed the differences in growth patterns between these new created strains and WT, figures 5-11 B, C. Apart from Cys- Δ *gapA*-*pfdxA*, all of new created strains have cjGAPDH activity close to WT. All of the newly created strains have a higher amount of GAPDH than WT. Overall, GAPDH enzymatic activity levels might not be the factor in releasing iron from Lf.

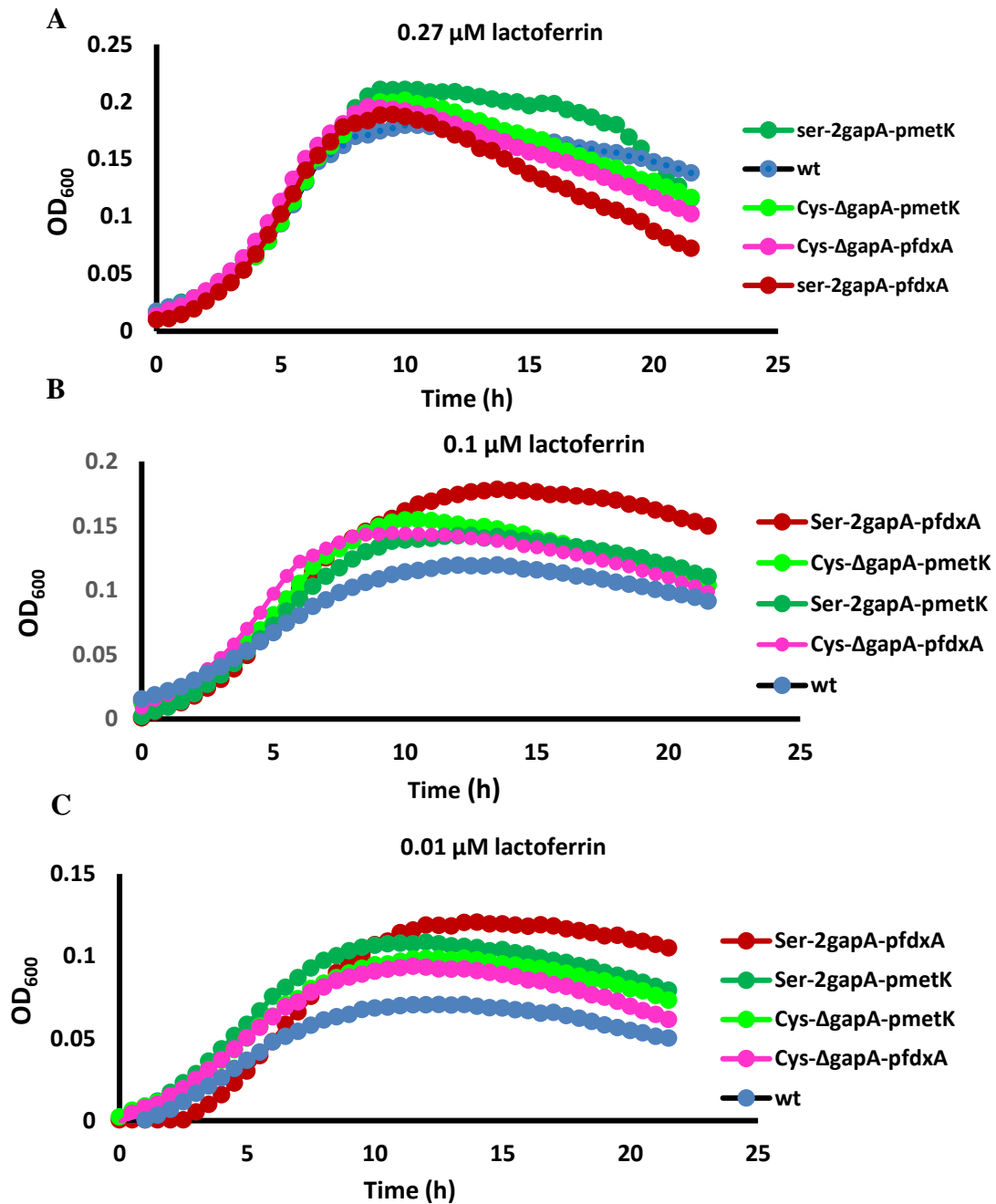


Figure 5-11 A, B, C. The growth curve assay of mutated gapA *C.jejuni* and wild type strains conducted in low concentrations of lactoferrin.

This graph shows the growth of *C. jejuni* strains WT (—●—), Ser-2gapA-pfdxA(—●—), Cys- Δ gapA-pfdxA (—●—), Ser-2gapA-pmetK (—●—) and Cys- Δ gapA-pmetK (—●—) in MEM α supplemented with different concentrations of ferric-Lf. (A) = 0.27 μ M, (B) = 0.1 μ M in and (C) = 0.01 μ M. Each data point is the mean of three replicates. The data presented is an average of at least three experiments carried out on different days. The error bars represent the standard deviation of WT.

Table 5.3. The growth rate of new *C. jejuni* strains in different concentrations of human ferric-Lf

Table shows the growth rate of each strain calculated from data given in figure (5-11 A, B, C) in MEM α supplemented by low concentrations (0.27, 0.1 and 0.01 μ M) of ferric-Lf. The growth rate was compared between Ser-2*gapA*-*pfdxA* and Cys- Δ *gapA*-*pfdxA* strains by student paired *t* test and no differences were observed $P > 0.05$.

Growth rate (h ⁻¹)	WT	Ser-2 <i>gapA</i> - <i>pfdxA</i>	Cys- Δ <i>gapA</i> - <i>pfdxA</i>	P value of Ser-2 <i>gapA</i> - <i>pfdxA</i> Vs Cys- Δ <i>gapA</i> - <i>pfdxA</i>
0.27 μ M (P value vs WT)	0.3 \pm 0.04	0.32 \pm 0.07 (0.75)	0.36 \pm 0.04 (0.13)	0.52
0.1 μ M (P value vs WT)	0.17 \pm 0.03	0.3 \pm 0.03 (0.005)*	0.32 \pm 0.04 (0.007)*	0.34
0.01 μ M (P value vs WT)	0.17 \pm 0.02	0.31 \pm 0.07 (0.03)*	0.27 \pm 0.03 (0.01)*	0.08

Table 5.4. The doubling time of new *C. jejuni* strains in different concentrations of human ferric-Lf

Table shows the doubling time of each strain calculated from data given in figure (4-5 A, B, C) in MEM α supplemented by low concentrations (0.1, 0.01 and 0.006 μ M) of ferric-Lf. The doubling time was compared between Ser-2*gapA*-*pfdxA* and Cys- Δ *gapA*-*pfdxA* strains via student paired *t* test and no differences were observed $P > 0.05$.

Doubling time (h)	WT	Ser-2 <i>gapA</i> - <i>pfdxA</i>	Cys- Δ <i>gapA</i> - <i>pfdxA</i>	P value of Ser-2 <i>gapA</i> - <i>pfdxA</i> Vs Cys- Δ <i>gapA</i> - <i>pfdxA</i>
0.27 μ M (P value vs Wt)	2.33 \pm 0.3	2.27 \pm 0.55 (0.89)	1.96 \pm 0.2 (0.14)	0.55
0.1 μ M (P value vs Wt)	4.13 \pm 0.67	2.3 \pm 0.28 (0.010)*	2.20 \pm 0.3 (0.01)*	0.38
0.01 μ M (P value vs Wt)	4.04 \pm 0.54	2.31 \pm 0.45 (0.01)*	2.54 \pm 0.23 (0.01)*	0.09

5.7 Binding assays with ferric- Lf

To investigate the capability of the hetero-diploid and *Cys-ΔgapA* reverted strains to bind Lf, binding assays were also carried out with ferric-Lf. In addition, a far Western blot assay was used to explore the binding between purified C150S-GAPDH (section 5.3.1), which lacks enzymatic activity, and Lf iron binding proteins. The main purpose of these assays was to determine if there is any relationship between GAPDH enzyme activity and binding to iron glycoproteins. The procedures of the binding assays were identical to previously mentioned (section 4.2.6), the binding of the cells with ferric-Lf was performed without inclusion of anti-GapA antibody.

The results are shown in figure 5-12, all examined strains can bind ferric-Lf to a different degree as indicated by image J analysis. The intensity of Lf band in WT was greater than other strains, it is 14% more than hetero-merodiploid *Ser-2gapA-pfdxA* and 33% greater than *Cys-ΔgapA-pfdxA*. The expression level of cjGAPDH in these new created strains is higher than WT, therefore, high amount of cjGAPDH might not be important in the binding of Lf under optimum concentration (0.27 μM) but probably important in the interaction with other proteins involved in this pathway of iron uptake.

On the other hand, far western blot analysis shows that C150S-cjGAPDH can bind a range of Lf iron binding proteins with high affinity to ferric-Lf than other iron binding proteins. Not binding with BSA indicates that the C150S-cjGAPDH maintained the specificity of wild type GAPDH in binding with Lfs. Binding of C150S-GAPDH with these glycoproteins indicates no relationship between GAPDH enzymatic activity and binding with Lf family of iron binding proteins.

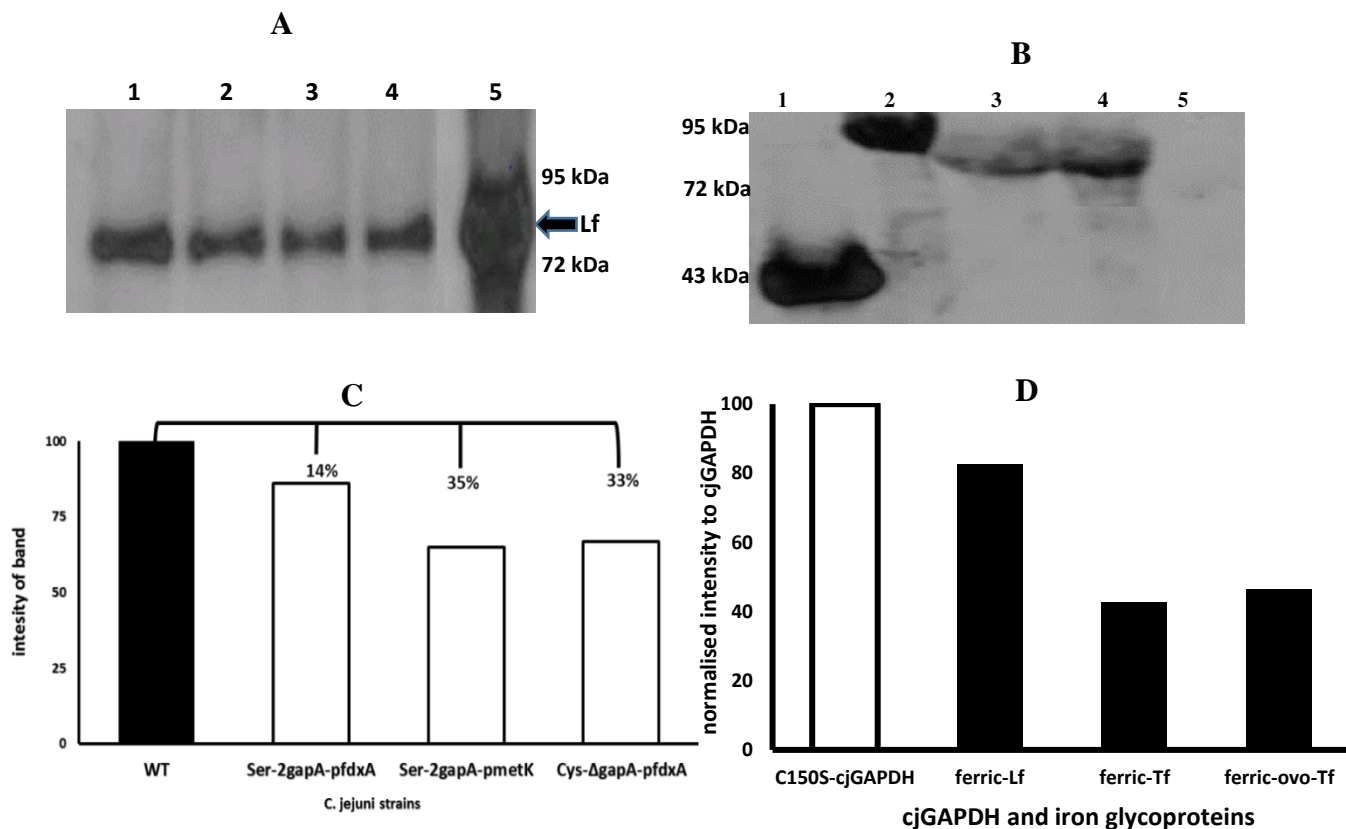


Figure 5-12 A, B, C, D. Western blot analysis of binding assays between *C. jejuni* with lactoferrin.

(A) Western blot analysis of solubilised *C. jejuni* proteins (approximately 25 μ g of protein separated by SDS-PAGE) prepared from cells incubated with 0.27 μ M ferric-Lf. 1= WT, 2= *Ser-2gapA-pfdxA*, 3= *Ser-2gapA-pmetK*, 4= *Cys- Δ gapA-pfdxA* and 5= human ferri-Lf (~5 μ g; positive control indicated by arrow at approximately 92 kDa). The blot was probed with rabbit anti-Lactoferrin antibody, protein ladder band sizes are indicated in kDa to the right of the blot. (B) is far Western blot, immobilised proteins on PVDF membrane: 1= purified C150S-cjGAPDH, 2= human ferric-Lf, 3= human ferric-Tf, 4= ferric-ovo-Tf and 5= BSA. The membrane incubated with 50 μ g/ml C150S-cjGAPDH in binding buffer, washed and probed with anti-GapA antibody, protein ladder band sizes are indicated in kDa on the left of the blot. (C) Bar chart displays the assessment of Western blot bands of the blot (A). Image J was used to estimate the intensity of the bands, the numbers indicate the differences between WT binding to ferric-Lf with other strains. (D) Bar chart estimation of binding by image J. The band intensity was normalised by mutated GAPDH in lane 1.

5.8 Discussion and conclusion

Recent studies have shown that GAPDH has multiple functions independent of its role in energy metabolism. Although there is substantial evidence demonstrating the capability of GAPDH to bind different proteins, various RNA species and telomeric DNA, the exact mechanism(s) behind most moonlight functions of GAPDH remains unclear (Nicholls *et al.*, 2012). In this chapter, the role of glycolytic function of GAPDH in iron uptake from ferric-Lf was investigated. The results of the binding assays indicate that the role of cjGAPDH in iron acquisition from ferric-Lf is not linked to its glycolytic activity function.

The results of binding between C150S-GAPDH with different iron binding proteins have given important indications of the role of glycolytic activity of GAPDH in releasing iron from ferric-Lf. The C150S-GAPDH showed similar features to wild type GAPDH in binding these iron glycoproteins, it has high affinity for ferric-Lf and lower affinities for ferric-ovo-Tf and ferric-Tf, thus this result suggests that the amino acid residue cys150 is not important in the binding of cjGAPDH with ferric-Lf. Additionally, it shows that the C150S-GAPDH has maintained the feature of wild type GAPDH in binding with iron glycoproteins. Importantly, it indicates that functions of GAPDH in glycolytic reactions and the binding with ferric-Lf are independent of each other. The binding of GAPDH mutant protein with ferric-Lf was also reported in *M. tuberculosis*, GAPDH acts as a receptor for Lf but GAPDH enzymatic activity and Lf binding were not related (Malhotra *et al.*, 2017). However, GAPDH function is extremely sensitive to the modification of this cysteine residue in the active site, human GAPDH lost ability to interact with some proteins such as nuclear RNA-binding protein (p54nrb) upon expression of mutated active site C152S-GAPDH (Hwang *et al.*, 2009).

The loss of GAPDH enzymatic activity due to site-directed mutagenesis of cys150 was reported before in purified mutated cjGAPDH of *C. jejuni* NCTC1118, it was unable to convert G3P in the presence of either NAD^+ or NADP^+ (Tourigny *et al.*, 2011). This finding was also reported in *B. stearothermophilus* and *S. aureus* MRSA252 (Didierjean *et al.*, 2003, Mukherjee *et al.*, 2010). In *M. tuberculosis*, the alterations of amino acids such as Asparagine at position 142 to Serine (N142S) and a Proline to Leucine at position 295 (P295L) also caused dramatic decrease in enzymatic activity with maintained binding to ferric-Lf comparable with wild type GAPDH (Malhotra *et al.*, 2017).

Furthermore, loss of enzymatic activity of C150S-GAPDH raises the question of whether this purified protein has been folded or not. The CD data revealed that C150S-GAPDH is a folded protein and like the wild type cjGAPDH is a α -helix protein. However, the negative bands in both proteins were not so distinct due to probable association of unknown residues in the buffer or improper concentrations of tested proteins. Additionally, it has been reported that CD method might fail in providing acceptable results on proteins with mixed α and β elements in their structure like GAPDH. This is due to spectral diversity of β -structures, thus this has been considered as intrinsic limitation of the technique (Micsonai *et al.*, 2015, Khrapunov, 2009).

Strains with similar expression levels but different glycolytic activity did not show any difference in utilisation of ferric-Lf, this suggests that glycolytic activity is not important for iron uptake from ferric-Lf, although it is not absolutely conclusive. However, the results of iron growth assay are in agreement with results obtained in section 4.2.4 which showed mutated *C. jejuni* strains grew significantly better than WT, this finding was more likely due to overexpression of GAPDH in these mutated strains.

Nevertheless, the role of cjGAPDH redundancy in iron uptake from ferric-Lf is still questionable. The intensity of binding of hetero-merodiploid and reverted strains with ferric-Lf was not greater than WT, although these newly created strains overexpressed GAPDH. This finding is inconsistent with the finding of Malhotra *et al.*, (2017), by use of fluorescence microscopy-based method, they reported that the overexpression of GAPDH in *M. tuberculosis* H37Ra cells resulted not only in a significant increase in binding and uptake of Lf but also in incorporation of associated iron into the cells (Malhotra *et al.*, 2017). Therefore, our finding requires further work to confirm with exploiting of the sophisticated approaches such as electronic and fluorescence microscopy based methods.

The reason for the reversion of the ser to cys when attempting to construct the knockout *gapA* strains is not clear, it is likely to be due to the selective pressure of mutating this essential gene. However, the reverting of mutated strains to wild type proves that cys150 is the critical amino acid in the metabolic function of cjGAPDH and has further confirmed the importance of GAPDH in the viability of *C. jejuni*. In this regard, it has been considered that creating of new *C. jejuni* strains with a metabolically inactive GAPDH might not be successful due to the essentiality of *gapA* in *C. jejuni*. Therefore, the creation of C150S-*gapA* mutants was in concurrence with constructing another mutation, which

was H177G. This new mutated gene was also cloned, overexpressed and purified similarly to the previously mentioned cjGAPDH forms in this research. The enzymatic activity of H177G-cjGAPDH was significantly higher than C150S-cjGAPDH but still drastically lower than wild type cjGAPDH protein (data not shown). Unfortunately, for unknown reasons the cloning of His177Gly-*gapA* into the *C. jejuni* pC46 plasmid delivery system was not successful.

To sum up, the function of cjGAPDH in binding with ferric-Lf appears to be irrelevant to metabolic role of this multiple function protein. The cys150 in the active site of cjGAPDH is extremely important residue for the viability of *C. jejuni*.

Chapter 6. General discussion

6.1 General discussion and future work

The main aim of this project was to investigate the function of cjGAPDH in iron uptake from ferric-Lf. Prior to this study, utilisation of ferric-Lf in iron uptake for growth of *C. jejuni* had been demonstrated (Rock, 2003, Miller *et al.*, 2008). The process of iron uptake from ferric-Lf is apparently operated by different proteins, the contribution of GAPDH in this iron uptake pathway has been reported in different organisms. Here, the results provide evidence of cjGAPDH's role in iron uptake from ferric-Lf, this new function of cjGAPDH is independent from the glycolytic function of the enzyme and it is likely that cjGAPDH acts as a receptor for ferric-Lf

6.1.1 Use of *C. jejuni* complementation system coupled with allelic replacement mutagenesis method clarified essentiality of *gapA*

Essential genes are defined as those that are critical for viability of the organism (Song *et al.*, 2005). Several studies have shown that *gapA* is essential in *C. jejuni* using different methodologies such as transposon mediated mutagenesis and transposon mutagenesis via transposon sequencing (Tn-seq) (Metris *et al.*, 2011, Gao *et al.*, 2014a, Mandal *et al.*, 2017). On the other hand, Stahl and Stintzi (2011) by employing transposon based mutagenesis combined with a microarray mapping approach, did not report *gapA* among the essential genes in *C. jejuni* NCTC11168 (Stahl and Stintzi, 2011). Tn-seq has been considered the most reliable method used to assign the essential genome (Mandal *et al.*, 2017). These differences in reporting the essentiality of *gapA* might be due to the techniques used, for example the mapping of the transposon insertion site was performed by either microarray in Stahl and Stintzi (2011) or next generation sequencing in Mandal *et al.*, (2017) and Gho *et al.*, (2014). Also the differences in experimental conditions such as temperature of growth, and agar culture media used might have led to discrepancies.

The *gapA* gene in *C. jejuni* is most likely essential, and there is no alternative homologue of *gapA* in *C. jejuni* that can exert the same essential metabolic function of cjGAPDH (Parkhill *et al.*, 2000). In the research reported here, deletion/insertion allelic replacement method was used to inactivate *gapA* and to clarify its essentiality. No colonies grew after attempted mutagenesis of the WT strain, while three different mutated *gapA* strains were obtained only by using a complementation system suggesting the observed essentiality of *gapA* was not due to a polar effect on adjacent genes or technical errors. The kanamycin

resistance cassette used to disrupt the mutated ORF of *gapA* was terminator-less and promoter-less, in order to avoid secondary polar effects on the downstream genes. Moreover, reversion of ser150 to wild type cys150-*gapA* was further evidence of *gapA* essentiality. The substitution of cys150 in the active site of GAPDH caused lethal effects on the cell due to the lack of glycolytic function of GAPDH, therefore, none of the grown strains maintained this mutation. They reverted to the wild type genotype in order to grow which indicates the importance of *gapA* for the viability of *C. jejuni*.

Due to the essentiality of *gapA* in *C. jejuni*, the pC46 plasmid complementation system was employed to create *C. jejuni* strains with an inactivated wild type *gapA*. The gene expression methods used to phenotype the newly created strains show that all strains have GAPDH expression levels greater than WT. Therefore, not obtaining a *C. jejuni* strain with *gapA* expression less than the wild type strain might be considered as a limitation of this *C. jejuni* complementation system. In future work, it might be worth performing site-directed mutagenesis on the other residues situated in the active site of *gapA*, which might significantly reduce the levels of glycolytic activity without fully inactivating it.

The complementation of *gapA* within the region of *cj0046* does not affect the growth rate of the new created *C. jejuni* strains except the Δ *gapA-porA* strain. The highly expressed cjGAPDH strains showed a growth defect upon entry into stationary phase compared to the other strains, which might be due to high level of cjGAPDH. In future work, performing a growth assay based on calculating CFU of each strain at a certain time point could be beneficial to relate these observations to the overexpression of GAPDH.

To date, there are not enough molecular genetics tools in research and experimental design for *C. jejuni*. Therefore, the available knowledge of *C. jejuni* pathogenicity is limited compared to other enteropathogenic bacteria such as *E. coli* and *Salmonella* spp. Establishing new systems in *C. jejuni* for the expression of recombinant genes such as a tetracycline inducible promoter system to allow inducible differential expression is highly recommended in future work.

6.1.2 The cjGAPDH is a membrane associated protein in *C. jejuni* NCTC11168

GAPDH is a key component of the glycolytic pathway. As such, its major functional location is cytoplasmic. GAPDH is lacking the signalling motifs for both extracellular transport and surface attachment (Eichenbaum *et al.*, 1996, Seidler and Seidler, 2012).

The results of the research reported here has indicated for the first time an outer membrane association of cjGAPDH. Localisation of GAPDH on the cell surface has been reported previously in different organisms (Egea *et al.*, 2007, D'Costa *et al.*, 2000, Modun and Williams, 1999, Gao *et al.*, 2014b, Dumke *et al.*, 2011).

The measurement of GAPDH enzyme activity was exploited to indicate surface localisation through three different ways, after treatment with Proteinase K, exposure to anti-GapA antibodies, and direct assay of enzyme activity in the outer membrane fraction. The GAPDH assay applied here was based on measurement of enzymatic activity without breakdown of the cell membranes. Treatment with Proteinase K resulted in significant reduction of GAPDH enzymatic activity due to digestion of GAPDH molecules by Proteinase K, and incubation of cells with anti-GapA antibodies blocked the majority of GAPDH on the cell surface. The antibody-protein complex was probably unable to convert G3P into 1,3 dPG leading to a significant decrease in whole cell GAPDH activity. However, detection of a considerable amount of GAPDH in treated cells either with Proteinase K or anti-GapA is proposed to be due to intracellular GAPDH in the enzymatic activity reaction. Use of microscopic examination probably was not enough to assess the levels of cell lysis, measurement of other cytoplasmic enzymes as markers for control intracellular leakage was in consideration. A number of enzymatic assays have been commonly reported in the literature such as succinate dehydrogenase (Johnston and Gotschlich, 1974), alkaline phosphatase (Alahari *et al.*, 2007), hippurate hydrolase (Steele *et al.*, 2005) and lactate dehydrogenase (Horikiri *et al.*, 2004). However, whole cell enzymatic activity of these enzymes in *C. jejuni* was not productive either due to the assays not being sensitive enough to detect enzymatic activity or the presence of enzyme inhibitors (for example, HEPES, Tris/HCl and EDTA) in the assay buffer (Hobb *et al.*, 2009). Therefore, these cytoplasmic markers were not measured to monitor the subcellular contamination.

Isolation of outer membrane fraction by *N*-laurylsarcosine (Sarkosyl) has been considered a reliable method for extraction of OMPs, which provides a large amount of OMPs with relatively few subcellular contaminating residues (Hobb *et al.*, 2009). Western blot analysis of the extracted fractions with anti-GroEL antibody revealed the outer membrane fraction was likely to be free from cytoplasmic contaminants, therefore,

the findings obtained by anti-GapA antibody confirm the likely association of GAPDH on the outer membrane and support the results of GAPDH enzymatic assay.

Furthermore, in the iron assay method, the inclusion of anti-GapA antibody into the cultures supplemented with Lf inhibited the growth of strains due to binding of this antibody with GAPDH. This cannot have occurred if cjGAPDH is not present on the surface of the cells. This observation was considered as further evidence of the surface localisation of cjGAPDH.

The precise mechanism of GAPDH trafficking and secretion onto the cell surface is still a mystery. The essentiality of GAPDH for bacterial survival made the mutagenesis of *gapA* not feasible, so it limits progression in characterising how GAPDH is exported to the bacterial surface and having multiple functions. However, attempts are still ongoing to understand the different GAPDH features and mechanisms. In *N. meningitidis*, which has two *gapA* genes, *gapA-1* and *gapA-2*, encoding GAPDH enzymes (Tunio *et al.*, 2010), the *gapA-1* mutated strain was grown normally relative to wild type but it lost surface localisation of GAPDH-1 (TUNIO *et al.*, 2013). The anti-GapA failed to detect the surface molecule in the capsulated cells, but this was probably due to steric hindrance of the antibodies to surface GapA-1. Fractionation experiments still showed the protein to be in the OM, and it still was able to mediate adhesion to human cells in vitro (Tunio *et al.*, 2010).

In the same context, one method to inactivate the essential GAPDH gene was introduced by Boel *et al.*, (2005) in the group A streptococcus. The wild type GAPDH allele was replaced by an allele encoding the functional protein with a 12-residue C-terminal hydrophobic peptide. Although the mutant strain grew normally in the same manner of wild type, the mutated GAPDH was not displayed on the cell surface and retained in the cytoplasm. The mutant cells showed a significant decrease in binding with plasminogen compared with wild type, also there was an entire loss of its anti-phagocytic activity (Boel *et al.*, 2005). In *C. jejuni*, our findings reveal that the deletion of C-terminal peptide converts recombinant GAPDH into inclusion bodies (data not shown). Therefore, this region contains important sequences which maintain the solubility of cjGAPDH. In future work, both wild and truncated C-terminal of *gapA* will be tagged with iLOV fluorophore and cloned into pC46 plasmids, followed by complementation into *C. jejuni* genome and

its influence on the localisation of GAPDH will be investigated by confocal fluorescence microscopy.

It still has to be elucidated which domains of this tetrameric molecule are important for its outer membrane association and non-metabolic function. The secretion of GAPDH in *C. albicans* was promoted by GAPDH protein itself. The first half of the GAPDH amino acid sequence directs the incorporation of polypeptides into the yeast cell wall and this integration is controlled by a region situated within the N-terminal half of the protein (Delgado *et al.*, 2003). Therefore, it has been suggested that the secretion of GAPDH in *C. albicans* is specific and induced by GAPDH itself (Delgado *et al.*, 2003). Regarding *C. jejuni*, in future work, the different sequences of N-terminal *gapA* in *C. jejuni* should be deleted and the resulting truncated gene tagged with suitable fluorophores such as iLOV before integration into *C. jejuni* genome. Fluorescence microscopy will determine the differences in localisation of GAPDH on the cell surface between iLOV labeled strains, N-terminal truncated and wild type GAPDH strains. The lack or decrease in cell surface localisation of iLOV-GAPDH in mutated strains can be compared to deleted N-terminal sequence proteins.

6.1.3 The cjGAPDH is an essential element for iron uptake from ferric-Lf

Several studies in different organisms have provided evidence of the role of GAPDH in iron uptake from ferric-Tf but few of studies have investigated the function of GAPDH in iron uptake from ferric-Lf. In this study, by using iron growth assays and binding assays between ferric-Lf and *C. jejuni* cells, it was demonstrated that *C. jejuni* can acquire iron from ferric-Lf utilising cjGAPDH. More specifically, binding assays revealed cjGAPDH as a potential receptor for ferric-Lf in a process independent to the glycolytic function of cjGAPDH. Inhibition of *C. jejuni* growth by inclusion of anti-GapA antibody to cultures supplemented by ferric-Lf as sole iron source, and also decreased binding of anti-GapA pre-exposed *C. jejuni* strains with ferric-Lf indicated the importance of cjGAPDH in iron uptake from iron-bound glycoproteins. The findings were proved by results obtained from anti-MOMP antibody which was used as control.

The binding assay of hetero-merodiploid, mutated reverted and WT strains with ferric-Lf show that the overexpression of cjGAPDH might not be important in the direct binding with ferric-Lf on the surface of *C. jejuni*, it might be important in other mechanisms such as internalisation of ferric-Lf to the cytoplasm of *C. jejuni*. Internalisation of ferric-Lf and

ferric-Tf by GAPDH into the cytoplasm was reported previously in *M. tuberculosis* and *M. smegmatis* by (Boradia *et al.*, 2014a, Malhotra *et al.*, 2017) using immuno-gold labelling transmission electron microscopy (TEM). Here, it was attempted to apply fluorescence-based techniques to characterise the role of cjGAPDH in iron uptake from ferric-Lf. Unfortunately, the construction of a pC46-*gapA*-mCherry plasmid was not successful. In future work, it could be better to try other fluorophores such as iLOV in labelling of cjGAPDH for examining the co-localisation of cjGAPDH with ferric-Lf on the surface of *C. jejuni*. In addition, Fluorescence Resonance Energy Transfer (FRET) Microscopy should be performed in order to confirm the interaction between mutated *C. jejuni* tagged GAPDH cells and fluorophore tagged Lf on the bacterial cell surface.

Far Western blot analysis showed both wild type and mutated cjGAPDH bind more tightly to ferric-Lf than ferric-ovo-Tf and ferric-Tf. The ferric-Lf is abundant in mucosal surfaces such as intestines; *C. jejuni* might be adapted to have high affinity to ferric-Lf in order to facilitate its colonisation in this niche. However, the binding of cjGAPDH with human ferric-Lf needs further characterisation. Structural investigations, such as protein X-ray crystallography, Nuclear Magnetic Resonance (NMR), and Electron Microscopy (EM), of GAPDH-Lf complex is highly recommended in future work. This will determine the binding between this metabolic enzyme and iron bound protein in a three-dimensional context. Additionally, it will highlight the orientation of the potential critical residues involved in these protein's interaction.

The iron uptake system from Lf iron binding proteins in *C. jejuni* might be a multifunctional system. The cjGAPDH might act as dual receptor for ferric-Lf and ferric-Tf, each of cjGAPDH, CtuA (cj0178) outer membrane receptor protein and perhaps other non-identified proteins might collaborate in this iron uptake system. In future work, the binding between CtuA and cjGAPDH protein should be performed by different methods such as Far Western blot, Pull-down assay and fluorescence-based assays. The study of this binding is important to understand the mechanism of iron uptake from this pathway.

The reduction of released ferric iron from Lf can occur on the surface of *C. jejuni*. Although several researchers reported visual activity of ferric reductase in different species of *Campylobacter* and other microorganisms (Grenier and Tanabe, 2011, Crossley *et al.*, 2007, Knight *et al.*, 2005), the reductase is not involved in the uptake of iron from lactoferrin by *C. jejuni* NCTC 11168 cells (Prof. Julian Ketley, unpublished

data; figure 3). There are no obvious candidate genes for cell surface ferric reductases in the NCTC 11168 genome (Parkhill *et al.*, 2000), therefore, it might be that a non-identified mechanism of ferric reduction could be involved and this is worth investigating in future work.

The ferrous iron can enter the cells by passive diffusion, CfbpA (Cj0175c) periplasmic binding protein, has been previously reported to preferentially bind ferrous iron and might transport ferrous iron in the periplasm (Tom-Yew *et al.*, 2005). However, the evidence of transport Fe^{+2} derived from Lf by CfbpA is required.

The role of the inner membrane ferrous iron transporter FeoB is not clear in this process, ferric reduction activity in *C. jejuni* has been shown to require riboflavin biosynthesis (Crossley *et al.*, 2007). However, growing of *ribB* mutant and wild-type strains did not show differences indicating that riboflavin biosynthesis might not be required for the successful uptake of iron from Lf (Prof. Julian Ketley, unpublished data; figure 5). In future work, the *feoB* gene in mutated *gapA* strains, which grew better than WT under low concentrations of ferric-Lf should be inactivated. The iron growth assay should be performed to determine the differences between these double mutants $\Delta feoB\text{-}\Delta gapA$ strains and single mutated *gapA* strains, which might be relevant to FeoB.

The role of the energy transduction system ExbBD-TonB1-3 was not proved in iron uptake from Lf iron binding proteins in *C. jejuni* (Prof. Julian Ketley, unpublished data; figure 6a-f). The growth kinetics of single and double *tonB* mutant strains showed no differences in the presence of ferri-Lf as sole iron source. However, CtuA appears to be a TonB-dependent ligand gated porin based on similarity to other outer membrane proteins and also redundancy of Ton-B thus further investigation of energy dependency might be required.

6.1.4 Proposed model for iron uptake from ferric-Lf by cjGAPDH

The experimental evidence of how iron is released by cjGAPDH protein from ferric-Lf into cells is required, the possible paradigm of iron removal from ferric-Lf can be assumed as shown in figure 6-1. This model is primarily based on evidence presented here or other publications, therefore, three different mechanisms of iron release from ferric-Lf have been proposed. The basic step in this model is binding of ferric-Lf to *C. jejuni* via GAPDH on the cell surface.

The first proposed mechanism is that ferric-Lf-cjGAPDH complex might be bound with CtuA located on the outer membrane, this binding might cause conformational changes of Lf resulting in release of ferric iron which is either internalised into the cells through CtuA or reduced into ferrous iron by a non-identified mechanism. The interaction between the complex and CtuA might also cause ferric reduction. Mutagenesis of *ctuA* caused incomplete failure of growth (Miller *et al.*, 2008); this might be because passive diffusion of ferrous iron through the outer membrane porins. The second potential mechanism of iron release might be due to cjGAPDH-Lf complex itself. The ferric iron might be removed from Lf by an organic phosphate produced from GAPDH glycolytic reaction. It has been previously reported that organic phosphate of 1,3- dPG produced from catabolic reaction of GAPDH is involved in the removal of iron from Tf (Morgan, 1977). Considering the close structural and functional homology between Tf and Lf, this assumption could be applicable for Lf. The third proposed mechanism would be internalisation of cjGAPDH-Lf complex into the cytoplasm where ferric-Lf is cleaved resulting in release of ferric iron, which is reduced into ferrous iron in the cytoplasm as previously reported (Malhotra *et al.*, 2017). However, this model is unlikely occurred due to inability of Lf to cross the membranes.

Within these proposed mechanisms, the collaboration of other factors is important. As mentioned above, the transport of Fe^{3+} across the outer membrane might occur via CtuA. The transport through the inner membrane could be by the Cj0175c-Cj0173c ABC transporter system. Alternatively, the ferric iron may be reduced on the cell surface then diffused through the membrane into the periplasm. Periplasmic CfbpA can bind ferrous iron and transport it in the periplasm. The entrance of ferrous iron into the cytoplasm might be mediated by FeoB on the inner membrane. The energy transduction system ExbBD-TonB1-3 is important to provide energy to CtuA. The redundancy of this energy transducer agent throughout the membranes suggests its importance to other non-identified co-players in this iron uptake system. Once in the cytoplasm, iron might be used in the cellular and metabolic processes or stored.

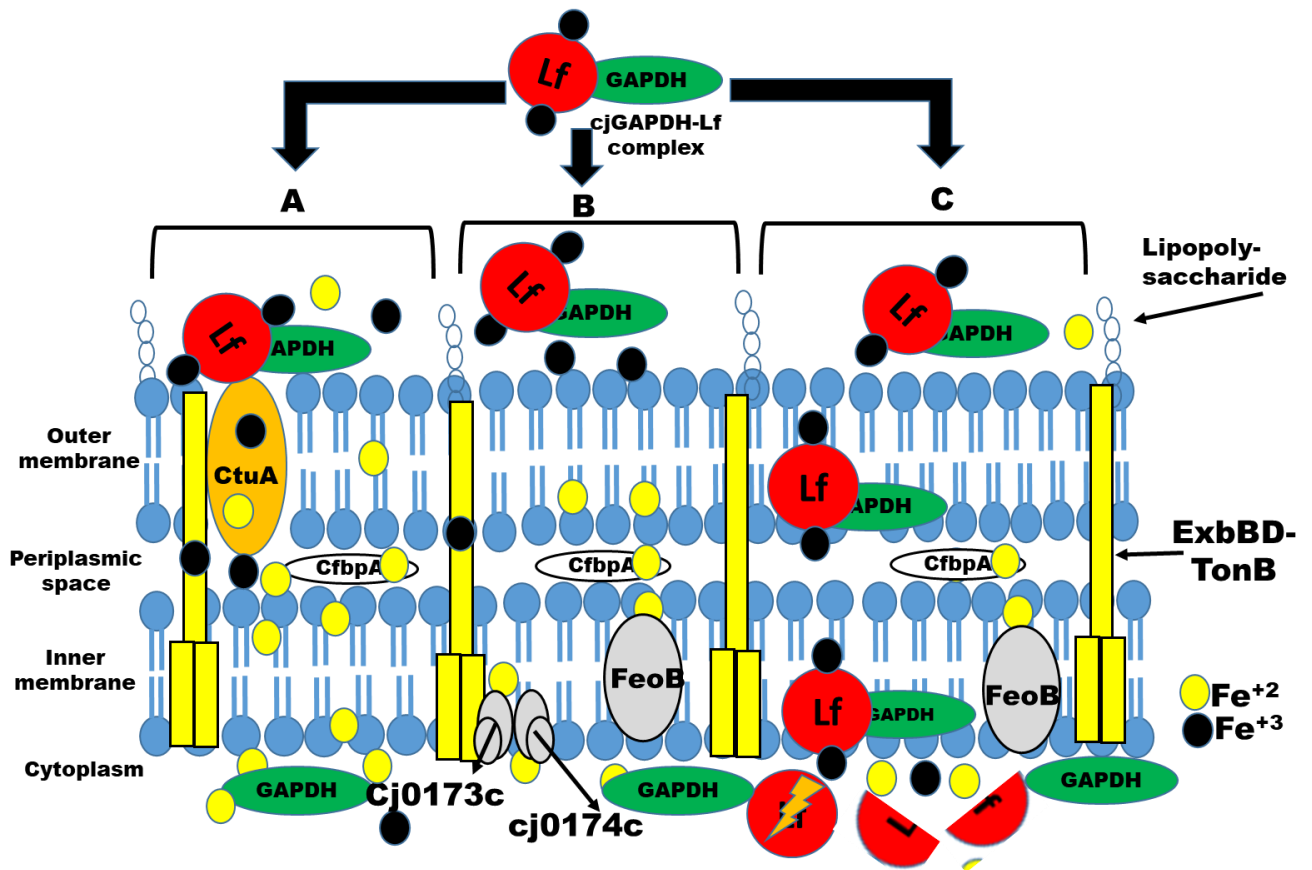


Figure 6-1. Proposed model of role of cjGAPDH in iron uptake from ferric-Lf.

The acquisition of iron from Lf by cjGAPDH is proposed via three potential mechanisms A,B,C. **A:** cjGAPDH acts as extracellular receptor of ferric-Lf so the cjGAPDH-Lf complex interacts with CtuA protein on the cell surface, the interaction causes liberation of ferric ions which might enter the cells via CtuA or reduced to ferrous ions. **B:** Once cjGAPDH bound ferric-Lf and forms a complex, the phosphate group produced from glycolytic reaction perhaps by itself or collaborated by other element/s should release iron from ferric-Lf. **C:** The cjGAPDH-Lf complex might be internalised into the cytoplasm of *C. jejuni* cells. Lf might be cleaved by proteases, ferric iron might be reduced by cytoplasmic ferric reductases. In all of these mechanisms, CfbpA bound Fe^{+2} in the periplasmic membrane, ExbBD-TonB1-3 is abundant through the membranes, it provides energy required for CtuA and probably some non-identified proteins. The FeoB is required for ferrous iron transporting into the cytoplasm. GAPDH is found throughout this simplified cell structure, although the mechanism of trafficking across the lipid bilayer still unclear.

6.2 Summary of findings and Conclusion

The current study revealed for the first time that GAPDH is efficiently utilised by *C. jejuni* NCTC11168 to uptake iron from ferric-Lf. The cjGAPDH protein acts as a *C. jejuni* receptor to bind iron bound glycoproteins. The findings also clarify the essentiality of *gapA* and the importance of the cys150 residue of cjGAPDH in the growth and survival of *C. jejuni*. In addition, there is strong evidence that cjGAPDH is a membrane associated protein, which opens questions about other potential functions of cjGAPDH such as virulence and pathogenicity of *C. jejuni*.

This study brings into consideration the importance of GAPDH in the biology of *C. jejuni*, provides evidence of how this house keeping protein has adapted to scavenge iron for *C. jejuni* growth, colonisation and probably disease association. These observations would make a worthwhile contribution in different biotechnological implications.

Appendix

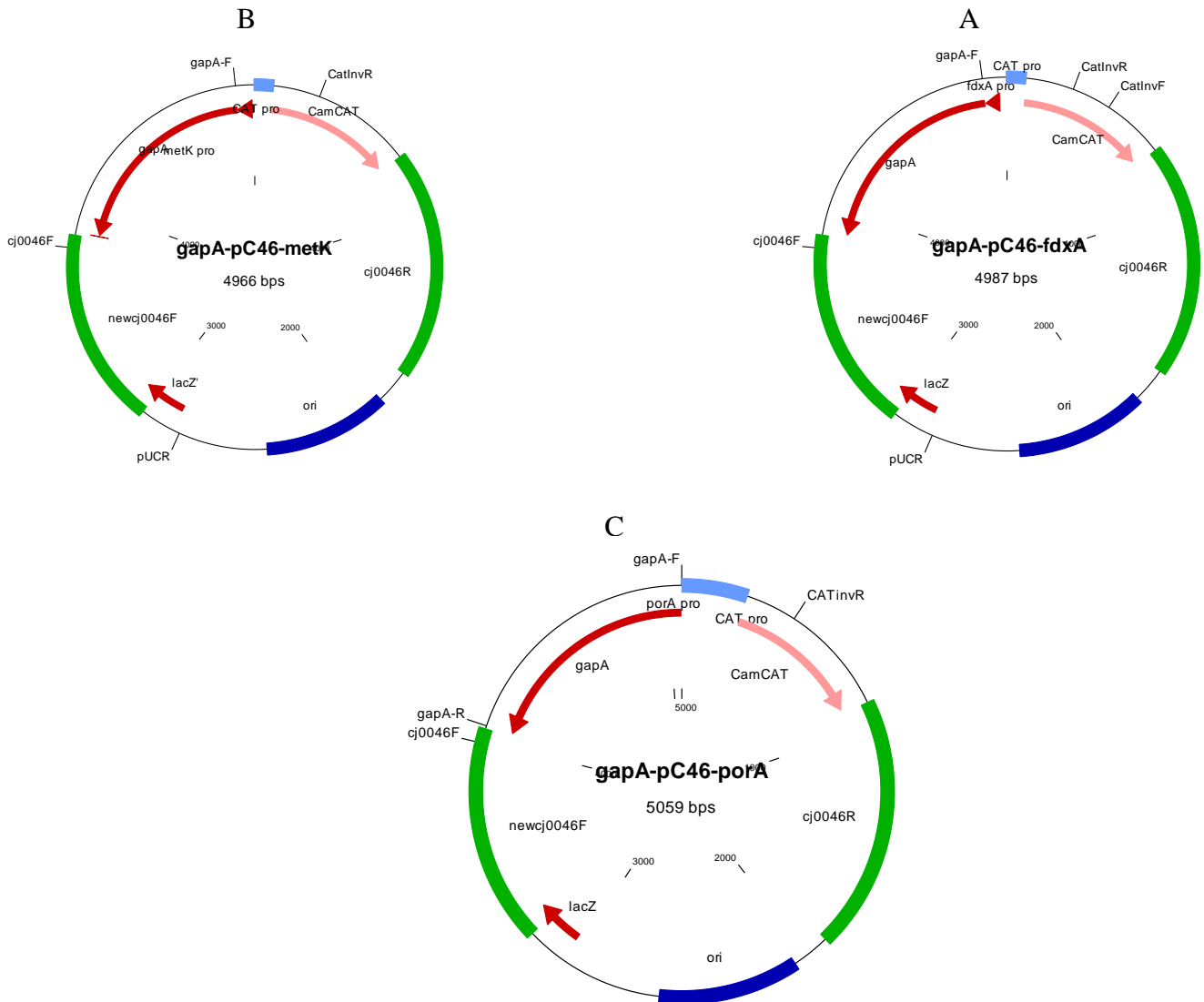


Figure A.1 The map of *gapA*-pC46 recombinant plasmids.

(a) *gapA*-pC46-*fdxA* has a medium strength promoter. (b) *gapA*-pC46-*metK* has a weak strength promoter. (c) *gapA*-pC46-*porA*, the strongest promoter. The green colours are forward and reverse fragments of *cj0046* pseudo gene, Chloroamphenicol (*CamCAT*) is selective gene (light red color). Primer positions for clarification of cloning are indicated: *cj0046F*; and *CATInvR*

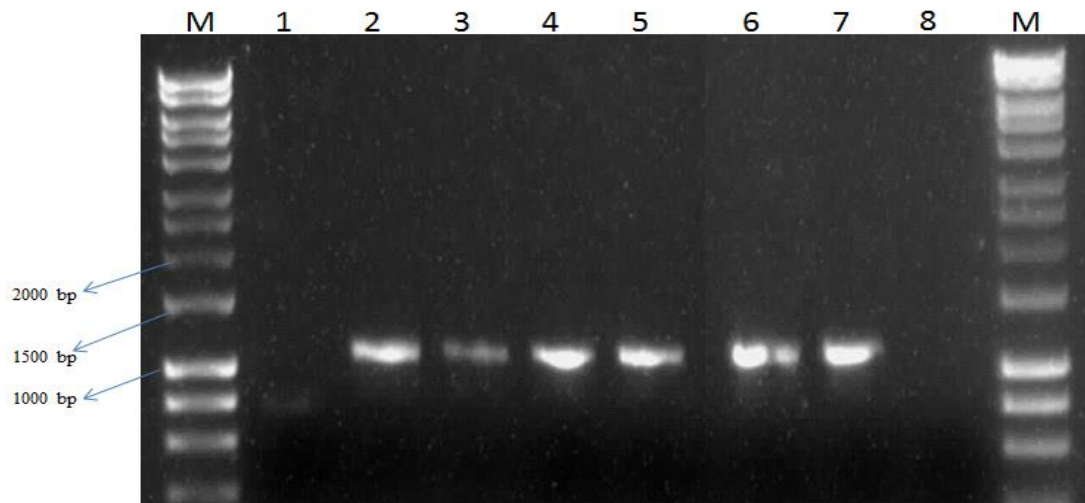


Figure A2. Agarose gel electrophoresis of colony PCR results to confirm the success of transformation by recombinant pC46-*gapA* plasmids. The primers used were *gapA-F* and *cj0046F*. The expected size of the amplicon is approximately 1080 bp. Lane M is hyperladder marker 1, lane 1 is empty and lane 8 is a PCR negative control (H₂O added), lanes 2,3, 4,5, 6, and 7 are PCR products from three different transformed colonies of *E.coli DH 5α*, each two lanes represent: *gapA-pC46-fdxA*, *gapA-pC46-metK*, and *(gapA-pC46-porA* strains harbouring plasmids respectively.

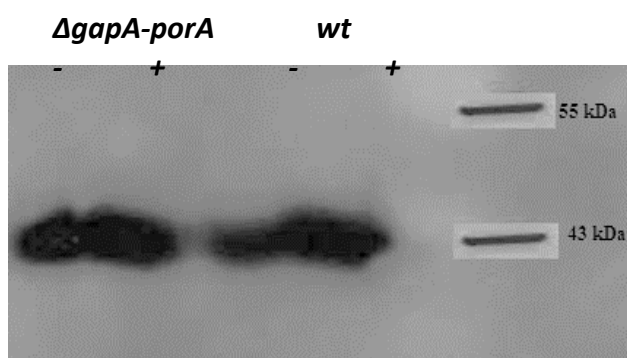


Figure A.3. Western blot analysis of GAPDH protein expression of whole *C. jejuni* strains in high and low iron conditions. (A) Iron conditions were represented by (+) repletion and (-) depletion. The titration of 1:5000 anti-GapA were used to probe the membrane, 1:5000 anti-rabbit as HRP secondary antibody. 10 ul of cell lysis were loaded. (43 kDa) prominent band among all strains was shown. No differences were seen.

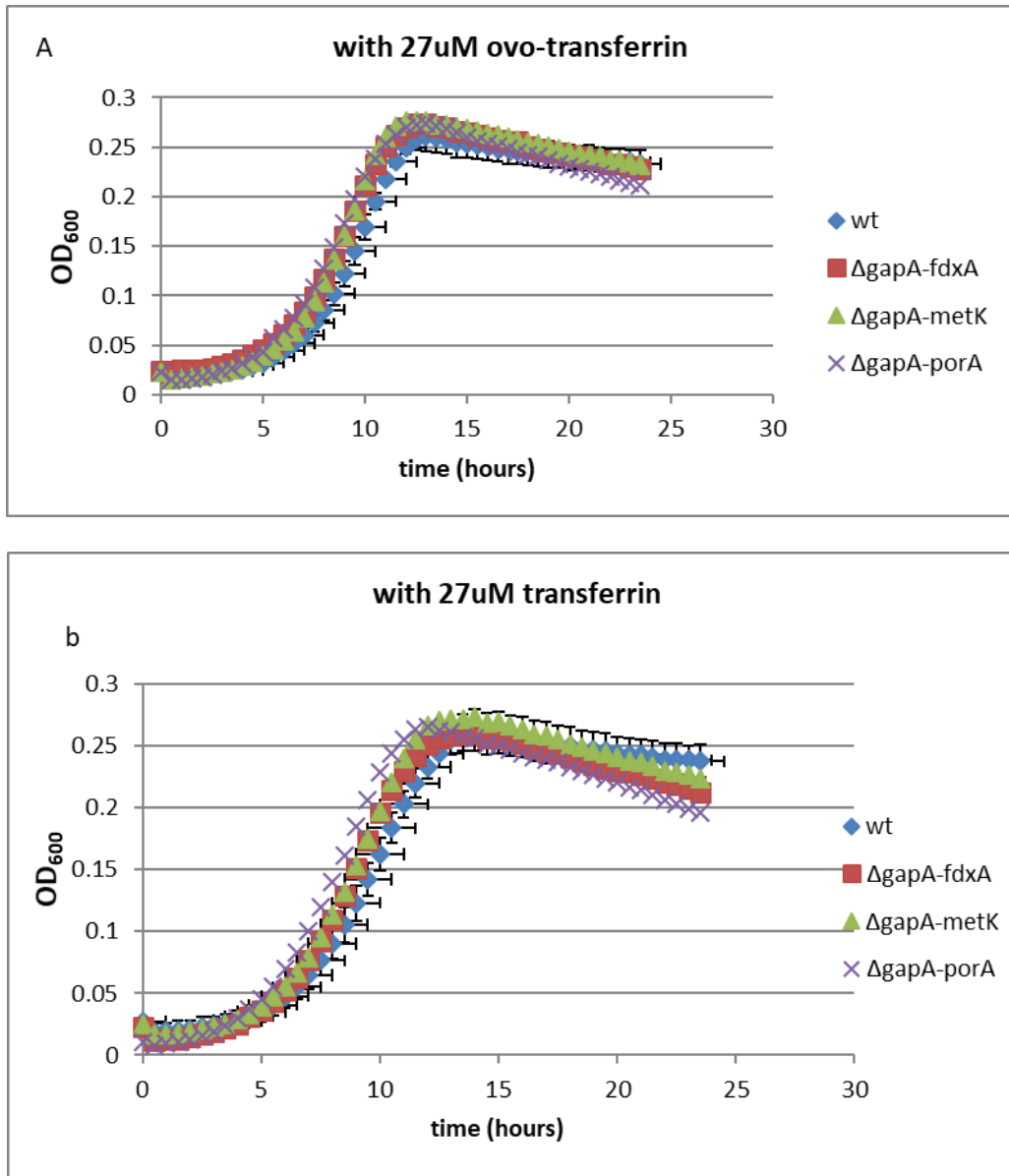


Figure A.4 the growth curve assay conducted in MEM α supplemented with transferrin and ovo-transferrin.

Each data point is the mean of the 3 replicates of wild and mutated *gapA* strains. (a) in ferri- ovo-transferrin supplemented MEM α (b) in ferric-transferrin supplemented MEM α . Error bar are represented by stansard deviations of wild strain.

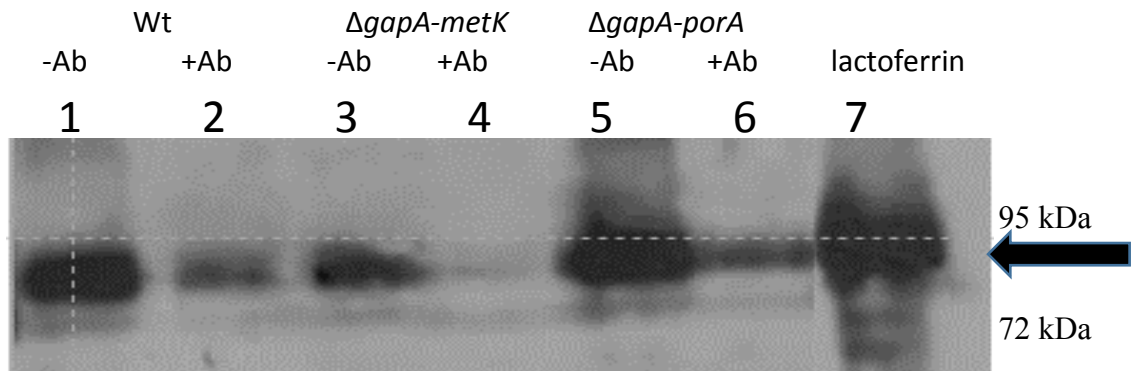


Figure A5. Western blot analysis of binding assay between anti-GapA pre-incubated whole cell *C. jejuni* with lactoferrin.

Certain number of cells $OD_{600}=0.1$ was loaded on the SDS-PAGE and transferred into PVDF membrane, 1,2= WT of *C. jejuni* NCTC11168. 3, 4= *ΔgapA-pmetK* and 5, 6= *ΔgapA-pporA* strain. Lane 7 lactoferrin (positive control). After overnight growing, the strains centrifuged and the number of the cells were equalised. The strains indicated as (+Ab) incubated in 1 ml tube with 1:200 of anti-GapA for 1 hour under conditions growth of *C. jejuni* without agitation, (-Ab) means without antibody and then washed with MEM α and 0.27 μ M lactoferrin were added for one hour then washed 3 times. Blot was probed with anti-lactoferrin, protein ruler is indicated at right of the blot. Human ferric-Lf was indicated by arrow with approximately 92 kDa on the left of the blot.

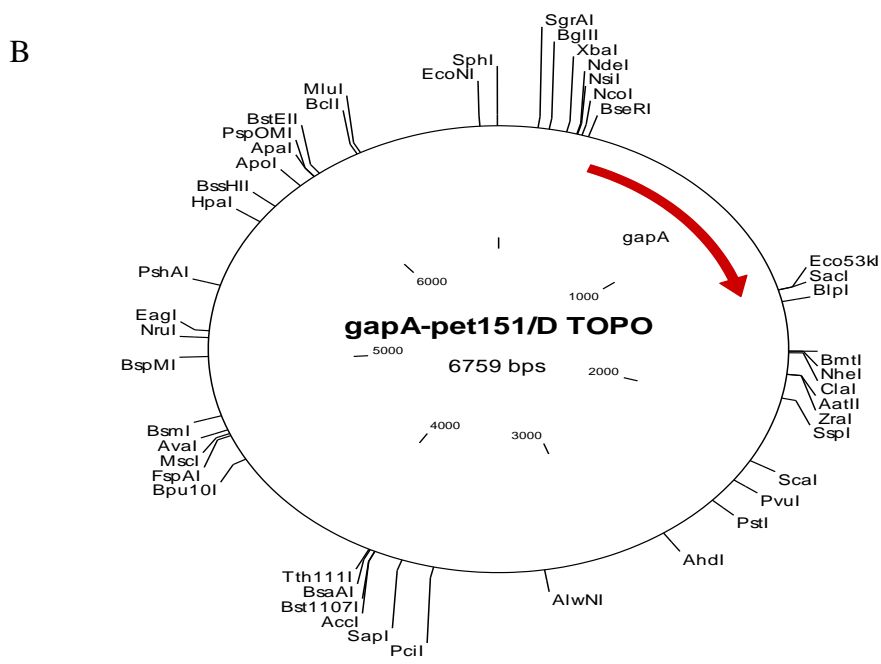
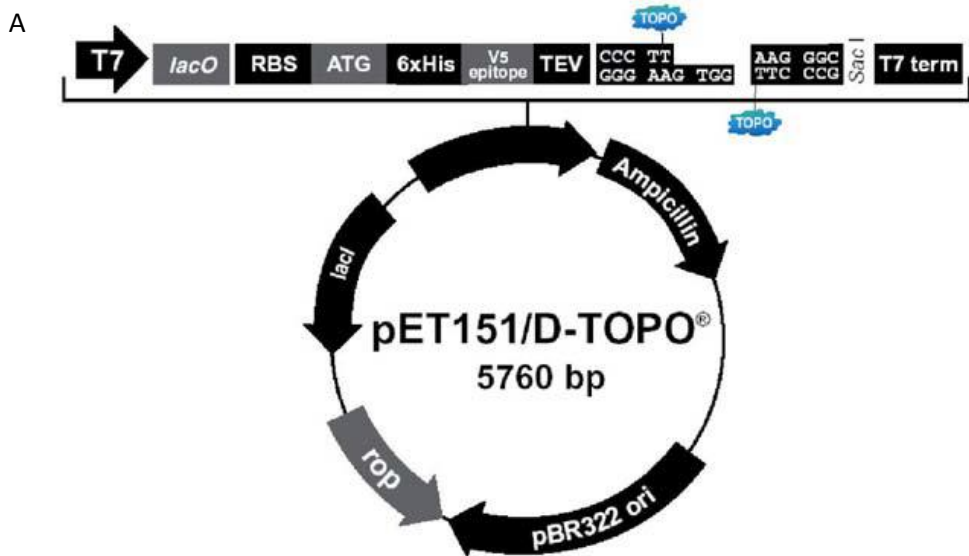


Figure A6, A & B. The map of pET151/D topoisomerase vector.

The upper panel (A) represents the naked plasmid not cloned with any gen and main components are indicated above the plasmid, whereas the lower panel (B) is cloned with interested gene *gapA*, the locations of restriction enzymes are indicated in the plasmid,

Table A1 The growth rate of new *C. jejuni* strains in different concentrations of MEM α compared with wild type

Table shows the growth rate of each strain calculated from data given in figure (5-10 A, B, C) in MEM α supplemented by low concentrations (0.27, 0.1 and 0.01 μ M) of ferric-Lf. The growth rate was compared between wild type and overexpressed strains by student paired *t* test and differences observed are significant $P < 0.05$.

Growth rate (h ⁻¹)	wt	2n-sermetK	2n-serfdxA	Ser-fdxA	Ser-metK
0.27 μM (P value vs Wt)	0.3 \pm 0.04	0.39 \pm 0.08 (0.15)	0.32 \pm 0.07 (0.75)	0.36 \pm 0.04 (0.13)	0.33 \pm 0.05 (0.43)
0.1 μM (P value vs Wt)	0.17 \pm 0.03	0.29 \pm 0.02 (0.003)*	0.3 \pm 0.03 (0.005)*	0.32 \pm 0.04 (0.007)*	0.3 \pm 0.03 (0.005)*
0.01 μM (P value vs Wt)	0.17 \pm 0.02	0.34 \pm 0.03 (0.006)*	0.31 \pm 0.07 (0.03)*	0.27 \pm 0.03 (0.01)*	0.32 \pm 0.06 (0.02)*

Table A2 The doubling time of new strains grew in low level of ferric-Lf.

Table shows the doubling time of each strain calculated from data given in figure (4-5 A, B, C) in MEM α supplemented by low concentrations (0.1, 0.01 and 0.006 μ M) of ferric-Lf. The doubling time was compared between wild type and overexpressed strains by student paired *t* test and differences observed are significant $P < 0.05$.

Doubling time (h)	wt	2n-sermetK	2n-serfdxA	Ser-fdxA	Ser-metK
0.27 μM (P value vs Wt)	2.33 \pm 0.3	1.81 \pm 0.35 (0.12)	2.27 \pm 0.55 (0.89)	1.96 \pm 0.2 (0.14)	2.13 \pm 0.38 (0.48)
0.1 μM (P value vs Wt)	4.13 \pm 0.67	2.37 \pm 0.14 (0.011)*	2.3 \pm 0.28 (0.010)*	2.20 \pm 0.3 (0.01)*	2.3 \pm 0.22 (0.01)*
0.01 μM (P value vs Wt)	4.04 \pm 0.54	2.05 \pm 0.2 (0.02)*	2.31 \pm 0.45 (0.01)*	2.54 \pm 0.23 (0.01)*	2.26 \pm 0.48 (0.01)*

Bibliography

- Abboud, S. & Haile, D. J. 2000. A novel mammalian iron-regulated protein involved in intracellular iron metabolism. *Journal of Biological Chemistry*, 275, 19906-19912.
- Abdallah, F. B. & Chahine, J.-M. E. H. 2000. Transferrins: iron release from lactoferrin. *Journal of molecular biology*, 303, 255-266.
- Adams, T. E., Mason, A. B., He, Q.-Y., Halbrooks, P. J., Briggs, S. K., Smith, V. C., Macgillivray, R. T. & Everse, S. J. 2003. The Position of Arginine 124 Controls the Rate of Iron Release from the N-lobe of Human Serum Transferrin A STRUCTURAL STUDY. *Journal of Biological Chemistry*, 278, 6027-6033.
- Adlerova, L., Bartoskova, A. & Faldyna, M. 2008. Lactoferrin: a review. *Veterinarni Medicina*, 53, 457-468.
- Aisen, P. & Leibman, A. 1972. Lactoferrin and transferrin: a comparative study. *Biochimica et Biophysica Acta (BBA)-Protein Structure*, 257, 314-323.
- Alahari, A., Saint, N., Campagna, S., Molle, V., Molle, G. & Kremer, L. 2007. The N-terminal domain of OmpATb is required for membrane translocation and pore-forming activity in mycobacteria. *Journal of bacteriology*, 189, 6351-6358.
- Alter, T., Gaull, F., Kasimir, S., Gürtler, M., Mielke, H., Linnebur, M. & Fehlhaber, K. 2005. Prevalences and transmission routes of *Campylobacter* spp. strains within multiple pig farms. *Veterinary microbiology*, 108, 251-261.
- Anderson, B. F., Baker, H. M., Norris, G. E., Rice, D. W. & Baker, E. N. 1989. Structure of human lactoferrin: Crystallographic structure analysis and refinement at 2.8 Å resolution. *Journal of molecular biology*, 209, 711-734.
- Andrews, S. C., Robinson, A. K. & Rodríguez-Quiñones, F. 2003. Bacterial iron homeostasis. *FEMS microbiology reviews*, 27, 215-237.
- Ascencio, F., Ljungh, Å. & Wadström, T. 1992. Lactoferrin binding properties of *Vibrio cholerae*. *Microbios*, 70, 103-117.
- Ayna, A. 2016. *Glyceraldehyde-3-phosphate Dehydrogenase and Fructose-1, 6-bisphosphatase of the Enteric Pathogens C. jejuni and H. pylori*. Department of Molecular and Cell Biology.
- Bacon, D. J., Alm, R. A., Burr, D. H., Hu, L., Kopecko, D. J., Ewing, C. P. & Guerry, P. 2000. Involvement of a plasmid in virulence of *Campylobacter jejuni* 81-176. *Infection and immunity*, 68, 4384-4390.
- Baker, E. 1994. Structure and reactivity of transferrins. *Advances in inorganic chemistry*, 41, 389-463.
- Baker, E. N. & Baker, H. M. 2009. A structural framework for understanding the multifunctional character of lactoferrin. *Biochimie*, 91, 3-10.
- Baker, H. M. & Baker, E. N. 2004. Lactoferrin and iron: structural and dynamic aspects of binding and release. *Biometals*, 17, 209-216.
- Bayliss, C. D. 2009. Determinants of phase variation rate and the fitness implications of differing rates for bacterial pathogens and commensals. *FEMS microbiology reviews*, 33, 504-520.
- Bayliss, C. D., Bidmos, F. A., Anjum, A., Manchev, V. T., Richards, R. L., Grossier, J.-P., Wooldridge, K. G., Ketley, J. M., Barrow, P. A. & Jones, M. A. 2012. Phase variable genes of *Campylobacter jejuni* exhibit high mutation rates and specific mutational patterns but mutability is not the major determinant of population structure during host colonization. *Nucleic acids research*, 40, 5876-5889.
- Bezine, E., Vignard, J. & Mirey, G. 2014. The cytolethal distending toxin effects on Mammalian cells: a DNA damage perspective. *Cells*, 3, 592-615.

- Biswas, D., Fernando, U., Reiman, C., Willson, P., Townsend, H., Potter, A. & Allan, B. 2007. Correlation between in vitro secretion of virulence-associated proteins of *Campylobacter jejuni* and colonization of chickens. *Current microbiology*, 54, 207-212.
- Biswas, G. D., Anderson, J. E. & Sparling, P. F. 1997. Cloning and functional characterization of *Neisseria gonorrhoeae* tonB, exbB and exbD genes. *Molecular microbiology*, 24, 169-179.
- Blaser, M. J. 1997. Epidemiologic and clinical features of *Campylobacter jejuni* infections. *Journal of Infectious Diseases*, 176, S103-S105.
- Boel, G., Jin, H. & Pancholi, V. 2005. Inhibition of cell surface export of group A streptococcal anchorless surface dehydrogenase affects bacterial adherence and antiphagocytic properties. *Infect Immun*, 73, 6237-48.
- Boradia, V. M., Malhotra, H., Thakkar, J. S., Tillu, V. A., Vuppala, B., Patil, P., Sheokand, N., Sharma, P., Chauhan, A. S., Raje, M. & Raje, C. I. 2014a. Mycobacterium tuberculosis acquires iron by cell-surface sequestration and internalization of human holo-transferrin. *Nat Commun*, 5, 4730.
- Boradia, V. M., Patil, P., Agnihotri, A., Kumar, A., Rajwadi, K. K., Sahu, A., Bhagath, N., Sheokand, N., Kumar, M. & Malhotra, H. 2016. Mycobacterium tuberculosis H37Ra: a surrogate for the expression of conserved, multimeric proteins of M. tb H37Rv. *Microbial cell factories*, 15, 140.
- Boradia, V. M., Raje, M. & Raje, C. I. 2014b. Protein moonlighting in iron metabolism: glyceraldehyde-3-phosphate dehydrogenase (GAPDH). Portland Press Limited.
- Boulton, I., Gorrings, A., Shergill, J., Joannou, C. & Evans, R. 1999. A dynamic model of the meningococcal transferrin receptor. *Journal of theoretical biology*, 198, 497-505.
- Braun, V. & Hantke, K. 2011. Recent insights into iron import by bacteria. *Current opinion in chemical biology*, 15, 328-334.
- Butcher, J. & Stintzi, A. 2013. The transcriptional landscape of *Campylobacter jejuni* under iron replete and iron limited growth conditions. *PLoS One*, 8, e79475.
- Butzler, J. P. 2004. *Campylobacter*, from obscurity to celebrity. *Clinical microbiology and infection*, 10, 868-876.
- Carniel, E. 2001. The *Yersinia* high-pathogenicity island: an iron-uptake island. *Microbes and infection*, 3, 561-569.
- Cerff, R. 1995. The chimeric nature of nuclear genomes and the antiquity of introns as demonstrated by the GAPDH gene system. *Tracing Biological Evolution in Protein and Gene Structures*, 205-227.
- Chan, A. C., Lelj-Garolla, B., Rosell, F. I., Pedersen, K. A., Mauk, A. G. & Murphy, M. E. 2006. Cofacial heme binding is linked to dimerization by a bacterial heme transport protein. *Journal of molecular biology*, 362, 1108-1119.
- Chang, Y.-C., Huang, Y.-H., Shih, C.-M. & Wu, J.-Y. 2006. One peptide derived from hen ovotransferrin as pro-drug to inhibit angiotensin converting enzyme. *Journal of Food and Drug Analysis*, 14.
- Chaudhuri, R. R. & Pallen, M. J. 2006. xBASE, a collection of online databases for bacterial comparative genomics. *Nucleic acids research*, 34, D335-D337.
- Chen, W.-P. & Kuo, T.-T. 1993. A simple and rapid method for the preparation of gram-negative bacterial genomic DNA. *Nucleic acids research*, 21, 2260.
- Christensen, J. E., Pacheco, S. A. & Konkel, M. E. 2009. Identification of a *Campylobacter jejuni*-secreted protein required for maximal invasion of host cells. *Molecular microbiology*, 73, 650-662.

- Cody, A. J., Mccarthy, N. D., Van Rensburg, M. J., Isinkaye, T., Bentley, S. D., Parkhill, J., Dingle, K. E., Bowler, I. C., Jolley, K. A. & Maiden, M. C. 2013. Real-time genomic epidemiological evaluation of human *Campylobacter* isolates by use of whole-genome multilocus sequence typing. *Journal of clinical microbiology*, 51, 2526-2534.
- Corry, J. & Atabay, H. 2001. Poultry as a source of *Campylobacter* and related organisms. *Journal of Applied Microbiology*, 90.
- Crossley, R. A., Gaskin, D. J., Holmes, K., Mulholland, F., Wells, J. M., Kelly, D. J., Van Vliet, A. H. & Walton, N. J. 2007. Riboflavin biosynthesis is associated with assimilatory ferric reduction and iron acquisition by *Campylobacter jejuni*. *Applied and environmental microbiology*, 73, 7819-7825.
- Crushell, E., Harty, S., Sharif, F. & Bourke, B. 2004. Enteric *Campylobacter*: purging its secrets? *Pediatric research*, 55, 3-12.
- D'costa, S. S., Romer, T. G. & Boyle, M. D. 2000. Analysis of expression of a cytosolic enzyme on the surface of *Streptococcus pyogenes*. *Biochemical and biophysical research communications*, 278, 826-832.
- Dasti, J. I. 2007. *Identification and characterization of Campylobacter jejuni factors relevant for the infection process*.
- Dasti, J. I., Tareen, A. M., Lugert, R., Zautner, A. E. & Groß, U. 2010. *Campylobacter jejuni*: a brief overview on pathogenicity-associated factors and disease-mediating mechanisms. *International Journal of Medical Microbiology*, 300, 205-211.
- Davis, L. & Dirita, V. 2008. Growth and laboratory maintenance of *Campylobacter jejuni*. *Current protocols in microbiology*, 8A. 1.1-8A. 1.7.
- De Guevara, C. L., Gonzalez, J. & Pena, P. 1994. Bacteraemia caused by *Campylobacter* spp. *Journal of clinical pathology*, 47, 174-175.
- Delgado, M. L., Gil, M. L. & Gozalbo, D. 2003. *Candida albicans* TDH3 gene promotes secretion of internal invertase when expressed in *Saccharomyces cerevisiae* as a glyceraldehyde-3-phosphate dehydrogenase-invertase fusion protein. *Yeast*, 20, 713-722.
- Delgado, M. L., O'connor, J. E., Azorín, I., Renau-Piqueras, J., Gil, M. L. & Gozalbo, D. 2001. The glyceraldehyde-3-phosphate dehydrogenase polypeptides encoded by the *Saccharomyces cerevisiae* TDH1, TDH2 and TDH3 genes are also cell wall proteins. *Microbiology*, 147, 411-417.
- Deng, J., Su, S., Lin, X., Hassett, D. J. & Lu, L. J. 2013. A statistical framework for improving genomic annotations of prokaryotic essential genes. *PLoS One*, 8, e58178.
- Dertz, E. A., Xu, J., Stintzi, A. & Raymond, K. N. 2006. Bacillibactin-Mediated Iron Transport in *Bacillus subtilis* 1. *Journal of the American Chemical Society*, 128, 22-23.
- Didierjean, C., Corbier, C., Fatih, M., Favier, F., Boschi-Muller, S., Branlant, G. & Aubry, A. 2003. Crystal structure of two ternary complexes of phosphorylating glyceraldehyde-3-phosphate dehydrogenase from *Bacillus stearothermophilus* with NAD and D-glyceraldehyde 3-phosphate. *Journal of Biological Chemistry*, 278, 12968-12976.
- Dierich, A., Gaub, M.-P., Lepennec, J.-P., Astinotti, D. & Chambon, P. 1987. Cell-specificity of the chicken ovalbumin and conalbumin promoters. *The EMBO journal*, 6, 2305.
- Dumke, R., Hausner, M. & Jacobs, E. 2011. Role of *Mycoplasma pneumoniae* glyceraldehyde-3-phosphate dehydrogenase (GAPDH) in mediating interactions with the human extracellular matrix. *Microbiology*, 157, 2328-2338.

- Egea, L., Aguilera, L., Gimenez, R., Sorolla, M. A., Aguilar, J., Badia, J. & Baldoma, L. 2007. Role of secreted glyceraldehyde-3-phosphate dehydrogenase in the infection mechanism of enterohemorrhagic and enteropathogenic *Escherichia coli*: interaction of the extracellular enzyme with human plasminogen and fibrinogen. *Int J Biochem Cell Biol*, 39, 1190-203.
- Eichenbaum, Z., Green, B. D. & Scott, J. R. 1996. Iron starvation causes release from the group A streptococcus of the ADP-ribosylating protein called plasmin receptor or surface glyceraldehyde-3-phosphate-dehydrogenase. *Infection and immunity*, 64, 1956-1960.
- Elli, M., Zink, R., Rytz, A., Reniero, R. & Morelli, L. 2000. Iron requirement of *Lactobacillus* spp. in completely chemically defined growth media. *Journal of applied microbiology*, 88, 695-703.
- Elliott, P. R. 2009. *Structure and function of enteric pathogen glyceraldehyde-3-phosphate dehydrogenases*. University of Leicester.
- Emery, T. & Neilands, J. 1961. Structure of the ferrichrome compounds^{1, 2}. *Journal of the American Chemical Society*, 83, 1626-1628.
- Faraldo-Gómez, J. D. & Sansom, M. S. 2003. Acquisition of siderophores in gram-negative bacteria. *Nature reviews Molecular cell biology*, 4, 105-116.
- Farnaud, S. & Evans, R. W. 2003. Lactoferrin—a multifunctional protein with antimicrobial properties. *Molecular immunology*, 40, 395-405.
- Fernando, U., Biswas, D., Allan, B., Willson, P. & Potter, A. A. 2007. Influence of *Campylobacter jejuni* *fliA*, *rpoN* and *flgK* genes on colonization of the chicken gut. *International journal of food microbiology*, 118, 194-200.
- Figge, R. M. & Cerff, R. 2001. GAPDH gene diversity in spirochetes: a paradigm for genetic promiscuity. *Molecular biology and evolution*, 18, 2240-2249.
- Fillinger, S. 2000. Two Glyceraldehyde-3-phosphate Dehydrogenases with Opposite Physiological Roles in a Nonphotosynthetic Bacterium. *Journal of Biological Chemistry*, 275, 14031-14037.
- Fouts, D. E., Mongodin, E. F., Mandrell, R. E., Miller, W. G., Rasko, D. A., Ravel, J., Brinkac, L. M., Deboy, R. T., Parker, C. T. & Daugherty, S. C. 2005. Major structural differences and novel potential virulence mechanisms from the genomes of multiple *Campylobacter* species. *PLoS Biol*, 3, e15.
- Fraenkel-Conrat, H. & Feeney, R. E. 1950. The metal-binding activity of conalbumin. *Archives of biochemistry*, 29, 101-113.
- Freestone, P. P., Lyte, M., Neal, C. P., Maggs, A. F., Haigh, R. D. & Williams, P. H. 2000. The mammalian neuroendocrine hormone norepinephrine supplies iron for bacterial growth in the presence of transferrin or lactoferrin. *Journal of Bacteriology*, 182, 6091-6098.
- Fugier, E., Salcedo, S. P., De Chastellier, C., Pophillat, M., Muller, A., Arce-Gorvel, V., Fourquet, P. & Gorvel, J. P. 2009. The glyceraldehyde-3-phosphate dehydrogenase and the small GTPase Rab 2 are crucial for *Brucella* replication. *PLoS Pathog*, 5, e1000487.
- Galindo, M. A., Day, W. A., Raphael, B. H. & Joens, L. A. 2001. Cloning and characterization of a *Campylobacter jejuni* iron-uptake operon. *Current microbiology*, 42, 139-143.
- Gao, B., Lara-Tejero, M., Lefebvre, M., Goodman, A. L. & Galán, J. E. 2014a. Novel components of the flagellar system in epsilonproteobacteria. *MBio*, 5, e01349-14.
- Gao, J.-Y., Ye, C.-L., Zhu, L.-L., Tian, Z.-Y. & Yang, Z.-B. 2014b. A homolog of glyceraldehyde-3-phosphate dehydrogenase from *Riemerella anatipestifer* is an

- extracellular protein and exhibits biological activity. *Journal of Zhejiang University Science B*, 15, 776-787.
- Gaskin, D., Van Vliet, A. & Pearson, B. The Campylobacter genetic toolbox: development of tractable and generally applicable genetic techniques for Campylobacter jejuni. *Zoonoses and Public Health*, 2007a. BLACKWELL PUBLISHING 9600 GARSINGTON RD, OXFORD OX4 2DQ, OXON, ENGLAND, 101-101.
- Gaskin, D., Vliet, A. V. & Pearson, B. 2007b. The Campylobacter genetic toolbox: development of tractable and generally applicable genetic techniques for Campylobacter jejuni. *Zoon Publ Health*, 54, 101.
- Ge, R. & Sun, X. 2012. Iron trafficking system in Helicobacter pylori. *Biometals*, 25, 247-258.
- Giansanti, F., Leboffe, L., Pitari, G., Ippoliti, R. & Antonini, G. 2012. Physiological roles of ovotransferrin. *Biochimica et Biophysica Acta (BBA)-General Subjects*, 1820, 218-225.
- Gibreel, A. & Sköld, O. 1998. High-level resistance to trimethoprim in clinical isolates of Campylobacter jejuni by acquisition of foreign genes (dfr1 and dfr9) expressing drug-insensitive dihydrofolate reductases. *Antimicrobial agents and chemotherapy*, 42, 3059-3064.
- Gomme, P. T., Mccann, K. B. & Bertolini, J. 2005. Transferrin: structure, function and potential therapeutic actions. *Drug discovery today*, 10, 267-273.
- González-Chávez, S. A., Arévalo-Gallegos, S. & Rascón-Cruz, Q. 2009. Lactoferrin: structure, function and applications. *International journal of antimicrobial agents*, 33, 301. e1-301. e8.
- Goulhen, F., Emmanuelle, D., Pagès, J.-M. & Bolla, J.-M. 2004. Functional refolding of the Campylobacter jejuni MOMP (major outer membrane protein) porin by GroEL from the same species. *Biochemical Journal*, 378, 851-856.
- Gray-Owen, S. D. & Schyvers, A. B. 1996. Bacterial transferrin and lactoferrin receptors. *Trends in Microbiology*, 4, 185-191.
- Green, E. R. & Meccas, J. 2016. Bacterial secretion systems—an overview. *Microbiology spectrum*, 4.
- Greenfield, N. J. 2006. Using circular dichroism spectra to estimate protein secondary structure. *Nature protocols*, 1, 2876-2890.
- Grenier, D. & Tanabe, S.-I. 2011. Transferrin as a source of iron for Campylobacter rectus. *Journal of oral microbiology*, 3.
- Guccione, E., Del Rocio Leon-Kempis, M., Pearson, B. M., Hitchin, E., Mulholland, F., Van Diemen, P. M., Stevens, M. P. & Kelly, D. J. 2008. Amino acid-dependent growth of Campylobacter jejuni: key roles for aspartase (AspA) under microaerobic and oxygen-limited conditions and identification of AspB (Cj0762), essential for growth on glutamate. *Molecular microbiology*, 69, 77-93.
- Hannibal, L., Collins, D., Brassard, J., Chakravarti, R., Vempati, R., Dorlet, P., Santolini, J. R. M., Dawson, J. H. & Stuehr, D. J. 2012. Heme binding properties of glyceraldehyde-3-phosphate dehydrogenase. *Biochemistry*, 51, 8514-8529.
- Hantke, K. 1987. Ferrous iron transport mutants in Escherichia coli K12. *FEMS microbiology letters*, 44, 53-57.
- Hantke, K. 2003. Is the bacterial ferrous iron transporter FeoB a living fossil? *Trends in microbiology*, 11, 192-195.
- Hensel, R., Zwickl, P., Fabry, S., Lang, J. & Palm, P. 1989. Sequence comparison of glyceraldehyde-3-phosphate dehydrogenases from the three urkingdoms: evolutionary implication. *Canadian journal of microbiology*, 35, 81-85.

- Hermans, D., Van Deun, K., Martel, A., Van Immerseel, F., Messens, W., Heyndrickx, M., Haesebrouck, F. & Pasmans, F. 2011. Colonization factors of *Campylobacter jejuni* in the chicken gut. *Veterinary research*, 42, 82.
- Herrington, D. & Sparling, P. 1985. Haemophilus influenzae can use human transferrin as a sole source for required iron. *Infection and immunity*, 48, 248-251.
- Hidalgo, E., Limon, A. & Aguilar, J. 1996. A second Escherichia coli gene with similarity to gapA. *Microbiologia (Madrid, Spain)*, 12, 99-106.
- Hobb, R. I., Fields, J. A., Burns, C. M. & Thompson, S. A. 2009. Evaluation of procedures for outer membrane isolation from *Campylobacter jejuni*. *Microbiology*, 155, 979-988.
- Hofreuter, D. 2014. Defining the metabolic requirements for the growth and colonization capacity of *Campylobacter jejuni*.
- Hofreuter, D., Novik, V. & Galán, J. E. 2008. Metabolic diversity in *Campylobacter jejuni* enhances specific tissue colonization. *Cell host & microbe*, 4, 425-433.
- Holmes, K., Mulholland, F., Pearson, B. M., Pin, C., McNicholl-Kennedy, J., Ketley, J. M. & Wells, J. M. 2005. *Campylobacter jejuni* gene expression in response to iron limitation and the role of Fur. *Microbiology*, 151, 243-57.
- Horikiri, S., Aizawa, Y., Kai, T., Amachi, S., Shinoyama, H. & Fujii, T. 2004. Electron acquisition system constructed from an NAD-independent D-lactate dehydrogenase and cytochrome c 2 in *Rhodospseudomonas palustris* no. 7. *Bioscience, biotechnology, and biochemistry*, 68, 516-522.
- Houry, W. A., Frishman, D., Eckerskorn, C., Lottspeich, F. & Hartl, F. U. 1999. Identification of in vivo substrates of the chaperonin GroEL. *Nature*, 402, 147-154.
- Hugdahl, M. B., Beery, J. & Doyle, M. 1988. Chemotactic behavior of *Campylobacter jejuni*. *Infection and immunity*, 56, 1560-1566.
- Humphrey, S., Chaloner, G., Kemmett, K., Davidson, N., Williams, N., Kipar, A., Humphrey, T. & Wigley, P. 2014. *Campylobacter jejuni* is not merely a commensal in commercial broiler chickens and affects bird welfare. *MBio*, 5, e01364-14.
- Humphrey, S., Lacharme-Lora, L., Chaloner, G., Gibbs, K., Humphrey, T., Williams, N. & Wigley, P. 2015. Heterogeneity in the infection biology of *Campylobacter jejuni* isolates in three infection models reveals an invasive and virulent phenotype in a st21 isolate from poultry. *PloS one*, 10, e0141182.
- Hwang, N. R., Yim, S.-H., Kim, Y. M., Jeong, J., Song, E. J., Lee, Y., Lee, J. H., Choi, S. & Lee, K.-J. 2009. Oxidative modifications of glyceraldehyde-3-phosphate dehydrogenase play a key role in its multiple cellular functions. *Biochemical Journal*, 423, 253-264.
- Ikeda, N. & Karlyshev, A. V. 2012. Putative mechanisms and biological role of coccoid form formation in *Campylobacter jejuni*. *European Journal of Microbiology and Immunology*, 2, 41-49.
- Iovine, N. M. 2013. Resistance mechanisms in *Campylobacter jejuni*. *Virulence*, 4, 230-240.
- Jackson, D. N., Davis, B., Tirado, S. M., Duggal, M., Van Frankenhuyzen, J. K., Deaville, D., Wijesinghe, M., Tessaro, M. & Trevors, J. 2009. Survival mechanisms and culturability of *Campylobacter jejuni* under stress conditions. *Antonie Van Leeuwenhoek*, 96, 377-394.
- Jacobs-Reitsma, W. 1995. *Campylobacter* bacteria in breeder flocks. *Avian diseases*, 355-359.

- Janvier, B., Constantinidou, C., Aucher, P., Marshall, Z., Penn, C. & Fauchere, J. 1998. Characterization and gene sequencing of a 19-kDa periplasmic protein of *Campylobacter jejuni/coli*. *Research in microbiology*, 149, 95-107.
- Javed, M. A., Cawthraw, S. A., Baig, A., Li, J., McNally, A., Oldfield, N. J., Newell, D. G. & Manning, G. 2012. Cj1136 is required for lipooligosaccharide biosynthesis, hyperinvasion, and chick colonization by *Campylobacter jejuni*. *Infection and immunity*, 80, 2361-2370.
- Jervis, A. J., Butler, J. A., Wren, B. W. & Linton, D. 2015. Chromosomal integration vectors allowing flexible expression of foreign genes in *Campylobacter jejuni*. *BMC microbiology*, 15, 230.
- Johnston, K. & Gotschlich, E. 1974. Isolation and characterization of the outer membrane of *Neisseria gonorrhoeae*. *Journal of bacteriology*, 119, 250-257.
- Jones, F., Orcutt, M. & Little, R. B. 1931. Vibrios (*Vibrio jejuni*, n. sp.) associated with intestinal disorders of cows and calves. *The Journal of experimental medicine*, 53, 853.
- Kanungpean, D., Kakuda, T. & Takai, S. 2011. Participation of CheR and CheB in the chemosensory response of *Campylobacter jejuni*. *Microbiology*, 157, 1279-1289.
- Kelley, L. A., Mezulis, S., Yates, C. M., Wass, M. N. & Sternberg, M. J. 2015. The Phyre2 web portal for protein modeling, prediction and analysis. *Nature protocols*, 10, 845-858.
- Kelley, L. A. & Sternberg, M. J. 2009. Protein structure prediction on the Web: a case study using the Phyre server. *Nature protocols*, 4, 363-371.
- Keo, T., Collins, J., Kunwar, P., Blaser, M. J. & Iovine, N. M. 2011. *Campylobacter* capsule and lipooligosaccharide confer resistance to serum and cationic antimicrobials. *Virulence*, 2, 30-40.
- Ketley, J. M. 1997. Pathogenesis of enteric infection by *Campylobacter*. *Microbiology*, 143, 5-21.
- Ketley, J. M. & Konkel, M. E. 2005. *Campylobacter: molecular and cellular biology*, Horizon Scientific Press.
- Khrapunov, S. 2009. Circular dichroism spectroscopy has intrinsic limitations for protein secondary structure analysis. *Analytical biochemistry*, 389, 174-176.
- Kim, J. W. & Dang, C. V. 2005. Multifaceted roles of glycolytic enzymes. *Trends Biochem Sci*, 30, 142-50.
- Knight, S. A., Vilaire, G., Lesuisse, E. & Dancis, A. 2005. Iron acquisition from transferrin by *Candida albicans* depends on the reductive pathway. *Infection and immunity*, 73, 5482-5492.
- Konkel, M., Joens, L. & Mixter, P. 2000. Molecular characterization of *Campylobacter jejuni* virulence determinants. *Campylobacter, 2nd ed. American Society for Microbiology, Washington, DC*, 217-240.
- Konkel, M. E., Christensen, J. E., Keech, A. M., Monteville, M. R., Klena, J. D. & Garvis, S. G. 2005. Identification of a fibronectin-binding domain within the *Campylobacter jejuni* CadF protein. *Molecular microbiology*, 57, 1022-1035.
- Konkel, M. E., Kim, B. J., Rivera-Amill, V. & Garvis, S. G. 1999. Bacterial secreted proteins are required for the internalization of *Campylobacter jejuni* into cultured mammalian cells. *Molecular microbiology*, 32, 691-701.
- Konkel, M. E., Klena, J. D., Rivera-Amill, V., Monteville, M. R., Biswas, D., Raphael, B. & Mickelson, J. 2004. Secretion of virulence proteins from *Campylobacter jejuni* is dependent on a functional flagellar export apparatus. *Journal of bacteriology*, 186, 3296-3303.

- Krewulak, K. D. & Vogel, H. J. 2008. Structural biology of bacterial iron uptake. *Biochimica et Biophysica Acta (BBA)-Biomembranes*, 1778, 1781-1804.
- Kumar, S., Sheokand, N., Mhadeshwar, M. A., Raje, C. I. & Raje, M. 2012a. Characterization of glyceraldehyde-3-phosphate dehydrogenase as a novel transferrin receptor. *Int J Biochem Cell Biol*, 44, 189-99.
- Kumar, S., Sheokand, N., Mhadeshwar, M. A., Raje, C. I. & Raje, M. 2012b. Characterization of glyceraldehyde-3-phosphate dehydrogenase as a novel transferrin receptor. *The international journal of biochemistry & cell biology*, 44, 189-199.
- Lau, C. K., Krewulak, K. D. & Vogel, H. J. 2015. Bacterial ferrous iron transport: the Feo system. *FEMS microbiology reviews*, 40, 273-298.
- Legrand, D., Pierce, A., Ellass, E., Carpentier, M., Mariller, C. & Mazurier, J. 2008. Lactoferrin structure and functions. *Bioactive Components of Milk*. Springer.
- Lenz, L. L., Mohammadi, S., Geissler, A. & Portnoy, D. A. 2003. SecA2-dependent secretion of autolytic enzymes promotes *Listeria monocytogenes* pathogenesis. *Proceedings of the National Academy of Sciences*, 100, 12432-12437.
- Lertpiriyapong, K., Gamazon, E. R., Feng, Y., Park, D. S., Pang, J., Botka, G., Graffam, M. E., Ge, Z. & Fox, J. G. 2012. *Campylobacter jejuni* type VI secretion system: roles in adaptation to deoxycholic acid, host cell adherence, invasion, and in vivo colonization. *PLoS One*, 7, e42842.
- Lewis, J. P. 2010. Metal uptake in host-pathogen interactions: role of iron in *Porphyromonas gingivalis* interactions with host organisms. *Periodontology 2000*, 52, 94-116.
- Lewis, L., Rohde, K., Gipson, M., Behrens, B., Gray, E., Toth, S., Roe, B. & Dyer, D. 1998. Identification and Molecular Analysis of lbpBA, Which Encodes the Two-Component Meningococcal Lactoferrin Receptor. *Infection and immunity*, 66, 3017-3023.
- Liberati, N. T., Urbach, J. M., Miyata, S., Lee, D. G., Drenkard, E., Wu, G., Villanueva, J., Wei, T. & Ausubel, F. M. 2006. An ordered, nonredundant library of *Pseudomonas aeruginosa* strain PA14 transposon insertion mutants. *Proceedings of the National Academy of Sciences of the United States of America*, 103, 2833-2838.
- Lin, J., Sahin, O., Michel, L. O. & Zhang, Q. 2003. Critical role of multidrug efflux pump CmeABC in bile resistance and in vivo colonization of *Campylobacter jejuni*. *Infection and immunity*, 71, 4250-4259.
- Liu, Y.-W., Hitchcock, A., Salmon, R. C. & Kelly, D. J. 2014. It takes two to tango: two TatA paralogues and two redox enzyme-specific chaperones are involved in the localization of twin-arginine translocase substrates in *Campylobacter jejuni*. *Microbiology*, 160, 2053-2066.
- Lottenberg, R., Broder, C., Boyle, M., Kain, S., Schroeder, B. & Curtiss, R. 1992. Cloning, sequence analysis, and expression in *Escherichia coli* of a streptococcal plasmin receptor. *Journal of Bacteriology*, 174, 5204-5210.
- Luo, N., Sahin, O., Lin, J., Michel, L. O. & Zhang, Q. 2003. In vivo selection of *Campylobacter* isolates with high levels of fluoroquinolone resistance associated with gyrA mutations and the function of the CmeABC efflux pump. *Antimicrobial agents and chemotherapy*, 47, 390-394.
- Macedo, M. F. & Sousa, M. D. 2008. Transferrin and the transferrin receptor: of magic bullets and other concerns. *Inflammation & Allergy-Drug Targets (Formerly Current Drug Targets-Inflammation & Allergy)*, 7, 41-52.

- Madureira, P., Baptista, M., Vieira, M., Magalhaes, V., Camelo, A., Oliveira, L., Ribeiro, A., Tavares, D., Trieu-Cuot, P. & Vilanova, M. 2007. Streptococcus agalactiae GAPDH is a virulence-associated immunomodulatory protein. *The Journal of Immunology*, 178, 1379-1387.
- Malhotra, H., Patidar, A., Boradia, V. M., Kumar, R., Nimbalkar, R. D., Kumar, A., Gani, Z., Kaur, R., Garg, P. & Raje, M. 2017. Mycobacterium tuberculosis Glyceraldehyde-3-phosphate dehydrogenase (GAPDH) functions as a receptor for human lactoferrin. *Frontiers in Cellular and Infection Microbiology*, 7.
- Mandal, R. K., Jiang, T. & Kwon, Y. M. 2017. Essential genome of Campylobacter jejuni. *BMC genomics*, 18, 616.
- Mcalister, L. & Holland, M. J. 1985. Isolation and characterization of yeast strains carrying mutations in the glyceraldehyde-3-phosphate dehydrogenase genes. *Journal of Biological Chemistry*, 260, 15013-15018.
- Mccarthy, N. & Giesecke, J. 2001. Incidence of Guillain-Barré syndrome following infection with Campylobacter jejuni. *American journal of epidemiology*, 153, 610-614.
- Mead, G., Hudson, W. & Hinton, M. 1995. Effect of changes in processing to improve hygiene control on contamination of poultry carcasses with Campylobacter. *Epidemiology and Infection*, 115, 495-500.
- Mendz, G. L., Ball, G. E. & Meek, D. J. 1997. Pyruvate metabolism in Campylobacter spp. *Biochimica et Biophysica Acta (BBA)-General Subjects*, 1334, 291-302.
- Metris, A., Reuter, M., Gaskin, D. J., Baranyi, J. & Van Vliet, A. H. 2011. In vivo and in silico determination of essential genes of Campylobacter jejuni. *BMC genomics*, 12, 535.
- Micsonai, A., Wien, F., Kernya, L., Lee, Y.-H., Goto, Y., Réfrégiers, M. & Kardos, J. 2015. Accurate secondary structure prediction and fold recognition for circular dichroism spectroscopy. *Proceedings of the National Academy of Sciences*, 112, E3095-E3103.
- Miller, C. E., Rock, J. D., Ridley, K. A., Williams, P. H. & Ketley, J. M. 2008. Utilization of lactoferrin-bound and transferrin-bound iron by Campylobacter jejuni. *Journal of bacteriology*, 190, 1900-1911.
- Miller, C. E., Williams, P. H. & Ketley, J. M. 2009. Pumping iron: mechanisms for iron uptake by Campylobacter. *Microbiology*, 155, 3157-3165.
- Modun, B., Morrissey, J. & Williams, P. 2000. The staphylococcal transferrin receptor: a glycolytic enzyme with novel functions. *Trends Microbiol*, 8, 231-7.
- Modun, B. & Williams, P. 1999. The Staphylococcal Transferrin-Binding Protein Is a Cell Wall Glyceraldehyde-3-Phosphate Dehydrogenase. *Infection And Immunity*, Vol. 67, 1086-1092.
- Monselise, A., Blickstein, D., Ostfeld, I., Segal, R. & Weinberger, M. 2004. A case of cellulitis complicating Campylobacter jejuni subspecies jejuni bacteremia and review of the literature. *European Journal of Clinical Microbiology and Infectious Diseases*, 23, 718-721.
- Monteville, M. R. & Konkel, M. E. 2002. Fibronectin-facilitated invasion of T84 eukaryotic cells by Campylobacter jejuni occurs preferentially at the basolateral cell surface. *Infection and immunity*, 70, 6665-6671.
- Morgan, E. 1977. Iron release from transferrin is mediated by organic phosphate compounds. *Proteins of Iron Metabolism*, 227-235.
- Mukherjee, S., Dutta, D., Saha, B. & Das, A. K. 2010. Crystal structure of glyceraldehyde-3-phosphate dehydrogenase 1 from methicillin-resistant

- Staphylococcus aureus MRSA252 provides novel insights into substrate binding and catalytic mechanism. *Journal of molecular biology*, 401, 949-968.
- Nachamkin, I., Allos, B. M. & Ho, T. 2000. Campylobacter jejuni infection and the association with Guillain-Barré syndrome. *Campylobacter*, 2nd ed. ASM Press, Washington, DC, 155-175.
- Nachamkin, I., Liu, J., Li, M., Ung, H., Moran, A. P., Prendergast, M. M. & Sheikh, K. 2002. Campylobacter jejuni from patients with Guillain-Barré syndrome preferentially expresses a GD1a-like epitope. *Infection and immunity*, 70, 5299-5303.
- Naikare, H., Palyada, K., Panciera, R., Marlow, D. & Stintzi, A. 2006. Major role for FeoB in Campylobacter jejuni ferrous iron acquisition, gut colonization, and intracellular survival. *Infection and immunity*, 74, 5433-5444.
- Nakajima, H., Amano, W., Fujita, A., Fukuhara, A., Azuma, Y.-T., Hata, F., Inui, T. & Takeuchi, T. 2007. The active site cysteine of the proapoptotic protein glyceraldehyde-3-phosphate dehydrogenase is essential in oxidative stress-induced aggregation and cell death. *Journal of Biological Chemistry*, 282, 26562-26574.
- Natale, P., Brüser, T. & Driessen, A. J. 2008. Sec-and Tat-mediated protein secretion across the bacterial cytoplasmic membrane—distinct translocases and mechanisms. *Biochimica et Biophysica Acta (BBA)-Biomembranes*, 1778, 1735-1756.
- Neilands, J. 1995. Siderophores: structure and function of microbial iron transport compounds. *Journal of Biological Chemistry*, 270, 26723-26726.
- Nicholls, C., Li, H. & Liu, J. P. 2012. GAPDH: a common enzyme with uncommon functions. *Clinical and Experimental Pharmacology and Physiology*, 39, 674-679.
- Nyati, K. K. & Nyati, R. 2013. Role of Campylobacter jejuni infection in the pathogenesis of Guillain-Barré syndrome: an update. *BioMed research international*, 2013.
- Okujo, N., Akiyama, T., Miyoshi, S.-I., Shinoda, S. & Yamamoto, S. 1996. Involvement of vulnibactin and exocellular protease in utilization of transferrin-and lactoferrin-bound iron by Vibrio vulnificus. *Microbiology and immunology*, 40, 595-598.
- Oliveira, L., Madureira, P., Andrade, E. B., Bouaboud, A., Morello, E., Ferreira, P., Poyart, C., Trieu-Cuot, P. & Dramsi, S. 2012. Group B streptococcus GAPDH is released upon cell lysis, associates with bacterial surface, and induces apoptosis in murine macrophages. *PloS one*, 7, e29963.
- Palamalai, V. & Miyagi, M. 2010. Mechanism of glyceraldehyde-3-phosphate dehydrogenase inactivation by tyrosine nitration. *Protein science*, 19, 255-262.
- Palyada, K., Threadgill, D. & Stintzi, A. 2004. Iron acquisition and regulation in Campylobacter jejuni. *Journal of bacteriology*, 186, 4714-4729.
- Pancholi, V. & Chhatwal, G. S. 2003. Housekeeping enzymes as virulence factors for pathogens. *International Journal of Medical Microbiology*, 293, 391-401.
- Pancholi, V. & Fischetti, V. A. 1992. A major surface protein on group A streptococci is a glyceraldehyde-3-phosphate-dehydrogenase with multiple binding activity. *The Journal of experimental medicine*, 176, 415-426.
- Park, S. F. & Richardson, P. T. 1995. Molecular characterization of a Campylobacter jejuni lipoprotein with homology to periplasmic siderophore-binding proteins. *Journal of bacteriology*, 177, 2259-2264.
- Parker, C. T., Quiñones, B., Miller, W. G., Horn, S. T. & Mandrell, R. E. 2006. Comparative genomic analysis of Campylobacter jejuni strains reveals diversity

- due to genomic elements similar to those present in *C. jejuni* strain RM1221. *Journal of clinical microbiology*, 44, 4125-4135.
- Parkhill, J., Wren, B., Mungall, K., Ketley, J., Churcher, C., Basham, D., Chillingworth, T., Davies, R., Feltwell, T. & Holroyd, S. 2000. The genome sequence of the food-borne pathogen *Campylobacter jejuni* reveals hypervariable sequences. *Nature*, 403, 665-668.
- Pei, Z., Burucoa, C., Grignon, B., Baqar, S., Huang, X.-Z., Kopecko, D. J., Bourgeois, A., Fauchere, J.-L. & Blaser, M. J. 1998. Mutation in the *peb1A* locus of *Campylobacter jejuni* reduces interactions with epithelial cells and intestinal colonization of mice. *Infection and immunity*, 66, 938-943.
- Pickett, C. 2000. *Campylobacter* toxins and their role in pathogenesis. *Campylobacter*, 2, 179-190.
- Pickett, C., Auffenberg, T., Pesci, E., Sheen, V. & Jusuf, S. 1992. Iron acquisition and hemolysin production by *Campylobacter jejuni*. *Infection and immunity*, 60, 3872-3877.
- Poly, F., Threadgill, D. & Stintzi, A. 2004. Identification of *Campylobacter jejuni* ATCC 43431-specific genes by whole microbial genome comparisons. *Journal of bacteriology*, 186, 4781-4795.
- Poly, F., Threadgill, D. & Stintzi, A. 2005. Genomic diversity in *Campylobacter jejuni*: identification of *C. jejuni* 81-176-specific genes. *Journal of clinical microbiology*, 43, 2330-2338.
- Purdy, D., Buswell, C., Hodgson, A., Mcalpine, K., Henderson, I. & Leach, S. 2000. Characterisation of cytolethal distending toxin (CDT) mutants of *Campylobacter jejuni*. *Journal of medical microbiology*, 49, 473-479.
- Purves, J., Cockayne, A., Moody, P. C. & Morrissey, J. A. 2010. Comparison of the regulation, metabolic functions, and roles in virulence of the glyceraldehyde-3-phosphate dehydrogenase homologues *gapA* and *gapB* in *Staphylococcus aureus*. *Infection and immunity*, 78, 5223-5232.
- Qing-Yu, H., Mason, A. B., Nguyen, V., Macgillivray, R. T. & Woodworth, R. C. 2000. The chloride effect is related to anion binding in determining the rate of iron release from the human transferrin N-lobe. *Biochemical Journal*, 350, 909-915.
- Raje, C. I., Kumar, S., Harle, A., Nanda, J. S. & Raje, M. 2007. The macrophage cell surface glyceraldehyde-3-phosphate dehydrogenase is a novel transferrin receptor. *J Biol Chem*, 282, 3252-61.
- Raphael, B. H. & Joens, L. A. 2003. *FeoB* is not required for ferrous iron uptake in *Campylobacter jejuni*. *Canadian journal of microbiology*, 49, 727-731.
- Ratledge, C. & Dover, L. G. 2000. Iron metabolism in pathogenic bacteria. *Annual reviews in microbiology*, 54, 881-941.
- Rawat, P., Kumar, S., Sheokand, N., Raje, C. I. & Raje, M. 2012. The multifunctional glycolytic protein glyceraldehyde-3-phosphate dehydrogenase (GAPDH) is a novel macrophage lactoferrin receptor 1 1 This article is part of Special Issue entitled Lactoferrin and has undergone the Journal's usual peer review process. *Biochemistry and Cell Biology*, 90, 329-338.
- Reeser, R. J., Medler, R. T., Billington, S. J., Jost, B. H. & Joens, L. A. 2007. Characterization of *Campylobacter jejuni* biofilms under defined growth conditions. *Applied and environmental microbiology*, 73, 1908-1913.
- Ridley, K. A., Rock, J. D., Li, Y. & Ketley, J. M. 2006. Heme utilization in *Campylobacter jejuni*. *Journal of bacteriology*, 188, 7862-7875.
- Riordan, J. F. 1977. The role of metals in enzyme activity. *Annals of Clinical & Laboratory Science*, 7, 119-129.

- Ritz, M., Garenaux, A., Berge, M. & Federighi, M. 2009. Determination of *rpoA* as the most suitable internal control to study stress response in *C. jejuni* by RT-qPCR and application to oxidative stress. *Journal of Microbiological Methods*, 76, 196-200.
- Rivera-Amill, V., Kim, B. J., Seshu, J. & Konkel, M. E. 2001. Secretion of the virulence-associated *Campylobacter* invasion antigens from *Campylobacter jejuni* requires a stimulatory signal. *The Journal of infectious diseases*, 183, 1607-1616.
- Rivera-Amill, V. & Konkel, M. E. 1999. Secretion of *Campylobacter jejuni* Cia proteins is contact dependent. *Mechanisms in the Pathogenesis of Enteric Diseases 2*. Springer.
- Rock, J. D. 2003. *Iron acquisition from host molecules by Campylobacter jejuni*. Genetics.
- Rompikuntal, P. K. 2012. *Outer membrane vesicle-mediated export of virulence factors from Gram-negative bacteria*. Umeå universitet.
- Saad, N., Urdaci, M., Vignoles, C., Chaignepain, S., Tallon, R., Schmitter, J.-M. & Bressollier, P. 2009. *Lactobacillus plantarum* 299v surface-bound GAPDH: a new insight into enzyme cell walls location. *J Microbiol Biotechnol*, 19, 1635-1643.
- Saier, M. 2006. Protein secretion systems in Gram-negative bacteria. *MICROBE-AMERICAN SOCIETY FOR MICROBIOLOGY*, 1, 414.
- Schaible, U. E. & Kaufmann, S. H. 2004. Iron and microbial infection. *Nature Reviews Microbiology*, 2, 946-953.
- Schefe, J. H., Lehmann, K. E., Buschmann, I. R., Unger, T. & Funke-Kaiser, H. 2006. Quantitative real-time RT-PCR data analysis: current concepts and the novel "gene expression's CT difference" formula. *Journal of molecular medicine*, 84, 901-910.
- Schryvers, A. B. & Stojiljkovic, I. 1999. Iron acquisition systems in the pathogenic *Neisseria*. *Molecular microbiology*, 32, 1117-1123.
- Seidler, K. A. & Seidler, N. W. 2012. Role of extracellular GAPDH in *Streptococcus pyogenes* virulence. *Missouri medicine*, 110, 236-240.
- Seidler, N. W. 2013a. Basic biology of GAPDH. *GAPDH: Biological Properties and Diversity*, 1-36.
- Seidler, N. W. 2013b. GAPDH, as a virulence factor. *Adv Exp Med Biol*, 985, 149-78.
- Sellars, M. J., Hall, S. J. & Kelly, D. J. 2002. Growth of *Campylobacter jejuni* supported by respiration of fumarate, nitrate, nitrite, trimethylamine-N-oxide, or dimethyl sulfoxide requires oxygen. *Journal of Bacteriology*, 184, 4187-4196.
- Senkovich, O., Ceaser, S., Mcgee, D. J. & Testerman, T. L. 2010. Unique host iron utilization mechanisms of *Helicobacter pylori* revealed with iron-deficient chemically defined media. *Infection and immunity*, 78, 1841-1849.
- Seta, F. D., Boschi-Muller, S., Vignais, M. & Branlant, G. 1997. Characterization of *Escherichia coli* strains with *gapA* and *gapB* genes deleted. *Journal of bacteriology*, 179, 5218-5221.
- Shang, Y. W., Ren, F. Z., Song, Z. J., Li, Q. C., Zhou, X. H., Wang, X. B., Xu, Z. L., Bao, G. Y., Wan, T., Lei, T. Y., Wang, N., Jiao, X. A. & Huang, J. L. 2016. Insights into *Campylobacter jejuni* colonization and enteritis using a novel infant rabbit model. *Scientific Reports*, 6.
- Sheokand, N., Kumar, S., Malhotra, H., Tillu, V., Raje, C. I. & Raje, M. 2013. Secreted glyceraldehyde-3-phosphate dehydrogenase is a multifunctional autocrine transferrin receptor for cellular iron acquisition. *Biochim Biophys Acta*, 1830, 3816-27.

- Sheokand, N., Malhotra, H., Kumar, S., Tillu, V. A., Chauhan, A. S., Raje, C. I. & Raje, M. 2014. Moonlighting cell-surface GAPDH recruits apotransferrin to effect iron egress from mammalian cells. *J Cell Sci*, 127, 4279-91.
- Silva, J., Leite, D., Fernandes, M., Mena, C., Gibbs, P. A. & Teixeira, P. 2011. *Campylobacter* spp. as a foodborne pathogen: a review. *Frontiers in microbiology*, 2.
- Sirover, M. A. 2011a. On the functional diversity of glyceraldehyde-3-phosphate dehydrogenase: biochemical mechanisms and regulatory control. *Biochim Biophys Acta*, 1810, 741-51.
- Sirover, M. A. 2011b. On the functional diversity of glyceraldehyde-3-phosphate dehydrogenase: biochemical mechanisms and regulatory control. *Biochimica et Biophysica Acta (BBA)-General Subjects*, 1810, 741-751.
- Sirover, M. A. 2014. Structural analysis of glyceraldehyde-3-phosphate dehydrogenase functional diversity. *The international journal of biochemistry & cell biology*, 57, 20-26.
- Skirrow, M. B. 2000. Clinical aspects of *Campylobacter* infection. *Campylobacter*, 69-88.
- Soares, M. J., Souto-Pradrón, T. & De Souza, W. 1992. Identification of a large pre-lysosomal compartment in the pathogenic protozoon *Trypanosoma cruzi*. *Journal of cell science*, 102, 157-167.
- Song, J.-H., Ko, K. S., Lee, J.-Y., Baek, J. Y., Oh, W. S., Yoon, H. S., Jeong, J.-Y. & Chun, J. 2005. Identification of essential genes in *Streptococcus pneumoniae* by allelic replacement mutagenesis. *Molecules & Cells (Springer Science & Business Media BV)*, 19.
- Sopwith, W., Ashton, M., Frost, J., Tocque, K., O'brien, S., Regan, M. & Syed, Q. 2003. Enhanced surveillance of *Campylobacter* infection in the North West of England 1997–1999. *Journal of Infection*, 46, 35-45.
- Stahl, M., Butcher, J. & Stintzi, A. 2012. Nutrient acquisition and metabolism by *Campylobacter jejuni*. *Front Cell Infect Microbiol*, 2, 5.
- Stahl, M. & Stintzi, A. 2011. Identification of essential genes in *C. jejuni* genome highlights hyper-variable plasticity regions. *Functional & integrative genomics*, 11, 241-257.
- Stahl, M. & Vallance, B. A. 2015. Insights into *Campylobacter jejuni* colonization of the mammalian intestinal tract using a novel mouse model of infection. *Gut microbes*, 6, 143-148.
- Steele, M., Marcone, M., Gyles, C., Chan, V. & Odumeru, J. 2005. Enzymatic activity of *Campylobacter jejuni* hippurate hydrolase. *Protein Engineering Design and Selection*, 19, 17-25.
- Stintzi, A., Van Vliet, A. H. & Ketley, J. M. 2008. Iron metabolism, transport, and regulation. *Campylobacter, Third Edition*. American Society of Microbiology.
- Stojiljkovic, I. & Hantke, K. 1995. Functional domains of the *Escherichia coli* ferric uptake regulator protein (Fur). *Molecular and General Genetics MGG*, 247, 199-205.
- Takahashi, R., Shahada, F., Chuma, T. & Okamoto, K. 2006. Analysis of *Campylobacter* spp. contamination in broilers from the farm to the final meat cuts by using restriction fragment length polymorphism of the polymerase chain reaction products. *International journal of food microbiology*, 110, 240-245.
- Takayama, S. & Reed, J. C. 1997. Protein Interaction Cloning by Far-Western Screening of λ -Phage cDNA Expression Libraries. *cDNA Library Protocols*, 171-184.

- Tan, A. & Woodworth, R. C. 1969. Ultraviolet difference spectral studies of conalbumin complexes with transition metal ions. *Biochemistry*, 8, 3711-3716.
- Tanaka, T., Abe, Y., Inoue, N., Kim, W. S., Kumura, H., Nagasawa, H., Igarashi, I. & Shimazaki, K. 2004. The detection of bovine lactoferrin binding protein on *Trypanosoma brucei*. *J Vet Med Sci*, 66, 619-25.
- Tarze, A., Deniaud, A., Le Bras, M., Maillier, E., Mollé, D., Larochette, N., Zamzami, N., Jan, G., Kroemer, G. & Brenner, C. 2007. GAPDH, a novel regulator of the pro-apoptotic mitochondrial membrane permeabilization. *Oncogene*, 26, 2606-2620.
- Taylor, D. E. & Courvalin, P. 1988. Mechanisms of antibiotic resistance in *Campylobacter* species. *Antimicrobial Agents and Chemotherapy*, 32, 1107.
- Taylor, J. M. & Heinrichs, D. E. 2002. Transferrin binding in *Staphylococcus aureus*: involvement of a cell wall-anchored protein. *Molecular microbiology*, 43, 1603-1614.
- Tenover, F., Williams, S., Gordon, K., Nolan, C. & Plorde, J. 1985. Survey of plasmids and resistance factors in *Campylobacter jejuni* and *Campylobacter coli*. *Antimicrobial agents and chemotherapy*, 27, 37-41.
- Thibodeau, S. N., Lee, D. C. & Palmiter, R. D. 1978. Identical precursors for serum transferrin and egg white conalbumin. *Journal of Biological Chemistry*, 253, 3771-3774.
- Tom-Yew, S. A., Cui, D. T., Bekker, E. G. & Murphy, M. E. 2005. Anion-independent iron coordination by the *Campylobacter jejuni* ferric binding protein. *Journal of Biological Chemistry*, 280, 9283-9290.
- Tourigny, D. S., Elliott, P. R., Edgell, L. J., Hudson, G. M. & Moody, P. C. 2010. Expression, purification, crystallization and preliminary X-ray analysis of wild-type and of an active-site mutant of glyceraldehyde-3-phosphate dehydrogenase from *Campylobacter jejuni*. *Acta Crystallographica Section F: Structural Biology and Crystallization Communications*, 67, 72-75.
- Tourigny, D. S., Elliott, P. R., Edgell, L. J., Hudson, G. M. & Moody, P. C. 2011. Expression, purification, crystallization and preliminary X-ray analysis of wild-type and of an active-site mutant of glyceraldehyde-3-phosphate dehydrogenase from *Campylobacter jejuni*. *Acta Crystallographica Section F: Structural Biology and Crystallization Communications*, 67, 72-75.
- Tunio, S., Oldfield, N., Wooldridge, K. & Turner, D. 2013. Molecular and Immunological Characterization of Glyceraldehyde-3-phosphate Dehydrogenase (GAPDH-1) of *Neisseria meningitidis* serogroup B strain MC58. *Sindh University Research Journal-SURJ (Science Series)*, 45.
- Tunio, S. A., Oldfield, N. J., Ala'aldeen, D. A., Wooldridge, K. G. & Turner, D. P. 2010. The role of glyceraldehyde 3-phosphate dehydrogenase (GapA-1) in *Neisseria meningitidis* adherence to human cells. *BMC microbiology*, 10, 280.
- Valenti, P., Antonini, G., Von Hunolstein, C., Visca, P., Orsi, N. & Antonini, E. 1983. Studies of the antimicrobial activity of ovotransferrin. *International journal of tissue reactions*, 5, 97-105.
- Van Der Oost, J., Schut, G., Kengen, S. M., Hagen, W. R., Thomm, M. & De Vos, W. M. 1998. The Ferredoxin-dependent Conversion of Glyceraldehyde-3-phosphate in the Hyperthermophilic Archaeon *Pyrococcus furiosus* Represents a Novel Site of Glycolytic Regulation. *Journal of Biological Chemistry*, 273, 28149-28154.
- Van Snick, J. L., Masson, P. L. & Heremans, J. F. 1974. The involvement of lactoferrin in the hyposideremia of acute inflammation. *Journal of Experimental Medicine*, 140, 1068-1084.

- Van Vliet, A. & Ketley, J. 2001. Pathogenesis of enteric *Campylobacter* infection. *Journal of Applied Microbiology*, 90.
- Van Vliet, A. H., Baillon, M.-L. A., Penn, C. W. & Ketley, J. M. 2001. The iron-induced ferredoxin FdxA of *Campylobacter jejuni* is involved in aerotolerance. *FEMS Microbiology Letters*, 196, 189-193.
- Van Vliet, A. H., Ketley, J. M., Park, S. F. & Penn, C. W. 2002. The role of iron in *Campylobacter* gene regulation, metabolism and oxidative stress defense. *FEMS microbiology reviews*, 26, 173-186.
- Van Vliet, A. H., Wooldridge, K. G. & Ketley, J. M. 1998. Iron-responsive gene regulation in a *Campylobacter jejuni* fur mutant. *Journal of bacteriology*, 180, 5291-5298.
- Vartivarian, S. & Cowart, R. E. 1999. Extracellular iron reductases: identification of a new class of enzymes by siderophore-producing microorganisms. *Archives of biochemistry and biophysics*, 364, 75-82.
- Vázquez-Zamorano, Z. E., González-López, M. A., Romero-Espejel, M. E., Azuara-Liceaga, E. I., López-Casamichana, M. & Olivares-Trejo, J. D. J. 2014. *Streptococcus pneumoniae* secretes a glyceraldehyde-3-phosphate dehydrogenase, which binds haemoglobin and haem. *Biometals*, 27, 683.
- Velayudhan, J., Jones, M. A., Barrow, P. A. & Kelly, D. J. 2004. L-serine catabolism via an oxygen-labile L-serine dehydratase is essential for colonization of the avian gut by *Campylobacter jejuni*. *Infection and immunity*, 72, 260-268.
- Velayudhan, J. & Kelly, D. J. 2002. Analysis of gluconeogenic and anaplerotic enzymes in *Campylobacter jejuni*: an essential role for phosphoenolpyruvate carboxykinase. *Microbiology*, 148, 685-694.
- Villamón, E., Villalba, V., Noguerras, M. M., Tomás, J. M., Gozalbo, D. & Gil, M. L. 2003. Glyceraldehyde-3-phosphate dehydrogenase, a glycolytic enzyme present in the periplasm of *Aeromonas hydrophila*. *Antonie Van Leeuwenhoek*, 84, 31-38.
- Walsh, B. W., Lenhart, J. S., Schroeder, J. W. & Simmons, L. A. 2012. Far Western blotting as a rapid and efficient method for detecting interactions between DNA replication and DNA repair proteins. *Single-Stranded DNA Binding Proteins: Methods and Protocols*, 161-168.
- Wassenaar, T. M. & Blaser, M. J. 1999. Pathophysiology of *Campylobacter jejuni* infections of humans. *Microbes and Infection*, 1, 1023-1033.
- Weinberg, E. D. 1984. Iron withholding: a defense against infection and neoplasia. *Physiological reviews*, 64, 65-102.
- White, M. R. & Garcin, E. D. 2016. The sweet side of RNA regulation: glyceraldehyde-3-phosphate dehydrogenase as a noncanonical RNA-binding protein. *Wiley Interdisciplinary Reviews: RNA*, 7, 53-70.
- Widdel, F. 2007. Theory and measurement of bacterial growth. *Di dalam Grundpraktikum Mikrobiologie*, 4.
- Wolz, C., Hohloch, K., Ocaktan, A., Poole, K., Evans, R. W., Rochel, N., Albrecht-Gary, A.-M., Abdallah, M. A. & Döring, G. 1994. Iron release from transferrin by pyoverdinin and elastase from *Pseudomonas aeruginosa*. *Infection and immunity*, 62, 4021-4027.
- Woodall, C. A., Jones, M., Barrow, P., Hinds, J., Marsden, G., Kelly, D., Dorrell, N., Wren, B. & Maskell, D. 2005. *Campylobacter jejuni* gene expression in the chick cecum: evidence for adaptation to a low-oxygen environment. *Infection and immunity*, 73, 5278-5285.
- Wooldridge, K. G. & Ketley, J. M. 1997. *Campylobacter*-host cell interactions. *Trends in microbiology*, 5, 96-102.

- Wooldridge, K. G., Williams, P. H. & Ketley, J. M. 1994. Iron-responsive genetic regulation in *Campylobacter jejuni*: cloning and characterization of a fur homolog. *Journal of bacteriology*, 176, 5852-5856.
- Workman, S. N., Mathison, G. E. & Lavoie, M. C. 2005. Pet dogs and chicken meat as reservoirs of *Campylobacter* spp. in Barbados. *Journal of clinical microbiology*, 43, 2642-2650.
- Wösten, M. M. S. M., Van Mourik, A. & Van Putten, J. P. M. 2008. Regulation of Genes in *Campylobacter jejuni*. *Campylobacter*, Third Edition. American Society of Microbiology.
- Xu, F., Wu, C., Guo, F., Cui, G., Zeng, X., Yang, B. & Lin, J. 2015. Transcriptomic analysis of *Campylobacter jejuni* NCTC 11168 in response to epinephrine and norepinephrine. *Frontiers in microbiology*, 6.
- Yang, H.-W., Yong, T.-S., Lee, J.-H., Im, K.-I. & Park, S.-J. 2002. Characterization of two glyceraldehyde 3-phosphate dehydrogenase genes in *Giardia lamblia*. *Parasitology research*, 88, 646-650.
- Yen, C.-C., Shen, C.-J., Hsu, W.-H., Chang, Y.-H., Lin, H.-T., Chen, H.-L. & Chen, C.-M. 2011. Lactoferrin: an iron-binding antimicrobial protein against *Escherichia coli* infection. *Biometals*, 24, 585-594.
- Yen, M.-R., Peabody, C. R., Partovi, S. M., Zhai, Y., Tseng, Y.-H. & Saier, M. H. 2002. Protein-translocating outer membrane porins of Gram-negative bacteria. *Biochimica et Biophysica Acta (BBA)-Biomembranes*, 1562, 6-31.
- Young, K. T., Davis, L. M. & Dirita, V. J. 2007. *Campylobacter jejuni*: molecular biology and pathogenesis. *Nature Reviews Microbiology*, 5, 665-679.
- Yuki, N. & Odaka, M. 2005. Ganglioside mimicry as a cause of Guillain–Barré syndrome. *Current opinion in neurology*, 18, 557-561.
- Zano, S. P., Pavlovsky, A. G. & Viola, R. E. 2014. Structure of an unusual S-adenosylmethionine synthetase from *Campylobacter jejuni*. *Acta Crystallographica Section D: Biological Crystallography*, 70, 442-450.
- Zhao, X., Zhong, J., Wei, C., Lin, C.-W. & Ding, T. 2017. Current Perspectives on Viable but Non-culturable State in Foodborne Pathogens. *Frontiers in microbiology*, 8.
- Ziprin, R. L., Young, C. R., Stanker, L. H., Hume, M. E. & Konkel, M. E. 1999. The absence of cecal colonization of chicks by a mutant of *Campylobacter jejuni* not expressing bacterial fibronectin-binding protein. *Avian diseases*, 586-589.